



University
of Glasgow

<https://theses.gla.ac.uk/>

Theses Digitisation:

<https://www.gla.ac.uk/myglasgow/research/enlighten/theses/digitisation/>

This is a digitised version of the original print thesis.

Copyright and moral rights for this work are retained by the author

A copy can be downloaded for personal non-commercial research or study, without prior permission or charge

This work cannot be reproduced or quoted extensively from without first obtaining permission in writing from the author

The content must not be changed in any way or sold commercially in any format or medium without the formal permission of the author

When referring to this work, full bibliographic details including the author, title, awarding institution and date of the thesis must be given

Enlighten: Theses

<https://theses.gla.ac.uk/>
research-enlighten@glasgow.ac.uk

**Analysis of Trafficking Motifs in the Insulin-Responsive
Glucose Transporter Isoform, GLUT4**

A thesis submitted to the
FACULTY OF SCIENCE
for the degree of
DOCTOR OF PHILOSOPHY

By

Derek Robert Melvin

Division of Biochemistry and Molecular Biology
Institute of Biomedical and Life Sciences
University of Glasgow
September 1998

ProQuest Number: 10647097

All rights reserved

INFORMATION TO ALL USERS

The quality of this reproduction is dependent upon the quality of the copy submitted.

In the unlikely event that the author did not send a complete manuscript and there are missing pages, these will be noted. Also, if material had to be removed, a note will indicate the deletion.



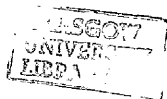
ProQuest 10647097

Published by ProQuest LLC (2017). Copyright of the Dissertation is held by the Author.

All rights reserved.

This work is protected against unauthorized copying under Title 17, United States Code
Microform Edition © ProQuest LLC.

ProQuest LLC.
789 East Eisenhower Parkway
P.O. Box 1346
Ann Arbor, MI 48106 – 1346



GLASGOW UNIVERSITY
LIBRARY

11322 (copy 2)

Abstract

The complex system that comprises the intracellular trafficking pathway of the insulin-responsive glucose transporter isoform, GLUT4, remains to be fully characterised. Many questions remain as to how the trafficking and targeting of this recycling protein occurs in the basal state and how this process is affected by treatment with the peptide hormone insulin. In this thesis I have attempted to address some of these issues.

Much of the trafficking of GLUT4 is thought to be governed by targeting motifs that are present in the cytoplasmic amino- and carboxy-termini of the protein. These sequences have previously been shown to be involved in the internalisation of the protein from the cell surface in both the basal and post-insulin-stimulated states. In this thesis I have undertaken to determine whether these signal motifs can also function in the trafficking of GLUT4 to specific intracellular locations. My results suggest that indeed these motifs may function at more than one intracellular loci and that they may have more than one role in the complex pattern of GLUT4 trafficking. These results have led to the proposal of an alternative intracellular trafficking pathway for GLUT4 within 3T3-L1 adipocytes.

I have also examined the role of the major phosphorylation site on the sequence of GLUT4, a serine residue at position 488, in the regulation of GLUT4 trafficking. Results suggest that the phosphorylation state of S⁴⁸⁸ is likely to play a role in the intracellular sorting of GLUT4, but is not involved in the insulin-stimulated recruitment of GLUT4 to the plasma membrane.

Further studies examined the role of residues distal to the carboxy-terminal dileucine motif in the cytoplasmic tail of GLUT4 in the targeting of this isoform in 3T3-L1 adipocytes. Such residues have previously been thought to be involved in the targeting of GLUT4 to specific intracellular compartments. Results suggest that the cytoplasmic carboxy-terminus of GLUT4 contains an additional targeting signal distal to the L⁴⁸⁹L⁴⁹⁰ motif that regulates sorting of GLUT4 from endosomes into a post-endocytic storage compartment.

To complement the above targeting studies, I undertook the construction and characterisation of a series of GLUT2/GLUT4 recombinant chimeric glucose transporters in a further attempt to define the roles of the cytoplasmic signal sequences on the trafficking of GLUT4. Results here were in concert with much of the published literature but also concurred strongly with the proposed alternative trafficking pathway of GLUT4.

My final study was undertaken during my period working at SmithKline Beecham as part of my CASE studentship. Analysis was performed into the expression levels of proteins known to be involved in the trafficking of GLUT4 in animal models of diabetes mellitus. This study identified selective changes in hindlimb skeletal muscle tissues from the Zucker diabetic *fa/fa* model of non-insulin-dependent diabetes mellitus and also demonstrated further alterations in levels of expression after treatment with a thiazolidinedione compound. It was concluded that these selective changes were a result of the state of hyperinsulinaemia that is prevalent in such animals.

Acknowledgements

I would like to thank my supervisor, Gwyn. His unyielding support, encouragement, and friendship have been an inspiration throughout the last three years. Quite simply, I could not have asked for a better supervisor. Thanks must go also to the University of Glasgow, the BBSRC and SmithKline Beecham Pharmaceuticals for providing me with a CASE Award Studentship.

Acknowledgments for this PhD would not be complete without mention of two special people. Firstly, Caroline, my twin. Thank you for being a great friend, colleague, and competitor...we really had some fun and I think that it is safe to say that we kept each other going! Secondly, I must thank the Captain: football team-mate, drinking buddy, and most importantly...fellow critic of the state of Scottish football! I would like to thank everyone that I have worked with over the years, both in C36 and the Davidson building, and Scientist Perry, for proof-reading this thesis through blue-tinted spectacles! Thanks must go also to my supervisor at SmithKline Beecham Pharmaceuticals, Dr. Greg Murphy, and all of the people who made my period of work there such a great experience.

Special thanks must go to my family. To my Gran and Granda: I think that everyone in the world (certainly Renfrew) knows that I was studying for a PhD, and if anyone does not then I am sure that my Gran will have told them by now!!! I know am very lucky to have them. I would also like to remember my paternal grandparents, who are in my thoughts.

Finally, I want to thank my Mum and Dad. All my life they have been there, helping and supporting...but never demanding. Their love and encouragement has meant more to me than I can ever explain. Thank you.

Dedication

I dedicate this thesis to my Mum and Dad,
without whom,
none of this would have been possible.

Quotations

"Our hope is like an anchor, stedfast and sure"

Hebrews, chapter 6 verse 19

"If a job is worth doing, it is worth doing well"

Robert McPhail Melvin

Contents

	Page
Title	i
Abstract	ii
Acknowledgements	iv
Dedication	vi
Quotes	vii
Contents	viii
List of Figures	xxii
List of Tables	xvii
Abbreviations	xxx

Chapter 1	Introduction	1
1.1	Introduction	2
1.2	Tissue-specific Distribution of the Facilitative Glucose Transporter Family	4
1.2.1	Overview	4
1.2.2	GLUT1	4
1.2.3	GLUT2	6
1.2.4	GLUT3	7
1.2.5	GLUT4	8
1.2.6	GLUT5	8
1.2.7	GLUT6	9
1.3	Structure and Membrane Topology of the Mammalian Facilitative Glucose Transporter Family	9
1.4	GLUT4 - The Insulin-Responsive Glucose Transporter Isoform	14
1.5	Regulation of GLUT4 Translocation	15
1.6	Regions Dictating GLUT4 Intracellular Sequestration	20
1.6.1	The Amino Terminus as a Targeting Domain	24
1.6.2	The Carboxy Terminus as a Targeting Domain	30
1.6.3	Analysis of Putative GLUT4 Targeting Signals in Insulin- Responsive Cell Lines	35

1.7	Constitutive Recycling of GLUT4	44
1.8	The Intracellular GLUT4 Compartment	45
1.9	GLUT4 Vesicle Trafficking	49
1.9.1	The SNARE Hypothesis	49
1.9.2	SNARE Complex-mediated Vesicle Docking and Fusion	50
1.9.3	SNARE Complex Structure	51
1.9.4	v-SNAREs Involved in GLUT4 Trafficking	52
1.9.5	t-SNAREs Involved in GLUT4 Trafficking	53
1.9.6	SNARE-binding Proteins Involved in GLUT4 Exocytosis	53
1.10	Insulin Resistance and Type II (Non-Insulin-Dependent) Diabetes Mellitus	57
1.10.1	The Role of the Insulin-Responsive Glucose Transporter Isoform, GLUT4, in Insulin resistance of NIDDM	58
1.10.2	GLUT4 Defects in Insulin Resistance of NIDDM	59
1.10.3	Effects of Insulin Resistance on GLUT4 Expression and Activity in Adipose Tissue	60
1.10.4	Insulin Resistance in Skeletal Muscle	61
1.11	Animal Models of Diabetes Mellitus	65
1.11.1	<i>ob/ob</i> Mouse	65
1.11.2	Obese Zucker Rat	65
1.11.3	Streptozotocin-induced Diabetic Rat	66
1.12	Aims of this study	67

Chapter 2	Materials and Methods	69
2.1	Materials	70
2.1.1	General Reagents	70
2.1.2	Antibodies	74
2.1.3	Cells	74
2.1.4	Cell Culture Media and Reagents	74
2.1.5	Cell Culture Plastics	75
2.1.6	Radioactive Materials	75
2.2	Buffers and Media	76
2.2.1	Cell Culture Media	76
2.2.2	General Buffers	76
2.2.3	SDS-Polyacrylamide Gel Electrophoresis Buffers	78
2.2.4	Protease Inhibitor Stocks	79
2.2.5	Western Blot Reagents	79
2.2.6	Muscle Buffer	79
2.2.7	Bacterial Media and Agar	80
2.2.8	Vesicle Immunoabsorption Buffer	80
2.3.	3T3-L1 Fibroblast Cell Culture	80
2.3.1	Growth of 3T3-L1 Fibroblasts	80
2.3.2	Trypsinisation of 3T3-L1 Fibroblasts	81
2.3.3	Preparation of 3T3-L1 Fibroblast Differentiation Media	81
2.3.4	Differentiation Protocol for 3T3-L1 Fibroblasts	82
2.3.5	Storage of 3T3-L1 Fibroblasts in Liquid N ₂	82
2.3.6	Resurrection of Frozen Cell Stocks from Liquid N ₂	83

2.3.7	Transfection of 3T3-L1 Fibroblasts Using the Calcium Phosphate Method	83
2.3.7a	Preparation of Cells for Transfection	83
2.3.7b	Transfection and Selection Protocol	83
2.3.7c	Isolation and Propagation of Individual Clones	84
2.4	Preparation of HRP-conjugated Transferrin	85
2.5	3T3-L1 Adipocyte Cell Preparations	86
2.5.1	Ablation Studies	86
2.5.2	DAB Cytochemistry	86
2.5.3	Subcellular Fractionation of Adipocytes	87
2.5.4	Sucrose Density Gradient Centrifugation	88
2.5.5	Vesicle Immunoabsorption from 3T3-L1 Adipocytes	88
2.6	Preparation of Animal Tissues	90
2.6.1	Dissection and Subcellular Fractionation of Adipose Tissue	90
2.6.2	Hindlimb Skeletal Muscle Dissection and Subcellular Fractionation	91
2.6.3	Insulin-stimulation of Sprague-Dawley Rats	92
2.6.4	Preparation and Use of Anaesthetic	93
2.6.5	Preparation of Insulin	94
2.7	Protein Concentration Assays	94
2.7.1	Quantigold Protein Concentration Determination	94
2.7.2	Bradford's Method of Protein Concentration Determination	95

2.8	SDS-Polyacrylamide Gel Electrophoresis	95
2.8.1	Hoefer Large Gel Apparatus	95
2.8.2	NuPAGE™ Electrophoresis System	96
2.9	Western Blotting of Proteins	97
2.9.1	Transfer of Proteins Using a BIO-Rad Trans-Blot Tank	97
2.9.2	Transfer of Proteins Using a BIO-Rad Semi-Dry Transfer Block	97
2.9.3	Immunodetection of Proteins on Transfer Membranes	98
2.9.4	Immunodetection Using HRP-linked Goat Anti-rabbit IgG	98
2.9.5	Detection of Immunoblotted Proteins Using the Enhanced Chemiluminescence (ECL) Kit	99
2.9.6	Detection of Immunoblotted Proteins Using the Enhanced Chemiluminescence Plus (ECL+Plus) Kit	99
2.10	Recombinant Polymerase Chain Reaction	100
2.10.1	Synthesis of Oligonucleotides	100
2.10.1a	3' External Primers	100
2.10.1b	5' External Primers	100
2.10.2	Precipitation of Oligonucleotides	101
2.10.3	Quantitation of Oligonucleotides	101
2.10.4	Reaction Conditions for Primary Polymerase Chain Reactions Using <i>Vent</i> DNA Polymerase	102
2.10.5	Thermal Cycling	103

2.11	Cloning PCR Products Using the Invitrogen Eukaryotic TA Cloning® Kit	104
2.11.1	Addition of 3' A-overhangs on to <i>Vent</i> ® DNA Polymerase PCR Products	104
2.11.2	Ligation of PCR Products into Eukaryotic Bidirectional TA Cloning Vector pCR®3.1	105
2.11.3	Transformation of One Shot™ TOP 10F' Competent Cells	106
2.12.	General Techniques Used for the Manipulation of cDNA	107
2.12.1	Agarose Gel Electrophoresis of cDNA	107
2.12.2	Alcohol Precipitation of cDNA	108
2.12.3	Restriction Digestion of cDNA	109
2.12.4	Separation of PCR Fragments by Agarose Gel Electrophoresis	109
2.12.5	Elution of DNA Fragments from Agarose Gel Slices by Electrophoresis	110
2.12.6	Preparation of Dialysis Tubing for Electroelution	110
2.12.7	Purification of DNA Using Elutip-d Affinity Columns	111
2.12.8	Dephosphorylation of Double Stranded DNA using Calf Intestinal Phosphatase (CIP)	112
2.12.9	Ligation of Double-Stranded cDNA	112
2.12.10	Preparation of Competent <i>E. coli</i> (JM109) Cells	113
2.12.11	Transformation of Competent <i>E. coli</i> (JM109) Cells	113
2.12.12	Transformation of Ultracompetent <i>E.coli</i> (JM109) Cells	114
2.12.13	Preparation of Small Amounts of Plasmid DNA Using the QIAGEN QIAprep 8 Turbo Miniprep Kit	114
2.12.14	Preparation of Small Amounts of Plasmid cDNA	116

2.12.15	Large Scale Preparation of Plasmid DNA using QIAGEN QIAprep Plasmid Maxi Preparation Kits	117
2.12.16	Large Scale Preparation of Plasmid cDNA	119
2.12.17	Calculation to Determine the Plasmid cDNA Concentration and Purity	121

Chapter 3 Analysis of Amino-and Carboxy-terminal GLUT4 Targeting Motifs in 3T3-L1 Adipocytes Using an Endosomal Ablation Technique 122

3.1	Aims	123
3.2	Introduction	124
3.3	Materials and Methods	129
3.3.1	Human GLUT3 Epitope-tagged GLUT4 Transporters	129
3.3.2	Expression Levels of Recombinant GLUT4 Constructs in Adipocyte Cell Lines	129
3.3.3	Immuno-electron Microscopy	133
3.3.4	Antibodies	133
3.3.5	Computer Modelling of GLUT4 Trafficking	133
3.4	Results	135
3.4.1	Buoyant Density Analysis of TAG, LAG and FAG Mutants	135

3.4.3	Co-localisation of Recombinant GLUT4 Mutants with Wild-type GLUT4 in 3T3-L1 Adipocytes	138
3.4.4	Colocalisation of GLUT4 with γ -adaptin	140
3.5	Discussion	162
3.5.1	Interpretation of Recombinant GLUT4 Mutant Trafficking Between Multiple Intracellular Compartments	165
3.5.2	LAG and FAG Mutant Distribution	166
3.5.3	An Alternative Model of GLUT4 Trafficking	168
3.6	Summary	180

Chapter 4 Analysis of the Carboxy-terminal Phosphorylation Site in GLUT4 Trafficking 181

4.1	Aims	182
4.2	Introduction	183
4.3	Materials and Methods	186
4.3.1	Human GLUT3 Epitope-tagged GLUT4 Transporters	186
4.3.2	Expression Levels of Recombinant GLUT4 Constructs in Adipocyte Cell Lines	186
4.3.3	Immuno-electron Microscopy	187
4.3.4	Antibodies	187

4.4	Results	190
4.4.1	Buoyant Density Analysis of TAG, SAG and DAG Mutants	190
4.4.2	Compartment Ablation Analysis of TAG, SAG and DAG Mutants	191
4.4.3	Subcellular Distribution of TAG and SAG in Basal and Insulin-stimulated Adipocytes	193
4.4.4	Co-localisation of TAG and SAG with γ -adaptin	195
4.4.5	The Effects of Okadaic Acid on the Intracellular Distribution of Wild-type and Recombinant GLUT4, vp165 and GLUT1 in 3T3-L1 Adipocytes	196
4.5	Discussion	220
4.6	Summary	228
Chapter 5	Analysis of Two Endosomal Targeting Motifs in the GLUT4 Carboxy-terminus	229
5.1	Aims	230
5.2	Introduction	231
5.3	Materials and Methods	234
5.3.1	Human GLUT3 Epitope-tagged GLUT4 Transporters	234
5.3.2	Expression Levels of Recombinant GLUT4 Constructs in Adipocyte Cell Lines	237

5.3.3	Antibodies	237
5.4	Results	238
5.4.1	Characterisation of the Carboxy-terminus of GLUT4	238
5.4.2	Compartment Ablation Analysis of GLUT4	
	Carboxy-terminal Tail Mutants	240
5.5	Discussion	246
5.6	Summary	250
Chapter 6	Construction and Analysis of GLUT2/GLUT4 Chimeric Glucose Transporters	252
6.1	Aims	253
6.2	Introduction	254
6.3	Methodology Used to Generate GLUT2/ GLUT4 Chimeric Glucose Transporters	257
6.3.1	Plasmid Constructs	257
6.3.2	Recombinant PCR Reactions	257
6.3.2a	GLUT4NT/2	258
6.3.2b	GLUT2NT/4	259

6.3.3	Cloning Strategies	259
6.3.3a	pNot.Not and pOP13CAT.aP2 Approach	259
6.3.3b	Cloning PCR Products Using the Invitrogen Eukaryotic TA Cloning® Kit	261
6.3.4	Expression of GLUT2/ GLUT4 Chimeras in 3T3-L1 Adipocytes	261
6.3.5	Complementary GLUT2/ GLUT4 Chimeras	262
6.3.5a	GLUT2/4	262
6.3.5b	GLUT4/2C	262
6.3.5c	GLUT2N/4/2C	263
6.4	Results	284
6.4.1	Subcellular Fractionation of GLUT2/ GLUT4 Chimeras	284
6.4.2	Compartment Ablation Analysis of GLUT2/ GLUT4 Chimeras	285
6.5	Discussion	292
6.6	Summary	296

Chapter 7	Analysis of the Expression Levels of SNARE Proteins Associated with GLUT4 Trafficking in Animal Models of Diabetes Mellitus	297
7.1	Aims	298
7.2	Introduction	299
7.2.1	Possible Defects in GLUT4 Trafficking Responsible for Non-Insulin-Dependent Diabetes Mellitus	299
7.2.2	Thiazolidinediones in the Treatment of NIDDM	301
7.2.3	ARF Proteins	303
7.3	Materials and Methods	306
7.3.1	Animal Models	306
7.3.1a	Sprague-Dawley Normal Rats	306
7.3.1b	Zucker <i>fa/fa</i> Rats (ZDF)	306
7.3.1c	Streptozotocin-treated (STZ) Sprague-Dawley Rats	307
7.3.1d	<i>ob/ob</i> Mice	307
7.3.2	BRL 49653 (Avandia)	308
7.4	Results	309
7.4.1	Analysis of SNARE Proteins in Adipose Tissue from Sprague-Dawley Normal Control Rats	309
7.4.2	Analysis of SNARE Proteins in Hindlimb Skeletal Muscle Tissue from Sprague-Dawley Normal Control Rats	310
7.4.3	Analysis of SNARE Proteins in Hindlimb Skeletal Muscle Tissue from ZDF Rats Treated with BRL 49653	311

7.4.4	Expression Levels of SNARE Proteins in Hindlimb Skeletal Muscle Tissue from Streptozotocin-treated (STZ) Rats	313
7.4.4a	Comparison of SNARE Protein Expression Levels in STZ -v- Normal SD Rats	313
7.4.4b	Effect of Hyperglycaemia on SNARE Protein Expression in STZ Rats	314
7.4.5	Expression Levels of SNARE Proteins in Hindlimb Skeletal Muscle Tissue from <i>ob/ob</i> Mice	314
7.4.6	Characterisation of ARF-5 in Adipose and Muscle Tissues	315
7.5	Discussion	331
7.5.1	Expression of SNARE Proteins in Animal Models of Diabetes Mellitus	331
7.5.2	Role of ARF-5 in GLUT4 Trafficking	336
7.6	Summary	337
Chapter 8	Discussion	339
References		345

Figures

Chapter 1 Introduction

1.1	Model for the Orientation of Mammalian Glucose Transporters in the Membrane	12
1.2	Diagrammatic Representation of GLUT4 Translocation in Skeletal Muscle and Adipose Tissue	17
1.3	GLUT4 Translocation in Adipose Tissue	19
1.4	Salient Targeting Motifs on the GLUT4 Sequence	23
1.5	Modified Three-Pool Model of GLUT4 Trafficking	41
1.6	Chimeric and Mutant GLUT4 Species	43
1.7	Time Course of Ablation of the Transferrin Receptor and GLUT4	48
1.8	SNARE Hypothesis	56
1.9	Potential Sites of Insulin Resistance in Adipose Tissue	64

Chapter 3 Analysis of Amino- and Carboxy-terminal GLUT4 Targeting Motifs in 3T3-L1 Adipocytes Using an Endosomal Ablation Technique

3.1	Schematic Representation of Human GLUT3 Epitope-Tagged Mutant GLUT4 Transporters	132
3.2	Buoyant Density Analysis of TAG, LAG and FAG Mutants	143
3.3	Buoyant Density Profiles of TAG, LAG and FAG Mutants	145

3.4	Compartment Ablation Analysis of TAG, LAG and FAG Mutants	147
3.5	Comparative Compartment Ablation Analysis of TAG	151
3.6	Immunoadsorption of Vesicles containing Mutant GLUT4 Species	153
3.7	Co-localisation of vp165 and Mutant GLUT4 Species in 3T3-L1 Adipocytes	155
3.8	Isolation of vp165 Vesicles and Co-localisation with Mutant GLUT4 Species	157
3.9	Immuno-electron Microscopy of γ -adaptin and Recombinant GLUT4 in Isolated Vesicles	159
3.10	Modified Three-Pool Model of GLUT4 Trafficking	175
3.11	Alternative Model of GLUT4 Trafficking	177

Chapter 4 Analysis of the Carboxy-terminal Phosphorylation Site in GLUT4 Trafficking

4.1	Schematic Representation of Human GLUT3 Epitope- Tagged Mutant GLUT4 Transporters	189
4.2	Buoyant Density Analysis of TAG, SAG and DAG Mutants	200
4.3	Buoyant Density Profiles of TAG, SAG and DAG Mutants	202
4.4	Compartment Ablation Analysis of TAG, SAG and DAG Mutants	204
4.5	Comparative Ablation of TAG, SAG and DAG Mutants	208

4.6	Subcellular Distribution of Wild-Type and Recombinant GLUT4 in 3T3-L1 Adipocytes	210
4.7	Subcellular Distribution of vp165 in Transfected and Non-transfected 3T3-L1 Adipocytes	212
4.8	Immuno-electron Microscopy Analysis of γ -adaptin and Epitope-tagged GLUT4 in 3T3-L1 Adipocytes	214
4.9A-C	The Effects of Insulin and Okadaic Acid on the Cell Surface Distribution of GLUT4, GLUT1 and vp165 in 3T3-L1 Adipocytes	217-19

Chapter 5 Analysis of Two Endosomal Targeting Motifs in the GLUT4 Carboxy-terminus

5.1	Schematic Representation of Carboxy-terminal GLUT4 Mutants	236
5.2	Compartment Ablation Analysis of Carboxy-terminal GLUT4 Mutants	243

Chapter 6 Construction and Analysis of GLUT2/GLUT4 Chimeric Glucose Transporters

6.1	Diagram of a GLUT cDNA Cloned into the pSP64T Vector	265
6.2	Generation of GLUT2/ GLUT4 Chimeras Using Recombinant PCR Technology	267

6.3	Schematic Representation of Recombinant GLUT4N/2 and GLUT2N/4 Chimeras	269
6.4	1% Agarose Gel of Primary PCR Products Used in the Construction of Recombinant GLUT2/ GLUT4 Chimeras	271
6.5	Cloning of Recombinant Chimeras Using pNot.Not and pOP13CAT.aP2	273
6.6	Cloning of Primary PCR Products Using the Invitrogen Eukaryotic TA Cloning® Kit	275
6.7	Restriction Digestion Analysis of Chimera GLUT4N/2	277
6.8	Restriction Digestion Analysis of Chimera GLUT2N/4	279
6.9	Schematic Representation of Complementary GLUT2/ GLUT4 Chimeras	281
6.10A-C	Subcellular Fractionation of GLUT2/ GLUT4 Chimeras	287-9
6.11	Compartment Ablation Analysis of GLUT2/ GLUT4 Chimeras	291

Chapter 7 Analysis of the Expression Levels of SNARE Proteins Associated with GLUT4 Trafficking in Animal Models of Diabetes Mellitus

7.1	SNARE Protein Expression Levels in Sprague-Dawley Normal Adipose Tissue	318
7.2	SNARE Protein Expression Levels in ZDF <i>fa/fa</i> Rat Hindlimb Skeletal Muscle Tissue	320
7.3	Expression Levels of GLUT1 and γ -adaptin in ZDF <i>fa/fa</i> Rat Hindlimb Skeletal Muscle Tissue	322

7.4	Comparison of Expression Levels of SNARE Proteins Between Sprague-Dawley Normal Rats and Streptozotocin-treated Diabetic Rats	326
7.5	Effect of Hyperglycaemia on SNARE Protein Expression in Streptozotocin-treated Diabetic Rats	328
7.6	SNARE Protein Expression Levels in <i>ob/ob</i> Mouse Hindlimb Skeletal Muscle Tissue	330

Tables

Chapter 1 Introduction

1.1	Major Sites of Expression of the Different Glucose Transporter Isoforms in Human and Rodent Tissues	13
1.2	Comparison of the Amino Acid Sequences of Recycling Membrane Proteins which Contain an Aromatic Amino Acid-Based Internalisation Motif	29
1.3	Comparison of the Amino Acid Sequences of Recycling Membrane Proteins which Contain an Di-leucine Motif	34

Chapter 3 Analysis of Amino- and Carboxy-terminal GLUT4 Targeting Motifs in 3T3-L1 Adipocytes Using an Endosomal Ablation Technique

3.1	Effect of Compartment Ablation on Intracellular GLUT4 Levels	149
3.2	Co-localisation of γ -adaptin and GLUT4 Mutants by Immuno-electron Microscopy	161
3.3	Computer Modelling of GLUT4 and LAG Subcellular Distributions	179

Chapter 4 Analysis of the Carboxy-terminal Phosphorylation Site in GLUT4 Trafficking

4.1	Effect of Compartment Ablation on Intracellular GLUT4 Levels	206
4.2	Percentage of Total Intracellular Vesicles Labelled for Either γ -adaptin or Recombinant GLUT4	215

Chapter 5 Analysis of Two Endosomal Targeting Motifs in the GLUT4 Carboxy-terminus

5.1	Endosomal Ablation Analysis of Carboxy-terminal GLUT4 Mutants	245
5.2	Comparison of the GLUT4 Carboxy-terminal and vp165 Amino-terminal Sequences	251

Chapter 6 Construction and Analysis of GLUT2/GLUT4 Chimeric Glucose Transporters

6.1	Sequences of Oligonucleotide Primers Used to Generate GLUT2/GLUT4 Chimeras	283
-----	---	-----

**Chapter 7 Analysis of the Expression Levels of SNARE
Proteins Associated with GLUT4 Trafficking
in Animal Models of Diabetes Mellitus**

7.1	Effects of BRL 49653 on ZDF <i>fa/fa</i> Rat <i>in vivo</i>	324
-----	---	-----

Abbreviations

Ac	Acetate
Amp	Ampicillin
ARF	ADP Ribosylation Factor
ARL	ARF-like
α SNAP	Alpha soluble NSF attachment protein
ATP	Adenosine 5'-triphosphate
bp	Base pairs
BSA	Bovine Serum Albumin
cDNA	Complementary deoxyribonucleic acid
CHO	Chinese Hamster Ovary
CIP	Calf intestinal phosphatase
CNS	Central Nervous System
cpm	Counts per minute
CTP	Cytidine 5'-triphosphate
DAB	Diaminobenzidine
DeGlc	2-Deoxy-D-glucose
DFP	Diisopropyl fluorophosphate
DMEM	Dulbecco's modified Eagle's medium
DMSO	Dimethylsulphoxide
DNA	Deoxyribonucleic acid
dNTPs	Deoxyribonucleic nucleoside 5'-triphosphates
dsDNA	Double stranded deoxyribonucleic acid
DTT	Dithiothreitol
ECL	Enhanced chemiluminescence
EDTA	Diaminoethanetetra-acetic acid, disodium salt
EM	Electron Microscopy

E64	Trans-epoxysuccinyl-L-leucylamido(4-guanido)-butane
FCS	Foetal calf serum
GDM	Gestational Diabetes Mellitus
GLUT	Glucose transporter
GTP	Guanosine 5'-triphosphate
HDM	High density microsome
HEPES	<i>N</i> -2-hydroxyethylpiperazine- <i>N</i> '-2-ethane sulphonic acid
hr	Hours
HRP	Horseradish peroxidase
IBMX	Isobutylmethylxanthine
IDDM	Insulin-Dependent Diabetes Mellitus
IgG	Immunoglobulin gamma
IGT	Impaired Glucose Tolerance
IR	Infra-red
IRS-1	Insulin receptor substrate-1
IRS-2	Insulin receptor substrate-2
KRH	Krebs ringer HEPES
KRP	Krebs ringer phosphate
LB	Luria-Bertani
LDM	Low density microsome
min	Minutes
NCS	New born calf serum
NIDDM	Non-Insulin-Dependent Diabetes Mellitus
NSF	<i>N</i> -ethylmaleimide sensitive factor
OD	Optical density
PAGE	Polyacrylamide gel electrophoresis
PBS	Phosphate buffered saline

PCR	Polymerase chain reaction
PEG	Polyethylene glycol
Pep A	Pepstatin A
PI-3' kinase	Phosphatidyl inositol-3 kinase
PM	Plasma membrane
PPAR	Peroxisome proliferator activated receptor
RNA	Ribonucleic acid
RNase A	Ribonuclease
rpm	Revolutions per minute
SD	Sprague-Dawley
SDS	Sodium dodecyl sulphate
SDS-PAGE	Sodium dodecyl sulphate polyacrylamide gel electrophoresis
sec	Seconds
SNAP25	Synaptosome-associated 25kDa protein
SNARE	SNAP receptor
ssDNA	Single stranded deoxyribonucleic acid
SSV	Small Synaptic Vesicle
STZ	Streptozotocin
TAE	Tris-acetate EDTA
TBE	Tris-borate EDTA
TCA	Trichloroacetic acid
TCR	T cell receptor
TE	Tris-EDTA
TEMED	<i>N, N, N', N'</i> -tetramethylenediamine
Tf-HRP	HRP-conjugated transferrin
Tf	Transferrin
TfR	Transferrin receptor

Tris	Tris(hydroxymethyl)aminoethane
TZD	Thiazolidinedione
VAMP	Vesicle-associated membrane protein
v/v	volume/ volume ratio
w/v	weight/ volume ratio

Chapter 1

Introduction

1.1 Introduction

Glucose is one of the most important molecules known to be involved in the cellular metabolism and homeostasis of a vast array of organisms encompassing all forms of life from microbes to mammals. In mammalian cells the metabolism of glucose provides ATP as an energy source under both aerobic and anaerobic conditions, and is especially crucial in tissues such as the brain, which rely almost solely on glucose as an energy source. As a result of the importance of glucose metabolism, it is not surprising that virtually all cells have naturally evolved a variety of mechanisms that allow selective catalysis of the movement of glucose across their plasma membranes [reviewed in Carruthers (1991)].

The transport of glucose across plasma membranes can occur by three discrete methods [reviewed in Carruthers (1990)]. The first of these functions through a simple, bi-directional diffusion system, which, because of the polar nature of the glucose molecule, is predicted to be too slow to satisfy the energy requirements of cells. The second method of transport is mediated by rapid, bi-directional, protein-mediated facilitated diffusion, which is not coupled to an energy requiring component such as ATP hydrolysis or an H^+ gradient. This form of transport is driven only by a concentration gradient, and although bi-directional, transport always occurs down the sugar's concentration gradient i.e. from high to low concentration. The third transport system operates through rapid, active, protein-mediated uptake and is found in cells that require to take up glucose against its concentration gradient, for example the transepithelial cells of the kidney and the small intestine. In these locations transport is mediated by a Na^+ /glucose

cotransporter that utilises a Na^+ gradient to couple the transport of glucose against its concentration gradient.

The transport of glucose in mammalian cells is achieved predominantly by the process of facilitated diffusion and this phenomenon is mediated by a family of proteins known as the facilitative glucose transporters, or GLUTs [Baldwin *et al.* (1982)].

The functional purification of the first member of this family was achieved independently in the early 1980s by two groups. Leinhard and colleagues used the specific binding of the transport inhibitor cytochalasin B as a basis for the purification procedure [Baldwin *et al.* (1979), Baldwin *et al.* (1981)], whilst the second group based their purification on the ability of reconstituted fractionated membrane proteins to transport glucose [Kasahara & Hinkle (1977)]. The result of these studies was the identification of a heterologously glycosylated integral membrane protein in human erythrocyte membranes which migrates on SDS-PAGE gels as a broad band with an approximate molecular mass of 55 kDa, which was reduced to a mass of 46 kDa after treatment with Endoglycosidase H. This protein was designated glucose transporter 1 (GLUT1) [Fukumoto *et al.* (1989)] and the subsequent members of the glucose transporter family have been named GLUTs 2-6, in chronological order of the isolation of their cDNAs.

1.2 Tissue-specific Distribution of the Facilitative Glucose Transporter Family

1.2.1 Overview

The discovery of a family of glucose transporters which were responsible for the transport of glucose in mammals was not surprising given the unique requirements of mammalian tissues for glucose. This is reinforced by previous findings which demonstrated that different tissues display unique kinetics for D-glucose uptake. This family comprises six members to date (GLUTs 1-6, of which GLUT6 is a pseudo-gene sequence) which are structurally very similar but are distinct from the mammalian active sodium-linked transporters of the intestinal and absorptive epithelia (the SGLT family) [Hediger *et al.* (1987), Bell *et al.* (1990)].

1.2.2 GLUT1

As the only member of the family to be purified to date in a functional form [Kasahara & Hinkle (1977)] this isoform has been the most extensively studied. GLUT1 was purified from erythrocytes which provide a rich source of this transporter, with it comprising about 3-5% of the membrane protein. Purification of the protein led to the generation of antibody probes, which in concert with partial sequence information from the protein, resulted in the isolation of a cDNA clone for the transporter in 1985 [Meuckler *et al.* (1985)]. Subsequently the gene encoding GLUT1 was also isolated [Fukumoto *et al.* (1988)].

Further studies utilising both cDNA and antibody probes have examined the expression levels of this transporter in the various tissue types. GLUT1 was found to be most abundantly expressed in erythrocytes [Allard & Leinhard (1985)] and is also enriched in the cells of the blood-tissue barriers such as the blood-brain/nerve barrier, the retina, the placenta etc. [Froehner *et al.* (1988)]. This isoform is also expressed in tissues which exhibit insulin-stimulated glucose transport, such as muscle and adipose tissue, but is only expressed at very low levels in the liver, the other major tissue involved in whole body glucose homeostasis [Flier *et al.* (1987)]. It has also been demonstrated that cultured cell lines possess elevated levels of GLUT1 protein and RNA levels [reviewed in Gould & Holman (1993)].

GLUT1 is located primarily on the plasma membrane and since it is expressed at some level in nearly all tissues it is regarded as the "house-keeping" glucose transporter, responsible for glucose uptake in the basal state [Flier *et al.* (1987)]. The K_m for zero-*trans* entry of D-glucose into cells at 37°C by GLUT1 is 7mM [Lowe & Walmsley (1986)]. This allows GLUT1 to efficiently transport glucose within its physiological concentration range.

The cloning and sequencing of GLUT1 cDNA clones from a range of species resulted in the rapid identification of homologous transporters from other mammalian tissues through the low stringency screening of appropriate cDNA libraries. All of the isoforms currently identified are between 40 and 80% identical in amino acid sequence, and hydropathy plots of their sequences are essentially superimposable. They must therefore all be very similar in secondary and tertiary structure to GLUT1.

1.2.3 GLUT2

The observation that GLUT1 was expressed at low levels in liver tissue, coupled to the fact that the kinetics of glucose transport in hepatocytes were radically different from those in erythrocytes [Elliot & Craik (1982)], led researchers to propose the existence of a related transporter in this tissue. The above low stringency screening approach led directly to the isolation of GLUT2 clones from human [Fukumoto *et al.* (1988)], rat [Thorens *et al.* (1988)], and mouse [Suzue *et al.* (1989)] cDNA libraries. Human GLUT2 has 55% sequence identity with GLUT1, with both proteins having essentially superimposable hydropathy plots. The major areas of diversity between GLUT1 and GLUT2 occur in the large extracellular loop and at the extreme C-terminus (Figure 1.1).

The tissue distribution of GLUT2 was determined by immuno-cytochemical screening, which displayed high GLUT2 protein levels in the β -cells of the Islets of Langerhans in the pancreas [Thorens *et al.* (1988), Orci *et al.* (1989)], in the transepithelial cells of the intestine and the kidney [Thorens *et al.* (1990)], as well as the hepatocytes of the liver itself. GLUT2 protein has also been discovered expressed at very low levels in many regions [Brant *et al.* (1993)].

Experimental analysis of this transporter revealed that it is a high-capacity, high K_m transporter, properties essential to allow the liver to function as one of the key elements in glucose homeostasis. In this tissue, GLUT2 is required for the influx of postprandial glucose, and under fasting conditions, for the release of glucose produced from glycogenolysis and gluconeogenesis into the bloodstream. The high concentration of GLUT2 in the plasma membrane of hepatocytes, in concert with the transporter's high K_m values for D-glucose

entry and exit [reviewed in Elliot & Craik (1982)], allows for the rapid, non-saturable translocation of D-glucose in either direction in times of stress.

1.2.4 GLUT3

The next isoform to be identified, GLUT3, was found to be the primary isoform present in brain and neural tissue. GLUT3 clones were isolated and cloned from human foetal skeletal muscle [Kayano *et al.* (1988)] and mouse [Nagamatsu *et al.* (1992)] cDNA libraries. These share 83% identity and the human isoform of GLUT3 has 64% identity with human GLUT1. GLUT3 is expressed at high levels in human foetal tissue, but Northern blot analysis of adult skeletal muscle revealed no trace of this isoform. In contrast, high expression of GLUT3 mRNA has been observed in a range of other tissues such as the placenta, liver, heart and kidney. However, these results are in discordance with the lower levels of GLUT3 protein expression displayed by such tissues, indicating that post-transcriptional regulation of this species of transporter may occur in non-neural tissues [Gould & Holman (1993)].

Thus it appears that high GLUT3 protein expression levels are confined generally to tissues which exhibit a high glucose demand, such as the brain and CNS, and therefore this isoform may be specialised to act in tandem with GLUT1 to meet the high energy demands of these tissues. This isoform displays the lowest K_m for hexoses of the facilitative glucose transporters characterised to date [Colville *et al.* (1993)], a kinetic ability that allows the brain to maintain function under conditions of either high glucose demand or hypoglycaemia by ensuring the efficient uptake of glucose even at low extracellular concentrations of blood glucose.

1.2.5 GLUT4

In 1989 five separate groups reported success in cloning and sequencing a fourth glucose transporter isoform. It was cloned from human [Fukumoto *et al.* (1989), James *et al.* (1989a)], rat [Birnbaum (1989), Charron *et al.* (1989)] and mouse [Kaestner *et al.* (1989)] cDNA libraries. This isoform occurs predominantly in muscle and adipose tissue and subsequent studies identified this isoform as being responsible for insulin-stimulated glucose transport. The properties of GLUT4 are examined in greater detail in section 1.4 of this thesis.

1.2.6 GLUT5

A further putative glucose transporter isoform was isolated from human small intestine by library screening with the GLUT1 cDNA probe [Kayano *et al.* (1988)]. Studies utilising specific anti-peptide antibodies demonstrated that this protein appears to be localised exclusively to the apical brush border on the luminal side of absorptive epithelial cells [Davidson *et al.* (1992)]. It has been shown that GLUT5 has a high-affinity for fructose and a low-affinity for glucose. Therefore, it has been rationalised that the primary role of GLUT5 involves the absorption of dietary fructose from the lumen [Burant *et al.* (1992)]. This transporter is expressed in a range of tissues, including muscle, brain and adipose tissue, where it may function in the provision of fructose. However, it remains to be discovered if other fructose transporters also exist [Shepherd *et al.* (1992)].

1.2.7 GLUT6

The homology screening approach led to the identification of a further transporter-like transcript which sequence analysis showed to have a high degree of homology (79.6%) with GLUT3 [Kayano *et al.* (1990)]. However, the GLUT6 cDNA sequence was also found to contain multiple stop codons and frame shifts, making it unlikely to encode a functional glucose transporter. It has been proposed that the glucose transporter-like region of GLUT6 may have arisen from the insertion of a reverse-transcribed copy of GLUT3 into the non-coding region of a ubiquitously expressed gene [Kayano *et al.* (1990)].

For a summary of the tissue distribution of the facilitative glucose transporters see Table 1.1.

1.3 Structure and Membrane Topology of the Mammalian Facilitative Glucose Transporter Family

After the success in purification and cloning of the GLUT family much effort was focused on analysis of the predicted amino acid sequences and modelling of the membrane topology of these transporters. This work demonstrated that the mammalian glucose transporters were highly homologous with one another. They possess a high level of sequence identity with transporters found in other species such as *Escherichia coli*, cyanobacteria, yeast, algae and protozoa [reviewed in Gould & Holman (1993)]. This high degree of sequence similarity is probably related to a common mechanism of transport catalysis, the transport of a common substrate, and also is indicative of evolution from a single ancestral gene.

Sequence alignment analysis of the GLUTs has revealed common features which include 12 predicted amphipathic helices arrayed so that both the N- and C- termini are at the cytoplasmic surface (Figure 1.1). There are large loops between helices 1 and 2 and between helices 6 and 7. The large intracellular loop between helices 6 and 7 divides the structure into two halves, commonly known as the N-terminal domain and the C-terminal domain. The loops between the remainder of the helices at the cytoplasmic surface are very short and the length of these loops (approximately 8 residues) is a conserved feature of the entire family. These short loops limit possible tertiary structures and suggest very close packing of the helices at the inner surface of the membrane in each half of the protein. The length and sequence identity of the loops at the extracellular surface of these proteins are varied but are generally longer than those at the cytoplasmic surface. Potentially this may result in a less helical packing at the external surface. The two-dimensional topography with the N- and C- termini on the cytoplasmic surface (Figure 1.1) was confirmed using anti-peptide antibodies which react only when the inner surface of the transporter is exposed, as in inverted vesicles containing human erythrocyte GLUT1 [Davies *et al.* (1987)]. Infra-red spectroscopy studies have suggested a high helical content for the GLUT1 protein [Chin *et al.* (1986), Alvarez *et al.* (1987)]. The above work supports the overall nature of the 12 membrane-spanning model and has been confirmed by further experimental analysis [reviewed in Gould & Holman (1993)].

Figure 1.1

Model for the Orientation of Mammalian Glucose Transporters in the Membrane

This model is based mainly on studies performed with human GLUT1, and so this model corresponds to that isoform. However, it is predicted from hydropathy analysis of the primary sequence of other mammalian transporters [Meuckler *et al.* (1985)] and numerous other studies that they will adopt an identical conformation. The 12 transmembrane helices are shown as boxes, numbered 1-12. The site marked 'CHO' between transmembrane helices 1 and 2 represents the potential site of *N*-linked glycosylation in the large exofacial loop. The amino- and carboxy-termini (NH₂ and COOH, respectively) are cytoplasmically disposed. Invariant residues are shown by single letter abbreviations. This diagram was taken from Bell *et al.* (1993).

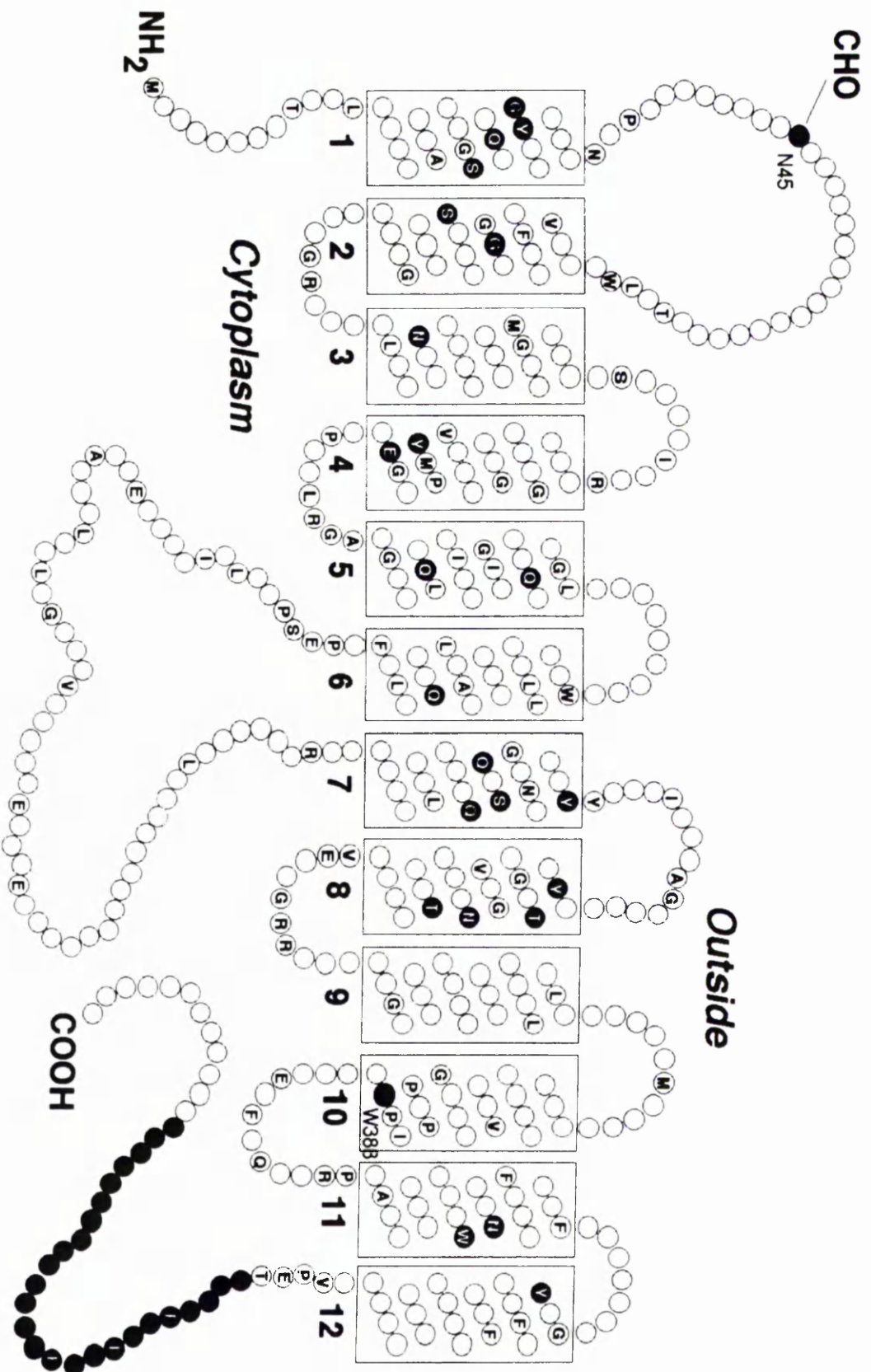


Table 1.1

**Major Sites of Expression of the Different Glucose
Transporter Isoforms in Human and Rodent Tissues**

Isoform	Tissue
GLUT1	Placenta, brain, blood-tissue barrier, adipose and muscle tissue (low levels), tissue culture cells, transformed cells
GLUT2	Liver, pancreatic β -cell, kidney proximal tubules, small intestine (basolateral membranes)
GLUT3	Brain and nerve cells in rodents; brain, nerve, placenta (low levels), kidney, liver, heart in humans
GLUT4	Muscle, heart, adipose tissue, brain (low levels)
GLUT5	Small intestine (apical membranes), brain, muscle (low levels), adipose tissue in humans; small intestine (apical membranes), kidney in rodents

1.4 GLUT4 - The Insulin-Responsive Glucose Transporter Isoform

In the context of insulin-stimulated glucose transport, and whole-body glucose homeostasis, the most important member of the GLUT family is the insulin-responsive glucose transporter (GLUT 4). This isoform is expressed only in tissues which exhibit acute, insulin-stimulated glucose transport, i.e. skeletal muscle and adipose tissue, and is physiologically the most dominant transporter in these tissues [James *et al.* (1989a)]. GLUT 4 is further characterised by its unique intracellular location in the absence of insulin [Slot *et al.* (1991b), Slot *et al.* (1997)]. It is this propensity to remain localised in the cytoplasmic tubulo-vesicular system that allows tissues possessing GLUT 4 to rapidly augment their glucose transport rate in response to insulin and other extrinsic factors, such as exercise, by as much as 10-20 fold. This occurs as a result of the rapid movement of GLUT4 from such intracellular membranes to the cell surface. The first evidence for this process of GLUT4 translocation was provided by Cushman and Wardzala in 1980 who analysed cytochalasin B binding to adipocyte subcellular fractions and independently by Suzuki and Kono [Cushman & Wardzala (1980), Suzuki & Kono (1980)]. Figure 1.2 is a diagrammatic representation of the process of GLUT4 translocation.

In the basal state GLUT4 is found almost exclusively within the cell in tubulo-vesicular elements that are clustered either in the *trans*- Golgi reticulum (TGN) or in the cytoplasm, often very close to the cell surface [Slot *et al.* (1991a), Slot *et al.* (1991b), Slot *et al.* (1997)]. Cell surface levels of GLUT4 are increased by as much as 30-fold in response to insulin (Figure 1.3). The studies of Tanner & Leinhard (1989), Slot *et al.* (1991a), and

Robinson *et al.* (1992) demonstrated co-localisation of GLUT4 with endocytic markers and with clathrin-coated lattices and pits in the plasma membrane, indicating that GLUT4 undergoes a process of constitutive recycling in the presence and absence of insulin.

1.5 Regulation of GLUT4 Translocation

The phenomenon of GLUT4 translocation has been discussed by a number of researchers who have suggested that the sequestration of GLUT4 could be caused either by the very rapid removal of this protein from the plasma membrane or by a very slow rate of exocytosis in the basal state [Slot *et al.* (1991a), Robinson *et al.* (1992), Piper *et al.* (1992)]. If this process is controlled at the level of endocytosis, then unique processing may occur at the plasma membrane, whereas if exocytosis is the control point, the targeting recognition events may occur intracellularly. In this context, it is probable that the GLUT4 protein sequence may contain information that allows unique cellular processing by vesicle trafficking and sequestration machinery.

Figure 1.2

Diagrammatic Representation of GLUT4 Translocation in Skeletal Muscle and Adipose Tissue

This figure illustrates the translocation of the insulin-stimulated glucose transporter isoform, GLUT4. Insulin binding to its cell surface receptor triggers the movement of a pool of intracellular vesicles to the cell surface. These vesicles contain abundant GLUT4 molecules such that the cell surface levels of GLUT4 increase by up to 20-fold in adipocytes and 7-fold in muscle.

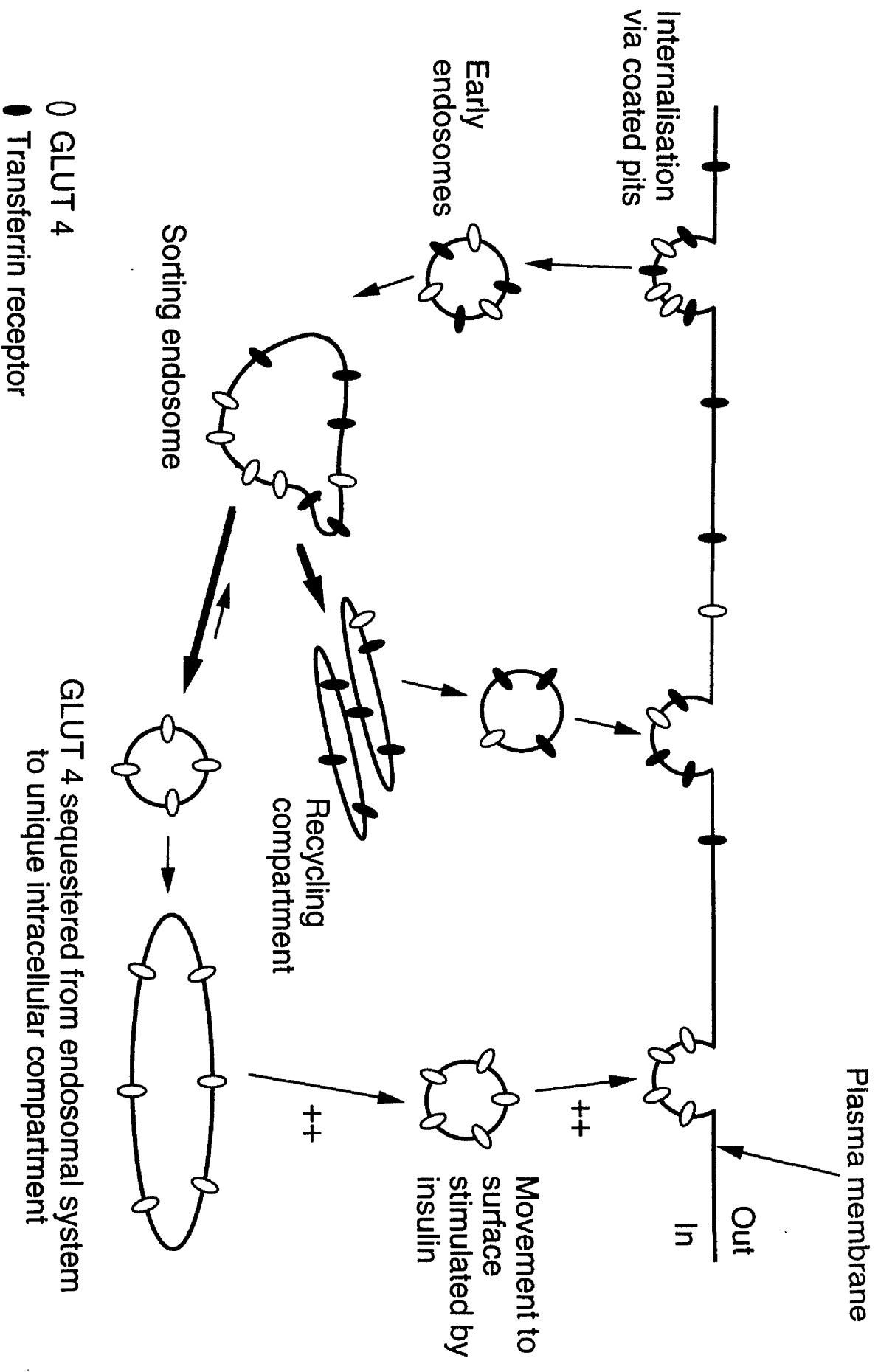
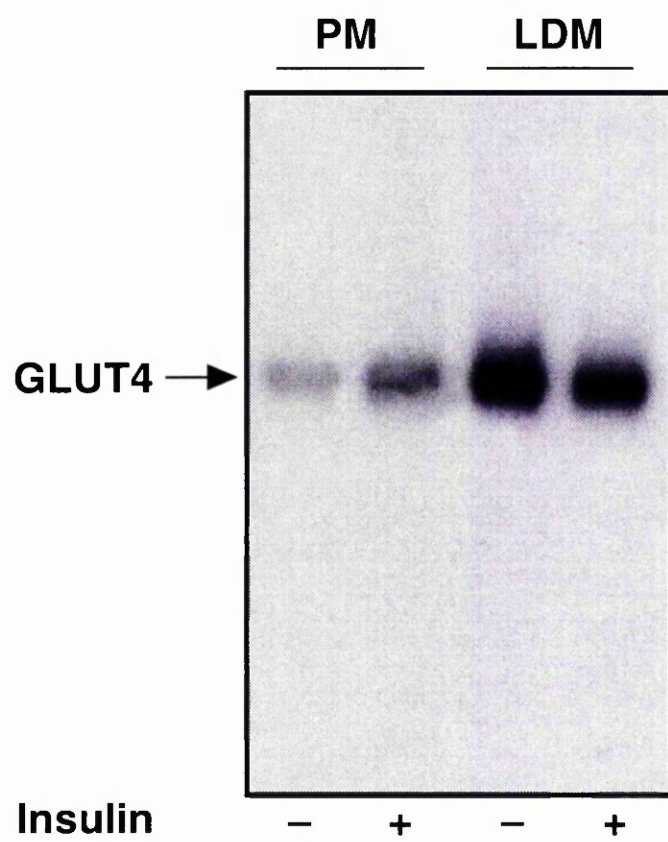


Figure 1.3

GLUT4 Translocation in Adipose Tissue

This representative immunoblot illustrates the changes in subcellular distribution of GLUT4 associated with the process of translocation. Insulin treatment results in increased levels of GLUT4 within the plasma membrane fraction, concomitant with a decrease in the level of GLUT4 in the intracellular low density microsomal fraction (LDM). Each lane contains 20 μ g of protein.



1.6 Regions Dictating GLUT4 Intracellular Sequestration

It has been well documented that GLUT4 is sequestered intracellularly in a range of cell types; such as 3T3-L1 adipocytes, rat adipocytes, HepG2 cells and oocytes, suggesting that the primary sequence of the protein contains targeting information which dictates this unique phenomenon [Haney *et al.* (1991), Slot *et al.* (1991b), Thomas *et al.* (1993)]. Such studies are reinforced by the observation that, when expressed in adipocytes, GLUT1 and GLUT2 are sequestered at the plasma membrane, providing further evidence that the intracellular sequestration of GLUT4 is unique amongst the GLUT family [Gould *et al.* (1989), Brant *et al.* (1994)].

In recent years a concerted attempt has been made by many researchers to define the relevant targeting domains that direct the intracellular sequestration of GLUT4. They have made use of the fact that the structural similarity of the different GLUT isoforms makes it possible to construct chimeric proteins which can be used to identify targeting domains while maintaining the overall structure of the protein. These studies have involved the exchange of reciprocal domains between GLUT4 and GLUT1 or GLUT2, and analysis of the subsequent subcellular distributions of these chimeras in a variety of cellular systems. The manipulations utilised here include swapping entire regions of GLUT4 and GLUT1/2; such as the C-terminal 30 amino acids or the entire amino-terminal cytoplasmic region, and also the introduction of specific amino acid mutations. These sorts of approaches have been successful in facilitating the identification of important domains, located in both the amino and carboxy termini (Figure 1.4), and also in transmembrane regions 7 and 8 [Asano *et al.* (1992)], that

are involved in the intracellular localisation of GLUT4. These regions will be discussed in detail below.

Epitope-tagged Recombinant GLUT-4

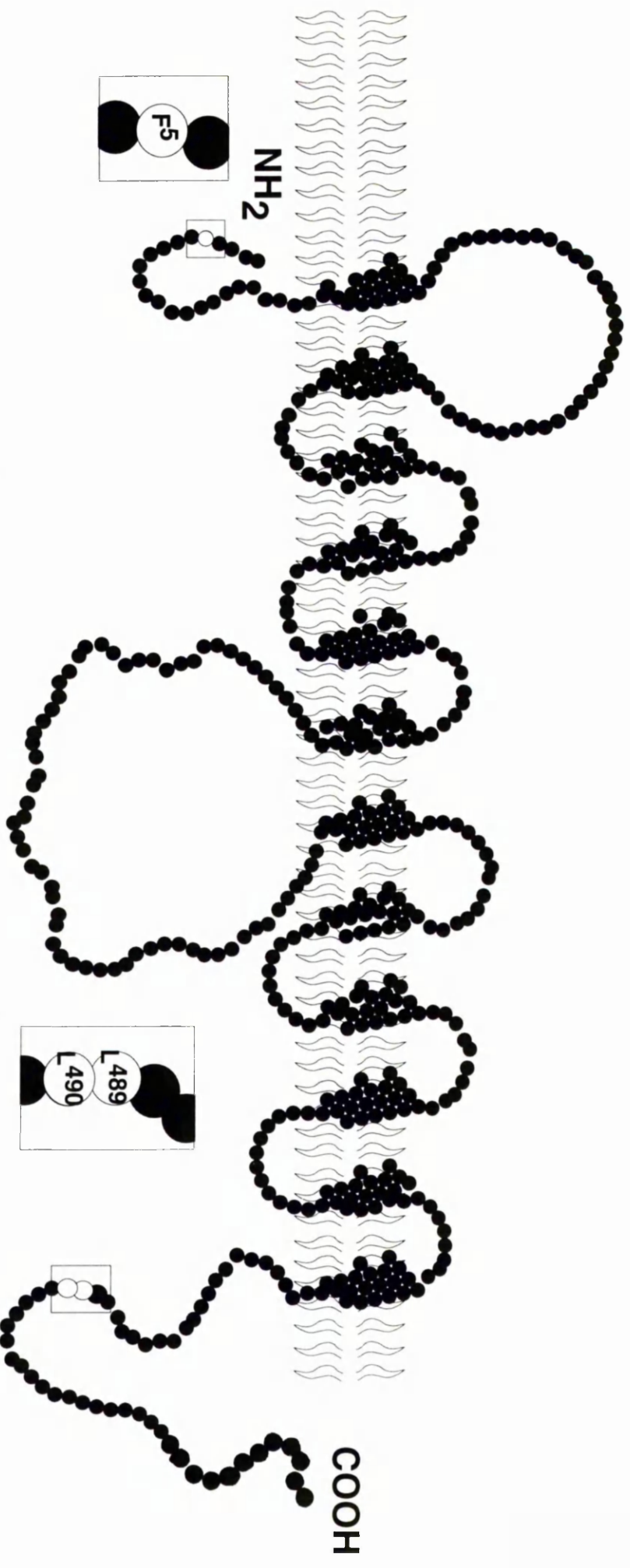


Diagram summarizing the location of amino acid mutations in recombinant GLUT-4 transporter protein. Amino acid residues are represented by the single letter code. The C-terminal region (shaded) represents a 12 amino acid epitope-tag encoded by the human GLUT-3 cDNA of the chimera constructs

1.6.1 The Amino Terminus as a Targeting Domain

The initial work carried out using chimeric GLUT4/GLUT1 transporters produced compelling evidence to suggest an important role for the extreme amino-terminal domain in the targeting of GLUT4. Piper *et al.* (1992) demonstrated that substitution of the amino-terminal region of GLUT4 with that of GLUT1 abolished the intracellular sequestration of GLUT4, and perhaps more importantly, that the reciprocal domain swap; introduction of the amino-terminus of GLUT4 into GLUT1, resulted in the intracellular sequestration of this chimera. These observations led to the conclusion that the amino-terminus of GLUT4 is both necessary and sufficient for the intracellular sequestration of this isoform [Piper *et al.* (1992)].

Further dissection of the GLUT4 amino-terminus has revealed that it shares homology with endocytic signals in cell surface receptors such as the low density lipoprotein receptor (LDLR) and the transferrin receptor (TfR) [Davis *et al.* (1986), Collawn *et al.* (1990)] (Table 1.2). Deletion analysis indicates that the targeting information is located within the first 8 amino acids and alanine scanning mutagenesis has elucidated P², S³, F⁵, and I⁸ as important amino acids within this domain. F⁵ has been shown to be a critical component of an amino-terminal targeting motif encoded by residues 2-8 (PSGFQQI) as mutation of this residue to alanine resulted in a large accumulation of GLUT4 at the plasma membrane [Piper *et al.* (1993b)]. The mutagenesis carried out on the other amino acids of this motif has shown that these residues, in particular P², S³, and I⁸, contribute to GLUT4 targeting but to a much lesser extent than the phenylalanine at position 5.

The essential features of the amino-terminal internalisation motifs in other proteins are the presence of an aromatic amino acid, usually tyrosine, at position 1 and a bulky hydrophobic amino acid at position 4 (YXXØ, where Y is an aromatic amino acid, X is any amino acid and Ø is an amino acid with a bulky hydrophobic group) [Trowbridge *et al.* (1993), Sandoval & Bakke (1994)]. Thus, the sequence FQQI within the GLUT4 amino-terminal tail broadly fits the consensus for an internalisation sequence [Trowbridge *et al.* (1993)]. These tyrosine-based motifs are known to be responsible for the efficient endocytosis of cell surface receptors and have been proposed to promote the association of these proteins with clathrin coated pits via interaction with plasma membrane adaptors [Mellman *et al.* (1998)]. This correlates with the findings of Piper *et al.* (1993b) who demonstrated that the colocalisation of GLUT4 with cell surface clathrin lattices was abolished when either the first thirteen amino acids of the amino-terminus were deleted or when the phenylalanine at position 5 was mutated to alanine.

In an attempt to ascertain whether the targeting information within the GLUT 4 amino-terminal targeting domain could function independently of the glucose transporter structure Piper *et al.* (1993b) inserted this domain into the cytoplasmic tail of the H1 subunit of the asialoglycoprotein receptor. Comparison of the subcellular distribution of the native receptor (which contains an efficient tyrosine-containing motif; YQDL) with the H1-GLUT4 mutant revealed important differences between the two motifs which will be discussed below. The resulting chimera was predominantly localised to an intracellular location similar to GLUT4 and was sequestered from the cell surface to a greater extent than the wild-type H1 protein. These results led to the conclusion that the amino-terminus of GLUT4 is capable of functioning as an autonomous motif mediating intracellular

sequestration at least in part by facilitating the interaction of the transporter with endocytic machinery at the cell surface.

Further analysis of the observations of Piper *et al.* (1993b) indicate that the GLUT4 amino-terminal motif identified does not behave in an identical fashion to the homologous motifs in recycling receptors. Indeed, it appears that the GLUT4 amino-terminus contains additional sorting information that is not present in tyrosine-containing internalisation motifs. As previously stated, the chimeric asialoglycoprotein receptor containing the GLUT4 amino-terminus was much more effectively excluded from the cell surface than the native receptor. In addition, the intracellular distribution of the heterologous protein containing the GLUT4 amino-terminus closely resembled that of GLUT4 in that it was very focused around the nucleus, while this was not the case for wild-type H1 [Piper *et al.* (1993b)]. The marked intracellular distribution of both chimeric glucose transporters and heterologous proteins containing the GLUT4 amino-terminus clearly indicates that this targeting is not due solely to the presence of a weak internalisation signal. Such a weak internalisation signal would be expected in GLUT4 because phenylalanine constitutes an inferior internalisation signal compared with the tyrosine present in a number of cytosolic receptor tails. Further evidence is provided by the observation that mutation of F⁵ to Y⁵ in the chimeric asialoglycoprotein receptor did not alter its GLUT4-like characteristics, suggesting that any additional targeting information present in the GLUT4 amino-terminus is not encoded merely by the presence of phenylalanine at position 5 instead of tyrosine [Garripa *et al.* (1994)].

James and colleagues have drawn the conclusion that the GLUT4 amino-terminus contains a weak internalisation signal, dictated by the phenylalanine at position 5. However, the observed difference in the localisation of the chimeric GLUT4-asialoglycoprotein receptor compared to the native receptor suggests the presence of additional targeting information; i.e. a discrete targeting signal within the sequence of GLUT4 which may be involved in directing the protein to a distinct compartment.

This hypothesis is supported by data published by Garripa *et al.* (1994). In an attempt to directly measure the effect of the GLUT4 amino-terminus on internalisation and subsequent recycling back to the plasma membrane, they constructed chimeric transporters in which the amino-terminal 19 amino acids of GLUT4 were substituted for the amino-terminal cytoplasmic domain of the human transferrin receptor. The endocytic behaviour of these chimeras was characterised by stable transfection into Chinese Hamster Ovary (CHO) cells. The GLUT4-transferrin receptor chimera was recycled back to the cell surface with a rate similar to the transferrin receptor, indicating that the GLUT4 amino-terminal sequence was not promoting intracellular retention of the chimera. The observed internalisation rate for the chimera was half the rate of the native transferrin receptor. Substitution of F⁵ by A⁵ slowed internalisation to a level characteristic of bulk membrane internalisation, whereas substitution of a tyrosine increased the rate of internalisation to the level of the transferrin receptor. However, it was noticeable that neither of these mutations significantly altered the rate of recycling of this chimera back to the plasma membrane. These results were interpreted as demonstrating that the major function of the GLUT4 amino-terminal domain is to promote the effective internalisation of the protein from the cell surface,

via a functional phenylalanine-based internalisation motif, rather than the retention of the transporter within intracellular structures.

Table 1.2

**Comparison of the Amino Acid Sequences of Recycling
Membrane Proteins which Contain an Aromatic Amino
Acid-Based Internalisation Motif**

Shown are the amino acid sequences which constitute aromatic amino acid-based internalisation motifs in other recycling membrane proteins. These proteins are lgp120: lysosomal protein; LAP: lysosomal acid phosphatase; M6PR: mannose 6-phosphate receptor; LDLR: low density lipoprotein receptor; TfR: transferrin receptor; ASGPR: asialoglycoprotein receptor; and GLUT4. Note that the key aromatic residue is in bold text, with the sequences written from the amino- to carboxy-terminus, left to right. In lgp120 and LAP these are the targeting domains within type I membrane proteins which are localised to lysosomes, in the cases of M6PR and LDLR these are type I membrane proteins which undergo efficient endocytosis, and the TfR and ASGPR are type II membrane proteins which are also efficiently endocytosed.

<u>Protein</u>	<u>Sequence</u>
GLUT4	MPSG F QQIGSED
lgp 120	..SHAG Y QTI....
LAP	..QPPG Y RHVAD..
M6PR	..VS Y KY S KV....
LDLR	..DNPV Y QKT....
TfR	...PLS Y TRFSLA.
ASGPR	...TK E YQDLQH..

1.6.2 The Carboxy Terminus as a Targeting Domain

The initial findings of James and colleagues implicating the amino-terminus of GLUT4 as being an important targeting domain have recently been contradicted by studies published by several other laboratories [Marshall *et al.* (1993), Czech *et al.* (1993), Verhey *et al.* (1993)] These studies have all provided evidence that suggests an important role for the carboxy-terminus in the intracellular sequestration of GLUT4. Furthermore, these researchers have questioned the importance of the role of the amino-terminus in this process.

In order to determine the primary sequence(s) responsible for the characteristic distribution of GLUT4, Verhey *et al.* (1993) constructed a series of chimeric glucose transporters in which reciprocal domains were exchanged between GLUT1 and GLUT4. In addition, a non-disruptive, species-specific epitope-tag was introduced into a neutral region of the transporter to allow analysis of the reciprocal chimeras using a single antibody. The recombinant transporters were stably expressed in NIH 3T3 and PC12 cells by retrovirus-mediated gene transfer, and were localised by indirect immunofluorescence and laser-scanning confocal microscopy, as well as by staining of plasma membrane sheets prepared from these cells. Chimeras which contained the carboxy-terminal 30 amino acids of GLUT4 were predominantly expressed in a perinuclear compartment similar to native GLUT4. The results also showed that expression of a chimera based upon GLUT1 but containing both residues 1 to 183 and the carboxy-terminal amino acids of GLUT4 was expressed in an intracellular compartment and exhibited a pattern of localisation very similar to that of native GLUT4. Chimeras in which amino acids 1 to 183 were contributed

by GLUT4 and the carboxy-terminal 30 amino acids from GLUT1 consistently showed a phenotype intermediate between native GLUT1 and native GLUT4 with localisation to both the plasma membrane and the perinuclear compartment. These data were interpreted to imply that the carboxy-terminal 30 amino acids contain the dominant signal for intracellular localisation of GLUT4, but indicate that regions in the amino-terminus also play a role in this regard.

A similar study was undertaken by Czech *et al.* (1993) who engineered GLUT1/GLUT4 chimeric glucose transporter constructs that contained the hemagglutinin (HA) epitope YPYDVPDYA in their major exofacial loops. Analysis of monoclonal anti-HA antibody binding to non-permeabilised COS-7 cells expressing HA-tagged transporter chimeras revealed that expression of transporters on the cell surface was strongly influenced by their cytoplasmic carboxy-terminal domain. More specifically, Czech and colleagues found that a chimera composed of GLUT1 with a GLUT4 carboxy-terminal 30 residue substitution exhibited a predominantly intracellular localisation.

Concurring results were produced by a study which used oocytes as an expression system to elucidate the targeting of GLUT1/GLUT4 chimeras [Marshall *et al.* (1993)]. These showed that two domains, the C-terminus and a region corresponding to amino acids 24-132 of GLUT4 appear to confer intracellular sequestration. However, the authors postulate that any effect caused by the amino-terminal region may arise as a consequence of the incomplete maturation of the protein during transit through the endoplasmic reticulum in this cell type.

Both of the above studies provide contrasting results to the data of James and colleagues in that they were unable to demonstrate an important role for the amino-terminus in GLUT4 intracellular sequestration. However they have clearly demonstrated a role for the carboxy-terminus in mediating the intracellular localisation of this protein.

In 1994 Verhey & Birnbaum (1994) undertook to discover the exact nature of the signal sequence found in the carboxy-terminus of GLUT4. Visual inspection of the amino acid sequence of the protein identified a di-leucine pair (L⁴⁸⁹ and L⁴⁹⁰) that is not present in the corresponding position in GLUT1. This motif was of special interest as di-leucine pairs had previously been identified as key internalisation and sorting signals in several recycling membrane proteins such as the T cell surface antigen CD4 and the cation-dependent and cation-independent mannose-6-phosphate receptors [Letourneur & Klausner (1992), Johnson & Kornfeld (1992a), Denzer *et al.* (1997)] (Table 1.3). To investigate the role of this potential di-leucine motif in the targeting of GLUT4, L⁴⁸⁹ and L⁴⁹⁰ were mutated to alanine-serine in the carboxy-terminus of GLUT4, and the subcellular location of the chimeras containing these mutations was compared with wild-type proteins. The results of this study demonstrated that alteration of the di-leucine amino acid pair to A⁴⁸⁹S⁴⁹⁰ is sufficient to alter the subcellular sorting of the transporter from its normally perinuclear localisation to the plasma membrane in fibroblasts [Verhey & Birnbaum (1994)].

The above results were reinforced by the data of Corvera *et al.* (1994), who observed that mutation of the unique double leucines 489 and 490 caused a decrease in the rate of endocytosis and an increase the steady-state cell surface display of chimeric GLUT1/GLUT4 glucose transporters containing the carboxy-terminal 30 amino acids of GLUT4. Both of the above results support a hypothesis that the di-leucine motif in the carboxy-terminus operates as a rapid endocytosis and retention signal in the GLUT4 transporter, causing its localisation to intracellular compartments in the absence of insulin [Verhey & Birnbaum (1994), Corvera *et al.* (1994)].

Table 1.3

**Comparison of the Amino Acid Sequences of Recycling
Membrane Proteins which Contain a Di-leucine Motif**

Shown are the amino acid sequences surrounding di-leucine-based internalisation signals in other recycling membrane proteins. The proteins are M6PR: mannose 6-phosphate receptor; LIMP: lysosomal integral membrane protein; IFN-G-R: interferon gamma receptor; Lip31 is a type II membrane protein which associates with MHC class II molecules. The sequences are written from the amino- to carboxy-terminus, left to right.

<u>Protein</u>	<u>Sequence</u>
GLUT4ISATFRRTPSLLEQV KPST....
M6PRGEESEERDDHLLPM.....
CD3 γ chainQDGV RQSRASKDQTL LQNEQLYQPLK..
CD3 δ chainHERGRPSGAAEVQAL LKNEQLYQPLR..
CD4QAERMSQIKRLLSEKKTCQCPH..
LIMPII	..RGQGSTDEGTADERAPLLRT.....
IFN-G-RSIILPKL ISV.....
Lip31MDDQRDL IS.....

1.6.3 Analysis of Putative GLUT4 Targeting Signals in Insulin-Responsive Cell Lines

Despite the apparent success of the above studies in elucidating the targeting sequences responsible for the unique insulin-regulated translocation of GLUT4 a potential problem required to be addressed. This was that these studies had been carried out in cells that do not exhibit insulin-stimulated glucose transport, and are therefore unlikely to contain the cell-specific factors that facilitate the insulin-regulated translocation of GLUT4 to the plasma membrane or mediate the correct intracellular targeting of this isoform. In addition, it is possible that the insulin-responsive intracellular pool may not exist in cells other than adipocytes or muscle cells. In respect of these problems two recent publications have analysed the expression of epitope-tagged mutant and chimeric GLUT4 species to further define aspects of the targeting and translocation of GLUT4.

Marsh and co-workers investigated the role of the N-terminal FQQI motif and the LL motif in the carboxy-terminus using GLUT4 mutants which they stably expressed in 3T3-L1 adipocytes, a cell type that exhibits insulin-regulatable glucose transport. [Marsh *et al.* (1995)]. Because these cells already express GLUT4, an epitope-tag was introduced into the mutant species in order to distinguish recombinant GLUT4 from the endogenous protein. These workers initially demonstrated that the epitope-tagged GLUT4 construct behaved indistinguishably from endogenous GLUT4 and then proceeded to examine the effects of mutating either of the identified targeting motifs. Their results showed that mutation of either F⁵ in the amino-terminal or L⁴⁸⁹L⁴⁹⁰ in the carboxy-terminal resulted in impaired

targeting of GLUT4 in 3T3-L1 adipocytes. Mutation of either of these motifs to alanine resulted in a pronounced accumulation of epitope-tagged GLUT4 at the cell surface in an insulin-independent manner. Interestingly these researchers observed that the disruption in targeting of the LL mutant in adipocytes was governed by the level at which it was expressed, whereas this phenomenon did not occur in the case of F⁵ mutants. When expressed at low to moderate levels the di-leucine mutant displayed a subcellular distribution similar to endogenous GLUT4. In marked contrast, significant accumulation of the mutant protein at the plasma membrane was observed when expressed at higher levels. It is thought that this apparent dependence of targeting on expression level may account for the inability of previous studies to demonstrate a role for the carboxy-terminus of GLUT4 in the process of intracellular sequestration [Marsh *et al.* (1995)].

A similar approach was utilised by Birnbaum and colleagues to assess the relative importance of the amino- and carboxy-terminal domains [Verhey *et al.* (1995)]. This involved introducing a species-specific epitope-tag into the intracellular loop between transmembrane helices 6 and 7 of the chimeric transporters. These chimeras were stably expressed in the insulin-sensitive 3T3-L1 adipocyte cell line and their subcellular localisation in basal and insulin-stimulated states and the influence of the carboxy-terminal LL motif was determined. The results of this study demonstrated that information contained within the amino-terminal 183 amino acids of GLUT4 was sufficient to confer a predominantly intracellular distribution when expressed in 3T3-L1 adipocytes. This result is in direct contrast to previous data obtained using cell expression systems such as CHO cells, oocytes, and fibroblasts [Robinson *et al.* (1992). Marshall

et al. (1993)]. Their data also shows that expression of chimeras containing the carboxy-terminal amino acids of GLUT4 either alone or in conjunction with the amino-terminal 183 amino acids of GLUT4 also displayed a predominantly intracellular pattern of expression. From such results these workers postulated that either or both of the amino-terminus and/or the carboxy-terminus are capable of sequestering chimeric GLUT1/GLUT4 transporters to an intracellular location.

In this study Birnbaum went on to address the effect of insulin on the steady state distribution of the mutant transporters in an attempt to identify the sequences responsible for the subcellular sorting of GLUT4 in its physiologically relevant cell type. It was observed that although a chimera containing the amino-terminal 183 amino acids of GLUT4 was intracellularly localised, no significant translocation from the intracellular site to the plasma membrane occurred in response to insulin. This was thought to imply that the amino-terminal domain of GLUT4 possesses sequences responsible for internalisation, but not for targeting to an insulin-responsive compartment. In contrast, expression of chimeras containing the carboxy-terminal 30 amino acids of GLUT4, either alone or in tandem with the amino-terminal 183 amino acids exhibited an intracellular pattern of expression and moreover translocated to the plasma membrane in response to insulin. This data led to the hypothesis that the carboxy-terminus of GLUT4 contains information sufficient to target the transporter to an intracellular storage site from which it is recruited to the plasma membrane in response to insulin [Verhey & Birnbaum (1994)].

In order to further investigate the importance of the di-leucine motif Birnbaum and co-workers constructed chimeras which possessed the carboxy-terminal region of GLUT4 but were mutated such that the LL motif was altered to alanine-serine. In adipocytes, these mutant transporters displayed an intracellular distribution in the basal state and exhibited translocation to the cell surface in response to stimulation of the cells by insulin. After removal of insulin the cells were re-internalised at a rate slower than the comparable chimera with an intact di-leucine motif. These results are interpreted to imply that sequences within the carboxy-terminus of GLUT4 distinct from the di-leucine motif are involved in targeting to an insulin-responsive compartment, but that the LL motif does play some role in the re-internalisation of GLUT4 from the plasma membrane into the recycling endosomal system

These results are in accord with those of James and colleagues who demonstrated efficient intracellular targeting of chimeric glucose transporters mutated at L⁴⁸⁹L⁴⁹⁰ when expressed at low to medium levels [Marsh *et al.* (1995)]. This result is taken to infer that the di-leucine motif is not the dominant internalisation signal within GLUT4. This hypothesis is supported by data showing that mutation of the FQQI motif (F⁵ to A⁵) caused GLUT4 to constitutively accumulate at the cell surface and that regardless of expression level the functional di-leucine motif retained by these chimeras was insufficient to restore a pattern of intracellular sequestration. Furthermore, James similarly reported that both of their chimeric transporters retained their insulin-dependent movement out of the intracellular LDM vesicle fraction suggesting that neither of these motifs directly regulate the insulin-dependent translocation of GLUT4 *per se* [Marsh *et al.* (1995)]. Hence, they proposed that the information that

encodes the insulin-regulatibility of GLUT4 must be located elsewhere in the protein [Marsh *et al.* (1995), Rea & James (1997)].

All of the above data has been assessed collectively by Birnbaum who favours a model in which the cellular localisation of GLUT4 is distributed among three compartments in adipocytes: the plasma membrane, a non-specialised endosomal compartment, and insulin-responsive vesicles [Verhey *et al.* (1995)] (Figure 1.5). In the basal state, the distribution of glucose transporters between endosomes and the other two compartments is isoform-specific: GLUT4 has a greater tendency than GLUT1 to remain in endosomes as opposed to the cell surface. Based upon all of the above data it is postulated that this propensity is conferred by the information in both the amino- and carboxy-termini of the GLUT4 protein. In addition, GLUT1 is excluded from the intracellular insulin-responsive vesicles whereas GLUT4 is rapidly and efficiently sorted to this storage pool. The signal dictating targeting to the insulin-responsive vesicles appears to be encoded by a di-leucine independent signal located within the carboxy-terminal 30 amino acids.

Figure 1.6 illustrates some examples of chimeric and mutant GLUT4 species that have been expressed in 3T3-L1 adipocytes and employed to investigate the putative targeting motifs on the sequence of GLUT4.

Figure 1.5

Modified Three-Pool Model of GLUT4 Trafficking

This model of GLUT4 trafficking proposes two major intracellular compartments, the endosomal pool (X_{ee}) and the "insulin-responsive" compartment (X_{irv}). In this model, GLUT4 can move from the "insulin-responsive" compartment to the cell surface (defined by the rate constant K_2). GLUT4 is viewed as being sequestered from the recycling pathway *via* a sequestration step (K_{seq}) in the basal state into the "insulin-responsive" compartment. This model is taken from Yeh *et al.* (1995).

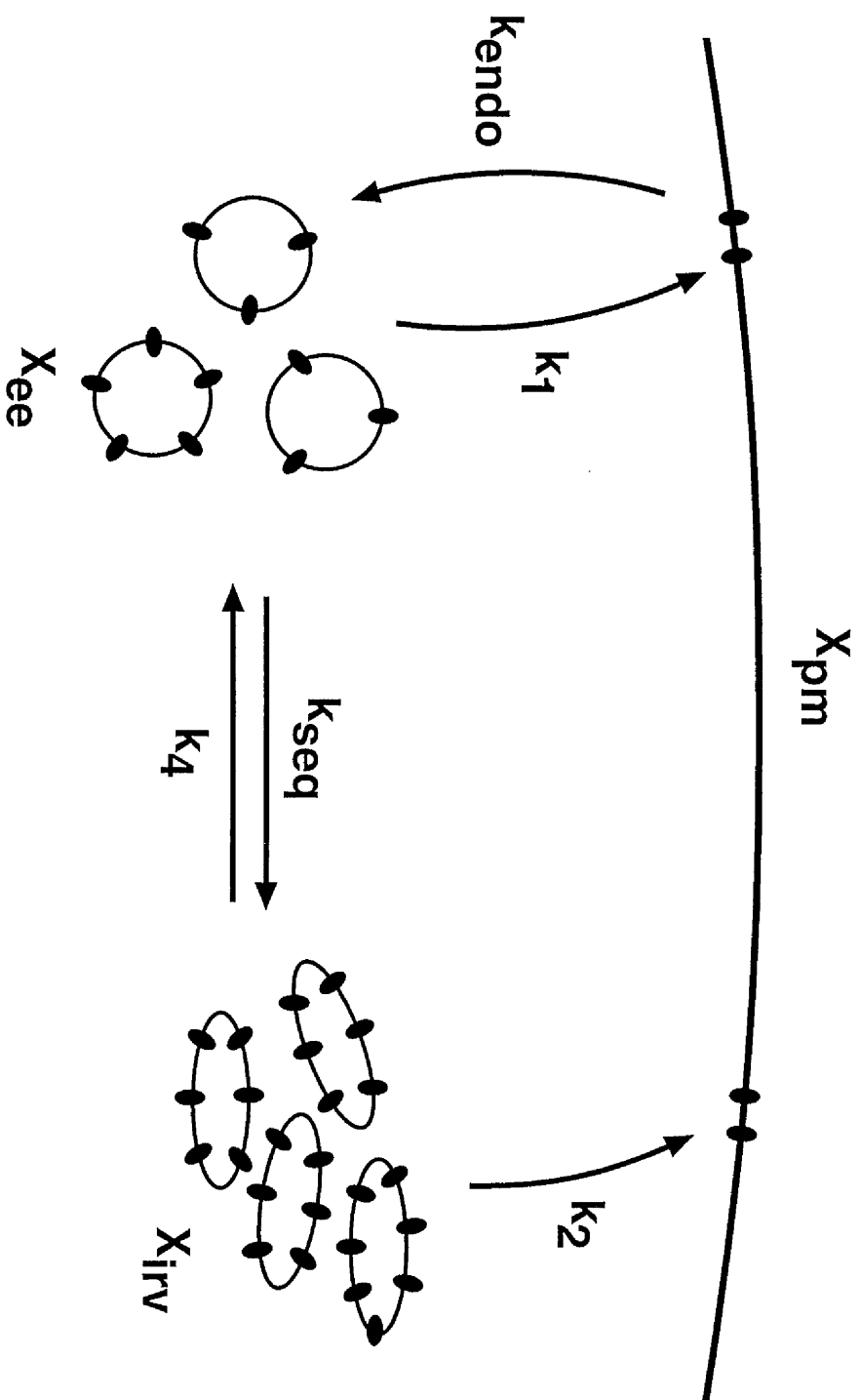












Figure 1.6

Chimeric and Mutant GLUT4 Species

This figure illustrates some examples of chimeric and mutant GLUT4 species which have been employed to investigate putative GLUT4 targeting motifs when expressed in 3T3-L1 adipocytes. Their subcellular localisation and insulin-responsiveness are shown. Collated from Marsh *et al.* (1995) and Yeh *et al.* (1995).

Name	Location	Translocation?
 Glut 1	Surface	No
 Glut 4	Intracellular	Yes
 4 HB4	Intracellular	Yes
 4 HB1	Mainly Intracellular but some at surface	No
 1 HB4	Intracellular	Yes
 4 HB4ΔLL	Intracellular	Yes
 1 HB4ΔLL	Intracellular	Yes
 TAG	Intracellular	Yes
 FAG	Surface	No
 LAG	Intracellular at low levels of expression only	Yes

1.7 Constitutive Recycling of GLUT4

The exact nature of the intracellular tubulo-vesicular compartment to which GLUT4 is trafficked is currently undefined and is the focus of intensive investigation. Two models have been formulated to describe the trafficking and biogenesis of GLUT4 and its storage compartment [reviewed in James *et al.* (1994), Rea & James (1997)]. Both of these models predict different modes of GLUT4 trafficking, as well as distinct loci of insulin action.

The first model proposes that under basal conditions, GLUT4 is sequestered within a topologically continuous subdomain of the endosomal system. This model assumes that the trafficking of GLUT4 through the general recycling pathway is regulated by its interaction with other proteins that constitute retention factors. Insulin and/or contraction are predicted to disrupt the interaction between GLUT4 and such retention factors, enabling GLUT4 to re-enter the constitutive recycling pathway and gain access to the cell surface. No specialised vesicular fusion machinery is required to accompany GLUT4 in this particular model, since, presumably, this function would be fulfilled by the constitutive machinery utilised by the endosomal system.

The second model suggests that GLUT4 is sorted and packaged into discrete storage vesicles at some stage during transit through the endosomal recycling system. An important feature of this model is that once formed, these vesicles have the potential to dock and fuse directly with the cells surface, independently of the endocytic recycling system. Hence, one predicted locus of insulin action in this model is the machinery that mediates the docking and fusion of GLUT4 containing vesicles with the plasma membrane. Recently, elements of such insulin-regulated docking machinery were found to be

identical to those used for small synaptic vesicle (SSV) endocytosis in neurones. These findings have provided strong support for the vesicle model of GLUT4 trafficking and also raised the possibility that GLUT4 is stored in intracellular vesicles that resemble SSVs. The discovery of vp165 [Ross *et al.* (1996)], an aminopeptidase that co-localises and traffics identically to GLUT4 in response to insulin, provides additional support for the storage vesicle model.

1.8 The Intracellular GLUT4 Compartment

The insulin-responsive glucose transporter isoform is one of many integral membrane proteins which recycle between the plasma membrane and specific intracellular loci by way of the endosomal system, which is composed of a series of discontinuous tubular and vesicular structures. Immuno-electron microscopy studies have shown that GLUT4 is localised to several elements of the endosomal recycling pathway: including the *trans*-Golgi network (TGN), clathrin-coated vesicles, and endosomes. However, the vast majority of GLUT4 (60%) is found in tubulo-vesicular elements clustered in the cytoplasm, often just beneath the cell surface [Slot *et al.* (1991a), Slot *et al.* (1991b), Slot *et al.* (1997)].

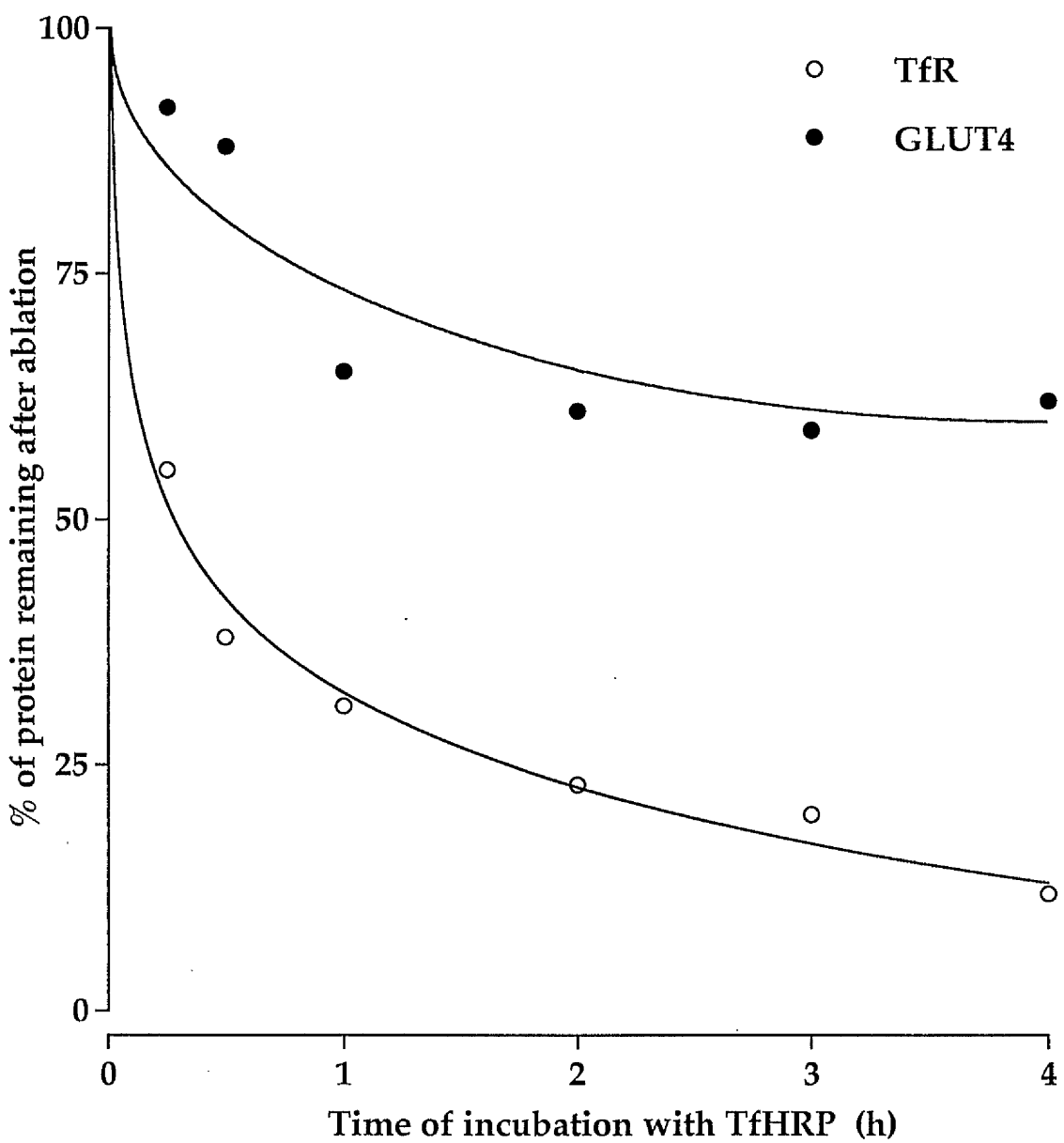
Researchers have found it difficult to distinguish the GLUT4 compartment from the other elements of the constitutive recycling pathway, but several observations have suggested that it is a separate compartment. Double-labelled immunofluorescence microscopy in 3T3-L1 adipocytes revealed differential targeting of GLUT1 and GLUT4 [Piper *et al.* (1991)]. Secondly, ablation experiments using transferrin conjugated to horse-radish peroxidase have demonstrated that endosomal recycling proteins such as

the transferrin receptor and clathrin can be extensively ablated, whereas a large portion of GLUT4 cannot [Livingstone *et al.* (1996), Martin *et al.* (1996)] (Figure 1.7). Thirdly, vesicle immunoadsorption studies have revealed sub-populations of vesicles in adipocytes, some of which are enriched for GLUT4, others are enriched for endosomal markers and some are enriched for both species [Zorzano *et al.* (1989), Robinson *et al.* (1992), Livingstone *et al.* (1996)]. Finally, glycerol gradient centrifugation revealed a population of small GLUT4-positive vesicles in adipocytes that are segregated from endosomes [Herman *et al.* (1994)].

Figure 1.7

Time Course of Ablation of the Transferrin Receptor and GLUT4

Shown is a comparison of the time courses of Tf-HRP conjugate incubation on both the transferrin receptor (TfR) and GLUT4 ablation from low density microsomal membranes (LDM) of 3T3-L1 adipocytes. The amount of protein lost on ablation, determined by immunoblot analysis, is expressed as a percentage of that measured in cells not exposed to peroxide at each time point. Even after complete 'ablation' of the recycling system containing the TfR, a significant pool of GLUT4 remains unablated, indicative of the presence of a GLUT4-containing compartment distinct from the recycling endosomal system. See also sections 2.5.1-2 and 3.2 for details.



1.9 GLUT4 Vesicle Trafficking

The present school of thought proposes that the unique GLUT4 storage compartment is mobile. Its motility could be regulated by factors such as insulin, and such a mobile compartment could be made to fuse directly with the cell surface. A paradigm for this type of regulated storage compartment is provided by the controlled release of small synaptic vesicles in neurones [Rothman & Warren (1994), Sudhof (1995)]. Several of the molecules that specifically mediate the targeting, docking and fusion of SSVs with the neuronal plasma membrane have been identified. Furthermore, homologues of many of these molecules have recently been identified in both adipocytes and myocytes; strongly indicating that the trafficking of the GLUT4 storage compartment in response to insulin is highly analogous to SSV exocytosis.

1.9.1 The SNARE Hypothesis

In 1993 Rothman provided a coherent conceptual framework within which to explain the molecular basis of vesicular transport between membrane-bound compartments [Sollner *et al.* (1993)]. This arose from the discovery of the SNARE proteins, membrane receptors for the cytosolic proteins α -SNAP and NSF, which were known to play a joint and generic role in numerous membrane trafficking events [Sollner *et al.* (1993)].

This work by Rothman and colleagues resulted in the proposal that different sets of proteins found in different membrane compartments were capable of interacting in a highly specific way, much like receptors and ligands. They suggested that each membrane involved in an NSF-

dependent fusion process would possess homologues of the synaptic proteins VAMP, syntaxin and SNAP-25, which were shown to mediate docking and fusion together with SNAPs and NSF. The generic NSF and SNAP proteins are not responsible for the specificity of this system, therefore specific pairing must occur between SNAREs in the vesicle and target membrane [Sollner *et al.* (1993)].

The SNARE hypothesis was subsequently formulated. It proposed that for all membrane trafficking events, a high-affinity match between a ligand in a transport vesicle (v-SNARE), generally VAMP homologues, and a receptor in the target membrane (t-SNARE), generally homologues of syntaxin, would be required to facilitate a specific docking and fusion reaction (Figure 1.8A).

1.9.2 SNARE Complex-mediated Vesicle Docking and Fusion

The original SNARE hypothesis proposed that the formation of a complex of an NEM-sensitive fusion protein (NSF), soluble NSF attachment proteins (SNAPs) and membrane-bound SNAP receptor proteins ensured docking specificity and led to membrane fusion driven by the ATPase activity of NSF (Figure 1.8B). However, recent results have challenged some aspects of this hypothesis and led to a reassessment of the models of SNARE interactions and the events leading to vesicle docking and fusion. Recent evidence from several *in vitro* systems suggests that NSF acts not directly in the membrane fusion step but in fact acts at a step before the fusion event [Banerjee *et al.* (1996), Ungermann *et al.* (1998)]. Such results led Wickner and co-workers to propose a different order of events in vacuole docking and fusion, in vacuolar trafficking. In this model, the v-

SNARE and t-SNARE form a complex followed by α -SNAP and NSF binding to the v-SNAREt-SNARE complex on the membrane. Upon ATP hydrolysis by NSF, α -SNAP is released from the SNAREs, and the SNARE complex is disassembled. At this stage LMA1, a complex of thioredoxin and the protease B inhibitor IB2, is required to stabilise the SNAREs. The next step, which involves docking of the vacuoles and v-SNAREt-SNARE pairing, requires the small GTPase Rab7. This step is followed by membrane fusion [Banerjee *et al.* (1996), Nichols *et al.* (1997), Ungermann *et al.* (1998)].

The data produced by the above studies has also demonstrated that NSF and α -SNAP dissociate a v-SNAREt-SNARE complex on one membrane, leading to the activation of the t-SNARE, but that NSF and α -SNAP are not directly involved in fusion. The dissociation of SNARE complexes by NSF and α -SNAP might be required for the recycling of v-SNAREs which may need to be returned to their original location for a new round of transport vesicle budding.

1.9.3 SNARE Complex Structure

Recent studies have provided evidence for structural changes during SNARE complex formation [Fasshauer *et al.* (1997)]. Monomeric SNAP-25 is largely unstructured, but it converts to a highly α -helical structure upon formation of a complex with syntaxin. In this binary t-SNARE complex, syntaxin and SNAP-25 are present in a 2:1 ratio. SNAP-25 is attached to the membrane by a palmitate in the middle of the molecule and may form a hairpin structure in which both the N- and C-terminal predicted coiled coils interact with syntaxin molecules. Monomeric synaptobrevin is also

largely unstructured. Upon formation of a ternary complex with syntaxin and SNAP-25, the α -helicity of synaptobrevin increases dramatically and the ternary complex exhibits a high degree of thermal stability. Synaptobrevin, syntaxin and SNAP-25 are present in a 1:1:1 stoichiometry, suggesting that synaptobrevin replaces one of the syntaxin molecules. The shape of the complex is consistent with a four- α -helix bundle [Hanson *et al.* (1997)].

It has been proposed that the thermodynamically favoured conformation of the highly stable SNARE complex is the driving force for the membrane fusion event, and evidence suggests that SNAREs alone may drive liposome fusion *in vitro*, albeit very inefficiently [Hanson *et al.* (1997), Weber *et al.* (1998)]. The stability of the SNARE complex would also explain the need for the ATPase NSF as an energy-converting enzyme to dissociate the complex and to prepare the SNAREs for subsequent fusion events.

1.9.4 v-SNAREs involved in GLUT4 Trafficking

Recent studies have demonstrated that several SNARE and SNARE-binding proteins play critical roles in the stimulated translocation of GLUT4 to the plasma membrane in response to insulin. The VAMP homologues, VAMP2 and cellubrevin were shown to be components of GLUT4 containing vesicles in adipocytes [Cain *et al.* (1992), Volchuk *et al.* (1995)]. A model postulating the specific roles of these proteins in GLUT4 trafficking has been proposed on the basis of studies using the transferrin-conjugated horse-radish peroxidase ablation technique [Martin *et al.* (1996)]. This model suggests that cellubrevin mediates the constitutive endosomal

trafficking of GLUT4, while VAMP2 specifically regulates the docking of GLUT4 vesicles in response to insulin stimulation.

1.9.5 t-SNAREs involved in GLUT4 Trafficking

Syntaxin4 is expressed at high levels in fat and muscle cells and is predominantly targeted to the plasma membrane. A functional role for this protein in GLUT4 trafficking has been established by studies showing that introduction of a recombinant fusion protein encoding the cytoplasmic tail of syntaxin4 or antibodies directed against syntaxin4 specifically blocked insulin-stimulated GLUT4 translocation in permeabilised 3T3-L1 adipocytes [Tellam *et al.* (1997), Volchuk *et al.* (1996)].

1.9.6 SNARE-binding Proteins involved in GLUT4 Exocytosis

In neuronal cells, several syntaxin-binding proteins have been identified including Munc-13, Munc-18 and SNAP-25 [Sudhof *et al.* (1995)]. Homologues of the latter two proteins have been identified in adipocytes. It appears that Munc-18 and SNAP-25 modulate vesicle docking efficiency by directly regulating the availability of syntaxin [Pevsner *et al.* (1994)]. SNAP-25 is thought to be a positive modulator for the interaction between VAMP2 and syntaxin. Munc-18a is a peripheral membrane protein that binds to syntaxin1A in neurones; an interaction that has been reconstituted *in vitro* and shown to reduce the affinity of syntaxin1A for VAMP2 [Sudhof *et al.* (1995)]. Protein kinase C phosphorylates Munc-18a *in vitro* preventing its interaction with syntaxin1A [Fujita *et al.* (1996)]. Thus, in contrast to SNAP-25, Munc-18 may be a negative regulator of vesicle docking.

Researchers have been unable to detect significant levels of SNAP-25 expression in adipocytes, but recently discovered a SNAP-25 homologue, known as Syndet [Wang *et al.* (1997)]. This protein is ubiquitously expressed and interacts with syntaxin4 *in vitro*. Peptides based on the C-terminus of Syndet inhibit GLUT4 translocation [Rea & James (1997)]. It is thought that there may be a Syndet-like isoform in muscle tissue which is also distinct from SNAP-25.

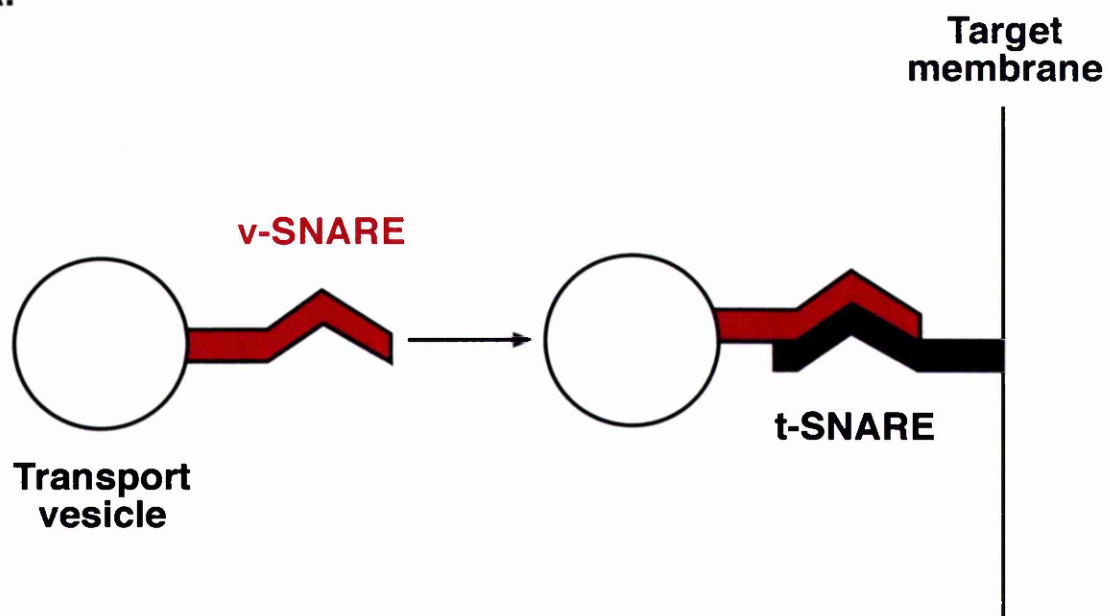
It has been demonstrated that there are at least three different Munc-18 isoforms participating in the endosomal recycling system of adipocytes (Munc18a-c) [Tellam *et al.* (1997)]. Of these, Munc-18c appears to be involved in GLUT4 exocytosis. This isoform is expressed at high levels in adipocytes and is primarily targeted to the cell surface, demonstrating a subcellular distribution indistinguishable from that of syntaxin4. Munc-18c reduces the interaction between syntaxin4 and VAMP2 *in vitro* similar to the effect observed for Munc-18a on the interaction between syntaxin1A and VAMP2 [Pevsner *et al.* (1994)]. These data suggest that Munc-18c may play a pivotal role in the insulin-regulated movement of GLUT4 and provides further support for the similarity between the regulation of GLUT4 exocytosis in fat cells and synaptic vesicles in neurones.

Figure 1.8

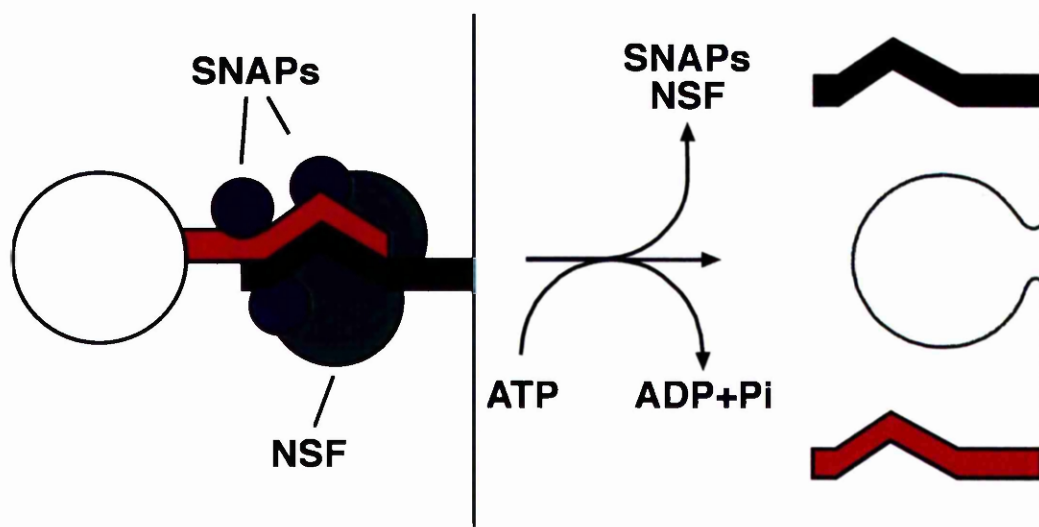
SNARE Hypothesis

- A.** Each transport vesicle is endowed with one or more unique v-SNAREs (generally related to VAMP) which pair with cognate t-SNAREs (generally related to syntaxin and/or SNAP-25), thereby docking the vesicle to the correct target membrane.
- B.** Fusion of vesicles is mediated by NSF and the SNAPs (no relation to SNAP-25). SNAP proteins bind to the SNARE (SNAP receptor) complex at the attachment site of the vesicle and its target. Hydrolysis of ATP by NSF disrupts the SNARE complex and initiates membrane fusion.

A.



B.



1.10 Insulin Resistance and Type II (Non-Insulin-Dependent) Diabetes Mellitus

Patients suffering from Type II or Non-Insulin-Dependent Diabetes Mellitus (NIDDM) display at least two major pathological defects. One is a decreased ability of insulin to act on peripheral tissues to stimulate glucose metabolism or inhibit hepatic glucose output. This phenomenon is known as insulin resistance. The other is the inability of the endocrine pancreas to fully compensate for this insulin resistance, termed relative insulin deficiency. In the context of this thesis I will concentrate on the phenomenon of insulin resistance and its role in NIDDM.

Insulin resistance is characterised by the patient displaying hyperglycaemia in the face of normal or even elevated circulating concentrations of insulin. One of the primary effects of insulin resistance is a marked decrease in insulin-stimulated glucose uptake into skeletal muscle and adipose tissue. Insulin resistance is a primary feature of NIDDM and is also associated with several other conditions that include obesity, Impaired Glucose Tolerance (IGT), hypertension, dyslipidaemia, coronary artery disease and the polycystic ovarian syndrome [reviewed in Reaven (1988)].

Longitudinal studies indicate that insulin resistance precedes the development of NIDDM [reviewed in Kahn (1994)]. In the pre-diabetic state this insulin resistance may occur with normal glucose tolerance and be asymptomatic, or it can be associated with the conditions listed above; a constellation sometimes referred to as Syndrome X [reviewed in Kahn (1995)]. NIDDM is characterised by the patient displaying hyperglycaemia in the face of normal or even elevated circulating concentrations of

insulin. Increased hepatic glucose production, impaired insulin secretion and insulin resistance all combine to generate the hyperglycaemic state. This disorder is also associated with vascular complications, neuropathy and increased infection rates, leading to morbidity and premature mortality [reviewed in Kahn (1995)].

The precise molecular causes of insulin resistance in NIDDM remain incompletely understood. It has been established that the abnormality impairing insulin's ability to stimulate glucose disposal into peripheral tissues *in vivo* generally lies distal to the binding of insulin to its plasma membrane receptor [Reaven *et al.* (1989)]. The series of cellular signalling events involved in insulin-stimulated glucose uptake have not yet been fully elucidated, thus the abnormality could lie anywhere from the generation of the signal to the process of glucose uptake itself. In both animal models of the disease and tissues taken from human patients there is a decrease in insulin receptor number (caused by a downregulation of receptors), a decrease in tyrosine kinase activity of the receptor, defects in a variety of intracellular enzymes involved in insulin action; including glycogen synthase, hexokinase and S6 kinases, and defects in the insulin stimulation of glucose transport [reviewed in Kahn (1994)]. For the purposes of this discussion I wish to focus on the latter defect of NIDDM.

1.10.1 The Role of the Insulin-Responsive Glucose Transporter Isoform, GLUT4, in Insulin Resistance of NIDDM

Insulin resistance is characterised above as a state in which ordinary circulating levels of insulin fail to result in efficient glucose disposal, and in particular as the failure of insulin to stimulate an increased rate of

glucose uptake in the major target sites of skeletal muscle and adipose tissue. The majority of studies on insulin resistance in NIDDM have been carried out in adipose tissue. This tissue accounts for only 5-20% of whole body glucose disposal but has been used as a classic insulin target tissue as it expresses GLUT4 and is readily isolated or grown in culture. Skeletal muscle is the main site of insulin-stimulated glucose disposal but is a much less convenient tissue to work with. In particular this tissue is difficult to isolate, grow in culture and separate in subcellular membrane fractions.

As stated previously (section 1.4), GLUT4 is the most important facilitative glucose transporter in whole body glucose homeostasis [Gould & Holman (1993)]. In the state of postprandial hyperglycaemia, circulating insulin signals GLUT4 to translocate from its unique intracellular location to the plasma membrane, where it facilitates a rapid and massive increase in glucose uptake. Following the cloning and purification of the transporter a considerable amount of effort has gone into understanding the process of GLUT4 translocation and its role in NIDDM.

1.10.2 GLUT4 Defects in Insulin Resistance of NIDDM

Several attempts have been made to identify specific mutations of the GLUT4 gene in NIDDM patients which might account for its dysfunction. Various point mutations have been observed but these occur in too small a percentage of cases for them to be considered an important aetiological factor in insulin resistance [reviewed in Gould (1997)]. Furthermore, specific genetic defects would be expected to underlie an irreversible form of insulin resistance, when in fact the phenomenon of insulin resistance

appears to be influenced by a number of other factors, and is not always irreversible, as in the case of gestational diabetes mellitus (GDM).

As a result of recent studies it has become apparent that a functional impairment of insulin-stimulated glucose transport in NIDDM patients is more fundamental than any genetic defects, and the nature of this fundamental impairment is becoming clearer.

1.10.3 Effects of Insulin Resistance on GLUT4 Expression and Activity in Adipose Tissue

It has been documented that in adipose tissue from obese and NIDDM patients there is a clear reduction in the expression of GLUT4 compared to that of lean control subjects [Garvey *et al.* (1988)]. Such tissues also display decreased rates of [¹⁴C]-D-glucose transport greater than can be explained by the reduced numbers of transporters present in both NIDDM and obesity. This phenomenon indicates impaired functional activity of GLUT4 and suggests that impaired glucose transport is caused by both a numerical and functional defect in transporters [Garvey *et al.* (1988)]. This study also demonstrated that NIDDM patients display more profound insulin resistance than their obese counterparts, and this is associated with a greater depletion in the number of glucose transporters as well as a further decrease in transporter functional activity.

Further studies by the same group showed that NIDDM sufferers displayed profoundly reduced levels of adipocyte GLUT4 mRNA compared with lean controls. Suppression of GLUT4 mRNA is thought to be caused by a pre-translational event and results in depleted numbers of GLUT4 glucose

transporters as the cellular content of these carriers is well correlated with the level of GLUT4 mRNA. Suppression of GLUT4 mRNA is also observed in adipocytes from subjects with IGT and could constitute an early lesion in the progressive pathogenesis of NIDDM [Garvey *et al.* (1991)].

Furthermore, insulin-stimulation of GLUT4 translocation has been shown to be impaired in adipocytes from NIDDM patients. This failure of the protein to translocate effectively to the plasma membrane may be caused by a defect in the signal pathway following binding of insulin to its receptor [reviewed in Gould (1997)], or defective targeting [Garvey *et al.* (1998)].

1.10.4 Insulin Resistance in Skeletal Muscle

The nature of insulin resistance in skeletal muscle tissue differs from adipose tissue, implying that there may be tissue-specific differences in the pathology of insulin resistance [Pedersen *et al.* (1990)]. Some published data suggests that plasma membrane levels of GLUT4 are reduced in obese Zucker rats, a phenomenon caused by an impairment in the insulin-stimulated translocation of GLUT4 [Brozinick *et al.* (1994)]. However, the majority of studies have shown little or no change in skeletal muscle cellular expression of GLUT4 mRNA or protein in insulin resistant patients [Pedersen *et al.* (1990)]. Thus, it is presently thought that altered GLUT4 expression does not contribute to skeletal muscle insulin resistance. It is generally accepted that muscle GLUT4 levels are broadly similar in individuals with NIDDM compared to age- and weight-matched control subjects [Pedersen *et al.* (1991)].

The above data suggests that the defect in insulin resistance in skeletal muscle may occur either on the insulin-signalling pathway or in the process of insulin-stimulated GLUT4 translocation. Potential sites of insulin resistance in relation to the translocation of GLUT4 are illustrated in Figure 1.9.

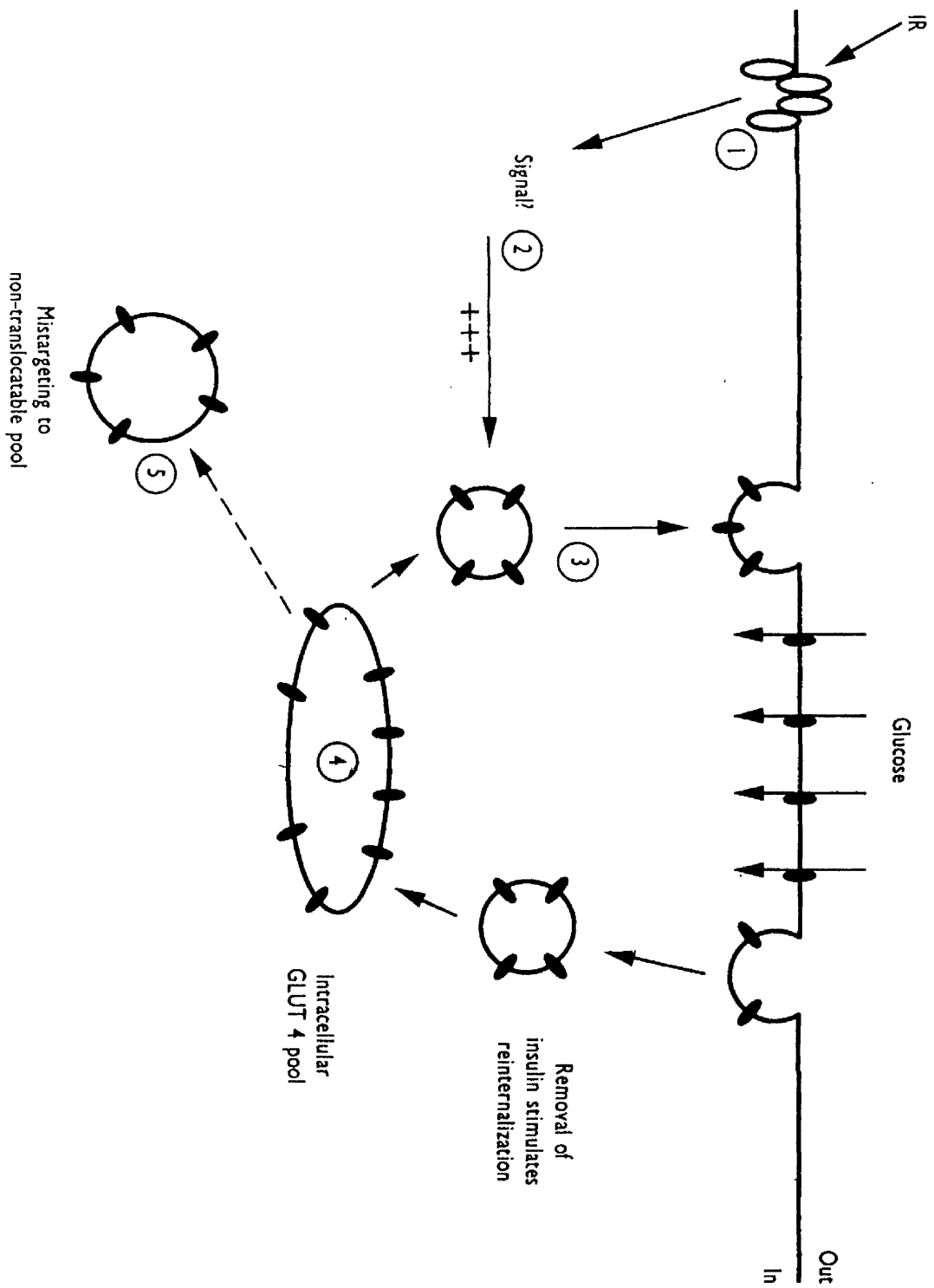
In consequence, a greater understanding of the precise defects in insulin-stimulated glucose transport underlying insulin resistance remains a key goal for future research.

Figure 1.9

Potential Sites of Insulin Resistance in Adipose Tissue

Under basal conditions, approximately 95% of GLUT4 is located intracellularly in a pool of vesicles, the nature of which is incompletely understood. GLUT4 undergoes a slow rate of constitutive recycling between the plasma membrane and this intracellular site; a process thought to occur via coated pits and entry into the endosomal system. On insulin stimulation, 40-50% of the intracellular pool translocates rapidly (within minutes), giving rise to 20-30 fold increases in cell surface GLUT4 levels, and so accounting for the large increase in glucose transport observed under such conditions. As circulating glucose and insulin levels fall, there is a reversal of this situation, with GLUT4 becoming sequestered in the intracellular pool. This model is based on studies in adipocytes.

Potential sites of insulin resistance marked are as follows: (1) Reduced binding of insulin to its plasma membrane receptor or impaired activation of the receptor-associated tyrosine kinase. (2) Impaired intracellular insulin signalling. Both of these defects would render cells insulin-resistant for glucose transport independent of any defects in GLUT4 expression or function. (3) Defective translocation of GLUT4 to the cell surface. In this case, normal levels of GLUT4 are present in the intracellular pool, but some defect in the mechanism responsible for translocation results in attenuated insulin-stimulated transport. (4) Reduction in the intracellular pool of GLUT4. Translocation of GLUT4 occurs normally, but insulin-stimulated transport is decreased because of a profound reduction in the GLUT4 available for translocation. (5) Mistargeting of GLUT4 to a non-translocatable pool. Defective targeting of GLUT4 to a site from which it cannot be translocated would have the effect of diminishing insulin-stimulated glucose transport.



1.11 Animal Models of Diabetes Mellitus

There exists a variety of animal species which develop spontaneous or induced NIDDM (Non-Insulin-Dependent-Diabetes Mellitus). These are valuable tools in the investigation into the aetiology and pathology of this disease. The multitude of animal species with NIDDM can provide a genetic and endocrine-metabolic basis for the subclassification of the variants of the NIDDM syndrome.

1.11.1 *ob/ob* mouse

Several strains of mice are known with mutations, either induced or spontaneous, which manifest both diabetes and obesity through most of their lifespan. The most extensively investigated representatives of this group are the *ob/ob* mice. These animals display an autosomal recessive mutation. Obesity is prevalent and they exhibit hyperinsulinaemia 10 to 50 times that of their non-obese litter-mates. Severe insulin resistance is associated with the hyperinsulinaemia and is accompanied by increased gluconeogenesis, although the animals are only moderately hyperglycaemic [Coleman (1982)]. The activity of the enzymes of both the glycolytic and gluconeogenic hepatic pathways are increased [Seidman *et al.* (1967), Lombardo & Menahan (1979)].

1.11.2 Obese Zucker Rat

This diabetic rat model was initially employed as a model for non-insulin-dependent diabetes mellitus [Peterson *et al.* (1990)] and has subsequently been used as a model of insulin resistance associated with obesity [Kahn *et al.* (1993)] The obese Zucker *fa/fa* rat model has been extensively studied with respect to insulin signalling and glucose uptake into the insulin-sensitive tissues. Such studies demonstrated that this model was indeed insulin resistant as the animal displayed mild hyperglycaemia in conjunction with elevated circulating levels of insulin and diminished insulin-stimulated glucose uptake in adipocytes and all major muscle groups [reviewed in Shafrir (1992)] . Further investigation revealed that this animal was hypertensive when compared to control strains and is therefore also a useful model for this condition.

1.11.3 Streptozotocin-induced Diabetic Rat

Administration of the glucose analogue, streptozotocin, to normal Sprague-Dawley rats results in the destruction of the β -cells of the pancreas. This mimics the autoimmune destruction of the pancreatic β -cells observed in patients suffering from Type-1 or Insulin-Dependent Diabetes Mellitus (IDDM). These animals display severe hyperglycaemia allied to glycosuria, water and electrolyte loss, and ketoacidosis.

1.12 Aims of this study

This thesis has two primary objectives. The first of these is to characterise the roles played in the complex process of intracellular trafficking of the insulin-responsive glucose transporter by targeting sequences present at the amino- and carboxy- termini of this protein. These targeting sequences are thought to control (a) the intracellular targeting of GLUT4 to an intracellular insulin-responsive pool, (b) internalisation of this transporter from the cell surface and (c) biogenesis of the GLUT4 storage compartment. Previous studies have identified two discrete motifs in GLUT4, both of which are thought to regulate internalisation from the cell surface. This study attempts to determine whether these sequences also influence the intracellular targeting of GLUT4 within the endosomal system.

As an extension to this work I have also carried out analysis of the role of the carboxy-terminal phosphorylation site in GLUT4 trafficking in an attempt to determine its possible involvement in the sorting of the glucose transporter in the Golgi network.

Further investigation was also made into the role of residues distal to the di-leucine motif in the carboxy-terminal cytoplasmic tail of GLUT4 in the targeting of this isoform in adipocytes.

The above studies were carried out in conjunction with the laboratory of Prof. D. E. James at the University of Queensland and where included results generated by James *et al.* are noted. These are included for the purposes of comparison only.

The other major aim of this thesis was to examine the expression levels of SNARE proteins involved in GLUT4 trafficking in a variety of animal models of insulin resistance, NIDDM and IDDM. These proteins are proposed to play an important role in regulating the transport of GLUT4 to the cell surface. Therefore knowledge of their expression levels in diabetic states may provide important information as to the defects present in glucose transport in such conditions.

Chapter 2

Materials and Methods

2.1 Materials

All reagents used in the course of this study were of good quality and were obtained from the following sources:

2.1.1 General Reagents

Amersham International Plc, Aylesbury, Buckinghamshire, UK

ECL Western Blotting Detection Kit

ECL+Plus Western Blotting Detection Kit

Bio-Rad Laboratories Ltd, Hemel Hempstead, Hertfordshire, UK

Extra-thick Filter paper

N, N, N', N' -tetramethylenediamine (Temed)

PVDF membrane

Boehringer Mannheim GmbH, Germany

Bovine Serum Albumin, Fraction V (Low Hormone)

Complete™ Protease Inhibitor Cocktail Tablets

Diversified Biotech, Boston, MA, USA

Quantigold Protein Assay Reagent

Fisons, Loughborough, Leicestershire, UK

Acrylamide

Ammonium persulphate

Diaminoethanetetra-acetic acid, disodium salt (EDTA)

Glucose

Glycerol

Glycine

HEPES

Hydrochloric acid

Methanol

N, N' methylene-bis-acrylamide

Potassium chloride

Sodium dodecyl sulphate (SDS)

Sodium chloride

Sodium dihydrogen orthophosphate dihydrate

Sodium diaminoethanetetra-acetic acid (EDTA)

Sodium hydrogen carbonate

Trichloroacetic acid

Gelman Sciences Ltd, Northampton, UK

Sterile Acrodisc® 0.2µm filters

Gibco BRL, Paisley, UK

Agarose (electrophoresis grade)

Tris base

Kodak Ltd, Hemel Hempstead, Hertfordshire, UK

RP X-Omat liquid fixer/replenisher

RP X-Omat liquid developer/replenisher

X-Omat AR film

X-Omat S film

Medicell International Ltd, London, UK

Dialysis tubing (Visking size 1-8/32")

Merck Ltd (BDH). Lutterworth, Leicestershire, UK

Calcium chloride hexahydrate

Chloroform (analytical reagent)

Dimethyl sulphoxide

Magnesium chloride hexahydrate

Magnesium sulphide hexahydrate

Millipore Corporation, Bedford, MA 01730, USA

Immobilon™-P Transfer Membranes (PVDF) 0.2µm

New England Biolabs, Hitchin, Hertfordshire, UK

Broad range pre-stained protein standards (6-175kDa)

Lambda ladder (*Bst*E II digested)

Ribonuclease A

Vent® DNA polymerase

Pierce, P.O. Box 117, Rockford, Illinois, USA

Albumin Standard

Coomassie Plus Protein Assay Reagent

Premier Brands UK, Knighton Adbaston, Staffordshire, UK

Marvel powdered milk

Promega, Southampton, UK

All restriction enzymes and corresponding 10X buffers

Calf intestinal phosphatase and 10X buffer

dNTPs

Nuclease-free H₂O

QIAGEN, UK

Plasmid Mini Preparation Kit

Plasmid Turbo Mini Preparation Kit

Plasmid Maxi Preparation Kit

Schleicher & Schuell, Dassel, Germany

Elutip-D DNA purification columns

Nitrocellulose membrane (0.45μm)

Sigma Chemical Company Ltd, Poole, Dorset, UK

Aprotinin

BSA (A-7030)

Bromophenol blue

Diisopropyl fluorophosphate

DL-dithiothreitol

E 64

Insulin (porcine monocomponent)

Pepstatin A

Sodium deoxycholate

Staphylococcus aureus cells

Trichloroacetic acid

Triton X-100

Whatman International Ltd, Maidstone, UK

Whatman 3mm filter paper

2.1.2 Antibodies

Amersham International Plc, Aylesbury, Buckinghamshire, UK

Horse-radish peroxidase (HRP)-conjugated donkey anti-rabbit IgG antibody

2.1.3 Cells

American Type Culture Collection, Rockville, USA

3T3-L1 fibroblasts

Prof D. E. James, University of Queensland, Australia

Stably transfected mutant 3T3-L1 fibroblast cell lines

2.1.4 Cell Culture Media and Reagents

Gibco BRL, Paisley, UK

Dulbecco's modified Eagle's medium (without sodium pyruvate, with 4500mg/L glucose) (DMEM)

Foetal calf serum (FCS)

10000U/ml penicillin, 10000U/ml streptomycin

Trypsin

Sigma Chemical Company Ltd, Poole, Dorset, UK

New born calf serum (NCS)

2.1.5 Cell Culture Plastics

AS Nunc, DK Roskilde, Denmark

50ml centrifuge tubes

6cm cell culture plates

75cm² cell culture flasks

6-well cell culture plates

Bibby Sterilin Ltd, Stone, Staffordshire, UK

13.5ml centrifuge tubes

Sterile pipettes

Fred Baker Scientific, UK

10cm cell culture plates

2.1.6 Radioactive Materials

NEN Dupont (UK) Ltd, Stevenage, Hertfordshire, UK

2-deoxy-D-[2, 6-³H] glucose

¹²⁵I-conjugated transferrin

2.2 Buffers and Media

All buffer recipes listed provide constituents required to produce 1 litre of the stated buffer.

2.2.1 Cell Culture Media

Serum-free DMEM

100U/ml penicillin, 100U/ml streptomycin in DMEM

10% NCS/DMEM

100U/ml penicillin, 100U/ml streptomycin, 10% (v/v) NCS in DMEM

10% FCS/DMEM

100U/ml penicillin, 100U/ml streptomycin, 10% (v/v) FCS in DMEM

Sterile trypsin solution for cell passage

25%(w/v) trypsin in PBS (see General Buffers) was syringe filtered through a sterile 2 μ m membrane and stored in 10ml aliquots in 50ml sterile centrifuge tubes at -20°C.

2.2.2 General Buffers

Citrate buffer

150mM NaCl, 20mM Tri-sodium citrate; pH 5.0

5X DNA gel-loading buffer

0.25% bromophenol blue, 30% glycerol in water

Glucose buffer

50mM glucose, 25mM Tris.HCl; pH 8.0, 10mM EDTA; pH 8.0

HBS buffer

50mM HEPES; pH 7.1, 280mM NaCl, 1.5mM Na₂HPO₄

HE buffer

20mM HEPES, 1mM EDTA; pH 7.4

HES buffer

20mM HEPES, 1mM EDTA, 225mM sucrose; pH 7.4

High Salt solution

1M NaCl, 20mM Tris; pH 7.4, 1mM EDTA

KRH buffer

0.1M NaCl, 5mM NaHCO₃, 5mM KCl, 1mM KH₂PO₄, 0.1mM MgSO₄.7H₂O,
25mM HEPES, 50mM glucose, 1mM CaCl₂; pH 7.4

KRP buffer

64mM NaCl, 2.5mM KCl, 2.5mM NaH₂PO₄.2H₂O, 0.6mM MgSO₄.7H₂O,
0.6mM CaCl₂; pH 7.4

Low Salt Solution

0.2M NaCl, 20mM Tris; pH 7.4, 1mM EDTA

Phosphate buffered saline (PBS)

150mM NaCl, 10mM NaH₂PO₄.2H₂O; pH 7.4

3M Potassium/5M Acetate buffer

60ml 5M KOAc, 11.5ml glacial acetic acid, 28.5ml water

SDS Buffer

0.2M NaOH, 1% SDS

50X Tris-acetate (TAE) buffer

242g Tris base, 57.1ml glacial acetic acid, 100ml 0.5M EDTA; pH 8.0

10X Tris-borate (TBE) buffer

108g Tris base, 55.0g Boric acid, 40ml 0.5M EDTA; pH 8.0

TE buffer

10mM Tris.HCl; pH 8.0, 1mM EDTA; pH 8.0

2.2.3 SDS-PAGE Buffers

Electrode buffer

25mM Tris base, 192mM glycine, 0.1% (w/v) SDS

Sample buffer

93mM Tris.HCl; pH 6.8, 20mM dithiothreitol, 1mM sodium EDTA, 10% (w/v) glycerol, 2% (w/v) SDS, 0.002% (w/v) bromophenol blue. The dithiothreitol was added immediately before use.

2.2.4 Protease Inhibitor Stocks

Pepstatin A

1mg/ml in DMSO

E 64

10mM in 2mM sodium EDTA

DFP

200mM in isopropanol

All protease inhibitor stocks were stored at -20°C.

2.2.5 Western Blot Buffers

Blotting buffer

25mM NaH₂PO₄·2H₂O; pH 6.5

TBST-1

2.42g Tris.HCl, 8.77g NaCl, 0.2ml Tween-20; pH 7.4

Towbin buffer

25mM Tris base, 192mM glycine, 20% (w/v) methanol; pH 8.3

2.2.6 Muscle Buffer

10mM NaHCO₃, 0.25M sucrose, 5mM NaN₃

2.2.7 Bacterial Media and Agar

Luria-Bertani Medium (LB)

10g Tryptone (Bactotryptone), 5g Yeast extract, 10g NaCl

LB Plates

10g Tryptone (Bactotryptone), 5g Yeast extract, 10g NaCl, 15g Agar

SOC Medium

20g Tryptone (Bactotryptone), 5g Yeast extract, 10ml 1M NaCl, 2.5ml 1M KCl, 1ml 2M Mg^{2+} stock, 1ml 2M glucose

2.2.8 Vesicle Immunoabsorption Buffer

20mM HEPES-KOH, 150mM KCl, 2mM $MgCl_2$; pH 7.2

2.3 3T3-L1 Fibroblast Cell Culture

2.3.1 Growth of 3T3-L1 Fibroblasts

3T3-L1 fibroblasts were grown on cell culture flasks and plates containing 10% (v/v) NCS/DMEM (see section 2.1). The medium was replaced every 2 days with the cells being stored in an incubator at 37°C in a humidified atmosphere containing 10% CO_2 .

2.3.2 Trypsinisation of 3T3-L1 Fibroblasts

When the cells were 70-80% confluent they were removed from the flasks using trypsin. The medium was aspirated from each flask and 5ml of 0.25% (w/v) trypsin was added. The flask was placed in the incubator for 5 min, allowing the cells to float, before trypsinisation was terminated by addition of the cells to a volume of 10% NCS/DMEM. The diluted cells were subsequently seeded onto new cell culture dishes. On average the cells from one 10cm plate were seeded onto ten 10cm plates.

2.3.3 Preparation of 3T3-L1 Fibroblast Differentiation Medium

Differentiation medium containing 10% FCS (v/v), 0.5mM methylisobutylxanthine (IBMX), 0.25mM dexamethasone, and insulin (1µg/ml) was prepared as follows:

A 500X stock solution of dexamethasone was prepared by a 1:20 dilution of 2.5mM dexamethasone in ethanol with 10% FCS/DMEM prior to use. A 500X sterile stock of IBMX was prepared by dissolving 55.6mg IBMX in 1.0ml of 0.35M KOH and passing the solution through a 0.22 micron filter. Insulin (1mg/ml) was prepared in 10mM HCl and again filtered by passing through a 0.22 micron filter.

3T3-L1 fibroblast differentiation medium was prepared by diluting both the dexamethasone and IBMX solutions to a 1X concentration in 10% (v/v) FCS/DMEM and finally adding insulin to a concentration of 1µg/ml.

2.3.4 Differentiation Protocol for 3T3-L1 Fibroblasts

Cells seeded in 10cm plates were grown and maintained in 10% (v/v) FCS/DMEM until 48hr post confluence (96 hr for GLUT4 mutants). At this time the medium was aspirated and replaced with 10ml per plate of differentiation medium which is described above in section 2.3.3. After a further 48hr this medium was aspirated and replaced with 10% (v/v) FCS/DMEM containing 1 μ g/ml insulin. The cells were incubated in this medium for a further 48hr, then the medium was aspirated and replaced with 10% (v/v) FCS/DMEM. Cells were fed every 48hr thereafter in this medium. Cells were used between 8-14 days post differentiation, at which time expression of GLUT4 is maximal.

2.3.5 Storage of 3T3-L1 Fibroblasts in Liquid N₂

Confluent cells were removed from a 75cm² flask by trypsinisation (section 2.3.2) and resuspended in 5ml of 10% (v/v) NCS/DMEM. The suspension was centrifuged at 1000 x g at room temperature for 5 min and the supernatant was removed by aspiration. 10% NCS/DMEM containing 10% (v/v) glycerol was equilibrated in 10% CO₂ for 1hr, and the cell pellet was resuspended in 1ml of this medium. Aliquots of the suspension were put into cryotubes, packed in cotton wool and frozen overnight at 80°C. The tubes were then transferred to liquid N₂ for long term storage.

2.3.6 Resurrection of Frozen Cells from Liquid N₂

The cryotube containing the stored cells was removed from liquid nitrogen and placed in the 37°C water bath. The tube was then transferred to the cell culture sterile flow hood where the cells were triturated gently with a sterile Pasteur pipette to disperse any large aggregates of cells. The 3T3-L1 fibroblasts were seeded onto 10cm cell culture plates containing 10% (v/v) NCS/DMEM medium. The cells were then maintained in an incubator at 37°C in an atmosphere containing 10% CO₂.

2.3.7 Transfection of 3T3-L1 Fibroblasts Using the Calcium Phosphate Method

2.3.7a Preparation of Cells for Transfection

3T3-L1 fibroblasts were seeded at a density such that on the day of transfection they were no more than 50% confluent. Generally, this required the cells to be seeded a day prior to transfection at a density of 1-2 x 10⁶/10cm plate. The cells were cultured overnight in 10% (v/v) NCS/DMEM medium at 37°C in an atmosphere containing 10% CO₂. 3-4hr prior to transfection, fresh media was added to the plates.

2.3.7b Transfection and Selection Protocol

10-20µg of DNA was added to a sterile 13.5ml Falcon tube. To this 36µl of CaCl₂ was added and the final volume was made up to 300µl with sterile H₂O. This solution was added dropwise using a Pasteur pipette to another 13.5ml Falcon tube containing 300µl 2X Hepes Buffered Saline (HBS) whilst

bubbling air through the solution with a second Pasteur pipette. This process was performed over a period of 1-2 min. After incubation at room temperature for 30 min, a fine precipitate forms which is then added dropwise to the prepared cells in 10cm plates. The cells were maintained at 37°C in a 10% CO₂ incubator for 48hr. At this point, the selection reagent, G418 at 500µg/ml was added to the medium which was subsequently changed every 48hr to remove cell debris and to allow the resistant cells to grow. This process was carried out for 7-14 days post-transfection until colonies became visible under a microscope. Individual colonies were isolated and cultured for further analysis.

2.3.7c Isolation and Propagation of Individual Clones

The selection medium was aspirated from the cells. A sterile cloning ring was then placed over an individual colony and secured to the plate using sterile Beckman Silicon grease. 200µl of trypsin-EDTA solution was pipetted into the cloning ring and after 2-3 min incubation the cells began to lift from the plate aided by gentle titration using a P200 Gilson pipette. The cells were then transferred by pipetting to a 6cm plate containing 4ml 10% (v/v) NCS/DMEM supplemented with G418 (200µg/ml). Cells were propagated under these conditions, with medium changes every 48hr until they reached 70-80% confluency. At this stage the cells could be split and grown for further analysis by cell preparation or frozen down in liquid N₂ for long term storage (see section 2.3.5).

2.4 Preparation of HRP-conjugated Transferrin

This procedure was performed by the carbodiimide method of Kishida *et al.* (1975). Horse-radish peroxidase (HRP) was dissolved in 1ml of 0.1M NaCl/10mM sodium phosphate; pH 7.2, at 4°C and dialysed overnight against 1 litre of the same buffer. Disodium succinate (200mg) and succinic anhydride (70mg) were added to the protein solution and this was stirred for 30 min at 0°C, then at room temperature for 30 min, and passed over an 8ml G-50 Sephadex column. The solution was concentrated to 0.5ml using an Amicon Centriprep concentrator. *N*-hydroxysuccinimide (25mg) and *N*-ethyl-*N*-(3-dimethylaminopropyl)carbodiimide hydrochloride (40mg) were added and the solution stirred for 3 hr at 0°C. This was again passed over an 8ml G-50 Sephadex column in 0.1M NaCl/1mM sodium phosphate; pH 7.2, and the eluate collected. Activated HRP was immediately added to 1ml of 10mg/ml transferrin containing approximately 1×10^7 cpm of ^{125}I -transferrin and stirred for 2 days at 2°C. The conjugation reaction was quenched by addition of glycine and a sample of the reaction was run on a 10% polyacrylamide gel to check, by autoradiography, for an increase in molecular mass of a proportion of the transferrin counts. Samples from three reactions were pooled and chromatographed on a 75cm x 2cm Sephacryl S-300 column in order to separate unconjugated transferrin from the Tf-HRP conjugate. Fractions were counted using an LKB 1275 Minigamma gamma counter and the appropriate fractions were pooled, concentrated and gel filtration was repeated as described above. Fractions were again pooled and concentrated and a sample again resolved on a polyacrylamide gel to ensure removal of unconjugated transferrin. A sample was assayed for protein concentration and the rest of the conjugate was iron-loaded by the addition of 375μl

FeSO₄ (0.278g/20ml) and 112.5μl KHCO₃ (0.5g/20ml). The iron-loaded conjugate was filtered through Whatman 3mm paper, divided into aliquots and stored at 80°C until required for use.

2.5 3T3-L1 Adipocyte Cell Preparations

2.5.1 Ablation Studies

After a 2hr incubation with serum-free DMEM, adipocytes (grown on 10cm plates) were incubated at either 37°C or 4°C (to prevent vesicle trafficking) with 20μg/ml Tf-HRP for periods of 1hr or 3hr. Cells were thereafter chilled by washing in ice-cold isotonic citrate buffer (section 2.2.2) and kept on ice in order to prevent any further vesicle trafficking during the DAB cytochemistry reactions (see below). Cell surface attached Tf-HRP was removed by acid washing for 10 min in ice-cold isotonic citrate buffer with three changes of buffer, then the monolayer was washed once in ice-cold PBS (section 2.2.2).

2.5.2 DAB Cytochemistry

DAB (freshly prepared as a 2mg/ml stock and filtered through a 0.22μm-pore-size filter) was added at 100μg/ml to all cells and H₂O₂ added to a final concentration of 0.02%, v/v, to one of each pair of 10cm plates. The cells were then incubated at 4°C in the dark for 60 min and the reaction was stopped by washing in PBS containing 5mg/ml BSA. This was then aspirated and samples were prepared for immunoblotting. In all experiments, duplicate plates were used, one of which was exposed to DAB

and H₂O₂, the other only to DAB as a negative control [Livingstone *et al.* (1996), Martin *et al.* (1996), Martin *et al.* (1997)]. All steps subsequent to the treatment of the cells with Tf-HRP and DAB were performed at 0-4°C.

2.5.3 Subcellular Fractionation of Adipocytes

Cells grown on 10cm cell culture dishes were rinsed three times with 10ml of ice-cold HES buffer (section 2.2.2). The cells were then scraped into HES buffer (5ml per 10cm plate) containing protease inhibitors (1µg/ml pepstatin A, 0.2M di-isopropyl fluorophosphate, 20µM E-64 and 50µM aprotinin) and homogenised by 10 strokes of a Teflon/glass homogeniser. The homogenate was centrifuged at 19000 x g for 20 min at 4°C. The pellet from this spin was resuspended in 2ml of HES buffer, layered onto 1ml of 1.12M sucrose in HES buffer and centrifuged at 100000 x g for 60 min at 4°C in a swing-out rotor. Plasma membranes were collected from the interface by careful aspiration, resuspended in HES buffer and collected by sedimentation at 41000 x g for 20 min at 4°C. The supernatant from the 19000 x g spin was recentrifuged at 41000 x g to yield a high density microsomal (HDM) pellet and the supernatant from this spin was centrifuged at 180000 x g for 75 min to collect a low density microsomal (LDM) pellet. All fractions were resuspended in equal volumes of HES buffer (cell equivalents), snap frozen in liquid nitrogen and stored at -80°C prior to use.

2.5.4 Sucrose Density Gradient Centrifugation

Adipocytes grown on 10cm cell culture plates were placed in serum-free media for 2hr to quiesce. Each plate of cells was then washed twice with 10ml ice-cold HES buffer (section 2.2.2). The cells were then scraped into HES buffer (5ml per 10cm plate) containing protease inhibitors (1 μ g/ml pepstatin A, 0.2M di-isopropyl fluorophosphate, 20 μ M E-64 and 50 μ M aprotinin) and homogenised by 10 strokes of a Teflon/glass homogeniser. The homogenate was centrifuged at 19000 x g for 20 min at 4°C. The supernatant from this spin was then centrifuged at 180000 x g for 60 min at 4°C to collect low density microsomes. The LDM fraction was resuspended in a small volume of HES buffer and aliquots of this fraction were loaded onto a discontinuous step gradient comprised of ice-cold 1.5-0.5M sucrose solutions prepared in 20mM HEPES, 1mM EDTA; pH 7.4. These gradients were then centrifuged at 75000 x g for 24 hours at 4°C. Samples were collected by tube puncture and the protein in each fraction precipitated by the addition of 0.15% Deoxycholate (w/v), and Trichloroacetic acid. These samples were resuspended in SDS/PAGE buffer, snap frozen in liquid nitrogen and stored at -80°C prior to immunological analysis.

2.5.5 Vesicle Immunoabsorption from 3T3-L1 adipocytes.

Recombinant GLUT4-containing vesicles were immunoabsorbed from the LDM fraction of 3T3-L1 adipocytes exactly as previously described, using a polyclonal anti-human GLUT3 antibody which has been previously characterised [Martin *et al.* (1994), Livingstone *et al.* (1996)]. This antibody recognises an epitope-tag at the extreme carboxy-terminus of each of the mutant species studied. Cells were washed three times with 8ml of ice-cold

Buffer A (section 2.2.8) then scraped and homogenised in the same buffer, containing protease inhibitors (section 2.2.4). The LDM fraction was isolated as outlined in section 2.5.3.

Formaldehyde-fixed *Staph. a.* cells were extracted and washed exactly as described prior to use [Shepherd *et al.* (1992)]. The cells were then washed twice in Buffer A containing 1% bovine serum albumin, and loaded with either affinity purified anti-GLUT3 antibodies or irrelevant IgG as a control by incubation on the bench for 2hr at room temperature with occasional agitation/mixing. The cells were washed three times in PBS/BSA.

Prior to immunoadsorption of the recombinant GLUT4 vesicle population, the low density microsomal fractions were 'pre-cleared' by incubation for 30 min at 4°C with irrelevant IgG-coated *Staph. a.* cells, as this has been shown to reduce non-specific binding [Shepherd *et al.* (1992)]. The *Staph. a.* cells were removed by centrifugation and immunoadsorption of recombinant GLUT4-containing vesicles was achieved by slow rotation of an aliquot of the LDMs with antibody-coated *Staph. a.* cells for 2hr at 4°C. After washing, recombinant GLUT4 containing vesicles were solubilised directly in SDS-PAGE sample buffer (section 2.2.3) and snap-frozen prior to use. The supernatants from the immunoadsorptions were centrifuged at 180000 x g for 1hr at 4°C to pellet all membranes which were directly resuspended in SDS-PAGE sample buffer and snap-frozen prior to use. 100µg of LDM membranes and 10µg of anti-GLUT3 antibody were employed per immunoadsorption. An identical procedure was employed to immunoisolate vp165-containing vesicles, except 2µg of affinity purified anti-vp165 was used per 100 µg of LDM membrane protein.

2.6 Preparation of Animal Tissues

2.6.1 Dissection and Subcellular Fractionation of Adipose Tissue

The epididymal fat pads were removed from male rats which had been sacrificed by cervical dislocation. The tissue was placed in pre-weighed universal containing KRH buffer, pH 7.4 (section 2.2.2), containing 1% (w/v) BSA and the weight of the tissue was determined. The tissue was then added to the relevant volume of KRH/BSA/collagenase such that 4ml KRH/BSA was added per gram of adipose tissue and 2mg of collagenase was added to each 1ml adipose tissue/KRH/BSA.

The adipose tissue was then minced through a plastic tea strainer into a 100ml siliconised flask and incubated at 37°C with gentle agitation in an H₂O bath for 1hr. The contents of the flask were filtered twice through a tea strainer and left to stand for 15 min to allow the adipocytes to float to the surface of the cell suspension. The supernatant was removed using an aspirator and the cells were washed in KRH buffer; pH 7.4, containing 1% (w/v) BSA. This procedure was repeated twice more to obtain a pure cell suspension. The cells were resuspended in an equal volume of KRH buffer; pH 7.4, containing 3% (w/v) BSA.

The cell suspension was then split into two equal volumes. One of these samples was stimulated with a dose of 10^{-7} M insulin and incubated at 37°C in a shaking H₂O bath for 15 min. After insulin stimulation a cocktail of protease inhibitors was added to both \pm insulin samples and these were homogenised by 20 up and down strokes of a hand-held homogeniser.

The homogenate was centrifuged in a JA-21 rotor for 15 min at 16000 x g at 4°C and the pellets were resuspended in 1ml KRH buffer; pH 7.4. This pellet represents a crude plasma membrane fraction which was homogenised using a 5ml syringe and needle, snap-frozen in liquid nitrogen and stored at -80°C until use.

The supernatant from the first spin was further centrifuged at 41000 x g at 4°C for 15 min. The pellet from this spin contained the 'heavy microsomes' which were resuspended in 1ml KRH buffer; pH 7.4, homogenised, snap-frozen in liquid nitrogen and stored at -80°C until use. The supernatant from the previous spin was transferred to a clean tube and centrifuged in a TLA 100.4 rotor at 100000 x g for 75 min at 4°C. After this, the pellets were resuspended in 2ml KRH buffer; pH 7.4, homogenised and re-centrifuged at 100000 x g for another 75 min at 4°C. The pellet from this step contained the 'light microsomes' which were resuspended in 1ml KRH buffer; pH 7.4, homogenised, snap-frozen in liquid nitrogen and stored at -80°C until use.

2.6.2 Hindlimb Skeletal Muscle Dissection and Subcellular Fractionation

The method of Klip *et al.* (1987) was used in the preparation and subcellular fractionation of hindlimb skeletal muscle membranes. The animals were sacrificed by cervical dislocation and the hindlimb muscle was dissected. All subsequent procedures were carried out on ice or at 4°C. The skeletal muscle was minced and diluted 1g/10ml in muscle buffer (see section 2.2.6) before being homogenised using an UltraTurrex for 1 minute. The homogenate was then centrifuged using a JA-20 rotor at 1200 x g for 10

min at 4°C. The pellet was discarded and the supernatant was centrifuged at 190000 x g for 60 min. The pellet from this latest step contained the 'crude membranes' which were subsequently hand-homogenised for 20 strokes in 1ml of muscle buffer.

The crude membrane fraction was then applied to a discontinuous sucrose gradient of 25%, 30%, and 35% (w/v) sucrose and centrifuged at 150000 x g for 16hr at 4°C. The 25% (w/v) sucrose fraction contained the purified plasma membranes and the 35% (w/v) fraction contained the intracellular membranes. These fractions were collected, diluted 5-fold in muscle buffer, then further centrifuged at 190000 x g for 60 min to wash out the sucrose. The pellets from the plasma membrane and intracellular membrane fractions were then resuspended and homogenised in 100 µl muscle buffer before being snap-frozen in liquid nitrogen and stored at -80°C until use.

2.6.3 Insulin Stimulation of Sprague-Dawley Rats

Normal Sprague-Dawley rats of an optimum weight of approximately 180-200g were selected for this procedure. These animals were anaesthetised by injection of Hypnorm/Hypnovel (see below) directly into the abdomen. An adequate period of time was allowed for the anaesthetic to take full effect (~5 min) and the animal's state of consciousness was assessed by the blink reflex and motor reflex tests. If the animal was sufficiently anaesthetised then the abdomen was dissected open using an incision approximately five centimetres in length. At this point removal of the epididymal fat pads could be carried out if desired. The abdomen was then dissected further to a point just distal of the diaphragm. The hepatic portal

vein was then cannulated using a needle and syringe, and injected with a bolus of insulin at a maximal dose of 10^{-5}M . An equivalent volume of 0.9% NaCl saline was administered to the control (-insulin) rats in an attempt to minimise/mimic any stress-induced effects caused by this procedure. A period of 90 sec was allowed to achieve adequate insulin stimulation, then the cannula was removed from the hepatic portal vein. The hind-legs of the animal were then removed and the desired muscle tissue was removed by dissection. The tissue was then freeze-clamped in liquid N_2 and stored at -80°C .

2.6.4 Protocol for Preparation and Use of Anaesthetic

Hypnorm/Hypnovel

Hypnorm:	Fentanyl citrate	0.315mg/ml
	Flaumisone	10mg/ml
Hypnovel	Midazolam HCl	5mg/ml

Preparation required dilution of each component 1:1 in an equal volume of H_2O . It was necessary to add the Hypnorm component to the H_2O first and then add the Hypnovel component.

i.e. 4ml of H_2O + 2ml Hypnorm then 2ml Hypnovel

The anaesthetic was administered at a dose of 0.3ml/100g

2.6.5 Preparation of Insulin

The insulin used in the above procedure was of the Human Actrapid® type. It was supplied as a 0.7mM stock solution. To obtain a 10^{-5} M solution it was necessary to perform a 1:70 dilution.

i.e. 75 μ l of 0.7mM stock solution + 5.18ml saline

2.7 Protein Concentration Assays

2.7.1 Quantigold Protein Concentration Determination

This method was used to determine the protein concentrations of sub-fractionated adipose and muscle preparations from individual animals or small groups of animals, where concentrations were very low and samples at a premium.

Using BSA as a standard, 10 μ l of sample was added to 800 μ l of Quantigold solution in a 1.5ml microfuge tube, vortexed and incubated at 37°C for 40-60 min. The samples were then transferred to a plastic cuvette and their absorbance was read in a spectrophotometer set at 595nm. The protein concentration was determined after plotting the standard curve of concentration of BSA against absorbance. This method of protein determination is extremely sensitive and is accurate to 5ng of protein and linear up to 200ng of protein.

2.7.2 Bradford's Method of Protein Concentration Determination

This method was used to determine the protein concentrations of sub-fractionated 3T3-L1 adipocyte cell preparations.

A 10 μ l aliquot of each sample was added to 2ml of Pierce-Lauryl Coomassie Blue solution and vortexed. The samples were incubated at room temperature for 5-10 min and the absorbance was read in a spectrophotometer at 595nm. The concentration of the sample was determined from a standard curve (0-150 μ g) constructed from 2mg/ml BSA and treated in the same manner as protein samples of unknown concentration.

2.8 SDS/Polyacrylamide Gel Electrophoresis

2.8.1 Hoefer Large Gel Apparatus

The Hoefer gels had a stacking gel of 4cm composed of 5% acrylamide/0.136% bisacrylamide in 125mM Tris.HCl, pH 6.8; 0.1% SDS, polymerised with 0.1% ammonium persulphate and 0.05% *N, N, N', N'*-tetramethylenediamine (TEMED).

The separating gel consisted of 10% acrylamide/0.28% bisacrylamide in 0.383mM Tris.HCl, pH 8.8; 0.1% SDS, polymerised with 0.1% ammonium persulphate and 0.019% *N, N, N', N'*-tetramethylenediamine (TEMED).

The protein samples were solubilised in 1x sample buffer (see section 2.2.3) and loaded onto the wells in the stacking gel. The gel was then immersed in electrode buffer (see section 2.2.3) and the gel electrophoresed until the tracking dye had migrated to the bottom of the gel. For the Hoefer large gel a constant current of 150mA for 3hr ensured adequate separation of the pre-stained SDS-PAGE markers. Alternatively the gels could be electrophoresed overnight at 15-20mA.

2.8.2 NuPAGE™ Electrophoresis System

Protein samples were prepared by addition of 4X NuPAGE™ sample buffer and 10% β -mercaptoethanol.

The Novex NuPAGE™ Electrophoresis system was used with pre-cast 4-12% Bis-Tris gel. The gel was placed in the gel tank (XCell II™ Mini-Cell) and the outer chamber was filled with MOPS SDS running buffer. Immediately prior to loading the gel the inner chamber was filled with MOPS SDS running buffer containing 0.25% antioxidant. The samples were then loaded and electrophoresed at 200V constant for approximately 50 min.

2.9 Western Blotting of Proteins

2.9.1 Transfer of Proteins Using a BIO-Rad Trans-Blot Tank

After separation of the proteins using the Hoefer apparatus as described above, the gels were removed from the plates and equilibrated in blotting buffer (see section 2.2.5) at room temperature for 30 minutes. Each gel was then placed on top of a piece of nitrocellulose paper (0.45 μ m pore size) which had been cut to the size of the gel and pre-soaked in blotting buffer. This was then "sandwiched" between 2 layers of 3mm filter paper which had also been pre-soaked with blotting buffer. The "sandwich" was then placed in a cassette and transfer of the proteins onto the nitrocellulose was performed using a BIO-Rad trans-blot tank.

Transfer was achieved at a constant current of 255mA for 3hr at room temperature. The nitrocellulose membranes were then removed ready for immunodetection and the quality and efficiency of transfer could be qualitatively determined by the presence and intensity of the pre-stained molecular weight markers.

2.9.2 Transfer of Proteins Using a BIO-Rad Semi-Dry Transfer Block

After separation of the proteins using the Novex NuPAGE™ Electrophoresis system as described above, the gels were carefully removed from their cassette using a gel knife. The stacking gel and the bottom lip of the gel were removed. The gel was then washed in Towbins buffer (see section 2.2.5) at room temperature for 15 minutes. PVDF membrane was

prepared by washing successively in 100% methanol, distilled H₂O and Towbins buffer. Extra-thick filter paper was soaked in Towbins buffer and placed horizontally on the BIO-Rad Semi-Dry Transfer Block. On top of the was placed the prepared PVDF membrane and on this the equilibrated gels were placed. To complete the transfer "sandwich" another sheet of extra-thick filter paper was placed on top. The lid of the Transfer Block was assembled and the proteins were transferred onto the PVDF membrane at 18V for approximately 20 min.

2.9.3 Blocking of Transfer Membranes and Probing with Primary Antibodies

To block non-specific binding sites on the transfer membranes, the membrane was shaken in 5% (w/v) non-fat milk/TBST-1 (see section 2.2.5) at 4°C overnight on an orbital shaking platform. The membrane was then placed into 1% (w/v) non-fat milk/TBST-1 containing the relevant primary antibody at the required dilution and shaken at 37°C for 1hr. Following this, the membrane was washed five times at 10 min intervals with TBST-1.

2.9.4 Immunodetection Using HRP-linked Goat Anti-rabbit IgG

The membrane was incubated in 1% non-fat milk/TBST-1 containing HRP-linked goat anti-rabbit IgG (1:1000) for 1hr at room temperature.

2.9.5 Detection of Immunoblotted Proteins Using the Enhanced Chemiluminescence (ECL) Kit

After incubation with HRP-linked goat anti-rabbit IgG, the nitrocellulose membrane was washed as before, and then submerged in a solution containing equal volumes of Amersham "detection reagent 1" and "detection reagent 2" from the ECL Western Blotting Detection Kit for 1 minute. The nitrocellulose was then removed from the solution, rinsed in distilled water, wrapped in cling-film and placed protein side up in an X-ray film cassette. The blots were then exposed to Kodak X-Omat S film and developed in an X-Omat film processor.

2.9.6 Detection of Immunoblotted Proteins Using the Enhanced Chemiluminescence Plus (ECL+Plus) Kit

After incubation with HRP-linked goat anti-rabbit IgG, the membrane was washed as before. Excess wash buffer was drained from the membranes and they were placed protein side up on a sheet of SaranWrap™. Amersham detection reagents A and B were mixed at a ratio of 40:1 and pipetted onto the membrane, ensuring that the entire surface area of the membrane was covered. The membranes were incubated at room temperature for 5 min. The excess detection reagent was drained off the membrane and the blot was placed face down onto a fresh piece of SaranWrap™. The blot was then wrapped up and any air bubbles were smoothed out. The wrapped blots were placed protein side up in an X-ray film cassette. The blots were then exposed to Kodak X-Omat S film and developed in an X-Omat film processor.

2.10 Recombinant Polymerase Chain Reaction

2.10.1 Synthesis of Oligonucleotides

Oligonucleotides (37-90'mers) with sequence identical to the relevant amino- or carboxy-terminal cytoplasmic region of GLUT2 and/or GLUT4 were synthesised (Dr. V. Math, Division of Biochemistry and Molecular Biology, University of Glasgow). All of the oligonucleotides used in this study will subsequently be referred to as either 5' or 3' external primers.

2.10.1a 3' External Primers

Two 37'mer oligonucleotides were synthesised: (a) a sense oligonucleotide with sequence complementary to the 3' untranslated end of GLUT2 incorporating a *Sal* I restriction site, which will be referred to as G2-End, and (b) a sense oligonucleotide with sequence complementary to the 3' untranslated end of GLUT4 incorporating a *Not* I restriction site, which will be referred to as G4-End.

2.10.1b 5' External Primers

Two 90'mer oligonucleotides were synthesised: (a) a sense oligonucleotide with sequence complementary to the first 30 bases of GLUT4 married to sequence complementary to bases 16-48 of GLUT2 incorporating a *Sal* I restriction site, which will be referred to as G4/G2, and (b) a sense oligonucleotide with sequence complementary to the first 30 bases of GLUT2 married to sequence complementary to bases 16-48 of GLUT4 incorporating a *Bam* HI restriction site, which will be referred to as G2/G4.

For full sequences of oligonucleotides see Table 6.1.

2.10.2 Precipitation of Oligonucleotides

Oligonucleotides (stored in 0.88M aqueous NH_4OH) were prepared for use in PCR reactions by ethanol precipitation. 360 μl of the oligonucleotide was added to an Eppendorf tube containing 40 μl 3M sodium acetate; pH5.5, and 1.2ml ice-cold ethanol. The solutions were mixed thoroughly before incubation at 20°C for at least 1 hour. The DNA was pelleted by centrifugation at 16000 x g in a microfuge for 30 min. The pellet was washed in 70% ethanol, dried in air for 5 min and resuspended in 100-250 μl sterile H_2O , depending on yield.

2.10.3 Quantitation of Oligonucleotides

The $\text{OD}_{260\text{nm}}$ was determined for each oligonucleotide. From this value the concentration of the solution can be calculated, since an $\text{OD}_{260\text{nm}}$ of 1 is equal to 33.3mg/ml. Measurement of the $\text{OD}_{260\text{nm}}$ value allows an estimation of the purity of the solution from the $\text{OD}_{260}/\text{OD}_{280\text{nm}}$ ratio (the closer the ratio is to a value of 2, the higher the purity of the solution).

2.10.4 Reaction Conditions for Primary Polymerase Chain Reactions Using *Vent* DNA Polymerase

1.2µg	sense primer
1.2µg	antisense primer
10ng	template dsDNA (GLUT2/GLUT4)
2µl	nucleotide mix (20mM dATP, 20mM dCTP, 20mM dGTP, 20mM dTTP)
4µl	MgSO ₄
10µl	<i>Vent</i> DNA polymerase reaction buffer
1µl	<i>Vent</i> DNA polymerase

Nuclease-free sterile water was added to give a final volume of 100µl.

Reactions were carried out in 0.5ml microfuge tubes. The reaction constituents were added sequentially, with *Vent* DNA polymerase added last. On completion of the thermal cycling programme (see below), 20µl of 5X DNA gel-loading buffer was added to each reaction and mixed, before loading the entire reaction volume onto a 1.3% agarose gel. Following electrophoresis (section 2.12.4), cDNA bands were identified and excised from the gel, electroeluted (section 2.12.5), purified (section 2.12.7) and ethanol precipitated (section 2.12.2). . The contents of 3-6 reactions were combined and passed through the same Elutip-D column (section 2.12.7) and the final DNA pellet was resuspended in a volume of 50µl of sterile water. 3-5µl of the DNA sample was analysed by electrophoresis on a 1.3% agarose gel to determine the recovery of the purified primary PCR product.

Alternatively the primary PCR products were taken and directly subjected to the protocols for cloning of PCR products using the Invitrogen Eukaryotic TA cloning® kit (section 2.11).

2.10.5 Thermal Cycling

PCR reaction tubes were placed in a Techne PHC-3 Thermal Cycler with a heated lid. The following thermal cycling protocol was programmed into the machine:

Initial extension	95°C	10 min
Cycling	27 cycles total, 1°Csec ⁻¹ ramp rate	
Separation	95°C	1 min
Reannealing	X°C	1 min
Extension	72°C	1.5 min
Final extension	72°C	10 min
Soak	4°C	Hold

X = 5°C below the melting temperature of the oligonucleotide having the lower melting temperature.

2.11 Cloning PCR Products Using the Invitrogen Eukaryotic TA Cloning® Kit

The Eukaryotic TA Cloning® Kit provides a quick, one-step system to directly ligate a PCR product into a mammalian expression vector. This means that once cloned, analysed, and transfected, the PCR product will express directly in mammalian cell lines i.e. 3T3-L1 fibroblasts without the requirement for additional subcloning.

This system takes advantage of the fact that *Taq* DNA polymerase has a non-template dependent activity which adds a single deoxyadenosine (A) to the 3' ends of duplex molecules. The linearised vector supplied with this kit has single 3' deoxythymidine (T) residues. This allows PCR inserts to ligate efficiently with the vector.

2.11.1 Addition of 3' A-overhangs on to *Vent* DNA Polymerase PCR Products

Thermostable DNA polymerases containing extensive 3' to 5' exonuclease activity, such as *Vent* and *Pfu*, do not leave 3' A-overhangs. Thus, to enable successful cloning of PCR products produced by these enzymes, it is necessary to add 3' A-overhangs by incubation with *Taq* DNA polymerase.

After amplification with *Vent* polymerase, vials containing primary PCR products were placed on ice and 0.7-1 unit of *Taq* polymerase was added per tube. The tubes were then mixed well and incubated at 72°C for 10 min. The PCR products were then extracted immediately with an equal volume of phenol-chloroform. Precipitation of the DNA was carried out by

addition of 0.1X volumes of 3M sodium acetate and 2X volumes of 100% ethanol. This was then spun in a microfuge at maximum speed for 5 min at room temperature to fully precipitate the DNA. The ethanol was discarded, and the pellet was rinsed with 80% ethanol and left to air dry. The pellets were resuspended in sterile H₂O to the starting volume of the DNA amplification reaction (usually 100µl) in preparation for ligation into the TA cloning vector pCR®3.1.

2.11.2 Ligation of PCR Products into Eukaryotic Bidirectional TA Cloning Vector pCR®3.1

The A-tailed primary PCR products were ligated into the plasmid pCR®3.1 by the following procedure. For each ligation reaction one vial of vector pCR®3.1 was centrifuged briefly to collect all of the sample at the bottom of the tube. In order to optimise the efficiency of the ligation reaction the formula below was used to estimate the amount of PCR product required to ligate with 60ng (20 fmoles) of pCR®3.1 vector:

$$X \text{ ng PCR product} = \frac{(Y \text{ bp PCR product}) (60 \text{ ng pCR®3.1 vector})}{(\text{size in bp of pCR®3.1: } 5044 \text{ bp})}$$

Where "X" ng is the amount of PCR product of "Y" base pairs to be ligated for a 1:1 (vector:insert) molar ratio. The protocol for this system recommends that a 1:2 (vector:insert) ratio be used. For the purposes of this study not only a 1:2 (vector:insert) molar ratio was used. 1:3 and 1:10 (vector:insert) molar ratios were also used in an attempt to optimise the ligation reaction.

A typical ligation reaction would consist of:

X μ l	Fresh PCR product
1 μ l	10X Ligation Buffer
2 μ l	pCR®3.1 vector (30ng/ml)
1 μ l	T4 DNA Ligase
Sterile H ₂ O to 10 μ l total volume	

The ligation reaction was incubated at 14°C for a minimum of 4 hours, usually overnight.

2.11.3 Transformation of One Shot™ TOP 10F' Competent Cells

Vials containing the ligation reactions were centrifuged briefly and placed on ice. For each ligation/transformation one 50 μ l vial of One Shot™ TOP 10F' competent cells were thawed on ice. 2 μ l of β -mercaptoethanol was added to each vial of the competent cells and mixed by stirring gently with the pipette tip. Then, 2 μ l of each ligation reaction was added directly into the competent cells and mixed gently. The reaction vials were then incubated on ice for 30 min. At this point, any remaining ligation mixtures were stored at -20°C. The reaction vials were then heat shocked for exactly 30 seconds in a 42°C water bath, taking care not to mix or shake the reactions at this point. The vials were removed from the 42°C water bath and immediately placed on ice for 2 min. Then 250 μ l of SOC medium (section 2.2.7) was added to each reaction (at room temperature). The reaction vials were then shaken at 37°C for 1 hour at 225rpm in a rotary shaking incubator. The vials containing the transformed cells were then placed on ice. Both 50 μ l and 200 μ l samples were taken from each

transformation vial and spread on separate LB agar plates containing 50µg/ml ampicillin. After all of the liquid had been absorbed, the plates were inverted and placed in a 37°C incubator overnight.

2. 12 General Techniques Used for the Manipulation of cDNA

2.12.1 Agarose Gel Electrophoresis of cDNA

Various agarose concentrations, gel volumes and combs were used for the separation of DNA fragments. The number of samples and the degree of separation required between DNA fragments determined the gel volume. The choice of comb was governed by the sample volume. Differing degrees of band separation were achieved by varying the agarose concentration. High molecular weight species are separated better at low agarose concentrations whereas lower molecular weight bands are resolved better at higher concentrations. 1.0% and 1.3% (w/v) were typical agarose concentrations used.

Example: For a 100ml 1.0% agarose gel, 1g of agarose was dissolved in 100ml distilled water by heating in a microwave until boiling point was reached. On cooling, 2ml 50x TAE buffer (section 2.2.2) was added and the solution was mixed before pouring onto an appropriate gel-former sealed with tape. A comb was inserted and the gel was left to set at room temperature for approximately 15 min. The tape was removed from the gel-former before transferring the gel and gel-former to the electrophoresis tank containing 1 litre of 1x TAE buffer, sufficient to completely cover the gel and fill the sample wells on removal of the comb. The samples to be

loaded were prepared by addition of approximately 1/4 volume 5x DNA loading buffer (section 2.2.2). This serves to ensure that the samples sink to the bottom of the wells as the loading buffer is more dense than the electrophoresis buffer because of the presence of glycerol. Samples were mixed and loaded directly into the wells by pipetting. 10 μ l of loading buffer containing 25 μ g/ml *BstE* II-cut lambda DNA ladder was loaded into a well adjacent to the samples. 50 μ l of 10mg/ml ethidium bromide was added to the electrophoresis buffer and the electrodes were connected such that the negative electrode was connected to the well-end of the gel. Samples were electrophoresed at 50-100mA using an LKB 2197 power supply until the dye front had migrated to the appropriate distance; usually approximately two thirds the length of the gel. DNA was visualised under ultra-violet light using an ultra-violet transilluminator. Correctly sized DNA species were identified by their migration relative to the lambda ladder markers. A gel photograph was taken using a Mitsubishi video copy processor.

2.12.2 Alcohol Precipitation of cDNA

0.2 volumes of ethanol, stored at 4°C, was added to the DNA sample in a 1.5ml Eppendorf tube. After vortexing, the solution was incubated at -20°C for at least 1 hour, or at -80°C for 30 min. DNA was pelleted by centrifuging at 16000 x g for 30 min. The supernatant was removed and the pellet washed with 300-500 μ l of 70% ethanol, centrifuging at 16000 x g for 15 min to re-pellet the DNA. The supernatant was removed and the pellet allowed to dry in air for 10 min before resuspending in an appropriate volume of sterile water.

2.12.3 Restriction Digestion of cDNA

Restriction digestion of cDNA and plasmid DNA was performed by the addition of restriction enzyme(s) to the DNA in an appropriate buffer containing the optimum salt concentration and pH for the individual enzyme. When DNA was to be cleaved with two enzymes, the digests were carried out simultaneously if both enzymes had the same buffer requirements. Alternatively, the DNA was first digested with the enzyme requiring the buffer of lowest ionic strength and/or temperature, and then the appropriate amount of sodium chloride and second enzyme was added. A typical reaction contained 0.5-1.0 μ g of DNA in a reaction volume of 10 μ l per 1 μ g of DNA. 1 volume of the appropriate 10x buffer was added to 9 volumes of the reaction volume before addition of the restriction enzyme. This was mixed and incubated for 3 hours at 37°C (unless otherwise stated, depending on the specific enzyme). Reactions were terminated by addition of 1/4 volume of 5x DNA loading buffer and the reaction volume loaded onto an agarose gel for analysis by electrophoresis.

2.12.4 Separation of PCR Fragments by Agarose Gel Electrophoresis

20 μ l of 5x DNA gel loading buffer was added to the PCR reaction mixture on completion of the cycling procedure. The entire reaction volume was loaded onto a 1.3% agarose gel alongside a lambda ladder marker (section 2.1.1). A current of 100mA was applied until the dye front had migrated a suitable distance to obtain sufficient resolution of PCR fragments to enable excision from the gel with minimal contamination of non-specific products.

2.12.5 Elution of DNA Fragments from Agarose Gel Slices by Electrophoresis

DNA fragments to be isolated were identified by size on an agarose gel under ultra-violet illumination. A gel slice containing the DNA band was excised from the gel and transferred to a piece of dialysis tubing, prepared as described in section 2.12.6, sealed at one end using a clip. 1ml of 1x TAE was added to the tubing which was then sealed at the other end. The tubing was transferred to an electrophoresis tank containing 1 litre of 1x TAE buffer. A weight (e.g. a gel comb) was applied to ensure that the gel slices were completely submerged in the buffer. A voltage of 150V was then applied for 2 hours. The direction of the current flow was reversed for approximately 30 sec before transferring the DNA solution to a sterile Eppendorf tube. At this point, the DNA solution was either stored frozen at -20°C or was passed through an Elutip-d column to further purify the DNA (see section 2.12.7)

2.12.6 Preparation of Dialysis Tubing for Electroelution

Approximately 10g of dialysis tubing (Visking, size 2 Inf Dia 18/32") was cut into pieces of 3-4cm in length and transferred to a 500ml glass beaker. 500ml of 2% NaHCO₃ 10mM EDTA was added and the tubing was incubated in the boiling solution for 10 min. After washing with distilled water, the tubing was stored in 50% ethanol, 50% water containing 1mM EDTA at 4°C. Prior to use the tubing was boiled in distilled water for 10 min.

2.12.7 Purification of DNA Using Elutip-d Affinity Columns

The DNA to be purified was extracted from the gel into 1x TAE buffer as described in section 2.12.5. An Elutip-d affinity column was firstly prepared by gently forcing 1-2ml of high salt solution (section 2.2.2) into the column. This serves to pre-wash the column matrix. A second syringe (5, 10 or 20ml depending on sample size) was loaded with 5ml of low salt solution (section 2.2.2) and this was passed through the column to ensure that all the high salt solution had been removed from the matrix before application of the DNA sample. The same syringe was loaded with the DNA sample and this, together with a 0.4 μ m cellulose acetate Elutip pre-filter was attached to the column. Use of the filter ensures the removal of any particulates from the sample. All of the sample was forced through the filter and column at a flow rate of 1-2ml/min to ensure complete absorption of the DNA to the column matrix. The same syringe was loaded with 2-3ml of low salt solution which was passed through the column, washing any remaining DNA sample from the filter and syringe into the column. 0.4ml of high salt solution was then passed through the column without the filter attached to elute the DNA from the matrix. The eluate was collected in a 1.5ml Eppendorf tube, and the DNA further concentrated by alcohol precipitation, as described in section 2.12.2

2.12.8 Dephosphorylation of Double Stranded DNA using Calf Intestinal Phosphatase (CIP)

CIP catalyses the removal of 5'-phosphate groups from DNA fragments to prevent re-ligation. Plasmid DNA was cleaved with the appropriate restriction enzyme(s) for 3 hours and then treated with RNase A for 15 min at 37°C. The reaction volume was made up to 100µl by addition of the dephosphorylation buffer (provided with the enzyme), 10 units of CIP and the appropriate volume of sterile water. Reactions were carried out at 37°C for 2 hours. Plasmid cDNA was isolated from the enzyme reagents by passing through an Elutip-d column and alcohol precipitation as described above.

2.12.9 Ligation of Double-Stranded cDNA

cDNA fragments were ligated to plasmid cDNA by the following procedure. In order to increase the efficiency of ligation, the reaction was performed with various chimeric GLUT cDNA: plasmid cDNA molar ratios; i.e. 2:1, 5:1 and 10:1. 100ng of plasmid which had been CIP-treated was added to chimeric GLUT cDNA at a relevant molar ratio and the mix incubated overnight at 14°C in the presence of 3 units of T4 DNA ligase in 10x ligation buffer. Ligation reactions were stored at -20°C. Competent bacteria were then transformed with 5-10ml of the ligation reaction as described in section 2.12.11.

2.12.10 Preparation of Competent *E. coli* (JM109) Cells

10µl of a frozen stock of JM109 cells were used to streak an LB plate. After incubation at 37°C for 12-16 hours, a single colony was used to inoculate 3ml of sterile LB medium which was incubated for 12-16 hours at 37°C whilst shaking. 500µl of this starter culture was transferred to a 1 litre flask containing 50ml of sterile LB. The cells were grown at 37°C whilst shaking for 2 hr before being harvested by centrifugation at 6000 x g at 4°C for 5 min. The supernatant was discarded and the cell pellet resuspended in 20ml of ice-cold 100mM CaCl₂ solution. The suspension was incubated on ice for 20 min before harvesting the cells as previously described. The cell pellet was resuspended in 4ml of ice-cold 100mM CaCl₂ solution and incubated at 4°C for at least 1hr (NB. Cells remain competent at 4°C for up to 24 hours).

2.12.11 Transformation of Competent *E. coli* (JM109) Cells

200µl of competent cells (section 2.12.10) were transferred to a pre-chilled 13.5ml Falcon tube to which 5-10µl of the ligation mix is added. The tubes were incubated on ice for 40 min to allow uptake of the DNA by the competent cells. Transformation is terminated by heat-shocking the cells at 42°C for 45 sec, followed by incubation on ice for 5 min. 0.8ml of sterile LB is then added and the cells incubated at 37°C whilst shaking for 1 hour. After centrifugation at 6000 x g for 5 min at 4°C, 0.9ml of the supernatant was discarded and the cells were resuspended in the remaining 100µl which was plated out immediately onto LB agar plates containing 50µg/ml ampicillin. The liquid was allowed to dry, the plates were inverted and incubated at 37°C for 12-16 hours.

2.12.12 Transformation of Ultracompetent *E.coli* (JM109) Cells

Ultracompetent cells were purchased from Promega and stored at -70°C. Cells were thawed by incubation in an ice-bath for 5 min and mixed by flicking the tube. A 100µl aliquot (per transformation) was transferred to a pre-chilled 1.5ml Eppendorf tube. 5-10µl of the ligation mixture was added to the cells which were mixed gently and immediately incubated on ice for 10 min. The transformation was terminated by heat-shocking the cells at 42°C for 45 sec, and incubating on ice for 2 min. 900µl of SOC medium (section 2.2.7) was added and the cells were grown for 1 hour at 37°C in a shaking incubator at 225rpm. 100µl of the transformation mixture was plated onto LB plates containing 500µg/ml ampicillin. The remaining 900µl was centrifuged at 6000 x g for 10 min to pellet the cells. 800µl of the medium was removed and the cells resuspended in the remaining 100µl which was also plated as described. The plates were incubated at room temperature for 15 min to dry, then inverted and incubated at 37°C for 12-16 hours.

2.12.13 Preparation of Small Amounts of Plasmid DNA Using the QIAGEN QIAprep 8 Turbo Miniprep Kit

Colonies of interest were picked with sterile tips and dropped into universals, each containing 3ml of LB medium containing 50µg/ml ampicillin. These were grown overnight at 37°C in a shaking incubator. 1.5ml of culture was removed, placed in a microfuge tube and centrifuged for 15 min in a microfuge at full power to pellet the cells. Pelleted bacterial cells were resuspended in 250µl of Buffer P1 until no cell clumps were visible. 250µl of Buffer P2 was added to each sample, the tubes were gently

inverted and the samples were incubated at room temperature for 5 min. During this incubation the QIAVac 6S vacuum manifold was prepared for use. 350µl of Buffer N3 was added to each sample and the tubes were inverted immediately 4-6 times. The resulting lysates were pipetted into the wells of the Turbofilter strips (850µl per well), and the vacuum was applied until all of the samples had passed through the Turbofilter. The QIAPrep strips containing the cleared lysates were then transferred to the top plate of the QIAVac 6S and the vacuum was re-applied until all samples were drawn through the QIAPrep strips. The QIAPrep strips were then washed by adding 1ml of Buffer PB to each well and applying the vacuum. A further wash of the QIAPrep strips was achieved by washing through with 1ml of Buffer PE and applying the vacuum. This step was then repeated. After Buffer PE in all wells had been drawn through, maximum vacuum was applied to the wells for 5 min in order to dry the membrane. The QIAPrep strips were then blotted with absorbent paper to remove any residual Buffer PE. To elute the DNA from the QIAPrep strips, 100µl of 10mM Tris-HCl; pH 8.5, or H₂O, was added to the centre of each well of the QIAPrep strips. The QIAPrep strips were allowed to stand for 1 min and then maximum vacuum was applied for 5 min. The DNA produced was stored at -20°C.

This technique was used to produce rapid, moderate yields of plasmid DNA that could be used in restriction digestion analysis to check that the correct plasmid construct was being expressed by the bacterial cells.

2.12.14 Preparation of Small Amounts of Plasmid cDNA

Colonies of interest were picked with sterile tips and dropped into universals, each containing 3ml of LB medium containing 50 μ g/ml ampicillin. These were grown overnight at 37°C in a shaking incubator. 1.5ml of culture was removed, placed in a microfuge tube and centrifuged for 15 min in a microfuge at full power to pellet the cells. The supernatant was then discarded and the pellet resuspended in 100 μ l of glucose buffer (section 2.2.2) with extensive vortexing. This was incubated on ice for 15 min, then 200 μ l of 1% SDS in 0.2M NaOH was added and the tube gently inverted 5 times. The tube was incubated on ice for 10-20 min, or until viscous. 300 μ l of 3M K⁺/5M Ac was added, the tube inverted gently 5 times, and incubated on ice for a further 5 min before centrifuging in a microfuge for 5 min. The supernatant was removed to a fresh tube, 5 μ l of 1mg/ml RNase A was added and incubated at 37°C for 15 min. One phenol extraction, two phenol/chloroform (1:1 v/v) extractions, and two chloroform/isoamylalcohol (24:1 v/v) washes of the supernatants were performed, retaining each time the upper aqueous phase. After the final wash, 0.3 volumes of 3M sodium acetate and 2.5 volumes of 100% ethanol were added to precipitate the cDNA. This was incubated at -20°C for at least one hour before pelleting the cDNA by centrifugation for 30 min in a microfuge. The ethanol was removed, the pellet washed with 70% ethanol, and centrifuged for another 30 min before drying under vacuum. The pellet was resuspended in 20 μ l of sterile water. 1 μ l of this was added to 1ml of sterile water and the absorbance measured at 260nm. The concentration was determined from the calculation described in section 2.12.7.

This technique was used to produce greater yields of high quality plasmid DNA that could be used in transfection and sequencing.

2.12.15 Large Scale Preparation of Plasmid DNA Using QIAGEN QIAprep Plasmid Maxi Preparation Kits

This method of plasmid preparation is based on the modified alkaline lysis procedure and on the adsorption of DNA onto an anion-exchange resin in the presence of low-salt. The kits contain various buffer solutions and columns and the protocols are designed for the purification of up to 500µg plasmid DNA from an appropriate volume of an overnight culture of *E. coli* cells in LB medium.

Components supplied with kits:

Buffer P1 (Resuspension Buffer)	50mM Tris.HCl; pH8.0, 10mM EDTA, 100µg/ml RNase A; stored at 4°C
Buffer P2 (Lysis Buffer):	200mM NaOH, 1% SDS
Buffer P3 (Neutralisation Buffer)	3M KOAc; pH5.5; stored at 4°C
Buffer QBT (Equilibration Buffer)	750mM NaCl, 50mM MOPS; pH7.0, 15% ethanol, 0.15% Triton-X-100
Buffer QC (Wash Buffer)	1M NaCl, 50mM MOPS; pH7.0, 15% ethanol
Buffer QF (Elution Buffer)	1.25M NaCl, 50mM Tris.HCl; pH8.5, 15% ethanol
TE	10mM Tris.HCl; pH8.0, 1mM EDTA

STE

100mM NaCl, 10mM Tris.HCl; pH8.0,
1mM EDTA

Plasmid Maxi Preparation Protocol

A colony of cells containing the plasmid to be purified was used to inoculate 3ml of sterile LB containing the appropriate antibiotic(s). This was incubated whilst shaking at 37°C for 12-16 hours. From this starter culture 0.5ml was transferred to 300ml of sterile LB plus antibiotic(s) which was then incubated whilst shaking at 37°C for a further 12-16 hours. Cells were then harvested by centrifugation at 4000 x g for 10 min at 4°C, and the bacterial pellet resuspended in 10ml of Buffer P1. The pellet was resuspended completely such that no cell aggregations remained. 10ml of Buffer P2 was added and the solution mixed gently by inverting the tube 4-6 times. After incubation at room temperature for 5 min, 10ml of chilled Buffer P3 was added, the tubes mixed gently and incubated on ice for 20 min. After centrifugation at 20000 x g for 30 min at 4°C in a Beckman JA-20 rotor, the supernatant was promptly transferred to clean tubes and recentrifuged for a further 15 min. The supernatant was removed promptly and transferred to a QIAGEN-tip 500 equilibrated with 10ml of Buffer QBT. The QIAGEN-tip was then washed with 2x 30ml of Buffer QC. Plasmid DNA was eluted by application of 15ml of Buffer QF to the tip, which was allowed to empty by gravity. DNA was precipitated with 0.7 volumes of room-temperature isopropanol, followed by immediate centrifugation at 15000 x g for 30 min at 4°C. The supernatant was carefully removed and the DNA pellet washed with 5ml of 70% ethanol. recentrifuged, air-dried for 5 min at room temperature and redissolved in a suitable volume of sterile H₂O. A sample of the plasmid solution was analysed by agarose gel electrophoresis.

2.12.16 Large Scale Preparation of Plasmid cDNA

Solutions:

Buffer 1	50mM glucose, 10mM EDTA, 25mM Tris; pH 8.0
Buffer2	1% SDS, 0.2M NaOH 5M KOAc (Prepared fresh on day of use)
Buffer3	60ml 5M KOAc, 11.5ml acetic acid, 28.5ml st. H ₂ O
PEG	20% PEG (Mol. wt. 6000), 2.5M NaCl
Other solutions	TE Buffer 5M Lithium Chloride 3M NaOAc

All procedures following initial cell harvesting were carried out on ice.

A colony of cells containing the plasmid to be purified was used to inoculate 3ml of sterile LB containing the appropriate antibiotic(s). This was incubated shaking at 37°C for 12-16 hours. From this starter culture 0.5ml was transferred to 500ml of sterile LB plus antibiotic(s) which was then incubated shaking at 37°C for a further 12-16 hours. Cells were then harvested by centrifugation at 4°C for 10 min at 4000 x g. The resulting supernatant was carefully decanted from the pellet which was resuspended completely in 25ml of Buffer 1. 25ml of Buffer 2 was slowly added whilst swirling the solution on ice. To this, 25ml of Buffer 3 was added followed by thorough mixing. Centrifugation at 4°C for 10 min at 4000 x g, resulted

in a clear supernatant which was transferred to clean 250ml Beckman centrifuge tubes by filtering through a double thickness of fine muslin. 100ml of isopropanol (room temperature) was added and mixed thoroughly before incubating at -20°C for 15 min. The DNA was precipitated by centrifugation at 4°C for 10 min at 4000 x g, and the resulting supernatant discarded. The pellet obtained from the entire 500ml culture was resuspended in 7.5ml TE buffer and transferred to 50ml Beckman centrifuge tubes to which 10ml of 5M LiCl solution was added. After incubating on ice for 2-5 min, the solution was centrifuged at 4°C for 10 min at 4000 x g in a Beckman JA-20 rotor. The resulting supernatant was retained and transferred to a clean centrifuge tube. Two volumes of ice-cold 100% ethanol was added, the DNA solution was incubated at -20°C for 20 min, and precipitated by centrifugation as described for 20 min. The resulting pellet was rinsed with 70% ethanol and air-dried before resuspension in 0.5ml TE buffer. RNase A was added to 40µg/ml and the tubes incubated at 37°C for 15 min. 0.5 volumes of PEG solution was added, followed by an incubation period of 15 min on ice. After centrifugation the resulting pellet was resuspended in 0.6ml TE buffer and the DNA extracted once with phenol:chloroform and twice more with chloroform. 0.1 volumes of 3M NaOAc and 2 volumes of ice-cold 100% ethanol was added to the final extract, the solutions mixed thoroughly and incubated at -20°C overnight. After centrifugation at 16000 x g in a microfuge for 30 min, followed by a 70% ethanol rinse, the DNA pellet was air dried and resuspended in a volume of 100-200ml of sterile H₂O, depending on the size of the pellet. The purity and yield of the plasmid was determined as described in section 2.12.7.

2.12.17 Calculation to Determine the Plasmid cDNA Concentration and Purity

absorbance value of 1.0 at 260nm = 50 μ g/ml of dsDNA

absorbance value of "y" at 260nm = "y" x 50 μ g/ml of dsDNA

$$\frac{\text{absorbance at 260nm}}{\text{absorbance at 280nm}} = \text{"Z"}$$

cDNA has a lower protein concentration and has a higher purity when the value of "Z" is nearer to 2.0.

Chapter 3

Analysis of Amino and Carboxy Terminal GLUT4 Targeting Motifs in 3T3-L1 Adipocytes Using an Endosomal Ablation Technique

3.1 Aims

The aims of this chapter are :

1. To determine the gross intracellular targeting of the recombinant GLUT4 species TAG, LAG and FAG by employing the technique of sucrose density gradient centrifugation.
2. To examine the role of the N-terminal FQQI motif in GLUT4 trafficking by applying the compartment ablation technique to a GLUT4 species containing the mutation F⁵ to A⁵.
3. To examine the role of the C-terminal LL motif in GLUT4 trafficking by applying the compartment ablation technique to a GLUT4 species containing the mutation L⁴⁸⁹L⁴⁹⁰ to A⁴⁸⁹A⁴⁹⁰.
4. To investigate the co-localisation of recombinant GLUT4 mutants with wild-type GLUT4 in 3T3-L1 adipocytes.
5. To interpret the roles of the FQQI and LL motifs in GLUT4 trafficking within the context of a revised multi-compartment model for GLUT4 trafficking in adipocytes.

3.2 Introduction

The targeting of the insulin-responsive glucose transporter, GLUT4, to an intracellular compartment in adipocytes and muscle is one of the key features responsible for the unique insulin sensitivity of this transporter. The translocation of GLUT4 from an intracellular site to the plasma membrane in insulin-exposed cells is largely responsible for the 20-30-fold increase in glucose transport observed in these tissues [reviewed in Gould & Holman (1993)]. Ectopic expression of GLUT4 in a variety of cells has shown that the primary sequence of this protein contains sufficient information to direct it to a predominantly intracellular location in many cell types [Haney *et al.* (1991), Hudson *et al.* (1992), Thorens & Roth (1996)]. This is in contrast to other members of the glucose transporter family which are expressed primarily at the cell surface [Hudson *et al.* (1992), Brant *et al.* (1994), Haney *et al.* (1995), Hughes *et al.* (1992), Thomas *et al.* (1993)].

Several laboratories have attempted to define the molecular features of GLUT4 which dictate its intracellular sequestration and unique targeting properties in adipocytes. These studies have identified two motifs, both of which are found within the cytoplasmic domains of GLUT4, and which appear to be involved in regulating the unique intracellular distribution of this protein [Piper *et al.* (1992), Piper *et al.* (1993b), Corvera *et al.* (1994), Verhey & Birnbaum (1994), Verhey *et al.* (1995), Haney *et al.* (1995), Marsh *et al.* (1995)] (reviewed in section 1.6).

The first of these motifs is found within the amino-terminal cytoplasmic domain of the protein (sequence F⁵QQI⁸) [Piper *et al.* (1992), Piper *et al.* (1993b), Marsh *et al.* (1995)]. Interestingly, this motif is similar to the

tyrosine-based internalisation motifs identified in plasma membrane proteins which undergo endocytosis, such as the mannose-6-phosphate receptor and transferrin receptor [Collawn *et al.* (1990), Johnson & Kornfeld (1992a), Johnson & Kornfeld (1992b)]. Such motifs are typically represented by an aromatic amino acid, usually tyrosine, at position 1 and a bulky hydrophobic amino acid at position 4 (YXXØ, where Y is an aromatic amino acid, X is any amino acid and Ø is an amino acid with a bulky hydrophobic group). Present knowledge suggests that there may be further subclasses of tyrosine-based endocytosis signals and it is possible that the phenylalanine-based motif identified within GLUT4 may be a further example of such a signal [Naim & Roth (1994)].

The second region identified within GLUT4 as being important in the control of subcellular distribution is contained within the carboxy-terminal cytoplasmic domain of the protein, and contains a di-leucine motif [Verhey *et al.* (1993), Corvera *et al.* (1994), Verhey & Birnbaum (1994)]. When expressed at relatively high levels in adipocytes GLUT4 containing the mutation L⁴⁸⁹L⁴⁹⁰ to A⁴⁸⁹A⁴⁹⁰ accumulated at the plasma membrane. In contrast, at more moderate levels of expression, the di-leucine mutant was targeted indistinguishably from endogenous GLUT4 in adipocytes. However, when expressed in CHO cells, this mutation causes a 10-fold reduction in the internalisation of GLUT4 from the cell surface [Garippa *et al.* (1996)]. Such observations are consistent with numerous other studies where di-leucine (or isoleucine-leucine) motifs have been shown to be important endocytosis signals in other proteins, such as mannose-6-phosphate receptors and the interferon γ -receptor [Letourneur & Klausner (1992), Hunziker & Fumey (1994), Marks *et al.* (1996)].

Both tyrosine-based endocytosis signals and di-leucine motifs have been suggested to interact with adaptor proteins which regulate entry into clathrin coated pits, either at the cell surface or at the TGN; the major site of protein sorting [Pearse & Robinson (1990), Heilker *et al.* (1996), Seaman *et al.* (1996)]. In the context of GLUT4 it has been suggested that both of these motifs can regulate internalisation of the protein from the plasma membrane [Verhey & Birnbaum (1994), Marsh *et al.* (1995), Yeh *et al.* (1995)]. As detailed above, previous studies in adipocytes have shown that GLUT4 mutants containing either F⁵ to A⁵ or L⁴⁸⁹L⁴⁹⁰ to A⁴⁸⁹A⁴⁹⁰ are targeted to the cell surface aberrantly [Marsh *et al.* (1995)]. This could either be due to decreased internalisation or reduced intracellular sequestration. It is not known if the above-mentioned motifs can perform other functions in GLUT4 trafficking. Such a scenario is possible as both aromatic and di-leucine based motifs have also been implicated in intracellular sorting; in particular in the assembly of proteins into TGN-derived clathrin and/or AP-3 coated vesicles [Letourneur & Klausner (1992), Pond *et al.* (1995), Ohno *et al.* (1996), Simpson *et al.* (1997), Dell'Angelica *et al.* (1997)]. These findings may be relevant to GLUT4, as it appears to traffic via the TGN as part of its normal recycling in 3T3-L1 adipocytes, rat adipocytes and cardiomyocytes [Slot *et al.* (1991a), Slot *et al.* (1991b), Slot *et al.* (1997)].

This study employed a technique known as compartment ablation (section 2.5.1-3) which enables greater resolution of the intracellular compartments containing GLUT4 in adipocytes [Martin *et al.* (1996), Livingstone *et al.* (1996)]. This technique relies on Tf-HRP internalisation via TfRs, and the delivery of the Tf-HRP ligand to the recycling endosomal system. Subsequent exposure of the cells to diaminobenzidine and hydrogen

peroxide generates a highly-reactive cross-linking species within the lumen of compartments which have taken up the Tf-HRP, and results in their subsequent ablation. This procedure selectively ablates markers for the recycling endosomal system (TfR, Rab5, cellubrevin) with little or no effect on markers for the TGN or lysosomes [Martin *et al.* (1996), Livingstone *et al.* (1996)]. Previous studies utilising this technique have shown that in resting 3T3-L1 adipocytes, GLUT4 is segregated into at least two discrete intracellular pools, one of which corresponds to recycling endosomes, contains ~40% of the intracellular GLUT4, and is enriched in markers for the recycling endosomal system (transferrin receptor, Rab5, cellubrevin). The second compartment is devoid of transferrin receptors, enriched in the synaptobrevin homologue VAMP2, contains ~60% of the intracellular GLUT4 and is not ablated after Tf-HRP loading. It is proposed that this represents a unique GLUT4 compartment which may function to regulate the plasma membrane GLUT4 content in response to insulin [Martin *et al.* (1996), Livingstone *et al.* (1996)].

In an effort to obtain a clearer picture of the role of the FQQI and di-leucine-containing motifs in the control of GLUT4 targeting, this study has applied the compartment ablation technique to the above mentioned GLUT4 mutants expressed in 3T3-L1 adipocytes. The study attempts to determine if disruption of either the FQQI motif in the GLUT4 amino-terminus or the di-leucine motif in the GLUT4 carboxy-terminus alters the distribution of GLUT4 between the recycling and the non-ablated compartments. The results show that mutation of L⁴⁸⁹L⁴⁹⁰ to A⁴⁸⁹A⁴⁹⁰ does not prevent GLUT4 from reaching the non-ablated compartment, but greatly reduces the amount of GLUT4 present in the recycling endosomal compartment. In the F⁵ to A⁵ mutant, the low levels of GLUT4 present

intracellularly are mainly accounted for by the presence of this species in the recycling endosomal system. These data are interpreted in light of new models for GLUT4 trafficking in adipocytes. In the context of these models I will argue that the FQQI and LL motifs play important role(s) in sub-endosomal trafficking of GLUT4 in adipocytes.

3.3 Materials and Methods

3.3.1 Human GLUT3 Epitope-tagged GLUT4 Transporters

The methodology detailing the construction of human GLUT3 epitope-tagged transporter cDNAs, and their stable transfection into 3T3-L1 fibroblasts is documented in Marsh *et al.* (1995).

3.3.2 Expression Levels of Recombinant GLUT4 Constructs in Adipocyte Cell Lines

The constructs employed in this study have been characterised in 3T3-L1 fibroblasts and adipocytes previously by subcellular fractionation and indirect immunofluorescence microscopy [Marsh *et al.* (1995)]. Multiple clonal cell lines expressing recombinant GLUT4 constructs at a range of expression levels were classified in two broad categories: low expressors, in which total GLUT4 expression was at a level comparable to that of endogenous GLUT4 in untransfected adipocytes, and high expressors, where total expression was >4-fold higher than endogenous GLUT4 expressed by non-transfected adipocytes. Hence, specific cell lines were selected for more detailed analysis based on the following:

(1) The distribution of epitope-tagged wild-type GLUT4 (hereafter referred to as TAG) is indistinguishable from endogenous GLUT4 in different cell lines with markedly different expression levels [Marsh *et al.* (1995)]. I have examined the clone expressing the highest levels of TAG (TAG3B1), as the intracellular sequestration of TAG in this cell line is maintained despite a level of total GLUT4 expression approximately 6-fold greater than that

observed in wild-type cells. Thus, the aim was to determine whether any evidence for the saturation of intracellular trafficking pathways could be found at this level of over-expression using endosomal ablation and immuno-electron microscopy. The immuno-electron microscopy studies detailed in this chapter were carried out by Sally Martin in the laboratory of Prof. D. E. James and are included for the purposes of comparison only.

(2) The aberrant targeting of GLUT4 containing the F⁵ to A⁵ mutation (FAG) is independent of expression level [Marsh *et al.* (1995)]. Thus, two clones expressing FAG at low levels, i.e. comparable to endogenous GLUT4 in non-transfected adipocytes (FAG3C2 and FAG2C5), were chosen to examine the effects of this mutation on the intracellular distribution of GLUT4.

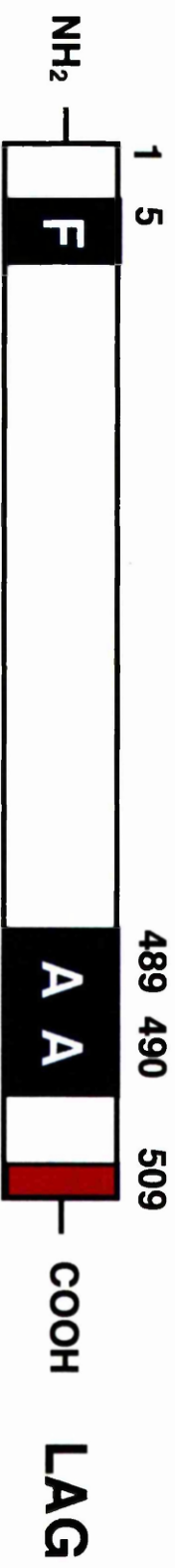
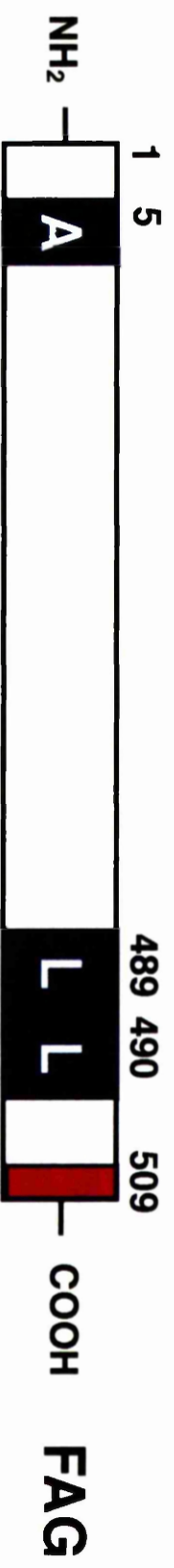
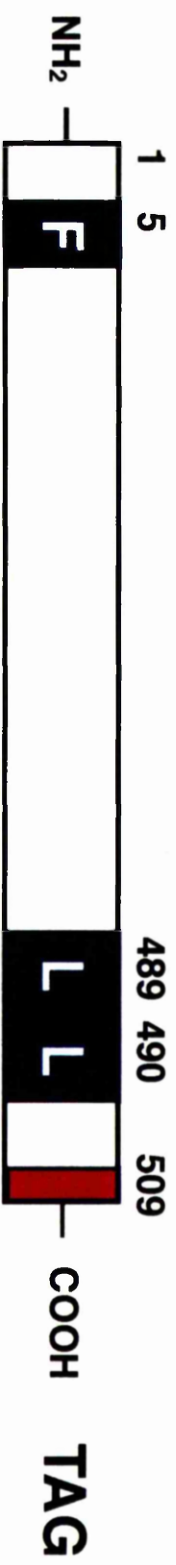
(3) The targeting of GLUT4 containing the L⁴⁸⁹L⁴⁹⁰ to A⁴⁸⁹A⁴⁹⁰ mutation (LAG) in adipocytes is dependent on the level at which it is expressed [Marsh *et al.* (1995)]. Thus, two clones with markedly different expression levels (LAG1D5 and LAG1D3, high and low expressors, respectively) were selected for further analysis by endosomal ablation and immuno-EM.

Figure 3.1 presents a schematic illustration of these mutants, and relative expression levels are listed in Table 3.1.

Figure 3.1

Schematic Representation of Human GLUT3 Epitope-Tagged Mutant GLUT4 Transporters

Summary of the recombinant GLUT constructs used in these studies. To discriminate between recombinant and endogenous GLUT4 in stably transfected 3T3-L1 adipocytes a foreign epitope encompassing the carboxy-terminal 12 amino-acid residues from human GLUT3 (red) was introduced at the extreme carboxyl-terminus of the full length GLUT4 cDNA. Wild-type GLUT4 epitope-tagged in this fashion is referred to as TAG. Epitope-tagged GLUT4 containing point mutations at either F⁵ or L⁴⁸⁹L⁴⁹⁰, are referred to as FAG and LAG respectively. The positions at which point mutations to alanine are present are shown in blue.



3.3.3 Immuno-electron Microscopy

Intracellular vesicles were prepared from 3T3-L1 adipocyte homogenates as described in section 2.5.5, and membrane vesicles fixed and stored at 4°C [Martin *et al.* (1996), Martin *et al.* (1997)]. Immunolabelling of vesicles was performed as described previously [Martin *et al.* (1997)]. Protein-A gold was provided by the Department of Cell Biology, University of Utrecht, The Netherlands. Anti-GLUT3 was diluted at 1:20, and anti- γ -adaptin diluted 1:100 for these studies.

3.3.4 Antibodies

The anti-GLUT4 antibodies used were a rabbit polyclonal antibody raised against a peptide comprising the carboxy-terminal 14 amino acid residues of the human isoform of GLUT4 [Brant *et al.* (1993)], or the corresponding region of the human isoform of GLUT3 [Shepherd *et al.* (1992)]. The affinity-purified polyclonal rabbit anti-serum generated against the cytoplasmic domain of the insulin-regulated aminopeptidase vp165 used in this study was provided by Prof. G. E. Leinhard (Dartmouth Medical School). Anti- γ -adaptin was supplied by Dr. M. S. Robinson (University of Cambridge) and anti-transferrin receptor antibody was from Upstate Biotechnology Inc. (Lake Placid, NY.).

3.3.5 Computer Modelling of GLUT4 Trafficking

This study modelled the distribution of GLUT4 between multiple intracellular compartments. Simulations were performed using models described previously [Holman *et al.* (1994), Verhey *et al.* (1995), Yeh *et al.*

(1995)]. The distribution of GLUT4 between three compartments at steady-state was modelled using the following equations [Yeh *et al.* (1995)]:

$$(k_{\text{endo}} \cdot X_{\text{pm}}) - (k_1 \cdot X_{\text{ee}}) - (k_{\text{seq}} \cdot X_{\text{ee}}) + (k_4 \cdot X_{\text{irv}}) = 0$$

$$(k_{\text{seq}} \cdot X_{\text{ee}}) - (k_4 \cdot X_{\text{irv}}) - (k_2 \cdot X_{\text{irv}}) = 0$$

$$(k_1 \cdot X_{\text{ee}}) - (k_{\text{endo}} \cdot X_{\text{pm}}) + (k_2 \cdot X_{\text{irv}}) = 0$$

X_{pm} = the fraction of GLUT-4 at the plasma membrane

X_{ee} = the fraction in the endosomal compartment

X_{irv} = the fraction in the insulin-responsive compartment

The rate constants employed in this analysis were k_{endo} , k_1 , k_{seq} , k_2 and k_4 and are shown in the schematic model of Figure 3.10. Values for these rate constants were derived from studies of GLUT4 trafficking in adipocytes described elsewhere [Yang *et al.* (1992a), Yang *et al.* (1992b), Yang & Holman (1993), Holman *et al.* (1994), Araki *et al.* (1996)]. The steady-state distribution of GLUT4 among these three compartments was determined from equations described in detail previously [Yeh *et al.* (1995), Araki *et al.* (1996)]. Estimated values of some of these rate constants for mutant GLUT4 species were based upon the results presented in [Garippa *et al.* (1994), Araki *et al.* (1996), Garippa *et al.* (1996)]. Simulations were performed on a PC using the kinetic simulation software package K-SIM (N. Miller, University of California, Los Angeles, CA) with the assistance of Dr. A. R. Warmsley, Division of Infection and Immunity, University of Glasgow.

3.4 Results

3.4.1 Buoyant Density Analysis of TAG, LAG and FAG Mutants

In an attempt to determine the effects of the F⁵ to A⁵ (FAG) and L⁴⁸⁹L⁴⁹⁰ to A⁴⁸⁹A⁴⁹⁰ (LAG) mutations on the trafficking of GLUT4, I initially employed the technique of sucrose density gradient centrifugation to investigate the buoyant density of these mutants in adipocyte subcellular membranes. This analysis provides information regarding the gross targeting of TAG, LAG and FAG rather than yielding detailed information on the specific intracellular compartments to which these exogenous GLUT4 mutants are trafficked. LDM membranes from these mutants were separated by centrifugation on sucrose gradients and the distribution of mutant GLUT4 determined by immunoblotting with anti-GLUT3 antibodies. This membrane fraction contains the majority of the intracellular endogenous GLUT4. The results of this analysis are presented in Figure 3.2.

Immunoblotting of the subcellular membrane fractions revealed that endogenous GLUT4 was observed to sediment primarily in fractions 3 to 8. Previous studies have shown that such fractions are also enriched for Rab5 (fractions 2 to 6), TGN38 and the transferrin receptor (fractions 3 to 9) [Livingstone *et al.* (1996)].

TAG was observed to sediment in a very similar fashion to endogenous GLUT4, confirming previous studies which have shown an identical subcellular distribution for this species [Marsh *et al.* (1995)] (Figure 3.2). The di-leucine mutant, LAG, was also found to sediment at similar

densities, suggesting that the gross targeting of this mutant was not significantly disrupted (Figure 3.2).

In contrast, analysis of the distribution of the small pool of intracellular FAG indicated that this protein was confined to a more restricted fraction of intracellular vesicles (fractions 3 and 4) (Figure 3.2). These fractions have been previously shown to be highly enriched for early endosomal markers such as Rab5 [Livingstone *et al.* (1996)]. Over 85% of the intracellular FAG was present in these two fractions, indicating that the intracellular distribution of FAG may be distinct from either endogenous GLUT4, TAG or LAG. It should be noted that the expression levels of the clones expressing FAG (FAG3C2 and FAG2C5) examined in this study resemble endogenous GLUT4 in non-transfected adipocytes, suggesting that the mistargeting of FAG within intracellular membranes is a consequence of mutation of the amino-terminal motif rather than of overexpression of this mutant species.

A graphical representation of the comparative buoyant density profiles of the above mutants is provided by Figure 3.3.

3.4.2 Compartment Ablation Analysis of TAG, LAG, FAG Mutants

In this study the technique of compartment ablation (sections 2.5.1-1, 3.2) was employed to examine the intracellular distribution of the recombinant GLUT4 constructs TAG, LAG and FAG, with the aim of determining whether such mutations alter the distribution of GLUT4 between the ablated (endosomal) and non-ablated pools.

In these experiments, duplicate plates of 3T3-L1 adipocyte clones were loaded with Tf-HRP for 1hr or 3hr at 37°C, or alternatively for 1hr at 4°C (as a control as no Tf-HRP is internalised under these conditions). The ablation reaction was performed on half of the plates ('ablated'), the other half were treated identically but peroxide was not added ('control'). The LDM fraction was then prepared from control and ablated cells, and the level of the heterologously expressed GLUT4 mutants determined by quantitative immunoblotting with GLUT3 antibodies. The results of this type of analysis for all of the clones are summarised in Table 3.1. TAG3B1 exhibits a pattern of ablation essentially identical to that of endogenous GLUT4 (Figure 3.4). Importantly, this demonstrates that despite a level of total GLUT4 expression approximately 6-fold greater than that observed in non-transfected adipocytes, over-expression of wild-type GLUT4, at least to the level achieved here, does not result in an increased proportion of GLUT4 residing in the endosomal system.

In contrast, intracellular LAG was found to be almost completely resistant to ablation after loading with Tf-HRP, implying that the majority of this protein is not present in the recycling endosomal system (Figure 3.4). FAG has previously been shown to exhibit a predominantly plasma membrane localisation [Marsh *et al.* (1995)]. The small intracellular fraction of this mutant however was readily ablated after Tf-HRP loading (Figure 3.4). Two clonal cell lines expressing FAG at low levels, or LAG at low and high levels, were independently examined and gave identical results for each mutant (Table 3.1). This strongly argues that the results do not reflect overexpression or clonal variation for either of the constructs. For each clone, the efficiency of ablation was monitored by parallel examination of the extent of ablation of the TfR (Figure 3.5).

3.4.3 Co-localisation of Recombinant GLUT4 Mutants with Wild-type GLUT4 in 3T3-L1 Adipocytes.

In an attempt to determine the extent of co-localisation of the mutant species with endogenous GLUT4 and the aminopeptidase vp165/IRAP (a protein known to co-localise with GLUT4 in adipocytes [Martin *et al.* (1997)]), intracellular vesicles containing the epitope-tagged constructs were immunoadsorbed using GLUT3 antibodies. The use of monoclonal IF8 (or other anti-GLUT4 antibodies) in this regard is disadvantaged by the fact that this epitope recognises both the endogenous GLUT4, and the expressed recombinant species; however, the use of anti-GLUT3 should result in only vesicles containing the mutant species being isolated.

Immunoisolations using anti-GLUT4 monoclonal antibody IF8 were performed for the recombinant GLUT4 mutants, TAG and LAG. Unfortunately the intracellular levels of FAG were too low to obtain reliable data using this approach. In all cases, it was observed that such immunoadsorptions quantitatively depleted the LDM fraction of both the expressed mutant species and the insulin-responsive aminopeptidase vp165/IRAP (data not shown). From such studies, it is not possible to definitively conclude that the expressed mutant species co-localise with GLUT4, nevertheless, the data are suggestive of such co-localisation. Further evidence in favour of such co-localisation was provided by the previous demonstration that both TAG and LAG exhibit insulin-stimulated translocation to the plasma membrane to an extent comparable to that exhibited by the endogenous GLUT4 [Marsh *et al.* (1995)]. If TAG or LAG were significantly mis-targeted, insulin-stimulated translocation would not be expected. Although neither of these observations are

definitive, both argue strongly that TAG and LAG populate the same intracellular compartments as the endogenous GLUT4.

More definitive conclusions can be drawn from experiments in which anti-GLUT3 antibodies were used to specifically immunoisolate vesicles containing the epitope-tagged mutant species from the intracellular membrane fractions. The results of these experiments are presented in Figure 3.6 for TAG and LAG. I was unable to quantitatively immunodeplete LDM membranes of immunoreactive GLUT3 using this approach, perhaps as a consequence of the low affinity of this antibody for its epitope. However, in several experiments of this type, I examined the depletion of intracellular membranes of GLUT3 and compared this to the depletion of vp165/IRAP in the same samples (Figure 3.7). For each of the clones examined, the depletion of GLUT3 from the LDMs (between 50 and 70% for both TAG and LAG; Figure 3.6) is mirrored by a depletion of vp165 from the same LDM fractions (Figure 3.7). It has recently been shown that in adipocytes, GLUT4 and vp165 exhibit essentially complete co-localisation using immuno-EM [Martin *et al.* (1997)]. Hence, the data of Figure 3.7 further argues that the recombinant expressed GLUT4 mutants exhibit a high degree of co-localisation with endogenous GLUT4. Recombinant GLUT4-containing vesicles isolated using anti-GLUT3 antibodies were also immunoblotted with antibodies specific for vp165 (Figure 3.7). Both TAG- and LAG- containing vesicles were observed to contain significant levels of vp165. These results, together with previous studies demonstrating that both TAG and LAG exhibit insulin-stimulated translocation, argue strongly that the recombinant species exhibit substantial co-localisation with endogenous GLUT4 and vp165/IRAP.

A parallel series of experiments were performed using anti-vp165 antibodies to immunoadsorb vesicles. Immunoadsorption with anti-vp165 antibodies was found to result in a significant depletion of the LDM membrane fraction of recombinant GLUT4 species. As was the case using anti-GLUT3 antiserum, I was unable to quantitatively deplete LDMs of either vp165 or recombinant GLUT4 using this approach. However, these results show that for both TAG and LAG, intracellular vesicles isolated using anti-vp165 antibodies contain recombinant GLUT4 (Figure 3.8). Taken together, these data argue that both TAG and LAG co-localise significantly with vp165/IRAP in these cells, and thus, by analogy, with endogenous GLUT4.

3.4.4 Co-localisation of GLUT4 with γ -adaptin

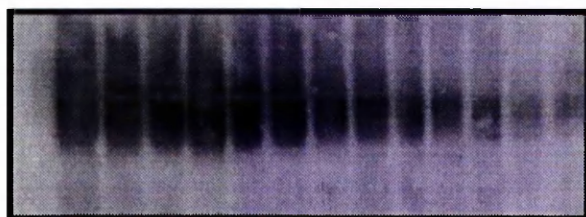
To complement my attempts to define the intracellular trafficking of the recombinant GLUT4 species LAG, immunogold-EM was employed (by Sally Martin in the laboratory of Prof. D. E. James, University of Queensland) to co-localise TAG and LAG with γ -adaptin, a component of the AP-1 complex (Figure 3.9 and Table 3.2). Unfortunately, the low level of intracellular FAG precluded similar analysis of this mutant. Comparison of TAG with the low-level expressing LAG clone (LAG1D3), demonstrates that in this case, LAG exhibits increased colocalisation with γ -adaptin (24.4% *cf.* 37.8%, respectively). However, inspection of the data obtained for the high-expressing clone LAG1D5 showed that it does not exhibit similar increased colocalisation (Table 3.2). This may be a consequence of the expression level-dependent mis-sorting of LAG [Marsh *et al.* (1995)]. The inability to detect differences in the level of γ -adaptin associated with TAG or LAG containing vesicles may be complicated by the

presence of endogenous GLUT4 within these vesicles which would be expected to interact with the γ -adaptin regardless of the presence of recombinant species within the same vesicle. Therefore, interpretation of the role of the L⁴⁸⁹L⁴⁹⁰ motif in interaction with AP-1 is not possible from these data. However, these results provide further evidence to show that a significant overlap exists between GLUT4 and γ -adaptin in intracellular membranes isolated from 3T3-L1 adipocytes, and provides a compelling argument in favour of the involvement of the TGN in the trafficking of GLUT4.

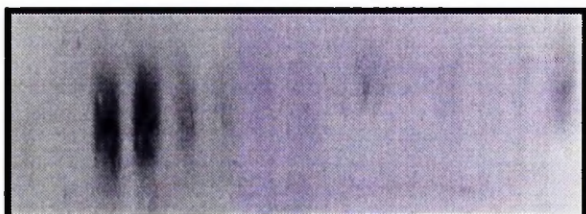
Figure 3.2

Buoyant Density Analysis of TAG, LAG and FAG Mutants

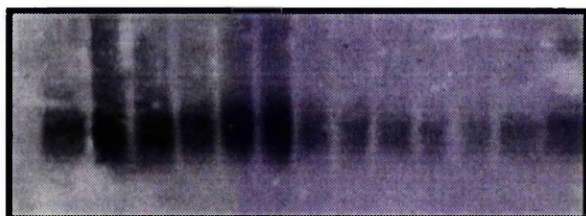
Low density microsomal membranes were prepared from the indicated 3T3-L1 adipocyte cell clone and analysed by sucrose gradient centrifugation as outlined in section 2.5.5. Fractions from a 1.5-0.5M sucrose gradient were loaded on a 10% SDS gel from left to right. 20µg protein from each fraction was loaded onto the gel. The position of the GLUT3 epitope-tagged mutant GLUT4 species was then determined by immunoblotting (section 2.9.3) with anti-GLUT3 antibodies. Data from a representative experiment is shown using TAG3B1 (TAG), FAG3C2 (FAG) and LAG1A5 (LAG). Similar data were obtained using FAG2C5 and LAG1D3 (data not shown). By way of comparison, the distribution of endogenous GLUT4 in non-transfected adipocytes is shown (GLUT4).



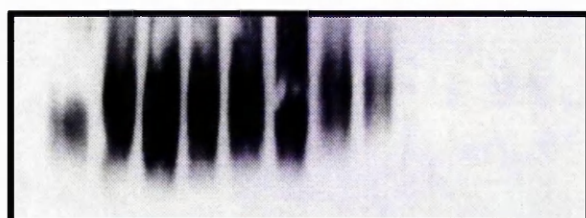
TAG



FAG



LAG



**Native
GLUT4**



[Sucrose]

Figure 3.3

Buoyant Density Profiles of TAG, LAG and FAG Mutants

This is a graphical illustration of the buoyant density profiles of the TAG, LAG and FAG mutants. The immunoreactivity of the fractions is represented by arbitrary units, with the fraction containing the highest level set = 1 unit.

Buoyant Density Profiles of TAG, LAG and FAG Mutants

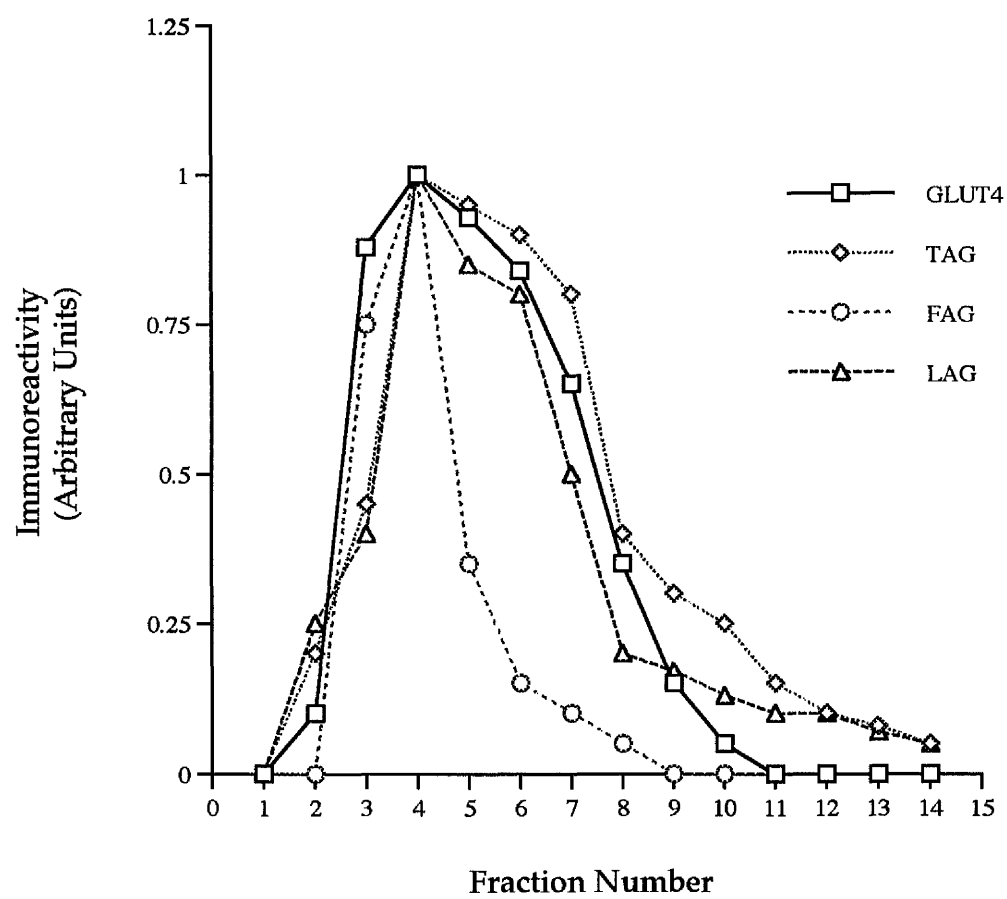
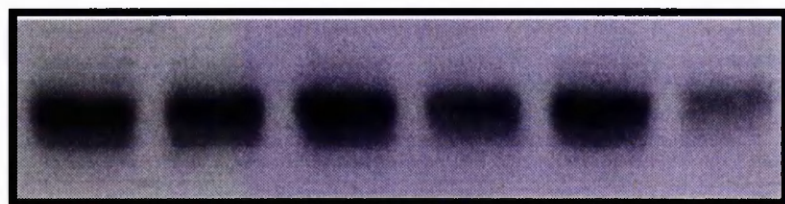


Figure 3.4

Compartment Ablation Analysis of TAG, LAG and FAG Mutants

LDM membranes were prepared from 3T3-L1 adipocytes loaded with Tf-HRP for 1hr at 4°C, 1hr at 37°C or 3hr at 37°C, before and after ablation (- and + hydrogen peroxide) as indicated. Figure 3.4 shows experiments for each of the mutant GLUT4 species examined (TAG=TAG3B1; FAG=FAG3C2; LAG=LAG1A5 experiments are shown). In these experiments, cells were loaded with Tf-HRP as indicated and the cells exposed to DAB in the presence and absence of peroxide as indicated. LDM membranes were prepared, 20µg of each fraction were electrophoresed and immunoblotted using anti-GLUT3 antibodies to study the effect of ablation on the intracellular content of each of the clones. Several blots of this type from at least three independent experiments were quantitated and the results are presented in Table 3.1.



TAG



FAG



LAG

- + - + - +
└───┘ └───┘ └───┘

4°C

1h 37°C

3h 37°C

Table 3.1

Effect of Compartment Ablation on Intracellular GLUT4 Levels

The relative levels of total GLUT4 expression (arbitrary units) in the cell lines examined in this study have been determined previously [Marsh *et al.* (1995)]. Clones were classified into two broad categories based on the total level of GLUT4 expressed by wild-type 3T3-L1 adipocytes. TAG3B1 and LAG 1A5 are high expressor clones, whereas FAG3C2, FAG2C5 and LAG 1D3 were classified as low expressors. Duplicate sets of 10cm plates were loaded with Tf-HRP for 1hr or 3hr at 37°C. After this time, the DAB cytochemistry was performed as described in section 2.5.2, with hydrogen peroxide added to one plate but not to the other. LDM membranes were prepared, and the GLUT3 immunoreactive signal quantified. The difference in signal between the plates incubated \pm peroxide represents the extent of protein ablation (Figure 3.4). Detailed opposite is the signal remaining in the LDM fraction **after** ablation expressed as a percentage of the signal in the LDM **before** ablation (mean \pm S.D. determined from three independent experiments). In all experiments, an additional control experiment was performed in which the cells were incubated with Tf-HRP at 4°C then ablated. Under these conditions, no internalisation of Tf-HRP is expected, and consistent with this no ablation of either the recombinant GLUT4 constructs or endogenous GLUT4 was observed (Figure 3.4). Values for endogenous GLUT4 were from plates of non-transfected adipocytes, measured using the same batches of Tf-HRP conjugate employed for analysis of the mutants.

Table 3.1**Effect of Compartment Ablation on Intracellular GLUT4 Levels**

<u>Species</u>	<u>Expression Level</u>	<u>% Signal Remaining after Ablation</u>	
		1hr at 37° C	3hr at 37° C
wt GLUT4	1.96	64 ± 3%	59 ± 8%
TAG3B1	11.48	62 ± 8%	60 ± 9%
FAG3C2	3.88	56 ± 7%	25 ± 10%*
FAG2C5	2.64	53 ± 5%	18 ± 9%*
LAG1A5	8.25	96 ± 7%	98 ± 3%
LAG1D3	2.54	92 ± 8%	89 ± 7%

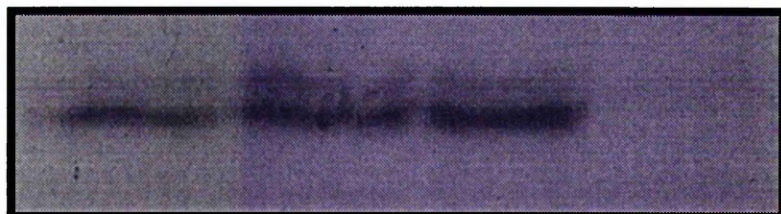
* Statistically significant difference from signal at 1hr (p<0.01)

Figure 3.5

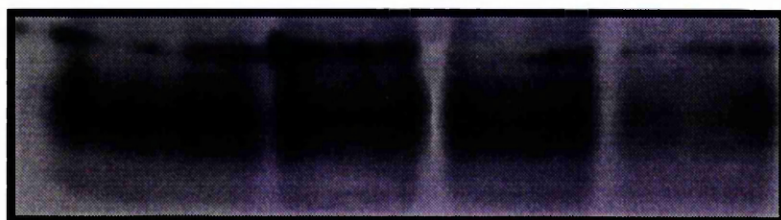
Comparative Compartment Ablation Analysis of TAG

LDM membranes (20 μ g protein) from TAG3B1 were immunoblotted with either anti-transferrin receptor (upper panel) or anti-GLUT3 antibodies (lower panel). Note that incubation of cells at 4°C with Tf-HRP did not result in any ablation of the transferrin receptor from the LDM membranes; in contrast, incubation of cells with Tf-HRP for 3hr at 37°C resulted in a peroxide-dependent loss of TfR from LDM membranes; under the same conditions, TAG3B1 ablation was much less pronounced.

α TFR



α Glut3



-

+

-

+

4°C
3h

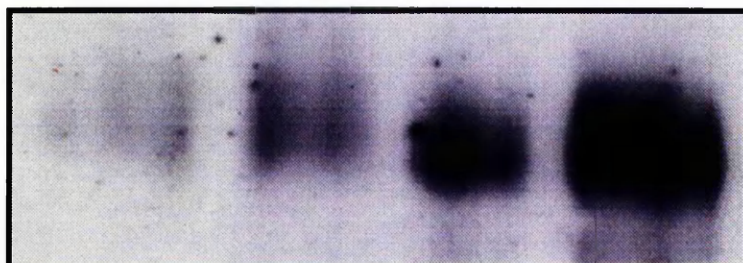
37°C
3h

Figure 3.6

Immunoabsorption of Vesicles containing Mutant GLUT4 Species

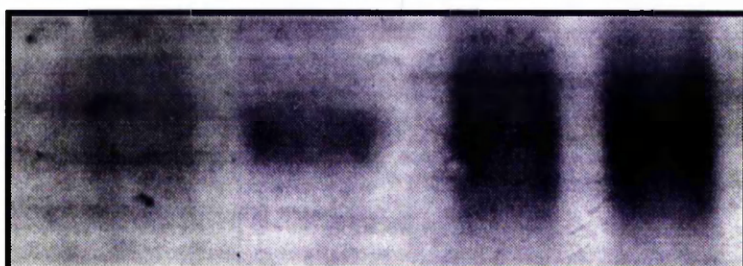
LDM membranes were incubated with anti-GLUT3 antiserum linked to *Staph. a.* cells to selectively immunoabsorb vesicles containing the expressed mutant GLUT4 species (section 2.5.5). 100µg of LDM membranes and 10µg of anti-GLUT3 antiserum were employed per immunoabsorption. Resultant vesicles and LDM fractions (20µg protein per fraction) were immunoblotted using anti-GLUT3 antiserum to determine the intracellular location of epitope-tagged mutant species.

TAG



Glut3

LAG



Glut3

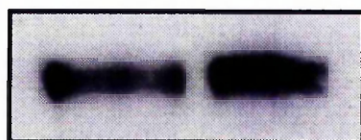
IgG	Glut3	Glut3	IgG
Vesicles		LDMs	

Figure 3.7

Co-localisation of vp165 and Mutant GLUT4 Species in 3T3-L1 Adipocytes

LDM membranes were incubated with anti-GLUT3 antiserum linked to *Staph. a.* cells to selectively immunoadsorb vesicles containing the expressed mutant GLUT4 species (section 2.5.5). 100µg of LDM membranes and 10µg of anti-GLUT3 antiserum were employed per immunoadsorption. Resultant vesicles and LDM fractions (20µg protein per fraction) were immunoblotted using affinity purified anti-vp165 antibody to determine the extent of co-localisation of vp165 and epitope-tagged mutant GLUT4 species.

TAG



Vp165/IRAP

LAG



Vp165/IRAP

IgG Glut3
└─────────┘
Vesicles

Glut3 IgG
└─────────┘
LDMs

Figure 3.8

Isolation of vp165 Vesicles and Co-localisation with Mutant GLUT4 Species

LDM membranes were incubated with affinity purified anti-vp165 antibody linked to *Staph. a.* cells to selectively immunoadsorb vesicles containing the aminopeptidase vp165 (section 2.5.5). 100µg of LDM membranes and 2µg of affinity purified anti-vp165 antibody were employed per immunoadsorption. Resultant vesicles and LDM fractions (20µg protein per fraction) were immunoblotted using anti-GLUT3 antiserum to determine the extent of co-localisation of vp165 and epitope-tagged mutant GLUT4 species.

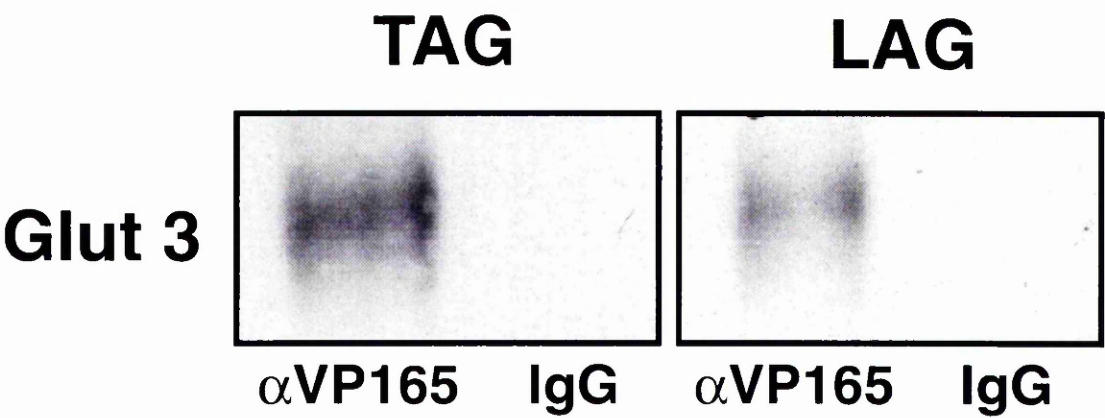
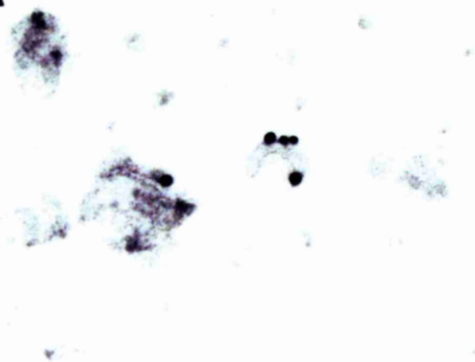


Figure 3.9

Immuno-electron Microscopy of γ -adaptin and Recombinant GLUT4 in Isolated Vesicles

Intracellular vesicles were prepared from 3T3-L1 adipocytes expressing either LAG (Panels A-D) or TAG (Panels E-F). Vesicles adsorbed to formvar/ carbon-coated copper grids were double-labelled using antibodies specific for γ -adaptin (15nm gold) and the human GLUT3 epitope (10nm gold). Bar = 100nm. Several experiments of this type were quantified and the results are presented in Table 3.1.

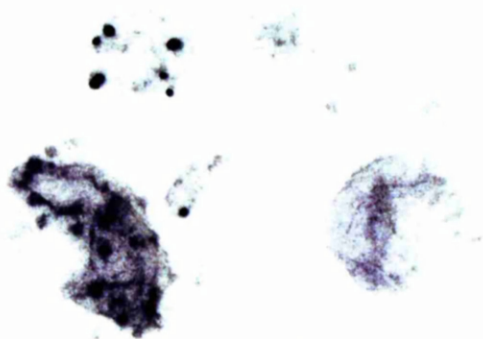
A



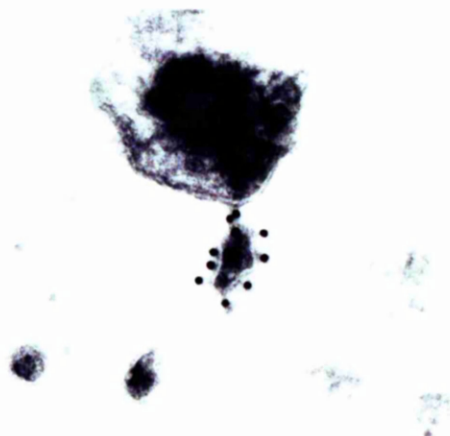
B



C



D



E



F

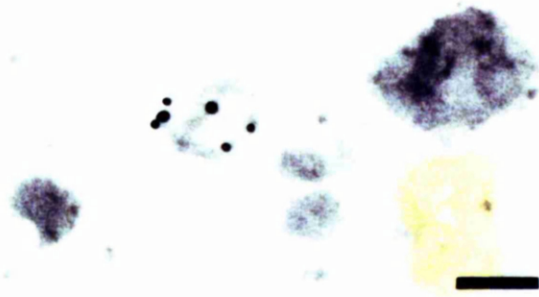


Table 3.2

**Co-localisation of γ -adaptin and GLUT4 Mutants by
Immuno-electron Microscopy**

Intracellular vesicles from the indicated mutant cell lines were used for immunogold EM as outlined in section 3.3.3. These results show the extent of colocalisation of epitope-tagged recombinant transporters with γ -adaptin, and are the results of four independent experiments. The number of vesicles labelled with the indicated antibodies is shown. Colocalisation was determined using two sizes of gold particles to detect either γ -adaptin or recombinant GLUT4 molecules. The percentage of TAG/LAG containing vesicles containing γ -adaptin is shown for TAG3B1 and the two LAG clones examined (LAG1A5 and LAG1D3). Also shown is the percentage of TAG or LAG gold particles present within γ -adaptin positive vesicles.

Table 3.2
Colocalisation of γ -adaptn and GLUT4 mutants by EM

Mutant	% total vesicles labelled with anti- γ -adaptn	% total vesicles labelled with anti-GLUT3	% TAG or LAG vesicles containing γ -adaptn	% TAG or LAG gold particles present in γ -adaptn containing vesicles
	(Mean \pm s.d.)	(Mean \pm s.d.)	(Mean \pm s.e.m)	(Mean \pm s.e.m)
TAG3B1	5.4 \pm 0.6	7.4 \pm 1.4	24.0 \pm 3.7	24.4 \pm 2.9
LAG 1A5	4.6 \pm 0.5	3.8 \pm 2.2	26.9 \pm 2.3	28.5 \pm 3.8
LAG1D3	7.5 \pm 0.9	6.0 \pm 3.4	37.1 \pm 2.7	37.8 \pm 3.8

3.5 Discussion

As a first step towards understanding the subcellular trafficking of the above mutants, I employed sucrose gradient centrifugation analysis to examine the gross targeting of the TAG, FAG and LAG mutants in the intracellular membranes of 3T3-L1 adipocytes (Figure 3.2). TAG and LAG exhibited broadly similar patterns of buoyant density on sucrose gradients to that observed for endogenous GLUT4, suggesting that these species were targeted to similar membrane compartments (Figure 3.2). In contrast FAG exhibited a much more restricted pattern of buoyant density and thus may be mis-targeted in the intracellular membranes of 3T3-L1 adipocytes (Figure 3.2).

It has been shown that the F⁵ to A⁵ substitution (FAG) results in the accumulation of the majority of FAG at the plasma membrane [Marsh *et al.* (1995)]. Despite this mis-targeting, the low level of the FAG mutant that remains in the intracellular LDM fractions retains its insulin-responsiveness in 3T3-L1 adipocytes. This indicates that the presence of FAG in the LDM fraction represents its targeting to an intracellular compartment, rather than a plasma membrane contamination of the LDM fraction. Furthermore, the insulin regulatability of FAG implies that it has not been grossly mis-targeted but rather is localised to a compartment similar to endogenous GLUT4. Using the Tf-HRP ablation procedure, I have observed that the intracellular fraction of this protein can be extensively ablated by Tf-HRP loading, to an extent far greater than either TAG or the native endogenous GLUT4 (Figure 3.4 and Table 3.1). This result argues that the portion of FAG present intracellularly is localised to a TfR containing compartment, most probably the recycling endosomal

system. Furthermore, this observation argues that FAG is unable to gain access to, or does not accumulate in, the non-ablated compartment.

The ablation efficiency of LAG expressed at either low or high levels was markedly reduced compared to either TAG or wild-type GLUT4, , implying that the majority of this mutant, in contrast to FAG, is not localised to the recycling endosomal system (Figure 3.4 and Table 3.1). The observation that LAG is expressed in an intracellular location and capable of insulin-stimulated translocation to the plasma membrane suggests that the gross targeting of this species to an insulin-sensitive location(s) is not impaired [Marsh *et al.* (1995)]. However, compared to either wild-type GLUT4 or TAG, this species exhibits little or no ablation after Tf-HRP load, implying that in the basal state, LAG is effectively sequestered into the non-ablated compartment and does not extensively populate the recycling endosomal system. One possibility is that LAG is shuttled into a separate intracellular compartment distinct from both the recycling endosome and that housing GLUT4. This is unlikely because (1) the buoyant density of LAG-containing membranes is similar to that of endogenous GLUT4, (2) insulin stimulates LAG translocation to an extent comparable to endogenous GLUT4 [Marsh *et al.* (1995)], and (3) vesicle immunoadsorption data has shown that LAG co-fractionates with another marker for the intracellular GLUT4 compartment, the aminopeptidase vp165 (see below).

The analysis of the epitope-tagged mutant species in this fashion does not, however, definitively address the issue of co-localisation with the endogenous GLUT4 protein. I therefore undertook a series of vesicle immunoadsorption experiments to study the overlap of the mutant GLUT4 species with the endogenous GLUT4 and the insulin-regulated

aminopeptidase vp165 to specifically address this point (Figures 3.6-8). This analysis employed anti-GLUT3 antiserum to selectively immunoadsorb membranes containing the expressed mutant species. Using this approach I was unable to quantitatively deplete intracellular membranes of GLUT3. For each clone of TAG and LAG examined, we have observed between 50 and 70% depletion of immunoreactive GLUT3 from the LDM fraction (Figure 3.6). Depletion of vp165 was consistently observed in the same membrane fractions (Figure 3.7) arguing in favour of co-localisation of these proteins. Furthermore, vp165 was also observed in intracellular vesicles isolated from both TAG and LAG clones using anti-GLUT3 antibodies (Figure 3.7). Such data provide compelling evidence that both TAG and LAG exhibit considerable co-localisation with endogenous vp165, and thus by analogy, endogenous GLUT4. Immunoadsorption of LDM membranes using anti-vp165 was also attempted as a means to study the co-localisation of these proteins. Recombinant GLUT4 was consistently observed in vp165-containing vesicles isolated from TAG and LAG, consistent with at least partial overlap of these proteins (Figure 3.8). The inability to quantitatively immunodeplete LDMs of either GLUT3 or vp165 using these two antibodies has precluded a more detailed analysis of their colocalisation in these cells. However, the fact that both TAG and LAG exhibit insulin-stimulated translocation to the plasma membrane to an extent similar to that of native GLUT4 strongly argues that these two recombinant proteins are appropriately localised in 3T3-L1 adipocytes.

3.5.1 Interpretation of Mutant GLUT4 Trafficking Between Multiple Intracellular Compartments

I have attempted to interpret this data in the light of the previous kinetic models describing the intracellular distribution of GLUT4 in adipocytes [Yeh *et al.* (1995), Araki *et al.* (1996)]. These studies imply that mutating either F⁵ to A⁵ or L⁴⁸⁹L⁴⁹⁰ to A⁴⁸⁹A⁴⁹⁰ disrupts the intracellular distribution of GLUT4 within the endosomal/TGN system. This supports the contention that GLUT4 is partitioned between at least two intracellular compartments in adipocytes, and that this distribution is signal mediated [Slot *et al.* (1991a), Slot *et al.* (1991b), Holman *et al.* (1994), Slot *et al.* (1997)]. Mathematical models of GLUT4 trafficking in adipocytes have suggested the presence of at least two intracellular GLUT4 pools [Holman *et al.* (1994), Yeh *et al.* (1995)]. The first corresponds to a recycling endosomal compartment (X_{ee} in Figure 3.10), which represents the compartment to which GLUT4 is internalised from the plasma membrane. The second pool is segregated from the recycling endosomal pool, and has been referred to as the tubulo-vesicular compartment (X_{tv} in Figure 3.10). It has been suggested that this pool may serve to regulate the cell surface levels of GLUT 4 in response to insulin [Holman *et al.* (1994), Yeh *et al.* (1995)]. Using this model, I argue that X_{ee} is analogous to the ablated compartment and X_{tv} to the non-ablated compartment; X_p is the plasma membrane pool.

This analysis of both endogenous GLUT4 and TAG3B1 using the ablation technique suggests that the distribution of these proteins between X_{ee} and X_{tv} is roughly 40% and 60% respectively. Using the model of Figure 3.10, simulations were performed to model this distribution (Table 3.3). By mathematical modelling of the steady-state distribution of GLUT4 between

the two intracellular compartments (X_{ee} and X_{tv} in Figure 3.10), it can be shown that at steady-state the ratio of the distribution of GLUT4 between these two compartments is given by:

$$X_{ee} / X_{tv} = (k_2 + k_4) / k_{seq}.$$

and that this ratio is independent of the endocytosis rate (k_{endo}) [Holman *et al.* (1994), Araki *et al.* (1996)]. To model a distribution akin to that proposed from ablation analysis dictates refinement of the estimate for the values of either k_{seq} or k_4 , which have been used in other studies [Holman *et al.* (1994)]. As shown in Table 3.3, it is possible to model a reasonable approximation of the subcellular distribution by decreasing k_{seq} , with no effect on k_4 . This model gives both a reasonable fit to the measured subcellular distribution, and also adequately models changes in GLUT4/TAG distribution in response to insulin. However, this model may be inadequate to explain all aspects of the phenotypes of the mutant species examined here. These are discussed further below.

3.5.2 LAG and FAG Mutant Distribution

Intracellular FAG exhibited increased ablation compared to either TAG or wild-type GLUT4, suggesting that this protein was not efficiently sorted into the non-ablated GLUT4 pool (X_{tv} in Figure 3.10). Furthermore, >90% of the LAG is in a non-ablated compartment. Invoking the model of Figure 3.10, this implies that one of the consequences of the di-leucine substitution is to decrease the ratio X_{ee} / X_{tv} , and in the case of FAG, this ratio is considerably increased. Thus, the phenotype of these mutants must be explained by alterations to one or more of three rate constants: k_2 , k_4 , or

k_{seq} . k_2 defines the movement of GLUT4 from the insulin-responsive intracellular compartment to the plasma membrane. k_2 is unlikely modulated by these mutations because (i) this rate is slow in the absence of insulin, and (ii) it is argued that the exocytosis of membrane/membrane proteins is defined by proteins which regulate movement of the vesicle rather than by the protein cargo itself (it should be noted that it has not been definitively established that the step defined by k_2 can actually occur *in vivo*). Hence, an explicit assumption of the model of Figure 3.10 argues that k_2 is regulated independently of the protein cargo.

Therefore, alterations in the ratio of X_{ee} / X_{tv} defined by ablation may reflect changes in k_4 and/or k_{seq} . Birnbaum and Holman have argued that k_4 is independent of transporter isoform (when comparing trafficking of GLUT4 and GLUT1 in adipocytes) [Yeh *et al.* (1995), Araki *et al.* (1996)]. Hence, one interpretation is that the di-leucine mutant may exhibit an increased rate of sequestration (k_{seq}). However, the assumption that k_4 is independent of transporter isoform has not been experimentally demonstrated. The possibility that sorting signals within GLUT4 may regulate such a step is plausible. I therefore set out to model the distribution of LAG within the model of Figure 3.10. Table 3.3 indicates that a reasonable fit to the observed data can be achieved by increasing k_{seq} by a factor of 2, coupled with a change in k_{endo} as has been proposed by others [Verhey *et al.* (1995), Yeh *et al.* (1995), Araki *et al.* (1996), Garippa *et al.* (1996)]. Because the ablation technique precludes kinetic analysis of trafficking, I have not attempted to further elaborate upon the kinetics outlined in Table 3.3. These simulations do however indicate that significant changes in transporter distributions can be modelled with only small changes in the rate constants for individual steps.

Within the context of the model of Figure 3.10, explaining the patterns of ablation of LAG requires that this mutation modulates sorting into the insulin-responsive (non-ablated) compartment, X_{tv} . Several studies have strongly argued that the di-leucine motif is not involved in the sorting of GLUT4 to an insulin-responsive compartment [Marsh *et al.* (1995), Verhey *et al.* (1995)]. As such, it is difficult to reconcile the behaviour of LAG within the model of Figure 3.10. I have therefore considered an alternative model of GLUT4 trafficking (Figure 3.11) which, although only hypothetical, can reasonably predict the behaviour of all the GLUT4 mutants studied to date.

3.5.3 An Alternative Model of GLUT4 Trafficking

I propose a modification of the model of Figure 3.10 to account for the behaviour of FAG and LAG in the ablation experiments. The revised model is shown in Figure 3.11. In this model, GLUT4 is initially internalised into an endosomal compartment (X_{ee}). From this compartment, GLUT4 is proposed to traffic into the TGN (X_{tgn}), and thence into the tubulo-vesicular storage compartment (X_{tv}) (this compartment may also derive in part directly from the endosomal compartment). The addition of the TGN in the trafficking scheme of GLUT4 was important for several reasons. Firstly, several studies using immuno-electron microscopy have provided compelling evidence in favour of GLUT4 recycling involving the TGN in both adipocytes and cardiomyocytes [Slot *et al.* (1991a), Slot *et al.* (1991b), Slot *et al.* (1997)]. Here it is shown that there is a significant overlap between GLUT4 and γ -adaptin, a component of the heterotetrameric adaptor complex associated with the TGN. Secondly, the addition of this extra compartment to the model of GLUT-4 trafficking

provides an attractive explanation for the observed phenotypes of LAG and FAG described above, and also for the sorting of further chimeric transporters observed by others without the need to invoke changes in k_{seq} and k_4 . Finally, it was felt important to consider that both X_{ee} and X_{tv} are capable of responding to insulin by moving cargo to the plasma membrane. X_{ee} is clearly insulin-responsive, as indicated by the insulin-stimulated movement of endosomal proteins (such as the TfR and GLUT1) to the plasma membrane [Tanner & Leinhard (1987), Calderhead *et al.* (1990), Robinson *et al.* (1992)]. Hence, in considering the behaviour of any mutant or chimeric GLUT4 species, this important point should be kept in mind. In the model of Figure 3.10 as considered by Yeh *et al.* (1995), X_{ee} was proposed to be minimally insulin-responsive. This important distinction will be returned to below.

This study proposes that the internalisation of GLUT4 into the early endosomes (X_{ee}) is dependent upon the well-characterised internalisation motifs, FQQI in the amino-terminus, and LL in the carboxy-terminus [Garripa *et al.* (1994), Garripa *et al.* (1996)]. The next step in this proposed trafficking pathway involves the sorting of GLUT4 into the TGN (X_{ee} to X_{tgn} in Figure 3.11). I suggest that this step is dependent upon the FQQI motif in the amino-terminus. If this were the case, FAG would be unable to sort further into the endosomal system, and thus be unable to reach the non-ablated compartments (X_{tgn} and X_{tv} in Figure 3.11). In contrast, both TAG and LAG would be predicted to gain access to X_{tgn} in this model, and thus be able to sort into X_{tv} . The possibility that the trafficking of GLUT4 from X_{ee} to X_{tgn} is dependent upon the interaction of coat-proteins with the FQQI motif in the amino-terminus is an attractive proposition. Recent studies have suggested that variants of the YXXØ-type sorting sequences

may exist which dictate subtly different sorting events for membrane proteins [Ohno *et al.* (1996)]. It is possible that FQQI may be a further example of this variation. If this motif were disrupted, then GLUT4 would be expected to become localised to the recycling endosomal system. Our ablation data (Table 3.1 and Figure 3.4) are consistent with this phenotype for the FAG mutant.

In the case of native GLUT4, recycling back to the cell surface would depend upon movement of GLUT4 from X_{tgn} to X_{ee} . On the basis of ablation results (Table 3.1 and Figure 3.4), I suggest that this step might be dependent upon the interaction of adaptor proteins with the LL motif within the carboxy-terminus. The sorting of some proteins at the TGN requires the formation of clathrin-coated vesicles, and is dependent upon the function of the AP-1 complex [Pearse & Robinson (1990), Page & Robinson (1995), Seaman *et al.* (1996)], although it should be noted that other proteins exit the TGN in non-clathrin coated vesicles. It has been shown that γ -adaptin (a component of the AP-1 complex) and GLUT-4 exhibit substantial co-localisation within 3T3-L1 adipocytes [Millar, C. A., Martin, S. M., James, D. E. and Gould, G. W. (unpublished data)]. Thus, the sorting of GLUT4 from X_{tgn} to X_{ee} might reasonably be proposed to be via a di-leucine motif-dependent interaction with AP-1. Such interactions of LL containing peptides with AP-1 have been clearly demonstrated for other recycling membrane proteins, such as the mannose-6-phosphate receptor [Sosa *et al.* (1993), Heilker *et al.* (1996)]. Thus, in the case of the LAG mutant, disruption of this motif would be predicted to result in LAG accumulation in either X_{tgn} or X_{tv} as a consequence of a reduced rate of movement from X_{tgn} to X_{ee} .

Based on evidence from several laboratories, it can be shown that Tf-HRP does not gain access to the TGN. This has been demonstrated by previous studies which showed no ablation of the TGN-marker protein TGN38 in adipocytes after Tf-HRP loading [Livingstone *et al.* (1996)], and also in other cell types using electron microscopy [Klumperman *et al.* (1993)]. Hence, the observed decrease in ablation of LAG compared to either native GLUT4 or TAG could be a consequence of this protein being preferentially localised to X_{tgn} and/or X_{tv} .

Although hypothetical, the model of Figure 3.11 offers an attractive framework within which to explain the expression level-dependent sorting of LAG, and also the behaviour of other mutant transporters. In a previous study, it was shown that when expressed at high levels, LAG exhibits mis-sorting to the cell surface [Marsh *et al.* (1995)]. This phenotype could be explained on the basis of a mis-sorting of LAG from X_{tgn} to X_{ee} when expressed at high levels. In this situation, the over-expression of the protein may effectively overcome the fidelity of sorting and result in the accumulation of LAG at the cell surface. Such a phenomenon has been reported for other recycling membrane proteins, notably the transferrin receptor [Warren *et al.* (1997)].

I have argued that FAG is confined to the ablated compartment (X_{ee}). However, some comment on the overall phenotype of FAG is appropriate. Previous studies have shown that although the majority of FAG is localised to the cell surface of adipocytes, insulin is capable of eliciting an increase in the cell surface FAG levels [Marsh *et al.* (1995)]. Thus, it could be proposed that the major function of firstly the FQQI motif and secondly the non-ablated compartment may be to remove GLUT4 from the recycling

pool and thus maintain low cell surface expression of GLUT4 in the absence of insulin. Although intracellular FAG is predominantly localised to the recycling pool, it still exhibits ready movement to the cell surface in response to insulin [Marsh *et al.* (1995)]. This suggests that the recycling endosomal pool (X_{ee}) is 'insulin-responsive', a suggestion which is consistent with the insulin-stimulated translocation of other proteins resident within endosomes, such as TfR and GLUT1 [Tanner & Leinhard (1987), Calderhead *et al.* (1990), Kandror *et al.* (1995), Kandror *et al.* (1996)]. For this reason, this study does not refer to the non-ablated compartment (X_{tv}) as the 'insulin-responsive' compartment. Although this pool is probably mobilised to the plasma membrane in response to insulin, we emphasise that the recycling pool should equally be considered insulin responsive.

This model can also provide a frame-work for interpreting other studies of GLUT4 targeting. For example, a chimera comprised of the GLUT4 amino-terminus and the GLUT4 carboxy-terminus: 4HB1 in [Verhey *et al.* (1995)] (Figure 1.6), would be predicted to sort into X_{tgn} but not gain access to X_{tv} . Thus, this protein would be efficiently sequestered away from the cell surface as a consequence of the presence of the FQQI motif; this would further allow movement of the chimeric species into X_{tgn} . However, subsequent sorting into X_{tv} would not be expected, as this sorting event is proposed to be mediated by signals in the carboxy-terminus of GLUT4 [Verhey *et al.* (1995), Marsh *et al.* (1995)]. Yeh and colleagues argue that 4HB1 is efficiently sequestered intracellularly, but is not insulin-responsive. In their kinetic analysis of the species, they explain this by suggesting that 4HB1 is localised to X_{ee} , which is minimally insulin-responsive [Yeh *et al.* (1995)]. As discussed previously, I propose that X_{ee} is

capable of insulin-stimulated movement to the plasma membrane, hence the addition of X_{tgn} provides a compelling explanation for the observed behaviour of this mutant [Verhey *et al.* (1995)].

The lack of kinetic data on the individual sorting events which define the model of Figure 3.11 preclude any kind of hypothetical kinetic analysis of the trafficking of GLUT4 through such a complex pathway. However, it can be argued that each component of this sorting pathway has a precedent in the published literature, and moreover the model offers an attractive scheme within which to interpret the behaviour of GLUT4 mutants defective in subcellular sorting. The application of the ablation technique to the study of GLUT4 mutants has clearly illustrated that individual targeting motifs within GLUT4 may function at more than one stage in the trafficking pathway of this protein. Both the amino-terminal FQQI motif and the carboxy-terminal LL motif could be reasonably argued to act at multiple points in the trafficking itinerary. Defining the mechanism behind these sorting events represents an important goal.

Figure 3.10

Modified Three-Pool Model of GLUT4 Trafficking

This model of GLUT4 trafficking proposes two major intracellular compartments, the endosomal pool (X_{ee}) and the "insulin-responsive" compartment (X_{irv}). In this model, GLUT4 can move from the "insulin-responsive" compartment to the cell surface (defined by the rate constant K_2). GLUT4 is viewed as being sequestered from the recycling pathway *via* a sequestration step (K_{seq}) in the basal state into the "insulin-responsive" compartment. This model is taken from Yeh *et al.* (1995).

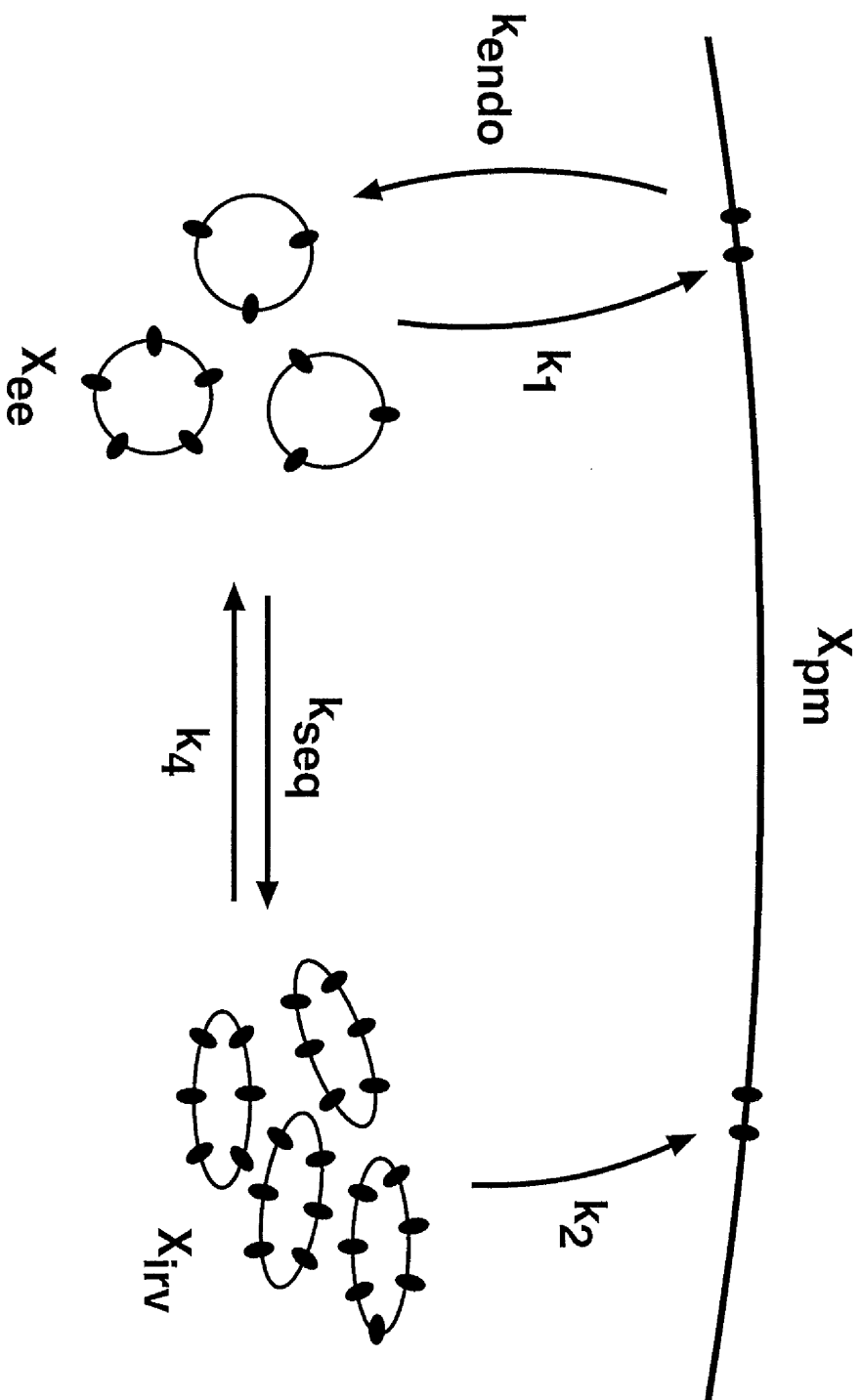


Figure 3.11

Alternative Model of GLUT4 Trafficking

This model represents a refinement of the 3-pool model of GLUT4 trafficking in Figure 3.10, in which an extra compartment, the *trans*-Golgi network (X_{tgn}), is considered as an integral compartment in GLUT4 recycling. Note that the sequestration of GLUT4 into X_{tv} may arise from either the endosomal (X_{ee}) or TGN (X_{tgn}) compartments in this model.

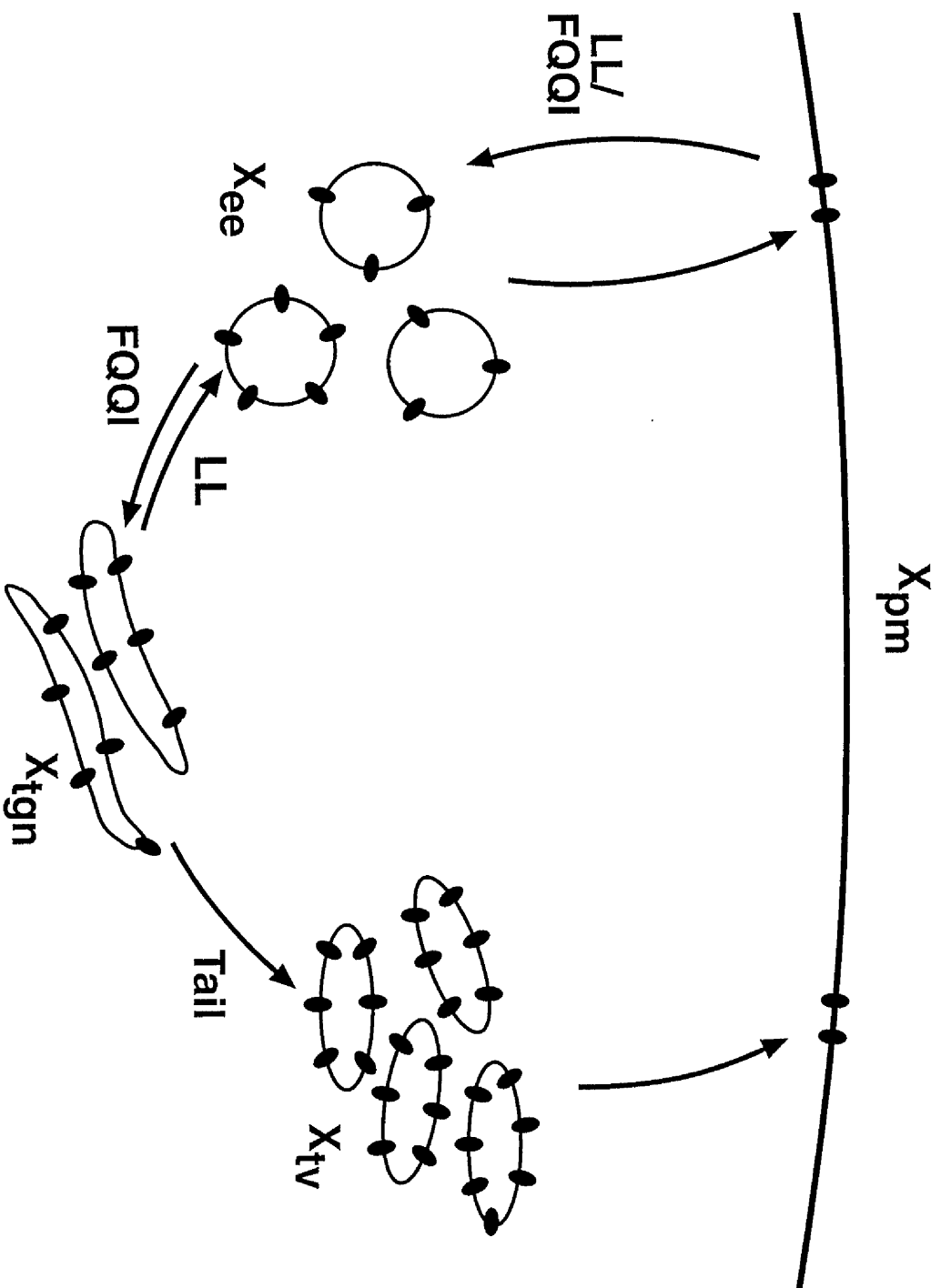


Table 3.3

Computer Modelling of GLUT4 and LAG Subcellular Distributions

Computer modelling of the steady-state distribution of GLUT4 between the three intracellular compartments shown in Figure 3.10 was performed. Shown are values of the individual rate constants employed in the simulations, and estimates of the % of GLUT4 between the three compartments is shown. In the case of the data indicated by *, the rate constants were those used by Yeh *et al.* (1995) to model GLUT4 distribution. In an effort to model a distribution between the X_{ee} and X_{irv} compartments more akin to the values obtained from the ablation experiments, some of the rate constants were modified and the resulting changes in GLUT4 distribution considered. The modified rate constants shown were those which gave the best fit to the data obtained from the ablation experiments. In the case of the LAG mutants, alterations to K_{endo} were in line with those reported by Yeh *et al.* (1996) and Garippa *et al.* (1996).

Table 3.3
Computer Modelling of GLUT4 and LAG Subcellular Distributions

	Rate Constants				Subcellular distribution (%)			
	k_{endo}	k_1	k_{seq}	k_4	k_2	PM	ENDO	IRV
GLUT4 (Bas)*	0.12	0.04	0.1	0.001	0.001	0.9	1.9	97.2
GLUT4 (Ins)*	0.08	0.012	0.1	0.001	0.1	41.1	29.6	29.3
GLUT4 (Bas)	0.12	0.04	0.005	0.001	0.001	7.5	26	65
GLUT4 (Ins)	0.06	0.015	0.005	0.001	0.1	71	27	1.4
LAG (Bas)	0.03	0.04	0.01	0.0005	0.001	13	11	74
LAG (Ins)	0.01	0.004	0.01	0.0005	0.1	82	16	1

3.6 Summary

In this study I have been able to resolve distinct effects of mutating either F⁵ (FAG) or L⁴⁸⁹L⁴⁹⁰ (LAG) to alanine residues, on the intracellular sorting of GLUT4 in adipocytes. FAG was predominantly expressed at the cell surface, but the small intracellular pool exhibited a more restricted pattern of buoyant density than the endogenous GLUT4. Furthermore, ablation analysis suggests that the intracellular population of FAG was extensively ablated in a fashion similar to other markers for the early endosomal compartment. I therefore propose that mutation of F⁵ to A⁵ results in the accumulation of GLUT4 in an early endosomal compartment, implying that this motif may be involved in the trafficking of GLUT4 out of early endosomes. LAG exhibited a normal distribution by buoyant density analysis, but in marked contrast to FAG, ablation analysis indicated that LAG was expressed predominantly in a non-ablated compartment. I suggest that the di-leucine motif may be involved in the movement of GLUT4 from the TGN to the recycling endosomal compartment. Based on these findings, I propose a new model for GLUT4 trafficking in adipocytes, which although only speculative at present, provides a rational model within which to interpret GLUT4 trafficking.

Chapter 4

Analysis of the Carboxy-terminal Phosphorylation Site in GLUT4 Trafficking

4.1 Aims

The aims of this chapter are:

1. To determine the gross intracellular targeting of the recombinant GLUT4 species TAG, SAG and DAG by employing the technique of sucrose density gradient centrifugation.
2. To examine the role of the major phosphorylation site on the sequence of GLUT4 in the trafficking of this glucose transporter isoform by applying the compartment ablation technique to a GLUT4 species containing the mutation S⁴⁸⁸ to A⁴⁸⁸.
3. To examine the role of the major phosphorylation site on the sequence of GLUT4 in the trafficking of this glucose transporter isoform by applying the compartment ablation technique to a GLUT4 species containing the mutation S⁴⁸⁸ to D⁴⁸⁸.
4. To determine the subcellular distribution of the recombinant GLUT4 species TAG, SAG and DAG in basal and insulin-stimulated adipocytes.

4.2 Introduction

It is widely acknowledged that the unique pattern of trafficking of the insulin-regulatable glucose transporter isoform, GLUT4, is responsible for its ability to facilitate the rapid and massive uptake of glucose observed in muscle and adipose tissue in response to insulin. Two models have been proposed to explain the regulated trafficking of GLUT4 in adipocytes [James *et al.* (1994)]. In the 'regulated exocytosis' model, GLUT4 is targeted to an insulin-responsive, intracellular storage compartment along with other proteins such as the aminopeptidase, vp165 [Ross *et al.* (1996), Malide *et al.* (1997)]. Insulin or other agonists might recruit GLUT4 to the cell surface by enhancing the exocytosis of this compartment. Thus, the distinguishing feature of this model is that insulin does not directly alter the intrinsic sorting of individual proteins but rather the compartment to which they are sorted into.

The second model, that of 'regulated recycling', suggests that proteins are differentially sequestered within endosomes as a function of the rate constants that direct their recycling through this system. These rate constants are determined by the efficiency of the targeting motifs within the cytoplasmic tails of different recycling proteins. The distinguishing feature of this model is that insulin may directly alter the rate constants that determine the recycling rates of each individual protein. This modification could involve an effect of insulin on the sorting machinery *per se*, or on the proteins themselves.

It has previously been shown that GLUT4 is directly phosphorylated by agents that regulate GLUT4 trafficking in adipocytes [James *et al.* (1989b), Lawrence *et al.* (1990a)]. This raises the possibility that this type of covalent modification may play an important role in the regulated recycling of GLUT4 in insulin-sensitive cells. β -adrenergic agonists such as isoproterenol, cAMP derivatives such as dibutyryl-cAMP and 8-bromo-cAMP, and the serine/threonine phosphatase inhibitor, okadaic acid, all cause a marked increase in GLUT4 phosphorylation *in vivo* [James *et al.* (1989b), Lawrence *et al.* (1990a), Lawrence *et al.* (1990b), Nishimura *et al.* (1991), Piper *et al.* (1993a)]. These agents have also been reported to induce GLUT4 translocation to the cell surface when added alone, or to inhibit GLUT4 movement when added in combination with insulin [Lawrence *et al.* (1990b), Corvera *et al.* (1991), Rampal *et al.* (1995). Livingstone *et al.* (1996), Rondinone & Smith (1996)].

The site of phosphorylation in GLUT4 has been mapped to a serine residue at position 488 within its cytoplasmic carboxy-terminal tail [Lawrence *et al.* (1990a)]. This site is unique to GLUT4, as no site corresponding to S⁴⁸⁸ is present in other glucose transporter isoforms [Lawrence *et al.* (1990a)]. Moreover, this residue is immediately adjacent to a di-leucine motif (L⁴⁸⁹L⁴⁹⁰) in the carboxy-terminus which plays an important role in the intracellular targeting of GLUT4 in adipocytes [Marsh *et al.* (1995), Verhey *et al.* (1995)]. Mutation of this di-leucine motif results in increased cell surface levels of GLUT4 in adipocytes as a consequence of impaired internalisation [Verhey *et al.* (1995)]. Di-leucine motifs have been shown to regulate both internalisation and intracellular sorting events in numerous recycling membrane proteins such as the T cell surface antigen CD4 [Shin *et al.* (1990), Shin *et al.* (1991)], the signal transducing component

(gp130) of the interleukin-6 receptor complex [Dittrich *et al.* (1996)], the CD3 γ subunit of the T cell receptor [Letourneur & Klausner (1992)], IGF II/MPR [Lobel *et al.* (1989), Johnson & Kornfeld (1992b)], and the CD-MPR [Johnson *et al.* (1990), Johnson & Kornfeld (1992a)]. Interestingly, changes in the phosphorylation state of serine residues juxtaposed to, and amino-terminal of, di-leucine motifs in all of these proteins have been proposed to modulate their sorting.

Phosphorylation of GLUT4 at S⁴⁸⁸ does not appear to be involved in the inhibitory effect of dibutyryl-cAMP on insulin-stimulated transporter function [Piper *et al.* (1993a)]. It has not been ascertained, however, if phosphorylation at this site is involved in triggering the movement of GLUT4 to the cell surface or in regulating its sorting intracellularly. The following results show that the regulatable movement of the S⁴⁸⁸ mutant to the cell surface is indistinguishable from wild-type GLUT4 in adipocytes, demonstrating that phosphorylation does not play a major role in the regulated exocytosis of GLUT4. However, the extent of co-localisation between GLUT4 and the γ -adaptin subunit of the Golgi adaptor complex, AP-1, was increased when S⁴⁸⁸ was mutated to alanine, suggesting that phosphorylation might modulate the sorting of GLUT4 at the TGN.

4.3 Materials and Methods

4.3.1 Human GLUT3 Epitope-tagged GLUT4 Transporters

The methodology detailing the construction of human GLUT3 epitope-tagged transporter cDNAs, and their stable transfection into 3T3-L1 fibroblasts is documented in Marsh *et al.* (1995).

4.3.2 Expression Levels of Recombinant GLUT4 Constructs in Adipocyte Cell Lines

The constructs employed in this study have been characterised in 3T3-L1 fibroblasts and adipocytes previously by subcellular fractionation and indirect immunofluorescence microscopy [Marsh *et al.* (1995)]. Multiple clonal cell lines expressing recombinant GLUT4 constructs at a range of expression levels were classified in two broad categories: low expressors, in which total GLUT4 expression was at a level comparable to that of endogenous GLUT4 in untransfected adipocytes, and high expressors, where total expression was >4-fold higher than endogenous GLUT4 expressed by non-transfected adipocytes. Hence, specific cell lines were selected for more detailed analysis based on the following:

- (1) Two independent clones, containing the S⁴⁸⁸ to A⁴⁸⁸ mutation (SAG), with differing expression levels (SAG2B3 and SAG1B6, high and low expressors, respectively) were selected for further analysis by endosomal ablation and buoyant density analysis.

(2) Two independent clones, containing the S⁴⁸⁸ to D⁴⁸⁸ mutation (DAG), with differing expression levels (DAG4B1 and DAG3B5, high and low expressors, respectively) were selected for further analysis by endosomal ablation and buoyant density analysis.

(3) As a comparison with wild-type GLUT4 targeting, the clone expressing the highest levels of TAG (TAG3B1) was selected for analysis (section 3.3.2.(1))

Figure 4.1 presents a schematic illustration of these mutants.

4.3.3 Immuno-electron Microscopy

This technique was carried out as detailed in section 3.3.3.

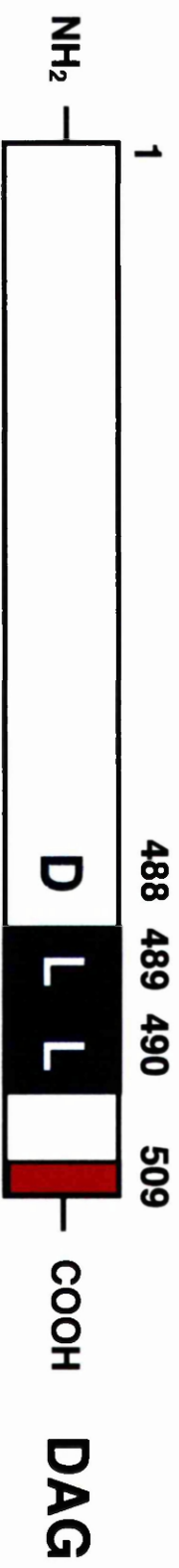
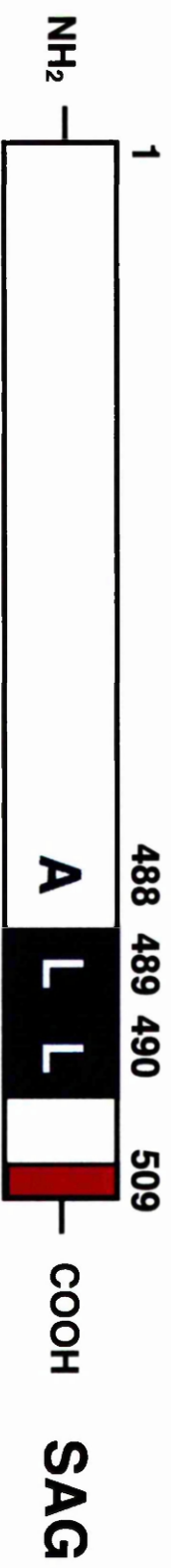
4.3.4 Antibodies

The antibodies used in this study were as detailed in section 3.3.4.

Figure 4.1

Schematic Representation of Human GLUT3 Epitope-Tagged Mutant GLUT4 Transporters

Summary of the recombinant GLUT constructs used in these studies. A foreign epitope encompassing the carboxy-terminal 12 amino-acid residues from human GLUT3 (red) is included as an additional tag at the 3' end of the full length GLUT4 cDNA. Wild-type GLUT4 epitope-tagged in this fashion is referred to as TAG. Epitope-tagged GLUT4 containing point mutations of S⁴⁸⁸ to either A⁴⁸⁸ or D⁴⁸⁸, are referred to as SAG and DAG respectively. The positions at which point mutations to alanine are present are shown in blue.



4.4 Results

4.4.1 Buoyant Density Analysis of TAG, SAG and DAG Mutants

In an attempt to determine the effects of the S⁴⁸⁸ to A⁴⁸⁸ (SAG) and S⁴⁸⁸ to D⁴⁸⁸ (DAG) mutations on the trafficking of GLUT4, I employed the technique of sucrose density gradient centrifugation to investigate the buoyant density of these mutants in adipocyte subcellular membranes. As stated previously, this analysis provides information regarding the gross targeting of SAG and DAG rather than yielding detailed information on the specific intracellular compartments to which these exogenous GLUT4 mutants are trafficked. LDM membranes from these mutants were separated by centrifugation on sucrose gradients and the distribution of mutant GLUT4 determined by immunoblotting with anti-GLUT3 antibodies. The results of this analysis are presented in Figure 4.2.

Immunoblotting of the subcellular membrane fractions revealed that endogenous GLUT4 was observed to sediment primarily in fractions 3 to 8 (Figure 4.2). TAG was observed to sediment in a very similar fashion to endogenous GLUT4, confirming previous studies which have shown an identical subcellular distribution for this species [Marsh *et al.* (1995)] (Figure 4.2). The S⁴⁸⁸ to A⁴⁸⁸ mutant, SAG, was also found to sediment at similar densities, suggesting that the gross targeting of this mutant within intracellular membranes of adipocytes is not significantly disrupted (Figure 4.2).

In contrast, analysis of the distribution of the intracellular pool of DAG revealed a different pattern of buoyant density (Figure 4.2). This

recombinant GLUT4 mutant was confined to a more restricted fraction of intracellular vesicles (fractions 1 to 4). This observed shift in the buoyant density of the S⁴⁸⁸ to D⁴⁸⁸ mutant provides evidence to suggest that the intracellular distribution of DAG may be distinct from either endogenous GLUT4, TAG or SAG.

A graphical representation of the comparative buoyant density profiles of the above mutants is provided by Figure 4.3.

4.4.2 Compartment Ablation Analysis of TAG, SAG and DAG Mutants

The technique of compartment ablation analysis was employed to examine the intracellular distributions of the SAG and DAG mutants. As stated in section 3.4.2, TfR-positive intracellular compartments loaded with a Tf-HRP conjugate for either 1hr or 3hr at 37°C are cross-linked and rendered insoluble ('ablated') by the addition of DAB/H₂O₂. Thus, this technique selectively ablates the endosomal recycling pathway but not intracellular compartments withdrawn from the endosomal system [Livingstone *et al.* (1996)].

The results of ablation experiments following either a 1hr or 3hr incubation with Tf-HRP are summarised in Table 4.1, and representative immunoblots are shown in Figure 4.4. Control experiments in which the cells were incubated for 1hr with Tf-HRP at 4°C and then ablated were performed. Under these conditions, no internalisation of Tf-HRP is expected, and consistent with this no ablation of the TfR, wild-type or recombinant GLUT4 was observed from LDM membranes.

In contrast, cells incubated with Tf-HRP for 3hr at 37°C exhibited a significant peroxide-dependent loss of TfR from the LDM membranes consistent with previous findings [Livingstone *et al.* (1996)] (Figure 4.4). The patterns of ablation exhibited by epitope-tagged wild-type GLUT4 (TAG) in transfected adipocytes were not significantly different from endogenous GLUT4 in native adipocytes and were consistent with previous findings [Livingstone *et al.* (1996)] (Figure 4.4).

Ablation experiments with adipocytes expressing SAG and DAG showed that these mutants appear to be distributed between ablated (~40%) and non-ablated (~60%) intracellular membranes similarly to TAG and endogenous GLUT4 in the basal state under the experimental conditions examined in this study (Figure 4.4). Thus, the patterns of ablation exhibited for SAG and DAG were not significantly different from endogenous GLUT4 in non-transfected adipocytes.

A further control experiment was performed in order to determine that the ablation procedure was functioning efficiently. Samples from the mutants cell lines were immunoblotted using an anti-TfR antibody, and as expected, after incubation at 4°C for 1hr no ablation was observed for each mutant (Figure 4.5). In contrast, cells incubated with Tf-HRP for 1hr at 37°C exhibited an almost complete peroxide-dependent loss of TfR from the LDM membranes consistent with previous findings [Livingstone *et al.* (1996)] (Figure 4.5).

NB. The results produced by the above analysis of the S⁴⁸⁸ to D⁴⁸⁸ (DAG) mutant are conflicting in nature. The buoyant density analysis suggests that the intracellular distribution of DAG may be distinct from either

endogenous GLUT4, TAG or SAG. However, using the compartment ablation technique I have shown that DAG displays a pattern of ablation not significantly different from endogenous GLUT4, indicative of a normal intracellular distribution in adipocytes. At present I am unable to resolve the conflicting nature of these results and as such the remaining studies in this chapter concentrate solely on the characterisation of the S⁴⁸⁸ to A⁴⁸⁸ (SAG) mutant. Further investigation is required to characterise the DAG mutant.

4.4.3 Subcellular Distribution of TAG and SAG in Basal and Insulin-stimulated Adipocytes

It has been previously shown that the recombinant GLUT4 mutant TAG exhibits a predominantly intracellular distribution in the absence of insulin, as assessed by immunoblotting membrane fractions prepared by differential centrifugation [Marsh *et al.* (1995)]. TAG, like wild-type GLUT4, was recovered in the LDM fraction, and was almost entirely excluded from the plasma membrane fraction. The basal distribution of TAG and wild-type GLUT4 are almost identical in adipocytes as indicated by the PM/LDM ratios calculated from subcellular fractionation data: (0.12 and 0.16, respectively). Thus, the intracellular sequestration of TAG was maintained despite a level of GLUT4 expression approximately 6-fold greater than that observed in non-transfected adipocytes (Figure 4.6). TAG exhibited a 5-fold increase in the PM fraction with insulin similar to that observed for wild-type GLUT4 (4-fold), with a corresponding decrease from intracellular membranes (Figure 4.6).

Two clonal cell lines expressing SAG were selected for study based on their relative expression levels. Western blots of subcellular membrane fractions prepared from adipocytes incubated in the absence of insulin treatment showed that SAG was found to be mostly absent from the PM fraction, and was retrieved predominantly within the intracellular (LDM) membrane fraction in a manner similar to TAG (Figure 4.6). Despite marginally higher PM/LDM ratios for SAG1B6 (0.28) and SAG2B3 (0.25) (calculated from the fractionation of non-insulin-stimulated adipocytes), these were not significantly different from the PM/LDM ratio of wild-type GLUT4. Furthermore, the PM/LDM ratios for SAG at both high and low levels of expression are in marked contrast with the PM/LDM ratios determined previously for GLUT4 mutants in which either the phenylalanine-based or di-leucine-based motifs were mutated (2.46 and 1.34, respectively), and which exhibited high cell surface distributions in the absence of insulin [Marsh *et al.* (1995)]. Following the addition of insulin, SAG exhibited a 5-fold and 4-fold increase in the PM fraction for cell lines with low (SAG1B6) and high (SAG2B3) levels of expression, respectively, with corresponding decreases in the level of SAG in intracellular membranes (Figure 4.6). The fold-increases in the PM fraction exhibited by adipocytes stably expressing SAG following insulin treatment were not significantly different from those described above for wild-type GLUT4 and for TAG.

As a control for the integrity of the differential centrifugation technique, the intracellular distribution of the endogenously expressed aminopeptidase, vp165, a protein co-localised with GLUT4 in adipocytes, was examined (Figure 4.7). In both transfected and non-transfected adipocytes, vp165 was recovered predominantly in the LDM fraction in the

absence of insulin (Figure 4.7). The determination of the overall PM/LDM ratio for vp165 (0.04) confirmed that it was largely absent from the PM fraction in basal adipocytes (Figure 4.7). With insulin treatment, the levels of vp165 in the PM fraction increased 10-fold in parallel with the increased levels of GLUT4, with a concomitant decrease in the levels of vp165 in the LDM fraction (Figure 4.7).

4.4.4 Co-localisation of TAG and SAG with γ -adaptin

A second technique employed to assess the distribution of GLUT4 among different intracellular compartments involved whole mount EM of intracellular vesicles prepared from 3T3-L1 adipocytes. Labelling of vesicles on an EM grid with two different primary antibodies followed by Protein-A tagged with different sized gold particles, enables a comparison of the distribution of two different proteins within individual vesicles. These studies compared the extent of overlap between recombinant GLUT4 proteins and the γ -adaptin subunit of the AP-1 adaptor complex. Phosphorylation has previously been implicated in the recruitment of proteins into Golgi-derived coated vesicles [Le Borgne *et al.* (1993), Mauxion *et al.* (1996)]. In the present study, the proportion of total vesicles that were γ -adaptin positive was not significantly different between the different adipocyte cell lines under investigation (Table 4.2 and Figure 4.8). The percentage of total vesicles labelled positively for TAG and SAG additionally reflects the differences in recombinant GLUT4 expression between different cell lines (Table 4.2). Recombinant GLUT4 was specifically labelled using an antibody to the human GLUT3 epitope-tag. Double-labelling revealed that both TAG and SAG were significantly co-localised with γ -adaptin in intracellular vesicles. Interestingly, there was a

small but statistically significant ($P < 0.05$) increase in the amount of SAG present in γ -adaptin positive vesicles (determined for two different cell lines expressing SAG at high and low levels) compared to TAG (Table 4.2).

4.4.5 The Effects of Okadaic Acid on the Intracellular Distribution of Wild-type and Recombinant GLUT4, vp165 and GLUT1 in 3T3-L1 Adipocytes

To complement the above studies, the following analysis was carried out in the laboratory of Prof. D. E. James.

In this set of experiments the effects of okadaic acid treatment and okadaic acid in combination with insulin on the subcellular distribution of TAG and SAG in comparison to wild-type GLUT4 have been examined. The site of okadaic acid-stimulated phosphorylation of GLUT4 *in vivo* has been shown to be restricted to the same cyanogen bromide cleavage fragment as the isoproterenol-stimulated phosphorylation site [Lawrence *et al.* (1990b)]. It has also been demonstrated that phosphorylation of the S⁴⁸⁸ to A⁴⁸⁸ mutant is abrogated in response to isoproterenol treatment in CHO cells and L6 myoblasts [Piper *et al.* (1993a)]. This study examines the effects of these treatments in parallel on the redistribution of endogenous GLUT1 and vp165, as these proteins co-localise with GLUT4 to different extents in 3T3-L1 adipocytes [Calderhead *et al.* (1990), Piper *et al.* (1991), Robinson *et al.* (1992), Ross *et al.* (1996)]. It is worth noting that the levels of vp165 expression were similar between the cell lines examined.

Treatment of non-transfected adipocytes with okadaic acid, in the absence or presence of insulin, stimulated wild-type GLUT4 translocation by 2.2- and 2.3-fold, respectively (Figure 4.9A). These increases in the level of GLUT4 in the PM fraction were less than for the insulin-elicited response (65% and 67%, respectively) (Figure 4.9A). The okadaic acid and okadaic acid plus insulin-mediated redistribution of endogenous GLUT1 and vp165 to the PM essentially mirrored the movement of GLUT4, and similarly, the increases at the PM were lower than for treatment with insulin alone (67% and 77% for GLUT1, and 64% and 56% for vp165) (Figures 4.9B and 4.9C).

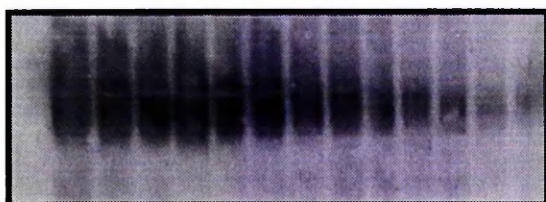
The levels of TAG at the PM increased 5.2- and 8.6-fold, respectively, following treatment with okadaic acid alone or in combination with insulin (data not shown). These increases were comparable to and greater than those observed with insulin treatment alone (110% and 181%, respectively). The increased cell surface distributions of endogenous GLUT1 and vp165 again essentially mimicked that of GLUT4 (TAG) in TAG-expressing adipocytes. While the okadaic acid-induced increases in the PM fraction for GLUT1 and vp165 were comparable to, or less than, the increases achieved with insulin stimulation alone (100% and 60%, respectively), an additive effect was demonstrated for treatment with okadaic acid in combination with insulin (127% for GLUT1 and 153% for vp165). These data further support the notion that phosphorylation of S⁴⁸⁸ is not involved in the translocation of GLUT-4 to the cell surface. Additionally, these results suggest that the stable expression of TAG in transfected adipocytes does not appreciably impair the fundamental properties of these two endogenous proteins to respond to a variety of agonists.

In concert with the previous findings that the distribution of SAG in basal adipocytes and in adipocytes incubated with insulin was not significantly different from TAG, the redistribution of SAG in response to treatment with either okadaic acid or okadaic acid with insulin closely resembled the results observed for TAG (Figure 4.9A). Okadaic acid alone elicited a 3.2-fold increase in the level of SAG in the PM fraction (78% of the insulin-mediated increase), while okadaic acid plus insulin resulted in a 4.8-fold increase in SAG at the cell surface (116% of the insulin-mediated increase) (Figure 4.9A). In parallel, okadaic acid alone stimulated increased cell surface levels of GLUT1 and vp165 which were 91% and 84% of insulin treatment alone (Figures 4.9B and 4.9C). Treatment with okadaic acid and insulin resulted in an additive effect over that of insulin (137% for GLUT1 and 151% for vp165) (Figures 4.9B and 4.9C).

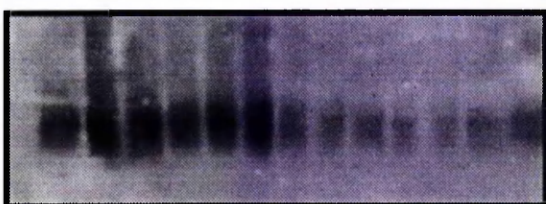
Figure 4.2

Buoyant Density Analysis of TAG, SAG and DAG Mutants

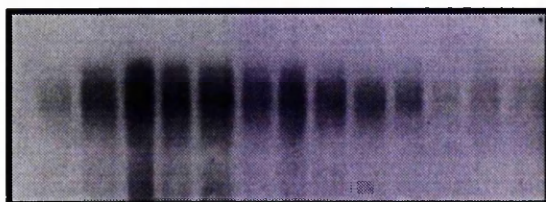
Low density microsomal membranes were prepared from the indicated 3T3-L1 adipocyte cell clone and analysed by sucrose gradient centrifugation as outlined in section 2.5.5. Fractions from a 1.5-0.5M sucrose gradient were loaded on a 10% SDS gel from left to right. 20 μ g protein from each fraction was loaded onto the gel. The position of the GLUT3 epitope-tagged mutant GLUT4 species was then determined by immunoblotting (section 2.9.3) with anti-GLUT3 antibodies. Data from a representative experiment is shown using TAG3B1 (TAG), SAG2B3 (SAG) and DAG3B5 (DAG). Similar data were obtained using SAG1B6 and DAG1D3 (data not shown). By way of comparison, the distribution of endogenous GLUT4 in non-transfected adipocytes and LAG in transfected adipocytes is shown (GLUT4).



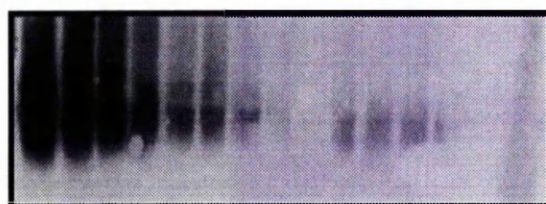
TAG



LAG



SAG



DAG



[Sucrose]

Figure 4.3

Buoyant Density Profiles of TAG, SAG and DAG Mutants

This is a graphical illustration of the buoyant density profiles of the TAG, SAG and DAG mutants. The immunoreactivity of the fractions is represented by arbitrary units, with the fraction containing the highest level set = 1 unit.

Buoyant Density Profiles of TAG, SAG and DAG Mutants

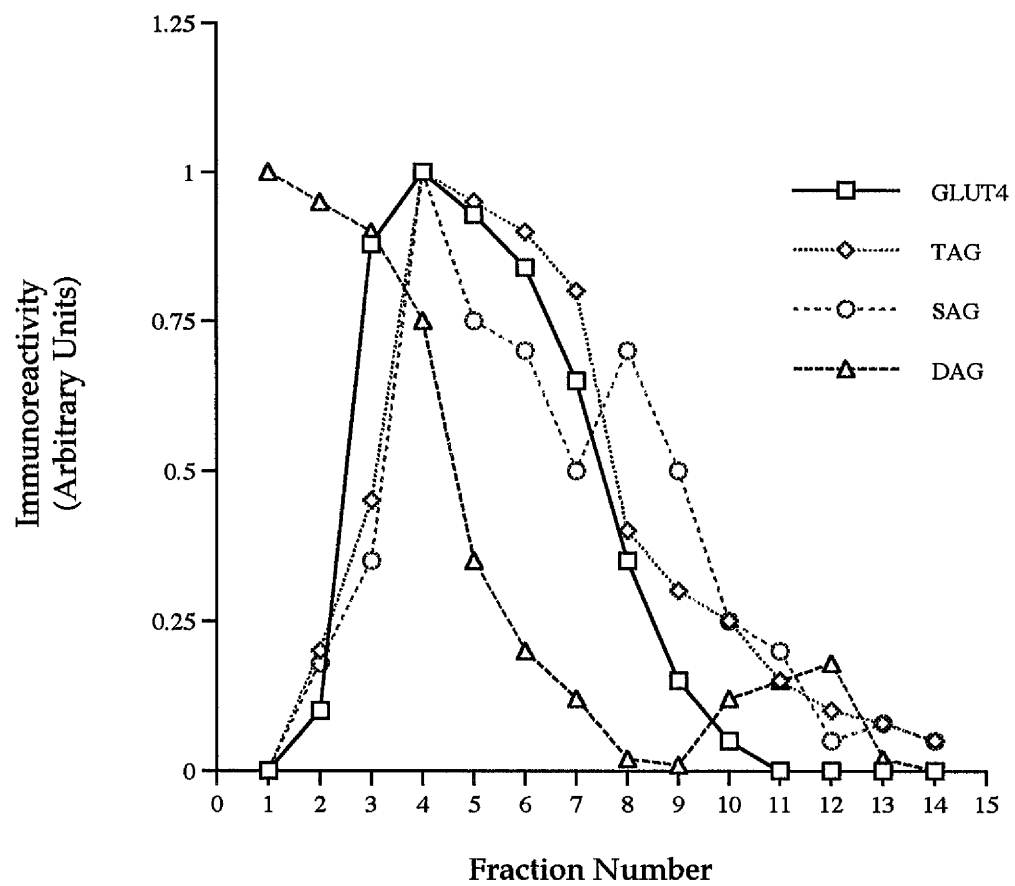


Figure 4.4

Compartment Ablation Analysis of TAG, SAG and DAG Mutants

LDM membranes were prepared from 3T3-L1 adipocytes loaded with Tf-HRP for 1hr at 4°C, 1hr at 37°C or 3hr at 37°C, before and after ablation (- and + hydrogen peroxide) as indicated. Figure 4.4 shows experiments for each of the mutant GLUT4 species examined (TAG=TAG3B1; SAG=SAG2B3; DAG=DAG3B5 experiments are shown). In these experiments, cells were loaded with Tf-HRP as indicated and the cells exposed to DAB in the presence and absence of peroxide as indicated. LDM membranes were prepared, 20µg of each fraction were electrophoresed and immunoblotted using anti-GLUT3 antibodies to study the effect of ablation on the intracellular content of each of the clones. Several blots of this type from at least three independent experiments were quantitated and the results are presented in Table 4.1.



TAG



FAG



LAG



SAG



DAG

- + - + - +

4°C

1h 37°C

3h 37°C

Table 4.1

Effect of Compartment Ablation on Intracellular GLUT4 Levels

Duplicate sets of 10cm plates of adipocytes were loaded with Tf-HRP for 1hr or 3hr at 37°C. The DAB cytochemistry was then performed as described in section 2.5.2, with hydrogen peroxide added to one but not both plates. LDM membranes were prepared, 20µg protein was electrophoresed, and the GLUT4 or GLUT3 immunoreactive signal quantitated. The difference in signals between the plates incubated \pm peroxide is a reflection of the extent of protein ablation (Figure 4.4). Shown above is the signal remaining in the LDM after ablation expressed as a percentage of the signal in the LDM before ablation. The results are expressed as the means \pm SEM of three experiments of this type on three separate platings of cells. Note that in all these experiments, an additional control experiment was performed in which cells were incubated with Tf-HRP at 4°C and then ablated. Under these conditions, no internalisation of Tf-HRP is expected, and consistent with this no ablation of either recombinant or wild-type GLUT4 was observed (Figure 4.4). Values for wild-type GLUT4 were from plates of non-transfected adipocytes, measured using the same batch of conjugate employed for the mutants.

Table 4.1**Effect of Compartment Ablation on Intracellular GLUT4 Levels**

<u>Species</u>	<u>% Signal Remaining after Ablation</u>	
	1hr at 37° C	3hr at 37° C
wt GLUT4	64 ± 3%	59 ± 8%
TAG3B1	62 ± 8%	60 ± 9%
SAG2B3	72 ± 3%	59 ± 6%
SAG1B6	70 ± 5%	62 ± 11%
DAG3B5	64 ± 5%	58 ± 8%
DAG4B1	56 ± 8%	55 ± 10%

Figure 4.5

Comparative Compartment Ablation of TAG, SAG and DAG Mutants

LDM membranes were prepared from 3T3-L1 adipocytes loaded with Tf-HRP for 1hr at 4°C and 1hr at 37°C , before and after ablation (- and + hydrogen peroxide) as indicated. Figure 4.5 shows experiments for each of the mutant GLUT4 species examined (TAG=TAG3B1; SAG=SAG2B3; DAG=DAG3B5 experiments are shown). In these experiments, cells were loaded with TfHRP as indicated and the cells exposed to DAB in the presence and absence of peroxide as indicated. LDM membranes were prepared, 20µg of each fraction were electrophoresed and immunoblotted using anti-TfR antibody as a control to ensure that the ablation procedure was functioning efficiently.

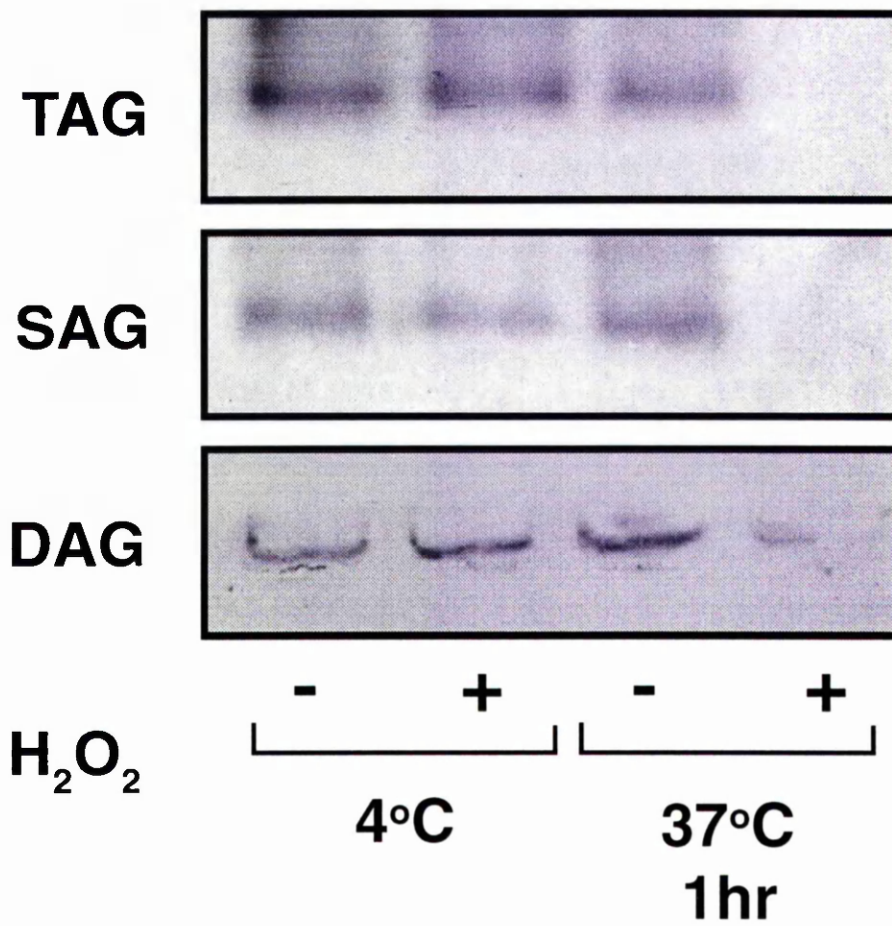


Figure 4.6

Subcellular Distribution of Wild-Type and Recombinant GLUT4 in 3T3-L1 Adipocytes

The subcellular distribution of GLUT4 and recombinant GLUT4 mutants are presented as the combined results of multiple independent differential centrifugation experiments. The amount of protein at the plasma membrane with insulin alone was normally assigned a value of 1 to normalise between separate experiments and between different cell lines. Values are expressed as means \pm SEM (arbitrary units/ μ g protein) determined from at least three independent experiments.

Subcellular Distribution of Wild-Type and Recombinant GLUT4 in 3T3-L1 Adipocytes

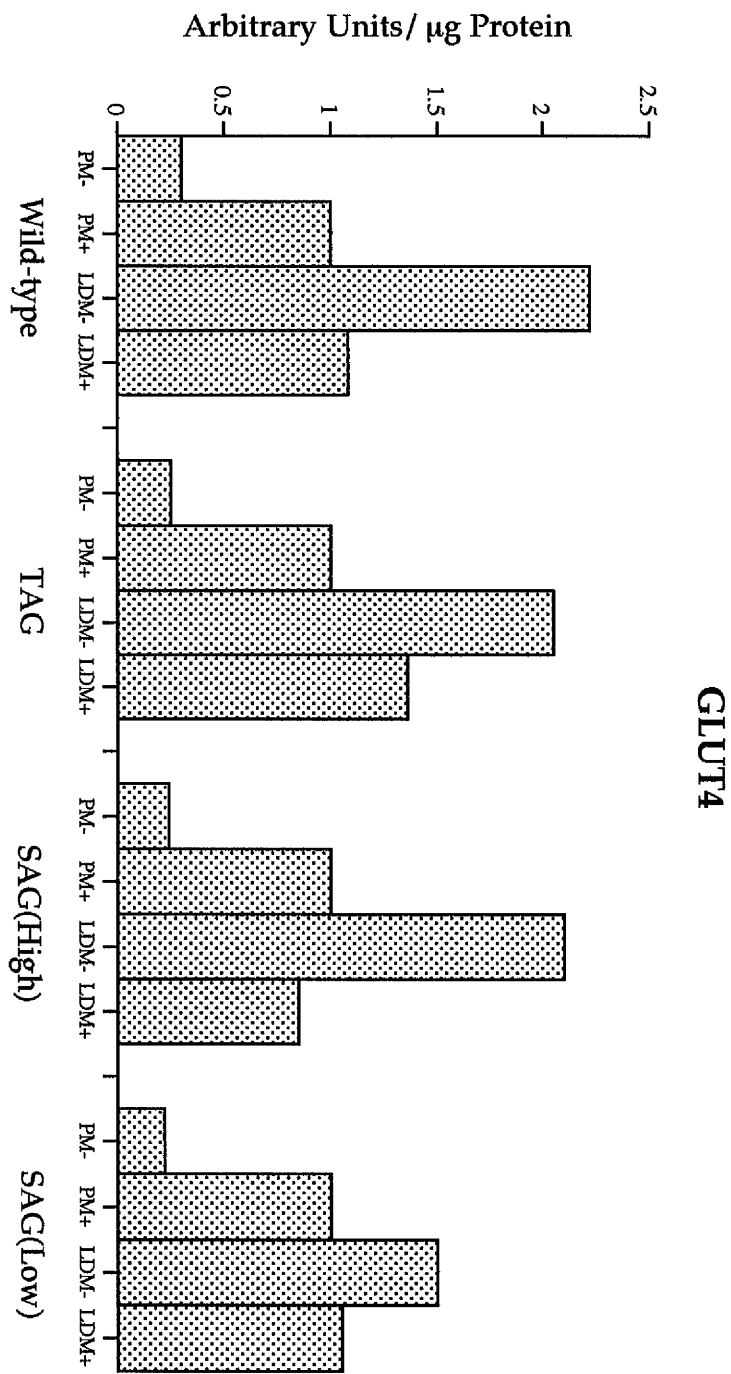


Figure 4.7

Subcellular Distribution of vp165 in Transfected and Non-Transfected 3T3-L1 Adipocytes

The subcellular distribution of vp165 is presented as the combined results of multiple independent differential centrifugation experiments. The amount of protein at the plasma membrane with insulin alone was normally assigned a value of 1 to normalise between separate experiments and between different cell lines. Values are expressed as means \pm SEM (arbitrary units/ μ g protein) determined from at least three independent experiments

Subcellular Distribution of vp165 in Transfected and Non-Transfected 3T3-L1 Adipocytes

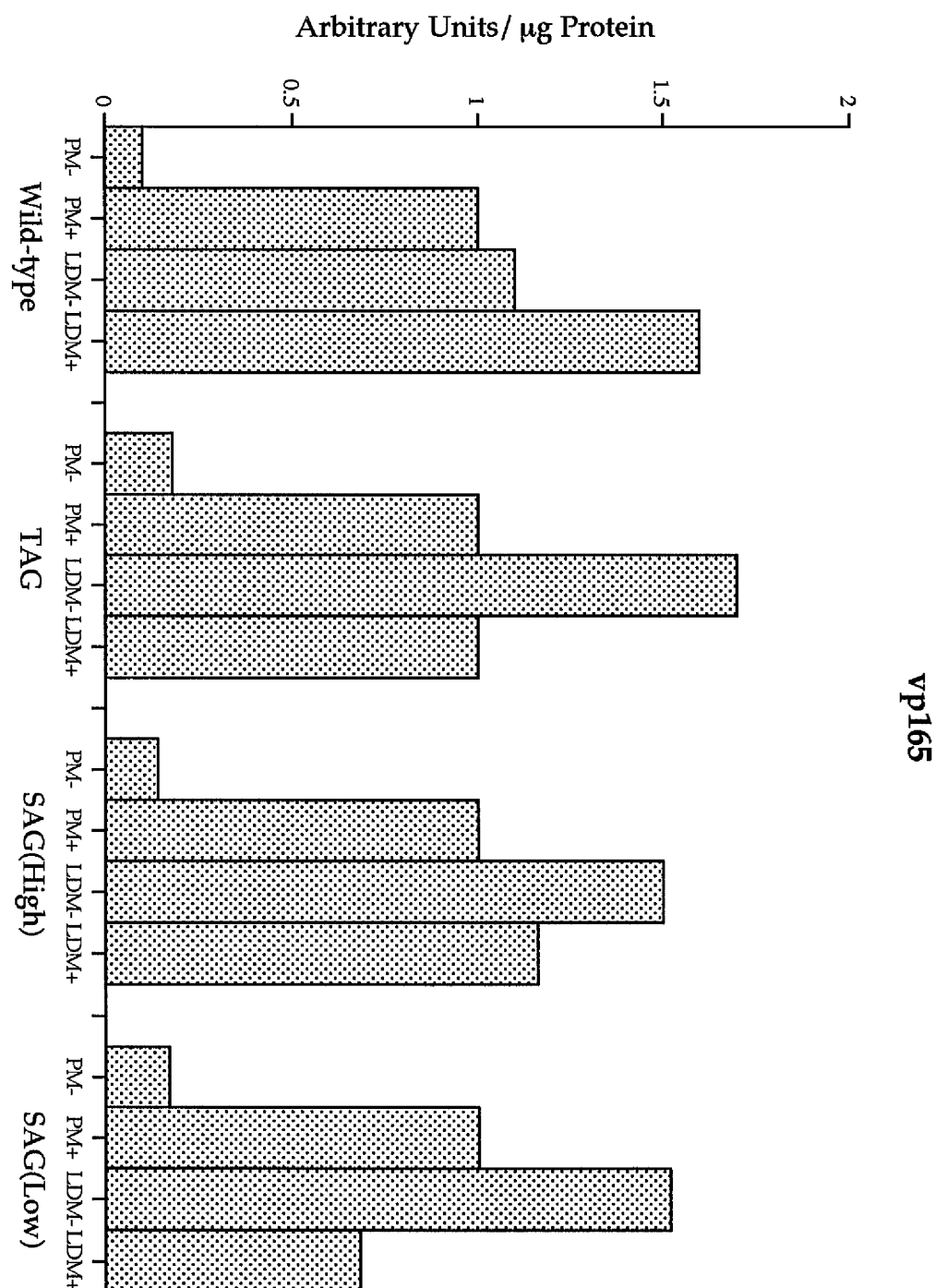


Figure 4.8

Immuno-electron Microscopy Analysis of γ -adaptin and Epitope-tagged GLUT4 in 3T3-L1 Adipocytes

Intracellular vesicles were prepared from basal 3T3-L1 adipocytes stably expressing either epitope-tagged wild-type (TAG) or mutant GLUT4 (SAG). Vesicles adsorbed to formvar/carbon-coated copper grids were double labelled using antibodies specific for γ -adaptin followed by protein-A gold (15nm), and GLUT3 followed by protein-A gold (10nm). The results of four independent labelling experiments were quantified and the values are presented as means \pm SEM.

Immuno-electron Microscopy Analysis of γ -adaptin and Epitope-tagged GLUT4 in 3T3-L1 Adipocytes

- ▤ % GLUT3 gold in γ -adaptin positive vesicles
- ▥ % GLUT3 positive vesicles containing γ -adaptin

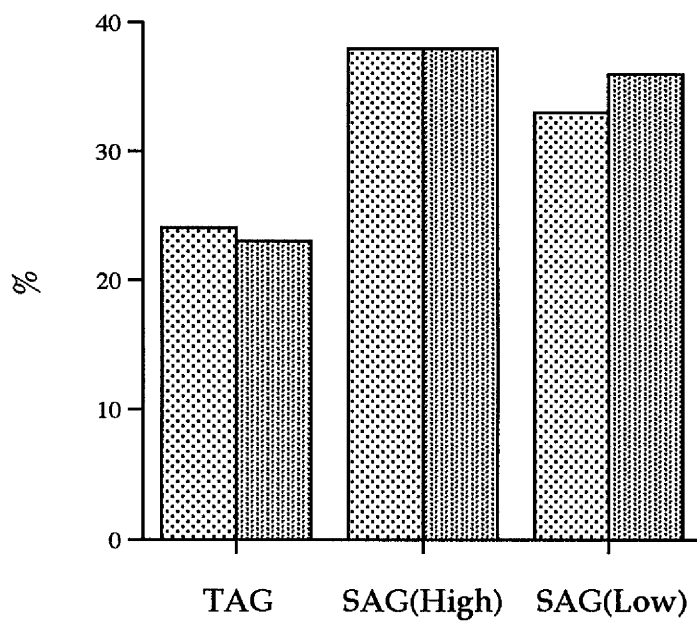


Table 4.2

**Percentage of Total Intracellular Vesicles Labelled for
Either γ -adaptin or Recombinant GLUT4**

Intracellular vesicles were prepared from basal 3T3-L1 adipocytes stably expressing either epitope-tagged wild-type (TAG) or mutant GLUT4 (SAG). Results of 4 independent labelling experiments were quantified; values are means. γ -adaptin vesicles were immuno-labelled with an antibody specific for γ -adaptin followed by protein A-gold (15nm). GLUT3 vesicles were immuno-labelled with an antibody specific for the human GLUT3 epitope-tag followed by protein A-gold (10nm).

Mutant	% total vesicles labelled with γ -adaptin	% total vesicles labelled with GLUT3
TAG3B1	5.4 \pm 0.4	7.4 \pm 0.7
SAG1B6	6.8 \pm 0.8	1.9 \pm 0.3
SAG2B3	7.9 \pm 1.6	4.1 \pm 0.7

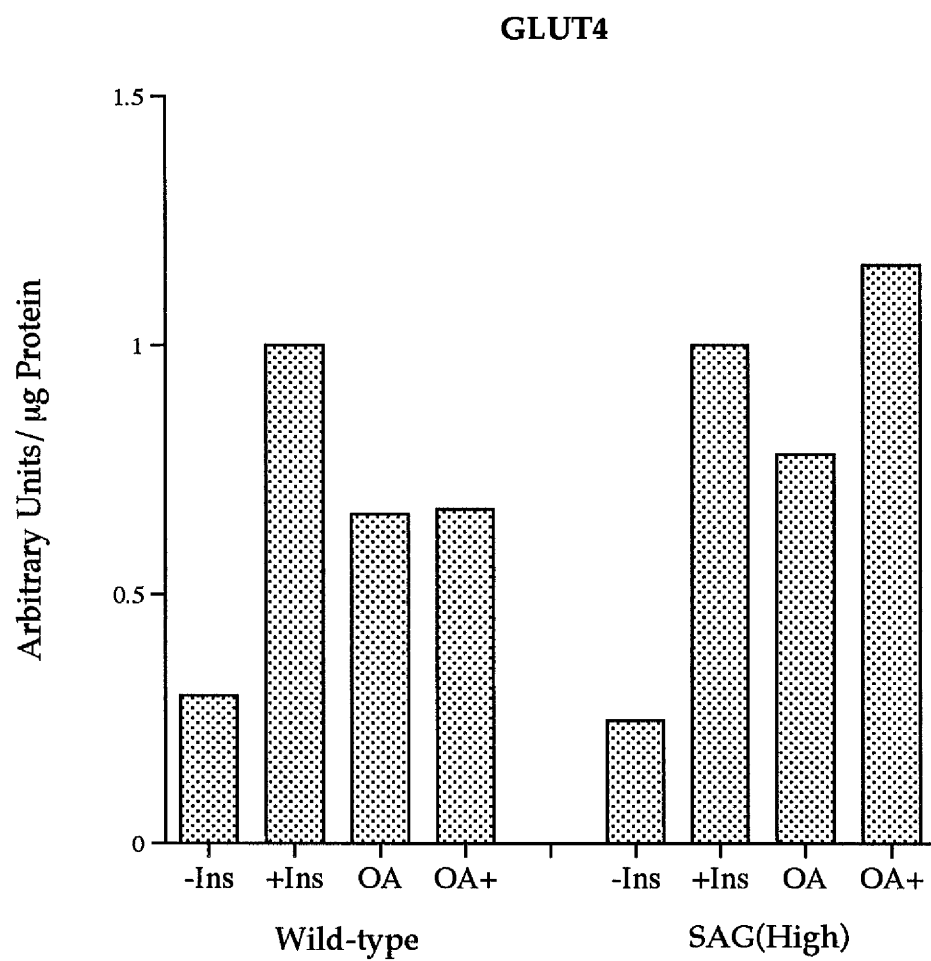
Figures 4.9A-C

The Effects of Insulin and Okadaic Acid on the Cell Surface Distribution of GLUT4, GLUT1 and vp165 in 3T3- L1 Adipocytes

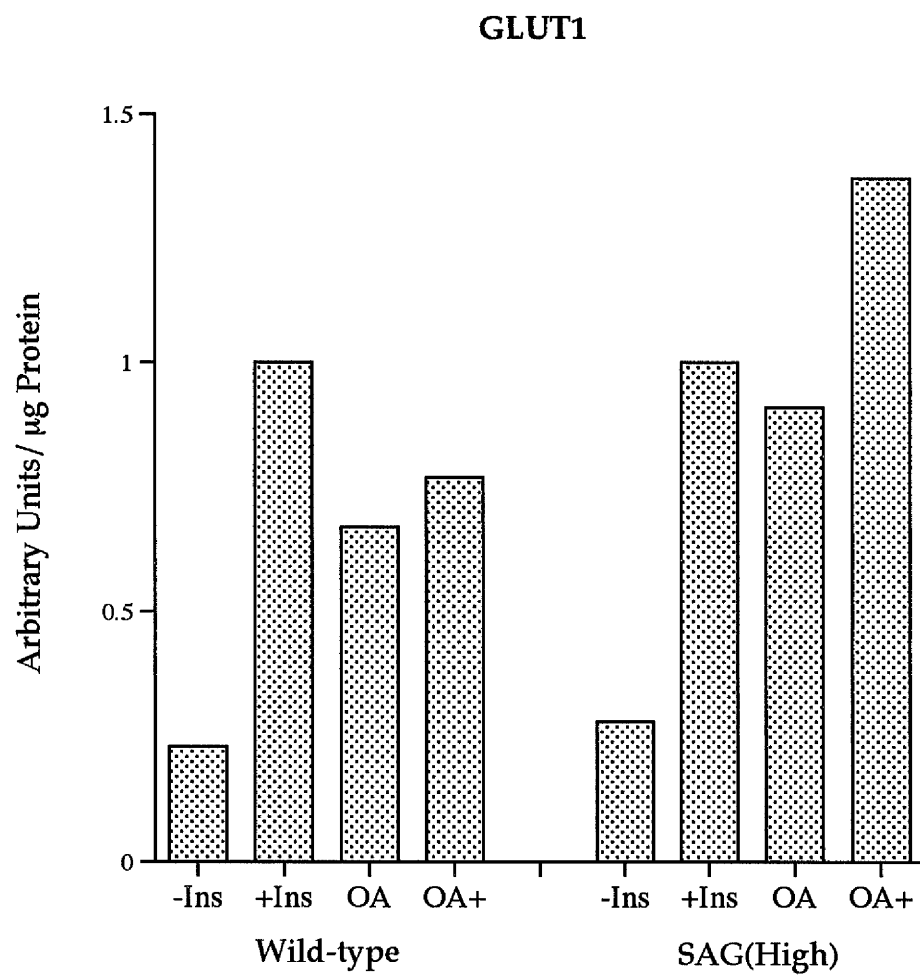
3T3-L1 adipocytes were incubated in serum-free medium for 2hr and then further incubated for 15 min at 37°C in the absence or presence of insulin (4µg/ml) with or without the addition of okadaic acid (10µM). Subcellular membrane fractions (10µg) from basal (Ins), insulin-stimulated (+Ins), okadaic acid-stimulated (OA) and okadaic acid plus insulin-stimulated (OA+) adipocytes prepared by differential centrifugation and subjected to SDS-PAGE were electrophoretically transferred to PVDF membranes and immunoblotted with antibodies specific for the carboxy-terminus of GLUT4, GLUT1 or human GLUT3, and the cytoplasmic domain of vp165. Immunoreactive signals were detected by ECL followed by densitometry of autoradiograms.

The plasma membrane distribution of (A) GLUT4, (B) GLUT1 and (C) vp165 are presented as the combined results of multiple independent differential centrifugation experiments. The amount of protein at the plasma membrane with insulin alone was normally assigned a value of 1 to normalise between separate experiments and between different cell lines. Values are expressed as means \pm SEM (arbitrary units/µg protein) determined from three independent experiments for wild-type adipocytes and four separate experiments for SAG-expressing adipocytes.

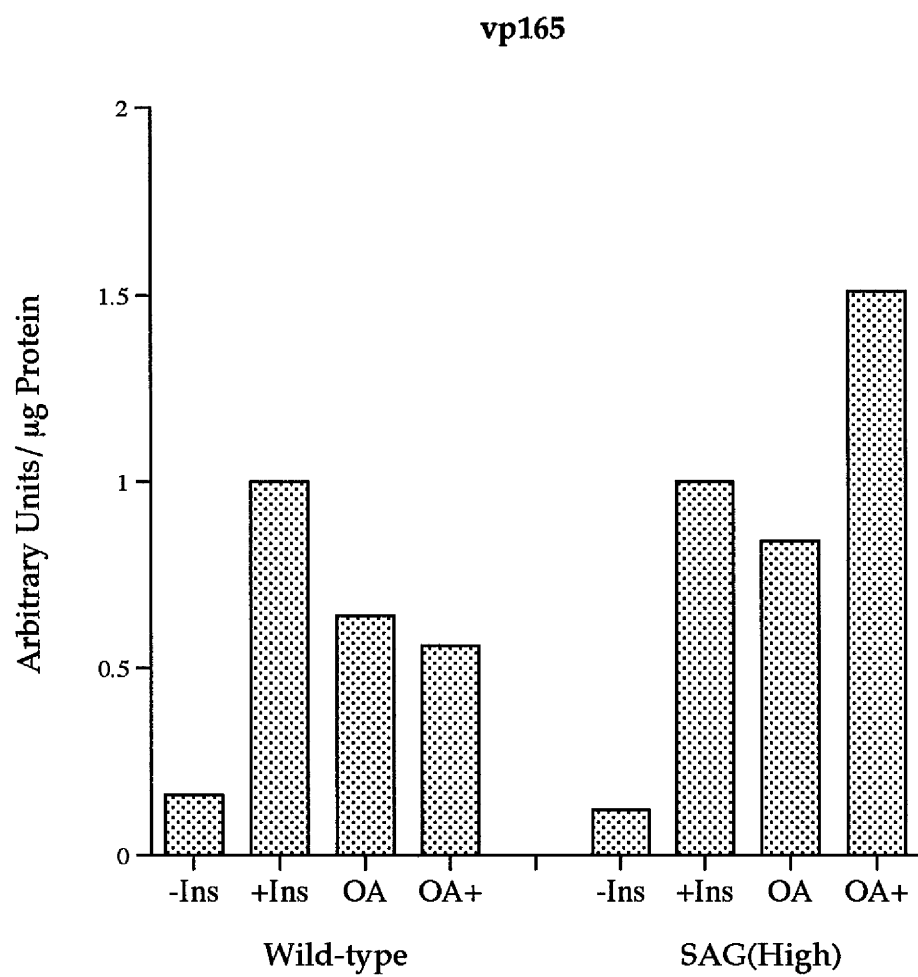
**A. The Effects of Insulin and Okadaic Acid on the Cell Surface
Distribution of GLUT4 in 3T3-L1 Adipocytes**



**B. The Effects of Insulin and Okadaic Acid on the Cell Surface
Distribution of GLUT1 in 3T3-L1 Adipocytes**



**C. The Effects of Insulin and Okadaic Acid on the Cell Surface
Distribution of vp165 in 3T3-L1 Adipocytes**



4.5 Discussion

With respect to the data reported above, I have been unable to demonstrate a major role for GLUT4 phosphorylation at S⁴⁸⁸ in promoting its insulin-dependent movement to the cell surface from intracellular membranes. The gross distribution of GLUT4 in which S⁴⁸⁸ was mutated to alanine (SAG) was not significantly different from either wild-type GLUT4 or epitope-tagged GLUT4 (TAG) in basal adipocytes. However, immuno-EM analysis of intracellular vesicles has revealed that the extent of co-localisation of SAG with the γ -adaptin subunit of AP-1 was significantly higher ($P<0.05$) than for TAG, suggesting that changes in the phosphorylation state of this site might regulate the intracellular sorting of GLUT4 to some extent. In adipocytes incubated in the presence of insulin, SAG translocated from intracellular membranes to the cell surface similarly to wild-type GLUT4 and TAG. Furthermore, James and co-workers found that the redistribution of SAG to the plasma membrane following okadaic acid treatment closely resembled that of GLUT4. These data demonstrate that the insulin- or okadaic acid-stimulated recruitment of GLUT4 to the plasma membrane is independent of the phosphorylation state of S⁴⁸⁸ in GLUT-4.

Phosphorylation of GLUT4 at S⁴⁸⁸ does not appear to play a role in the inhibitory effects of counter-regulatory hormones on glucose transport [Nishimura *et al.* (1991), Schurmann *et al.* (1992), Piper *et al.* (1993a)]. Hence, in this study, a primary objective was to determine if phosphorylation plays a role in the regulated trafficking of GLUT4 in adipocytes. Variations in subcellular distribution between glucose transporter isoforms have been attributed to heterologous amino acid

sequences residing in the cytoplasmic domains of these transporter proteins [Bell *et al.* (1990), Bell *et al.* (1993), James *et al.* (1993)]. As no site corresponding to S⁴⁸⁸ is found in other GLUT isoforms, it has been proposed that the targeting of GLUT4 may be uniquely regulated by phosphorylation ([Lawrence *et al.* (1990a)]. Recently, it has been shown that a carboxy-terminal di-leucine motif (L⁴⁸⁹L⁴⁹⁰) in the cytoplasmic domain of GLUT4 plays an important role in its trafficking in 3T3-L1 adipocytes [Marsh *et al.* (1995), Verhey *et al.* (1995)] (Chapter 3 of this thesis). This motif has the capacity to facilitate efficient and rapid internalisation from the cell surface, presumably via clathrin-coated pits [Corvera *et al.* (1994), Verhey *et al.* (1995), Garippa *et al.* (1996)]. Hence, it seemed possible that S⁴⁸⁸ might be involved in regulating GLUT4 trafficking in some way given its proximity to this di-leucine motif.

Changes in the phosphorylation state of serine residues flanking di-leucine motifs within the cytoplasmic tails of the T cell surface antigen, CD4 [Shin *et al.* (1990), Shin *et al.* (1991)], the IGF II/MPR [Le Borgne *et al.* (1993)], the CD-MPR [Mauxion *et al.* (1996), Breuer *et al.* (1997)], and gp130 [Dittrich *et al.* (1996)], are proposed to promote either internalisation or intracellular sorting events by inducing conformational changes in the relevant targeting motifs. For example, the phosphorylation of a serine residue within the cytoplasmic tail of the CD3 γ subunit of the T-cell receptor (TCR) facilitates the interaction of an adjacent di-leucine-based internalisation signal with the plasma membrane adaptor protein subunit, AP-2, resulting in increased internalisation of the TCR via clathrin-coated pits [Dietrich *et al.* (1997)]. In view of the fact that no significant differences could be observed in the steady-state distribution of SAG under basal, insulin- or okadaic acid-stimulated conditions compared to wild-type GLUT4, it is

unlikely that phosphorylation of S⁴⁸⁸ in the GLUT4 carboxyl terminus plays a major role in regulating the trafficking of this protein. It is noteworthy that previous studies have examined the effects of mutating the di-leucine motif (L⁴⁸⁹L⁴⁹⁰) in GLUT4 to in adipocytes. At low expression levels the steady state distribution of this mutant was indistinguishable from wild-type GLUT4, most likely because targeting motifs elsewhere in the protein were able to compensate for this defect. However, at high expression levels this mutant accumulated at the plasma membrane in the absence of insulin [Marsh *et al.* (1995)], presumably due to reduced internalisation efficiency [Verhey *et al.* (1995)].

This study has examined the distribution of two clonal cell lines expressing SAG at either low or high expression levels, and in neither case could I detect any disruption in gross targeting. While the possibility cannot be dismissed that at even higher expression levels a disruption in the insulin-dependent redistribution of GLUT4 would have been evident or that following insulin stimulation an internalisation defect may have been ascertained, it seems clear from these findings that phosphorylation at this site does not play a major role in the trafficking of GLUT4 at these steps either under basal or insulin-stimulated conditions in adipocytes. Consistent with these observations, a rigorous assessment of carboxy-terminal GLUT4 targeting motifs in CHO cells revealed that although S⁴⁸⁸ may play a modulatory role in regulating GLUT-4 endocytosis, it is relatively minor compared to that played by the di-leucine motif *per se* [Garippa *et al.* (1996)]. To characterise the trafficking motifs contained in the carboxyl terminus of GLUT4, these researchers constructed a chimera (GTCTR) in which the carboxy-terminal 30 amino acids of GLUT4 were substituted for the amino-terminal cytoplasmic domain of the transferrin

receptor (TfR). Mutations of GTCTR were constructed in which either the di-leucine motif at position 489-490 was mutated to di-alanine (GTCTR-AA), or the serine residue at position 488 was mutated to either alanine or aspartate. Each of these substitutions resulted in a shift in distribution of the mutated GTCTR constructs towards the cell surface. The shift in distribution of GTCTR-AA resulted from a 10-fold decrease in internalisation, whereas mutation of S⁴⁸⁸ resulted in only a 3-fold reduction in internalisation.

It has previously been reported, particularly with respect to the CD-MPR and IGF II/MPR, that phosphorylation of serine residues adjacent to di-leucine motifs in the cytoplasmic tails of recycling membrane proteins regulates their entry into clathrin-coated vesicles exiting the Golgi apparatus at the *trans*-Golgi network [Le Borgne *et al.* (1993), Mauxion *et al.* (1996)]. In an attempt to explore the possibility that a similar mode of regulation facilitates GLUT4 exit from the TGN, this study investigated the co-localisation of either TAG or SAG with the γ -adaptin subunit of the Golgi adaptor complex, AP-1. There was significant overlap between TAG and SAG with γ -adaptin, suggesting that GLUT4 must follow a similar trafficking pathway to the mannose 6-phosphate receptors. Interestingly, the localisation of SAG with γ -adaptin was significantly higher ($P < 0.05$) than TAG, suggesting that changes in the phosphorylation state of S⁴⁸⁸ might play a role in GLUT4 sorting at the TGN.

It has recently been shown using a chemical ablation technique following uptake of Tf-HRP, that GLUT4 is distributed between endosomes and a post-endocytic compartment in 3T3-L1 adipocytes [Livingstone *et al.* (1996), Martin *et al.* (1996)]. To determine if phosphorylation of GLUT4 might be

involved in regulating its distribution between these distinct compartments, Tf-HRP ablation analysis was performed on 3T3-L1 adipocytes expressing either wild-type GLUT4 or the S⁴⁸⁸ mutant. However, no significant differences could be determined between wild-type GLUT4 and SAG in terms of their susceptibility to ablation following uptake of Tf-HRP for 1-3 hours at 37°C. However, reversible phosphorylation events might act only to 'fine tune' the intracellular sorting of GLUT4. Recently, it has been postulated that reversible protein phosphorylation may act to modulate the relative affinities of aromatic- and di-leucine-based motifs for either internalisation or intracellular sorting events [Trowbridge *et al.* (1993)]. The possibility remains that mutation of S⁴⁸⁸ might only result in minor shifts rather than gross changes in the intracellular distribution of GLUT4 within TfR-negative pools. If these changes were confined to the recycling of GLUT4 between the TGN and insulin-responsive membranes, they would not be detectable using the ablation technique. For example, in the context of the model of GLUT4 trafficking that I have proposed in section 3.5.3, this means that mutation of S⁴⁸⁸ may result in shifts in intracellular distribution between the TGN compartment (X_{TGN}) and the tubulo-vesicular compartment (X_{TV}). These two compartments are both elements of the non-ablatable pool and as such, movement of proteins between them would not be detected by the compartment ablation approach.

It is conceivable that SAG may have formed hetero-oligomers with endogenous GLUT4, thus over-riding any potential disruptive effects the S⁴⁸⁸ mutation may have had on targeting. This seems unlikely however, because estimations demonstrate that the expression of SAG in the high expressing clone was 3-fold higher than endogenous GLUT4 expression in

wild-type cells. Furthermore, immunofluorescence microscopy of SAG in 3T3-L1 fibroblasts, in which endogenous GLUT4 is absent, revealed no discernible abnormalities in targeting compared to wild-type GLUT4 (TAG) stably-expressed in 3T3-L1 fibroblasts. Even so, based upon the 'regulated exocytosis' model proposed for the trafficking of GLUT4 [James *et al.* (1994)], the possibility cannot be excluded that endogenous GLUT4 molecules containing functional phosphorylation sites within insulin-responsive vesicles, facilitate the efficient exocytosis of these vesicles in which SAG additionally resides, to the cell surface in response to insulin or okadaic acid.

Previous studies have shown that the phosphatase inhibitor, okadaic acid, causes a significant shift in the distribution of GLUT4 to the cell surface [Lawrence *et al.* (1990b), Corvera *et al.* (1991), Rampal *et al.* (1995), Livingstone *et al.* (1996), Rondinone & Smith (1995)]. This is of potential interest because okadaic acid additionally results in a marked increase in GLUT4 phosphorylation [Lawrence *et al.* (1990b)]. However, okadaic acid stimulated the movement of SAG to the plasma membrane to a similar extent as wild-type GLUT4. Furthermore, okadaic acid additionally caused a shift in both GLUT1 and vp165 to the cell surface in adipocytes. Hence, these data are more consistent with an effect of okadaic acid on elements of the signal transduction pathway that regulate the movement of these proteins to the cell surface. Along these lines, in addition to increasing the cell surface levels of GLUT4, okadaic acid also inhibits the insulin-dependent movement of GLUT4 to the plasma membrane.

Treatment of wild-type cells with okadaic acid in combination with insulin inhibited the insulin-stimulated translocation of GLUT4 to the plasma membrane (67% of the insulin response) to levels observed with okadaic acid alone (65% of the insulin response), consistent with the findings of others [Lawrence *et al.* (1990b), Corvera *et al.* (1991), Rampal *et al.* (1995), Livingstone *et al.* (1996)]. Similarly, the extent of the movement of SAG to the cell surface following treatment with okadaic acid and insulin together was less than for insulin alone. This inhibitory effect of okadaic acid on the insulin-signalling pathway in 3T3-L1 and rat adipocytes is presumed to result from increased serine/threonine phosphorylation of insulin receptor substrate-1, which prevents its tyrosine phosphorylation and thus reduces its ability to dock phosphatidylinositol 3-kinase [Jullien *et al.* (1993), Tanti *et al.* (1993), Tanti *et al.* (1994)]. These results further reinforce the conclusion that phosphorylation of S⁴⁸⁸ in GLUT4 is not directly involved in its redistribution to the cell surface.

While the possibility exists that changes in the phosphorylation state of S⁴⁸⁸ in GLUT4 act to 'fine tune' either its internalisation from or insulin-dependent movement to the plasma membrane, based upon the above data it seems reasonable to conclude that phosphorylation of this residue does not play a major role in these aspects of GLUT4 trafficking. If changes in the phosphorylation state of S⁴⁸⁸ intricately regulate either the dileucine-mediated internalisation from the plasma membrane, or the intracellular sorting of GLUT4 at the TGN, it is perhaps not surprising that I have been unable to demonstrate any gross targeting defects for this mutation given both the levels of expression examined and the techniques employed in this study. Previous studies have failed to demonstrate a role for S⁴⁸⁸ phosphorylation in the isoproterenol- and dibutyryl-cAMP-

mediated inhibition of insulin-stimulated glucose transport also [Nishimura *et al.* (1991), Piper *et al.* (1993a)]. Therefore, other yet unidentified motifs with more dominant roles in these steps of GLUT4 trafficking must exist. It will be of interest to identify such motifs and the roles that they might play in regulating the intracellular trafficking of GLUT4. This data does support a role for phosphorylation/dephosphorylation events in regulating the entry of GLUT-4 into γ -adaptin positive vesicles. However, as is the case for other proteins such as the CD-MPR, disruption of this site is without significant effect on the regulated trafficking of GLUT-4 in adipocytes [Breuer *et al.* (1997)].

4.6 Summary

The carboxy-terminus of GLUT4 contains a functional internalisation motif (L⁴⁸⁹L⁴⁹⁰) that helps maintain its intracellular distribution in basal adipocytes. This motif is flanked by the major phosphorylation site in this protein (S⁴⁸⁸), which may play a role in regulating GLUT4 trafficking in adipocytes. In the present study, the targeting of GLUT4 in which S⁴⁸⁸ has been mutated to alanine (SAG) has been examined in stably-transfected 3T3-L1 adipocytes. The trafficking of SAG was not significantly different from GLUT4 in several respects. Firstly, in the absence of insulin, the distribution of SAG was similar to GLUT4, in that it was largely excluded from the cell surface and was enriched in small intracellular vesicles. Secondly, SAG exhibited insulin-dependent movement to the plasma membrane (4-5-fold) comparable to GLUT4 (4-5-fold). Furthermore, SAG exhibits patterns of buoyant density and compartment ablation similar to endogenous GLUT4. Finally, okadaic acid, which has previously been shown to stimulate both GLUT4 translocation and its phosphorylation at S⁴⁸⁸, also stimulated the movement of SAG to the cell surface similarly to GLUT4. Using immuno-electron microscopy, it has been shown that GLUT4 is localised to intracellular vesicles containing the Golgi-derived γ -adaptin subunit of AP-1, and that this localisation is enhanced when S⁴⁸⁸ is mutated to alanine. The above results suggest that the carboxy-terminal phosphorylation site in GLUT4 (S⁴⁸⁸) may play a role in intracellular sorting at the TGN, but does not play a major role in the regulated movement of GLUT4 to the plasma membrane in 3T3-L1 adipocytes.

Chapter 5

Analysis of Two Endosomal Targeting Motifs in the GLUT4 Carboxy-terminus

5.1 Aims

The aim of this chapter is:

1. To investigate the role of residues distal to the di-leucine motif in the carboxy-terminal tail of GLUT4 in the targeting of this isoform in 3T3-L1 adipocytes.

5.2 Introduction

The presence of discrete sorting signals in the cytoplasmic tails of membrane proteins regulates their differential distribution within the endo-lysosomal system. In many cases, these signals bind to coat components which are thought to selectively transport molecules from one compartment to another [Bremnes *et al.* (1998), Rapoport *et al.* (1998), Robinson (1994), Rodionov & Bakke (1998)]. Two major types of signals have been described which are identified either by the sequence YXXØ (where Y is an aromatic amino acid, X is any amino acid and Ø is an amino acid with a bulky hydrophobic group) or LL (where L is leucine or isoleucine) [Marks *et al.* (1997), Mellman (1996), Pond *et al.* (1995)]. Both of these motifs have been found to bind AP-1 or AP-2 adaptor complexes that regulate clathrin assembly at either the *trans*-Golgi network (TGN) or the cell surface [Bremnes *et al.* (1998), Heilker *et al.* (1996), Rapoport *et al.* (1998), Robinson (1994), Rodionov & Bakke (1998)]. Hence, these motifs facilitate the efficient delivery of both newly synthesised and internalised proteins to the endosomal system, from where they may either be recycled or transported to the lysosome [Marks *et al.* (1996), Mellman (1996)]. The presence of multiple sorting signals within the cytoplasmic tails of proteins with complex trafficking itineraries is thus likely required to facilitate their interaction with different adaptor protein subunits at multiple sites throughout the cell. Certain motifs, such as those found in CD3 γ , CD4 and the insulin-like growth factor II/mannose 6-phosphate receptor (IGFII/MPR), have been shown to bind more avidly to AP-1 than to AP-2, which correlates with their roles in sorting at the TGN [Johnson & Kornfeld (1992b), Le Borgne *et al.* (1993), Rapoport *et al.* (1998)]. In contrast, other signals appear to preferentially bind AP-2, suggesting that these

motifs predominantly regulate internalisation from the cell surface [Glickman *et al.* (1989), Heilker *et al.* (1996), Jing *et al.* (1990), Marks *et al.* (1996), Ohno *et al.* (1995), Zhang & Allison (1997)]. In some cases, the differential affinity of targeting signals for discrete adaptor subunits appears further influenced by amino acids either proximal or distal to the primary signal [Heilker *et al.* (1996), Marks *et al.* (1997), Matter *et al.* (1994), Motta *et al.* (1995), Ohno *et al.* (1995), Pond *et al.* (1995)].

More specialised compartments related to the endosomal system that give rise to cell-specific functions such as synaptic vesicle exocytosis and antigen presentation, have been described in a variety of cell types [Simonsen *et al.* (1997), West *et al.* (1994)]. The insulin-regulated movement of the glucose transporter GLUT4 to the cell surface in muscle and adipocytes may provide another example of this type of regulated recycling. In the resting state GLUT4 is localised to tubulo-vesicular elements that are clustered either in the TGN, endosomes or in the cytoplasm [Slot *et al.* (1991a), Slot *et al.* (1991b)]. The extremely low levels of GLUT4 at the plasma membrane under these conditions appears to be an essential feature of this protein that distinguishes it from many other recycling proteins. Thus, it has been proposed that GLUT4 is targeted to a unique intracellular compartment in muscle and fat cells that facilitates both its storage as well as its exocytosis, enabling GLUT4 to move transiently to the cell surface in response to stimuli such as insulin [Verhey *et al.* (1995), Livingstone *et al.* (1996), Martin *et al.* (1996)].

Several studies have attempted to identify targeting motifs in GLUT4 in the hope of defining the molecular machinery that regulates the intracellular sequestration of this protein [Marshall *et al.* (1993), Piper *et al.*

(1992), Verhey *et al.* (1993)]. Two distinct motifs, a phenylalanine-based motif (FQQI) in the amino-terminus and a di-leucine motif in the carboxy-terminus have been identified [Corvera *et al.* (1994), Piper *et al.* (1993), Verhey & Birnbaum (1994)]. Both of these motifs function autonomously as internalisation motifs and so presumably interact with AP-2 at the cell surface [Garippa *et al.* (1994), Garippa *et al.* (1996), Piper *et al.* (1993b), Verhey *et al.* (1995)]. These are discussed more extensively in Chapters 1 and 3 of this thesis.

It has been suggested that the cytoplasmic carboxy-terminus of GLUT4 contains additional targeting information, based on analyses of chimeric transporter proteins expressed in insulin-responsive cells [Haney *et al.* (1995), Verhey *et al.* (1995)]. In a previous study which examined the roles of both the ⁵FQQI⁸ and L⁴⁸⁹L⁴⁹⁰ motifs in GLUT4 trafficking in 3T3-L1 adipocytes, an epitope-tag was introduced at the carboxy-terminus of GLUT4 to distinguish between recombinant and endogenous proteins [Marsh *et al.* (1995)]. These researchers also generated a chimeric GLUT4 transporter by replacing the last 12 amino acids of GLUT4 with the corresponding sequence from GLUT3 and found that this protein was aberrantly targeted to the cell surface (Figure 5.1).

Thus, this study has proceeded to map the residues within this region of GLUT4 by alanine-scanning mutagenesis, in an effort to more specifically determine residues that might constitute an additional targeting motif involved in the sorting of this protein to its intracellular storage compartment. The studies reveal an important role for the residues ⁴⁹⁸TELEYLGP⁵⁰⁵ within the extreme carboxyl terminus of GLUT4 in determining the steady state distribution of this protein in adipocytes.

5.3 Materials and Methods

5.3.1 Human GLUT3 Epitope-tagged GLUT4 Transporters

The methodology detailing the construction of human GLUT3 epitope-tagged transporter cDNAs, and their stable transfection into 3T3-L1 fibroblasts is documented in Marsh *et al.* (1995).

The mutants used in this study are as follows:

TAIL: a recombinant GLUT4 transporter in which the GLUT4 sequence coding for the carboxy-terminal 12 amino acid residues is replaced with the corresponding sequence from human GLUT3.

498: a recombinant GLUT4 transporter in which the residues 498^{TELE}501 are mutated to alanines.

502: a recombinant GLUT4 transporter in which the residues 502^{YLGP}505 are mutated to alanines.

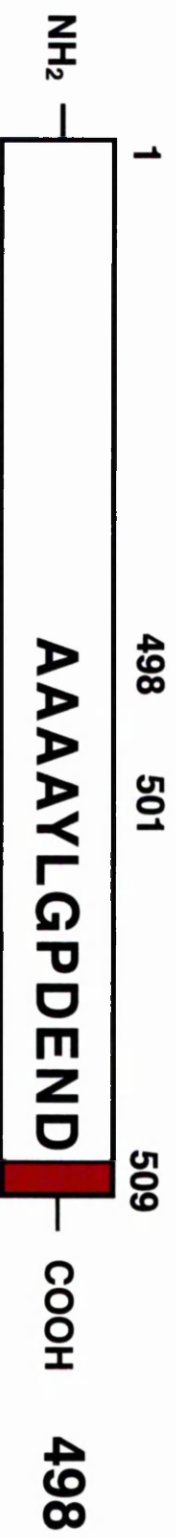
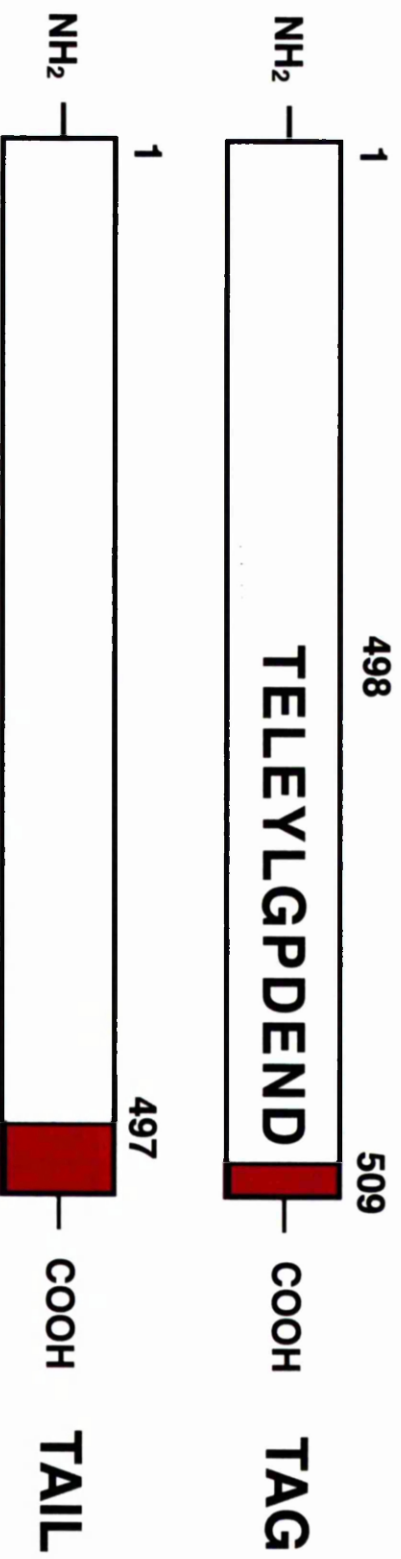
506: a recombinant GLUT4 transporter in which the residues 506^{DEND}509 are mutated to alanines.

For a diagrammatic representation of the above recombinant mutants see Figure 5.1.

Figure 5.1

Schematic Representation of Carboxy-terminal GLUT4 Mutants

Summary of the carboxy-terminal GLUT4 mutants used in these studies. To discriminate between recombinant and endogenous GLUT4 in stably transfected 3T3-L1 adipocytes a foreign epitope encompassing the carboxy-terminal 12 amino-acid residues from human GLUT3 (red) was introduced at the extreme carboxyl-terminus of the full length GLUT4 cDNA. The mutant referred to as TAIL is a recombinant GLUT4 transporter in which the GLUT4 sequence coding for the carboxy-terminal 12 amino acid residues is replaced with the corresponding sequence from human GLUT3. 498 is a recombinant GLUT4 transporter in which the residues ⁴⁹⁸TELE⁵⁰¹ are mutated to alanines. 502 is a recombinant GLUT4 transporter in which the residues ⁵⁰²YLGP⁵⁰⁵ are mutated to alanines. 506 is a recombinant GLUT4 transporter in which the residues ⁵⁰⁶DEND⁵⁰⁹ are mutated to alanines. The positions at which point mutations to alanine are present are shown in black.



5.3.2 Expression Levels of Recombinant GLUT4 Constructs in Adipocyte Cell Lines

A variety of clones for each construct that expressed the mutants at variable levels between 2-6-fold higher than endogenous GLUT4 were selected. It has previously been shown that the targeting of epitope-tagged DNA is indistinguishable from endogenous GLUT4 over this expression range, both under basal and insulin-stimulated conditions [Marsh *et al.* (1995)]. The cell lines were broadly classified as either low expressors, in which expression of the mutants was 1-3-fold that of the endogenous transporter, or high expressors, where total expression was >3-fold endogenous GLUT4.

5.3.3 Antibodies

The anti-GLUT4 antibodies used were a rabbit polyclonal antibody raised against a peptide comprising the 15 amino-terminal amino acid residues of the human isoform of GLUT4 [James *et al.* (1989a)], the carboxy-terminal 14 amino acid residues of the human isoform of GLUT4 [Brant *et al.* (1993)], or the corresponding region of the human isoform of GLUT3 [Shepherd *et al.* (1992)].

5.4 Results

5.4.1 Characterisation of the Carboxy-terminus of GLUT4

The following is a summary of the results of our collaborators in the laboratory of Prof. D. E. James which precede my work in this study.

No major differences were observed in targeting between the mutants TAG (representing wild-type GLUT4) and TAIL in 3T3-L1 fibroblasts by immunofluorescence microscopy. However, in differentiated cells a significant difference in the steady state distribution of these two proteins is apparent. The distribution of TAG was similar to endogenous GLUT4, and not significantly different at expression levels of TAG that were approximately 6-fold higher than endogenous levels of GLUT4. In contrast, a large proportion of TAIL was found at the cell surface even under basal conditions. Despite the accumulation of this construct at the PM under steady state basal conditions, an insulin-dependent movement of TAIL from the LDM fraction to the PM was still observed.

It is unlikely that the GLUT3 carboxy-terminal amino acids caused the aberrant targeting of TAIL in 3T3-L1 adipocytes, as inclusion of this sequence in TAG had no effect on GLUT4 targeting. This suggests that the last 12 amino acids in the carboxy-terminus of GLUT4 may contain intracellular targeting information. To more accurately define the amino acid constituents of this putative motif, alanine-scanning mutagenesis was performed on this domain in the context of TAG. Three constructs, designated 498, 502 and 506 were generated by replacing amino acids at

positions 498-501 (TELE), 502-505 (YLGP) or 506-509 (DEND) with alanines, respectively (Figure 5.1).

In general, the targeting of the 498 mutant was disrupted compared to TAG, with the cell surface expression of this mutant increased in the absence of insulin. It must be noted that the relative steady state accumulation of 498 at the PM appeared to be proportional to the expression level of the mutant. The level of PM expression of 498 is lower than that observed for TAIL, but similar to that observed for GLUT1. Parallel analysis of TAIL and 498 at almost identical expression levels revealed that PM levels of both TAIL and 498 were significantly higher than endogenous GLUT4, but the cell surface expression of 498 was intermediate between that of TAIL and GLUT4. This data suggests that residues distal to the TELE sequence may also contribute to the targeting information contained within the carboxy-terminus. Despite the impaired steady state distribution of 498 in basal adipocytes, insulin still elicited a redistribution of this mutant from LDMs to the cell surface.

The distribution of the 502 mutant in basal and insulin-treated adipocytes was not significantly different from endogenous GLUT4. Consistent with TAIL and 498 mutants, there was no demonstrable abnormality in the response to insulin for this mutant.

No significant change was observed in the subcellular distribution of the 506 mutant compared to endogenous GLUT4 or the TAG mutant. The redistribution of 506 from intracellular membranes to the cell surface following insulin stimulation (4.5-fold) closely resembled that of TAG (4-fold). Thus, the terminal 4 residues (DEND) appear to have no major contribution in targeting GLUT4 in 3T3-L1 adipocytes.

5.4.2 Compartment Ablation Analysis of GLUT4 Carboxy-terminal Tail Mutants

To determine whether the putative carboxy-terminal GLUT4 targeting motif is located within the sequences ⁴⁹⁸TELE⁵⁰¹, ⁵⁰²YLGP⁵⁰⁵ or ⁵⁰⁶DEND⁵⁰⁹, the technique of compartment ablation (sections 2.5.1-1, 3.2) was employed to examine the intracellular distribution of the recombinant GLUT4 constructs TAG, 498, 502 and 506, with the aim of determining whether such mutation of the above sequences alters the distribution of GLUT4 between the ablated (endosomal) and non-ablated pools.

Consistent with previous studies (section 3.4.2) the sensitivity of epitope-tagged GLUT4 (TAG) to ablation analysis was indistinguishable from wild-type GLUT4 (~40% reduction in the %GLUT4 signal in the LDM fraction after ablation), suggesting that this protein is partitioned normally between the ablated (endosomal) and non-ablated pools.

Ablation experiments with adipocytes expressing 502 and 506 showed that these mutants appear to be distributed between ablated (~40%) and non-ablated (~60%) intracellular membranes similarly to TAG and endogenous GLUT4 in the basal state under the experimental conditions examined in

this study (Figure 5.2 and Table 5.1). Thus, the patterns of ablation exhibited for 502 and 506 were not significantly different from endogenous GLUT4 in non-transfected adipocytes. Two independent clonal cell lines expressing 502 at low levels (5022A3) and intermediate levels (5027B2) were independently examined, yielding identical results for each mutant (no high expressing 502 clones that reproducibly expressed this mutant following differentiation into adipocytes were available for analysis). Similarly, two independent clones of 506 were examined, the low expressor (5063B2) and the high expressor (5067C1), producing identical results. This argues strongly that the results do not reflect overexpression or clonal variation for either of the constructs.

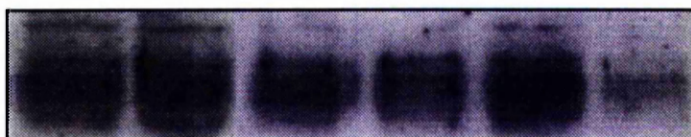
In contrast, the intracellular pool of the 498 mutant was readily ablated. This mutant was ablated to a much more significant degree (~80%) than either TAG or wild-type GLUT4 (~40%) (Figure 5.2 and Table 5.1). This result implies that the majority of this protein is present in the recycling endosomal system and not the non-ablatable GLUT4 pool. Three clonal cell lines expressing 498 at low levels (4981D3), intermediate levels (4987B1) and high levels (4981D4) were independently examined and gave identical results for each mutant (Table 5.1). As stated above, this argues strongly that the results do not reflect overexpression or clonal variation for this construct. I performed these experiments by preparing duplicate plates of 3T3-L1 adipocyte clones loaded with Tf-HRP for 1hr or 3hr at 37°C, or alternatively for 1hr at 4°C (as a control as no Tf-HRP is internalised under these conditions). Also, for each clone, the efficiency of ablation was monitored by parallel examination of the extent of ablation of the TfR.

Figure 5.2

Compartment Ablation Analysis of Carboxy-terminal GLUT4 Mutants

LDM membranes were prepared from 3T3-L1 adipocytes loaded with Tf-HRP for 1hr at 4°C, 1hr at 37°C or 3hr at 37°C, before and after ablation (- and + hydrogen peroxide) as indicated. Figure 5.2 shows experiments for each of the mutant GLUT4 species examined (498=4987B1; 502=5027B2; 506=5067C1 experiments are shown). In these experiments, cells were loaded with Tf-HRP as indicated and the cells exposed to DAB in the presence and absence of peroxide as indicated. LDM membranes were prepared, 20µg of each fraction were electrophoresed and immunoblotted using anti-GLUT3 antibodies to study the effect of ablation on the intracellular content of each of the clones. Several blots of this type from at least three independent experiments were quantitated and the results are presented in Table 5.1.

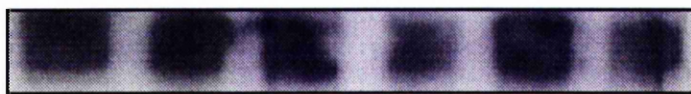
498 ID3



502 3A3



506 3B2



-

+

-

+

-

+

H₂O₂

4°C
1hr

37°C
1hr

37°C
3hr

Table 5.1

**Compartment Ablation Analysis of Carboxy-terminal
GLUT4 Mutants**

Duplicate sets of 10cm plates of adipocytes were loaded with Tf-HRP for 1hr or 3hr at 37°C. The DAB cytochemistry was then performed as described in section 2.5.2, with hydrogen peroxide added to one but not both plates. LDM membranes were prepared, 20µg protein was electrophoresed, and the GLUT4 or GLUT3 immunoreactive signal quantitated. The difference in signals between the plates incubated \pm peroxide is a reflection of the extent of protein ablation (Figure 5.2). Shown above is the signal remaining in the LDM **after** ablation expressed as a percentage of the signal in the LDM **before** ablation. The results are expressed as the means \pm SEM of three experiments of this type on at least three separate platings of cells. Membranes blotted in parallel with an antibody specific for the TfR showed >85% ablation of this protein in all cell lines studied (data not shown). Note that in all these experiments, an additional control experiment was performed in which cells were incubated with Tf-HRP at 4°C and then ablated. Under these conditions, no internalisation of Tf-HRP is expected, and consistent with this no ablation of either recombinant or wild-type GLUT4 was observed. Values for wild-type GLUT4 were from plates of non-transfected adipocytes, measured using the same batch of conjugate employed for the mutants.

Table 5.1**Compartment Ablation Analysis of Carboxy-terminal
GLUT4 Mutants**

<u>Species</u>	<u>% Signal Remaining after Ablation</u>	
	1hr at 37° C	3hr at 37° C
TAG1AB	55 ± 9%	59 ± 3%
4981D4	43 ± 5%	17 ± 2%
4981D3	45 ± 7%	18 ± 4%
4987B1	42 ± 2%	16 ± 3%
5023A3	74 ± 8%	65 ± 3%
5027B2	67 ± 6%	55 ± 7%
5063B2	64 ± 3%	58 ± 4%
5067C1	66 ± 4%	61 ± 6%

5.5 Discussion

This study utilised alanine-scanning mutagenesis and compartment ablation analysis in an attempt to identify additional targeting information in the carboxy-terminus of GLUT4 that appears to direct the endosomal sorting of the protein. The findings, summarised here, indicate that the residues ⁴⁹⁸TELEYLGP⁵⁰⁵, but not ⁵⁰⁶DEND⁵⁰⁹, are involved in targeting GLUT4 correctly in 3T3-L1 adipocytes. Replacing the last 12 amino acids in GLUT4 with the corresponding sequence from GLUT3 (TAIL) had a considerably greater effect on the targeting of GLUT4 than mutation of either ⁴⁹⁸TELE⁵⁰¹ or ⁵⁰²YLGP⁵⁰⁵ alone, suggesting that both of these regions contribute to the targeting information. As the ⁴⁹⁸TELEYLGP⁵⁰⁵ sequence is located 10 amino acids membrane-distal to the di-leucine motif in GLUT4 (L⁴⁸⁹L⁴⁹⁰), it is tempting to conclude that the targeting signal in this study may simply interact with or contribute information to the upstream di-leucine signal. However, significant available evidence tends to rule out this possibility. Firstly, by expressing chimeric glucose transporter proteins in either L6 myoblasts or 3T3-L1 adipocytes, it has been shown that the carboxy-terminal 30 amino acids of GLUT4 can direct the protein to a highly insulin-responsive intracellular location independent of the di-leucine motif [Haney *et al.* (1995), Verhey *et al.* (1995)]. Secondly, there are phenotypic differences between di-leucine mutants and carboxy-terminal tail mutants. Using an endosomal ablation technique, I find that the 498 mutant becomes much more susceptible to ablation than wild-type GLUT4 (Figure 5.2), consistent with it accumulating in endosomes. Conversely, I have found that the extent of ablation of di-leucine mutants becomes much less than for the wild-type protein (section 3.4.2), suggesting that these sequences regulate distinct trafficking steps.

The structural similarity between different types of endosomal sorting motifs [Marks *et al.* (1996) Mellman (1996), Marks *et al.* (1997)], combined with the realisation that both tyrosine- and di-leucine-based signals bind to adaptor complexes that mediate clathrin assembly [Ohno *et al.* (1995), Heilker *et al.* (1996), Rodionov & Blake (1998), Bremnes *et al.* (1998)] strongly suggests that both motifs can fulfil similar functions in the endocytic pathway. Acidic residues or phosphorylation sites juxtaposed to, and amino-terminal of di-leucine motifs in the T cell surface antigen CD4 [Shin *et al.* (1990), Shin *et al.* (1991)], the signal transducing component (gp130) of the interleukin-6 receptor complex [Dittrich *et al.* (1996)], the CD3 γ subunit of the T cell receptor (TCR) [Letourneur & Klausner (1992)], the IGFII/MPR [Lobel *et al.* (1989), Johnson & Kornfeld (1992b)] and the cation-dependent mannose 6-phosphate receptor [Johnson *et al.* (1990), Johnson & Kornfeld (1992a)], have been proposed to modulate the sorting of these proteins at different loci in the cell. Moreover, mutation of residues amino-terminal but not carboxy-terminal of these di-leucine motifs abrogates their function, consistent with a structural contribution from these adjacent residues [Motta *et al.* (1995), Pond *et al.* (1995)]. While no acidic residues are found at similar positions amino-terminal of the di-leucine motif in GLUT4, the major phosphorylation site in GLUT4 (S⁴⁸⁸) is immediately adjacent to and amino-terminal of this site [Lawrence *et al.* (1990)]. However, we have recently mutated this site and could find no major disruption to GLUT4 targeting in adipocytes [Chapter 4 and Marsh *et al.* (1998)]. The possibility remains, however, that other residues amino-terminal of this site in GLUT4 could contribute to the structure and function of the di-leucine motif, or vice versa, and this remains to be explored.

Defining the precise functions for each of the trafficking motifs thus far defined in the cytoplasmic domains of GLUT4 will require more detailed analysis. The ⁵FQQI⁸ and L⁴⁸⁹L⁴⁹⁰ signals both appear to regulate internalisation [Piper *et al.* (1993b), Verhey *et al.* (1995)]. However, because similar motifs in other proteins have been shown to function at multiple intracellular loci we cannot exclude the possibility that these motifs also contribute to GLUT4 sorting elsewhere in the cell. Indeed, my data (Chapter 3) suggests that this is the case. Most of the studies performed so far in adipocytes have simply measured the steady state distribution of the protein and mutations in each of the motifs so far described have resulted in an accumulation of GLUT4 at the cell surface in an insulin-independent manner [Marsh *et al.* (1995), Verhey *et al.* (1995)]. However, such a phenotype could result from impaired sorting at the TGN, endosomes or the plasma membrane. In an effort to further define the role of the distal carboxy-terminal signal in the present study, we have quantified the distribution of mutants between intracellular compartments that are readily accessible to recycling Tf-HRP, versus those that are not. While the nature of the latter compartment(s) remains ill-defined [Martin *et al.* (1996), Martin *et al.* (1997)], mutation of the ⁴⁹⁸TELE⁵⁰¹ sequence clearly resulted in an accumulation of GLUT4 in endosomes. This increased endosomal localisation of the 498 mutant supports our view that GLUT4 is normally actively sorted out of endosomes in insulin-sensitive cells, and that this step is at least in part regulated by the carboxy-terminal distal motif. Importantly, it remains to be determined whether this sequence can function autonomously in the context of a heterologous protein. The lack of a shift of the 502 mutant into endosomes was somewhat surprising in view of the data obtained for the 498 mutant. The possibility that this domain (⁴⁹⁸TELEYLGP⁵⁰⁵) comprises two separate motifs serving different

functions cannot be ruled out. However, it is noteworthy that I was only able to ablate cell lines expressing 502 at low levels, and in which the mutant did not exhibit an altered distribution compared to either TAIL or 498 as assessed by subcellular fractionation analysis. As noted previously [Marsh *et al.* (1995)], the expression level of GLUT4 mutants in adipocytes is an important variable to be considered in targeting studies such as these, presumably due to compensatory effects by motifs located elsewhere in the protein. The fact that this sequence does not at least superficially resemble targeting motifs found in most other proteins is consistent with this being a relatively specific sorting step. It might be noteworthy that a similar sequence (PDEVEYEP) is found adjacent to and membrane-distal from a dileucine motif in the cytoplasmic tail of vp165, a protein targeted similarly to GLUT4 in both adipocytes and cardiomyocytes [Ross *et al.* (1996), Malide *et al.* (1997), Martin *et al.* (1997)] (Table 5.2). In addition, an acidic sequence (CPSDSEEDeg) within the cytoplasmic tail of furin that functions independently of either the Y- or LL-based signals in this protein, and is located membrane-distal to them, has been shown to direct its localisation to the TGN [Schafer *et al.* (1995), Voorhees *et al.* (1995)].

Mutation of each of the targeting domains in GLUT4 has so far failed to abrogate the insulin-regulated movement of this protein from an intracellular compartment to the cell surface. These data are consistent with the notion that the primary and cumulative function of the targeting signals identified in GLUT4 is to sequester the protein in a post-endocytic storage locale, from where the protein can readily gain access to the plasma membrane following stimulation with agonists such as insulin. Defining the nature of this post-endocytic storage compartment, and how it relates to the endo-lysosomal system, should facilitate a better understanding of

how multiple targeting signals within the cytoplasmic tails of GLUT4 direct its intracellular trafficking in insulin-sensitive cells.

5.6 Summary

This study has investigated the role of residues distal to the di-leucine motif in the carboxy-terminal cytoplasmic tail of GLUT4 in targeting this isoform in adipocytes. Mutation of residues 498-505 (TELEYLGP), but not 506-509 (DEND), resulted in a redistribution of the protein to the cell surface in an insulin-independent manner. Mutation of TELE appeared to have a more dominant effect on targeting, resulting in an accumulation of GLUT4 in endosomes. None of these mutations abrogated the ability of insulin to translocate GLUT4 to the cell surface. These data suggest that the cytoplasmic carboxy-terminus of GLUT4 contains an additional targeting signal distal to the di-leucine motif that regulates sorting of GLUT4 from endosomes into a post-endocytic storage compartment.

Comparison of the GLUT4 Carboxy-terminal and vp165 Amino-terminal Sequences

GLUT4 Carboxy-terminus

...METFTNDRLQLPRNMI...ENSMFEEEPDVVDLAKEPC..**LHPLEPDEVE**...

251

Chapter 6

Construction and Analysis of GLUT2/GLUT4 Chimeric Glucose Transporters

6.1 Aims

The aims of this chapter are:

1. To construct chimeric GLUT2/GLUT4 glucose transporters using recombinant PCR technology. These recombinant transporters will be constructed by swapping the cytoplasmic amino- and carboxy-terminal domains of these transporter isoforms.
2. To introduce the above chimeric transporters into 3T3-L1 adipocytes for use as a tool enabling investigation of the contribution of the N- and C-terminal targeting motifs in GLUT4 trafficking.

6.2 Introduction

Various studies carried out over the last decade have clearly established that the signal sequences present in the amino- and carboxy-terminal cytoplasmic sequences of GLUT4 are fundamentally important in the regulation of the unique pattern of recycling and subcellular distribution displayed by this facilitative glucose transporter isoform [reviewed in Chapter 1 and Gould (1997)].

More than any other, the use of one technique has been responsible for the discoveries made into the roles of the above domains in GLUT4 trafficking: the construction of chimeric glucose transporters in which reciprocal domains were exchanged between GLUT4 and the ubiquitous glucose transporter isoform, GLUT1, and the subsequent analysis of the subcellular distributions of these chimeras in a variety of cellular systems. This technique was employed in studies carried out by various groups, including those of Birnbaum, James and Meuckler [Piper *et al.* (1992), Piper *et al.* (1993b), Czech *et al.* (1993), Marshall *et al.* (1993), Verhey *et al.* (1993), Verhey *et al.* (1995), Verhey & Birnbaum (1994)].

In all of the above studies the recombinant chimeric transporters were constructed by fusing portions of the GLUT1 and GLUT4 cDNAs at common restriction sites either present in the wild-type sequence or engineered by polymerase chain reaction (PCR)-based mutagenesis. Some examples of the chimeric species employed in the above studies are listed in Figure 1.6. These chimeras were introduced into various cellular systems including CHO cells, PC12 cells, COS cells and oocytes.

The key information that emerged from these studies was the initial identification of the ⁵FQQI⁸ and L⁴⁸⁹L⁴⁹⁰ sequences as being important motifs in the process of GLUT4 trafficking. It was demonstrated that both of these motifs were responsible for the internalisation of GLUT4 from the cell surface and that other motifs present in the carboxy-terminus of the protein may be responsible for its targeting to an insulin-responsive intracellular compartment. I have previously discussed in detail the results of these studies in section 1.6 of this thesis.

It is noteworthy that the majority of the previous studies involving GLUT4 chimeras made use of the ubiquitous glucose transporter isoform GLUT1 as the chimeric partner. This method has an inherent fundamental drawback in that it is recognised that GLUT1 exhibits a pattern of constitutive recycling in insulin-responsive cells in the basal state, and is also translocated to the plasma membrane, albeit to a lesser extent than GLUT4, in response to insulin [Zorzano *et al.* (1989). Holman *et al.* (1990)]. As a consequence, it could be argued that any alteration in GLUT4 trafficking observed after swapping GLUT1 and GLUT4 sequences could be attributed to the influence of dominant GLUT1 signals and not simply as a result of the removal or introduction of specific GLUT4 targeting sequences.

In an attempt to overcome this problem, I chose to construct a series of chimeric transporters using the liver-type glucose transporter isoform, GLUT2, as the chimeric partner. GLUT2 was chosen because previous studies have shown that this isoform is predominantly localised at the basolateral membrane of intestinal and kidney absorptive epithelial cells and the sinusoidal membrane of hepatocytes, and displays little or no

recycling characteristics [Thorens *et al.* (1990), Brant *et al.* (1994)]. Brant *et al.* also established that GLUT2 is predominantly localised at the PM of 3T3-L1 adipocytes when stably expressed in this cell type. This suggested that GLUT2 may be a more informative chimeric partner than GLUT1 for the identification of targeting motifs.

A further point to note is that the majority of the previous studies utilising chimeras were carried out in non-insulin-responsive cell lines. This presents another problem as such cells (e.g. CHO cells, COS cells and oocytes) may not possess cell-specific factors which mediate the insulin-regulated trafficking of GLUT4 and furthermore, the insulin-responsive intracellular pool may not exist in cells other than adipose or muscle tissue. As a consequence I have carried out all of these studies in 3T3-L1 adipocytes, a classic model for insulin-stimulated glucose transport.

Finally, it is apparent that the use of GLUT1/GLUT4 chimeras offers no simple method of undertaking functional transport assays because as both chimeric partners only have the capacity to transport glucose they cannot be distinguished from endogenous glucose transporters. The employment of GLUT2, a fructose transporter, overcomes this problem as it makes it possible to assay fructose transport in order measure such parameters as the translocation of the chimeric transporters to the PM after insulin stimulation, thus allowing kinetic analysis of the contributions of the amino- and carboxy-terminal signal motifs in GLUT4 trafficking.

6.3 Methodology Used to Generate GLUT2/GLUT4 Chimeric Glucose Transporters

6.3.1 Plasmid Constructs

Human glucose transporter cDNAs encoding GLUT2 and GLUT4 have been cloned into pSP64T as described previously [Gould *et al.* (1991)] to form pHTL.217 and pSPGT4, respectively (Figure 6.1). These constructs contain the protein coding region of the cDNAs and various amounts of the 5'- and 3'-untranslated regions. The cDNA sequences are flanked by 89bp of 5'- and 141bp of 3'-untranslated regions of the β -globin gene of *Xenopus laevis* [Kayano *et al.* (1990)]. The plasmids contain an SP6 polymerase promoter located 5' to the transporter sequence, a gene conferring ampicillin resistance, and encode functional transporters [Gould *et al.* (1991)].

6.3.2 Recombinant PCR Reactions

The GLUT2 cDNA-containing construct pHTL.217 and the GLUT4 cDNA-containing construct pSPGT4 were used as templates in the recombinant PCR reactions described below.

Two sets of oligonucleotide primers were designed for use in the following PCR reactions. These are referred to as the 5' or 3' external primers. The 3' external primers are 37'mers that correspond to the extreme 3' antisense strands of GLUT2 and GLUT4, which bind to the 3' untranslated region of the sense strand of the respective GLUT isoform, and are called G2-End and G4-End, respectively. These primers encode *Sal* I and *Not* I restriction sites,

respectively, to enable subcloning into the polylinker site of a suitable vector. The 5' external primers are 90 bases and 57 bases in length and are called G2/G4 and G4/G2, respectively. G2/G4 is designed such that it encodes the first 15 bases of GLUT2 together with bases 58-87 of GLUT4 and encodes a *Bam* HI restriction site. G4/G2 encodes the first 30 bases of GLUT4 together with bases 16-48 of GLUT2 and encodes a *Sal* I restriction site. Both of the 5' external primers bind to the 5' untranslated region of the antisense strand of the respective GLUT isoform. The sequences of these primers are displayed in Table 6.1.

Both of the recombinant chimeric transporters that I am going to discuss at this stage were produced by a primary PCR reaction involving the GLUT2 and GLUT4 templates and a combination of a 5' external primer and a 3' external primer (Figure 6.2).

6.3.2a GLUT4N/2

This chimeric transporter is a primary PCR product produced by the recombination of the amino-terminal cytoplasmic region of GLUT4 to helices 1-12 of GLUT2. It was designed to reveal the influence of the putative amino-terminal targeting signals by their introduction into this predominantly GLUT2-based chimera. In this case, the GLUT2 template was used in conjunction with the 5' external primer, G4/G2, and the 3' external primer, G2-End, to produce and amplify the desired recombinant product (Figure 6.3).

6.3.2b GLUT2N/4

This mutant is a primary PCR product produced by the recombination of the amino-terminal cytoplasmic region of GLUT2 to helices 1-12 of GLUT4. This chimera should reveal the effect caused by deleting the amino-terminal targeting signals, thus providing further information as to the extent to which they are involved in the trafficking of GLUT4. This reaction utilised the GLUT4 cDNA template along with the 5' external primer, G2/G4, and the 3' external primer, G4-End, to produce and amplify the desired recombinant product (Figure 6.3).

PCR reactions were carried out using *Vent* DNA polymerase under reaction conditions which were altered according to the manufacturers instructions. Details of the reaction conditions and thermal cycling programmes used are listed in sections 2.10.4 and 2.10.5. The size of the primary PCR products were approximately 1500 bp in each case (Figure 6.4).

6.3.3 Cloning Strategies

Two different cloning strategies were employed in the production of the above recombinant chimeric transporters.

6.3.3a pNot.Not and pOP13CAT.aP2 Approach

Primary PCR products were purified by agarose-gel electrophoresis followed by electroelution of the DNA and passage through an Elutip-d column (sections 2.12.4-5 and 2.12.7). The purified PCR product GLUT4N/2 encoded *Sal* I restriction sites at the 5' and 3' ends allowing subcloning into the polylinker

site of the shuttle vector pNot.Not (a pGEM11z and pBluescript polylinker fusion kindly provided by Prof. K. Siddle, University of Cambridge) (Figure 6.5). pNot.Not was digested with *Sal* I and the linearised vector was purified by electrophoretic extraction from agarose gel slices, followed by passage through an Elutip-d column and ethanol precipitation (section 2.12.2). The primary PCR fragment was also digested with *Sal* I and purified using the same procedure before ligation to the linearised vector and transformation into competent *E. coli* cells (sections 2.12.9-11). Plasmid DNA was prepared from several clones to identify potential positive clones by restriction digestion analysis (sections 2.12.14 and 2.12.3). On identification of positive clones, large scale plasmid preparations (section 2.12.15) were performed to obtain sufficient quantities of DNA in order to facilitate further subcloning into the adipocyte-specific promoter-containing vector pOP13CAT.aP2 (Figure 6.5).

The DNA produced from positive clones was digested with *Not* I to release the primary PCR fragment from the shuttle vector pNot.Not. This desired fragment was purified as above. pOP13CAT.aP2 was also digested with *Not* I to excise the CAT reporter gene and produce a linearised vector backbone. The linearised vector was then purified using the same procedure before ligation with the GLUT4N/2 fragment and transformation into competent *E. coli* cells. As before plasmid mini-preps were carried out, followed by screening by restriction digestion analysis. Positive clones were then prepared on a large scale.

A similar strategy was adopted for the subcloning of the PCR fragment GLUT2N/4, except that it involved digestion of the fragment with *Bam* HI and *Not* I, followed by subcloning into pNot.Not and then pOP13CAT.aP2.

6.3.3b Cloning PCR Products Using the Invitrogen Eukaryotic TA Cloning® Kit

The protocols for this technique are discussed in detail in section 2.11.

Briefly, the primary PCR products were incubated with *Taq* DNA polymerase to produce the 3' A-overhangs that are essential in order for PCR fragments to be subcloned using this technique. The fragments, complete with 3' A-overhangs, were then directly ligated into the eukaryotic bidirectional TA cloning vector pCR®3.1 and transformed into One Shot™ TOP 10F' competent cells (Figure 6.6). Small scale plasmid preparations were carried out using the QIAGEN QIAprep 8 Turbo Miniprep Kit to provide sufficient DNA for restriction digestion analysis (section 2.12.13) (Figures 6.7 and 6.8). Positive clones were then prepared on a large scale (section 2.12.16).

6.3.4 Expression of GLUT2/GLUT4 Chimeras in 3T3-L1 Adipocytes

The GLUT2/GLUT4 recombinant transporters were introduced into the cell line chosen for analysis, 3T3-L1 adipocytes, using the Calcium Phosphate method of transfection. This procedure is detailed in section 2.3.7.

6.3.5 Complementary GLUT2/GLUT4 Chimeras

Large scale plasmid preparations were performed on a series of complementary GLUT2/GLUT4 chimeras, the DNA for which was supplied by Dr. Bernard Thorens, University of Lausanne, Switzerland (Figure 6.9). These recombinant transporters were expressed in 3T3-L1 adipocytes using the Calcium Phosphate method.

6.3.5a GLUT2/4

This chimera is a product of the recombination of the cytoplasmic amino-terminus and first extracellular loop of GLUT2 with helices 2-12 and the carboxy-terminal cytoplasmic region of GLUT4. It is similar in nature to mutant GLUT2N/4 but should also allow more detailed analysis of the amino-terminal sequence, especially putative signals present in the extracellular loop between helices 1+2.

6.3.5b GLUT4/2C

This chimera is composed of the native sequence of GLUT4 from the amino-terminus to the carboxy-terminal residue of transmembrane helix 12 attached to the carboxy-terminal cytoplasmic region of GLUT2. This mutant will allow analysis of the contribution of the carboxy-terminal cytoplasmic sequences of GLUT4 to its unique intracellular distribution.

6.3.5c GLUT2N/4/2C

This chimera is constructed by recombination of the cytoplasmic amino-terminus and first extracellular loop of GLUT2, helices 2-12 of GLUT4, and the carboxy-terminal cytoplasmic region of GLUT4. Such a composition will allow observation of the effects of removing both of the salient signalling domains of GLUT4.

Figure 6.1

Diagram of a GLUT cDNA Cloned into the pSP64T Vector

GLUT2 cDNA was ligated to *Bgl* II DNA linkers and cloned into the untranslated regions of the *Xenopus* β -globin gene, which had previously been cloned into the multiple cloning site of pSP64 [Kreig & Milton (1984)]. The GLUT4 cDNA was ligated to *Sal* I DNA linkers and cloned into the untranslated regions of the *Xenopus* β -globin gene. The 5' untranslated region (UTR) is 89bp long and the 3' untranslated region is 141bp long. The GLUT cDNA and its flanking sequences are located 3' of the SP6 polymerase promoter.

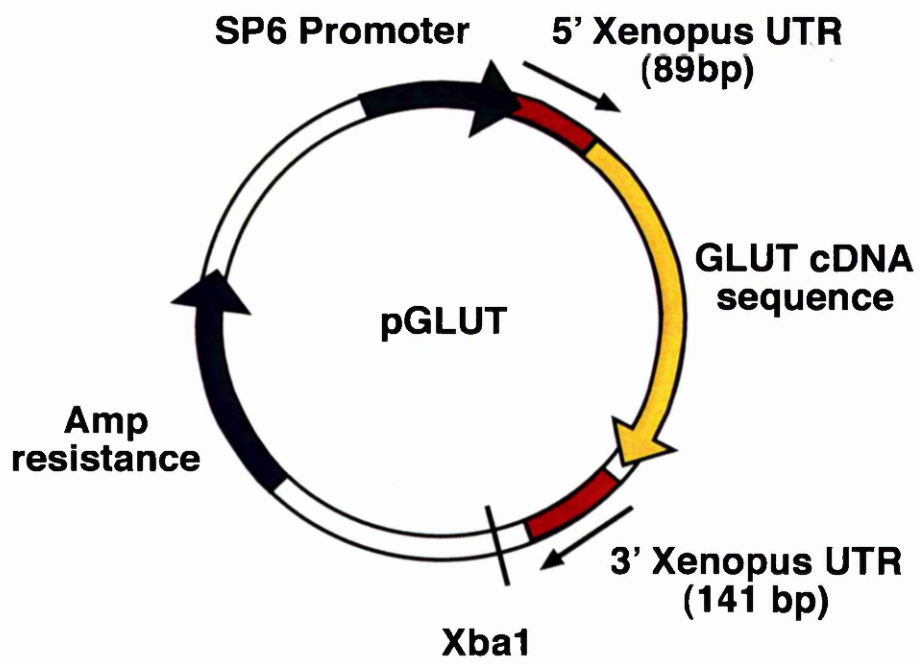
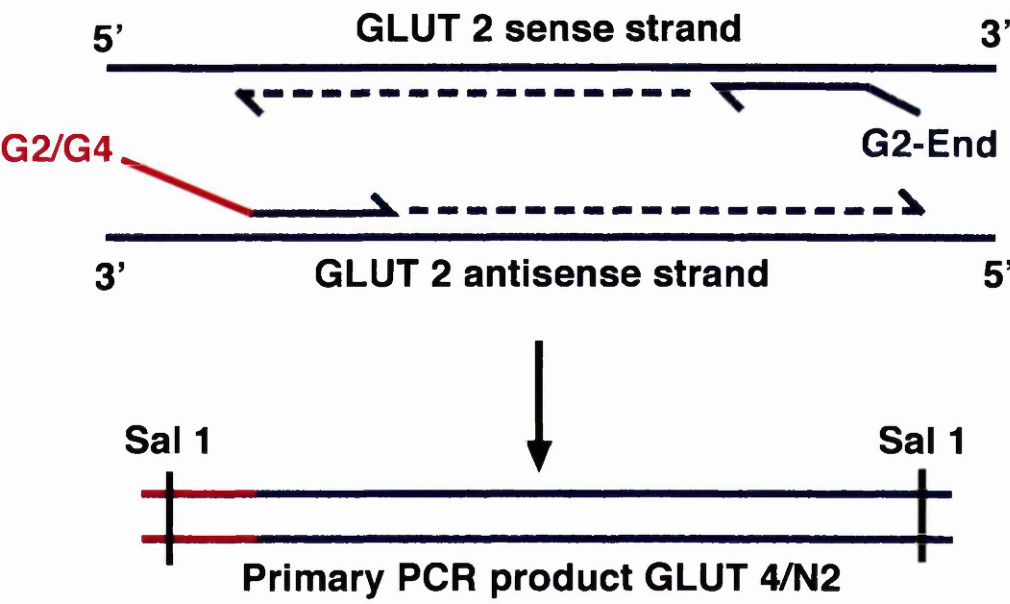


Figure 6.2

Generation of GLUT2/GLUT4 Chimeras Using Recombinant PCR Technology

This diagram describes the PCR method used to construct GLUT4N/2 and GLUT2N/4, which comprise the amino-terminal cytoplasmic region of GLUT4 or GLUT2 respectively, followed by the sequence of GLUT2 or GLUT4 from transmembrane helix 1 to the carboxy-terminus, respectively. These PCR products were generated by primary PCR reactions in which GLUT2 or GLUT4 template DNA were incubated with the appropriate primers. The 3' external primers anneal to the sense strands of GLUT2 and GLUT4 cDNA and have tails encoding *Sal* I and *Not* I restriction sequences for use in subsequent cloning procedures. The 5' external primers anneal to the antisense strand of GLUT2 and GLUT4 cDNA and have tails encoding *Sal* I and *Bam* HI restriction sequences, respectively. Thus, in a single primary PCR reaction, GLUT2 or GLUT cDNA act as templates, which under the reaction conditions, undergo strand dissociation allowing the extension of new strands from the primers in a 5' to 3' direction by *Vent* DNA polymerase. Melting, re-annealing and extension occur 27 times producing primary PCR products of ~1500bp.

PRIMARY PCR - GLUT 4N/2



PRIMARY PCR - GLUT 2N/4

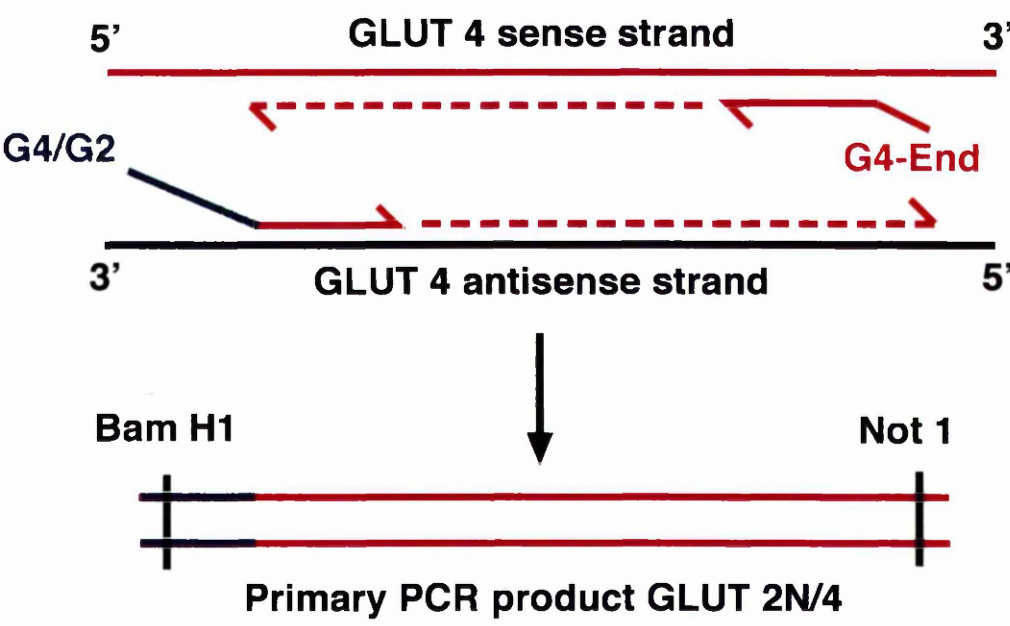
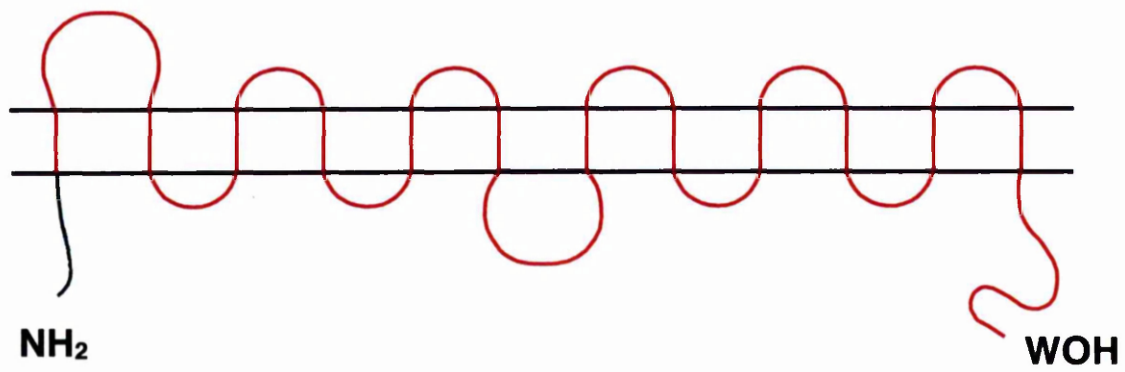


Figure 6.3

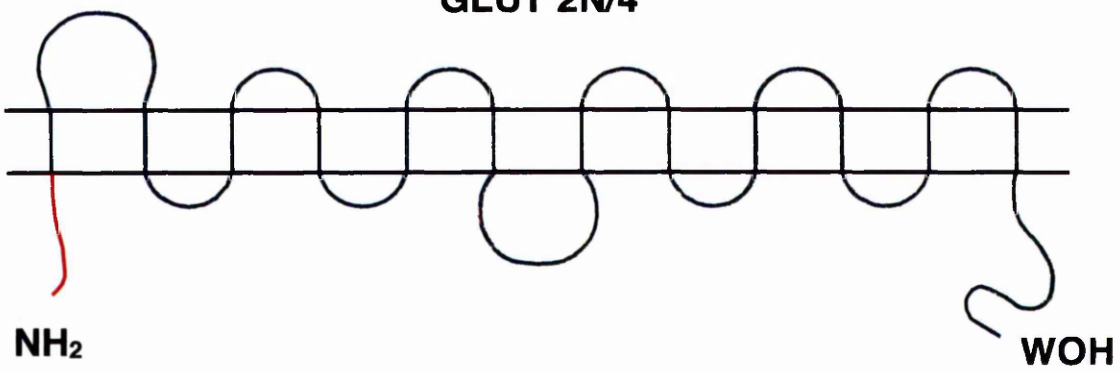
Schematic Representation of Recombinant GLUT4N/2 and GLUT2N/4 Chimeras

This is a schematic representation of the GLUT2/GLUT4 transporters generated by recombinant PCR technology. GLUT2 sequence is represented in red and GLUT4 sequence is represented in blue.

GLUT 4N/2



GLUT 2N/4



— GLUT 2
— GLUT 4

Figure 6.4

1% Agarose Gel of Primary PCR Products Used in the Cloning of Recombinant GLUT2/GLUT4 Chimeras

This figure shows a photograph of primary PCR products which had been subjected to 1% agarose gel electrophoresis and stained with ethidium bromide. Lane 1 contains 0.625mg of *Bst*E II-digested lambda DNA, Lanes 2-7 contain 5 μ l (from a total of 100 μ l) of GLUT4N/2 primary PCR product generated using *Vent* DNA polymerase.

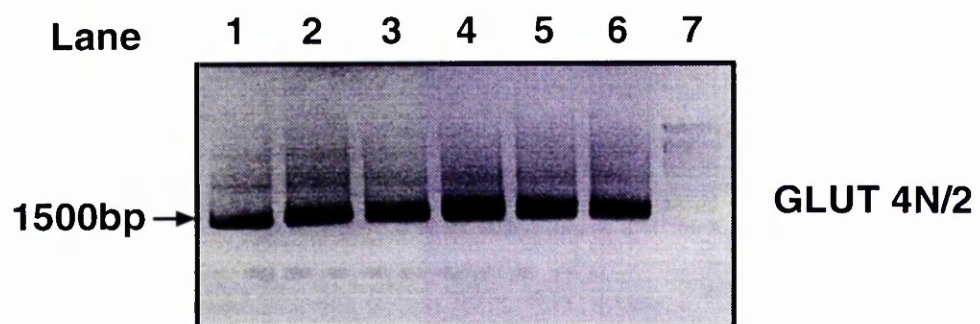
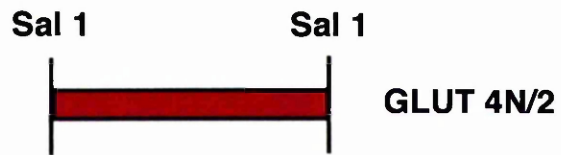


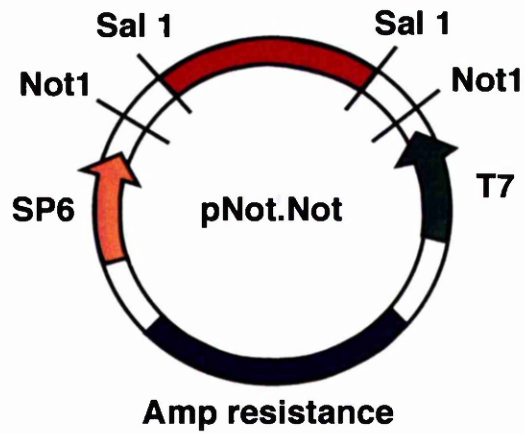
Figure 6.5

Cloning of Recombinant Chimeras Using pNot.Not and pOP13CAT.aP2

This diagram illustrates a cloning strategy utilising the shuttle vector pNot.Not and the vector pOP13CAT.aP2 which includes an adipocyte-specific promoter. The recombinant GLUT2/GLUT4 cDNAs were digested using either *Sal* I (GLUT4N/2) or *Bam* HI and *Not* I (GLUT2N/4) and ligated into the polylinker site of pNot.Not which had been digested with the appropriate enzymes. Positive clones were then digested with *Not* I to release the primary PCR fragment from the polylinker site of pNot.Not which was then inserted into pOP13CAT.aP2 which had been linearised using *Not* I. This produced an intact pOP13CAT.aP2 vector incorporating the chimeric GLUT2/GLUT4 cDNA under the control of the adipocyte-specific promoter aP2.



Ligate into
pNot.Not polylinker



Excise with Not 1



Ligate into
pOP13CAT.aP2

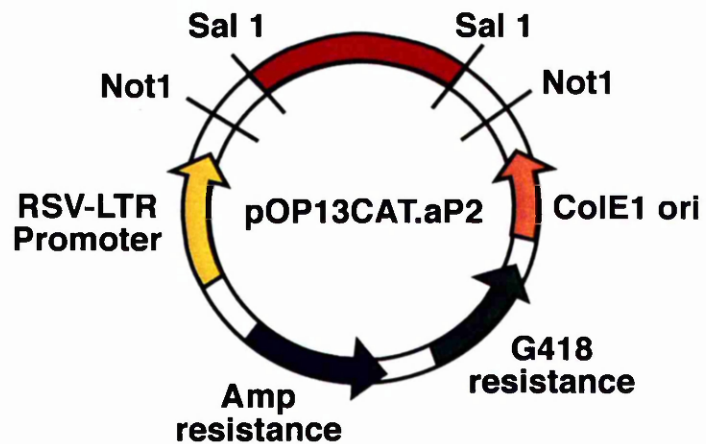


Figure 6.6

**Cloning of Primary PCR Products Using the Invitrogen
Eukaryotic TA Cloning® Kit**

This diagram illustrates a cloning strategy employing the Invitrogen Eukaryotic TA Vector. Recombinant GLUT2/GLUT4 primary PCR products were incubated with *Taq* DNA polymerase to produce the 3' A-overhangs that are essential when using this cloning strategy. The fragments, complete with 3' A-overhangs, were then directly ligated into the linear eukaryotic bidirectional TA cloning vector pCR®3.1.

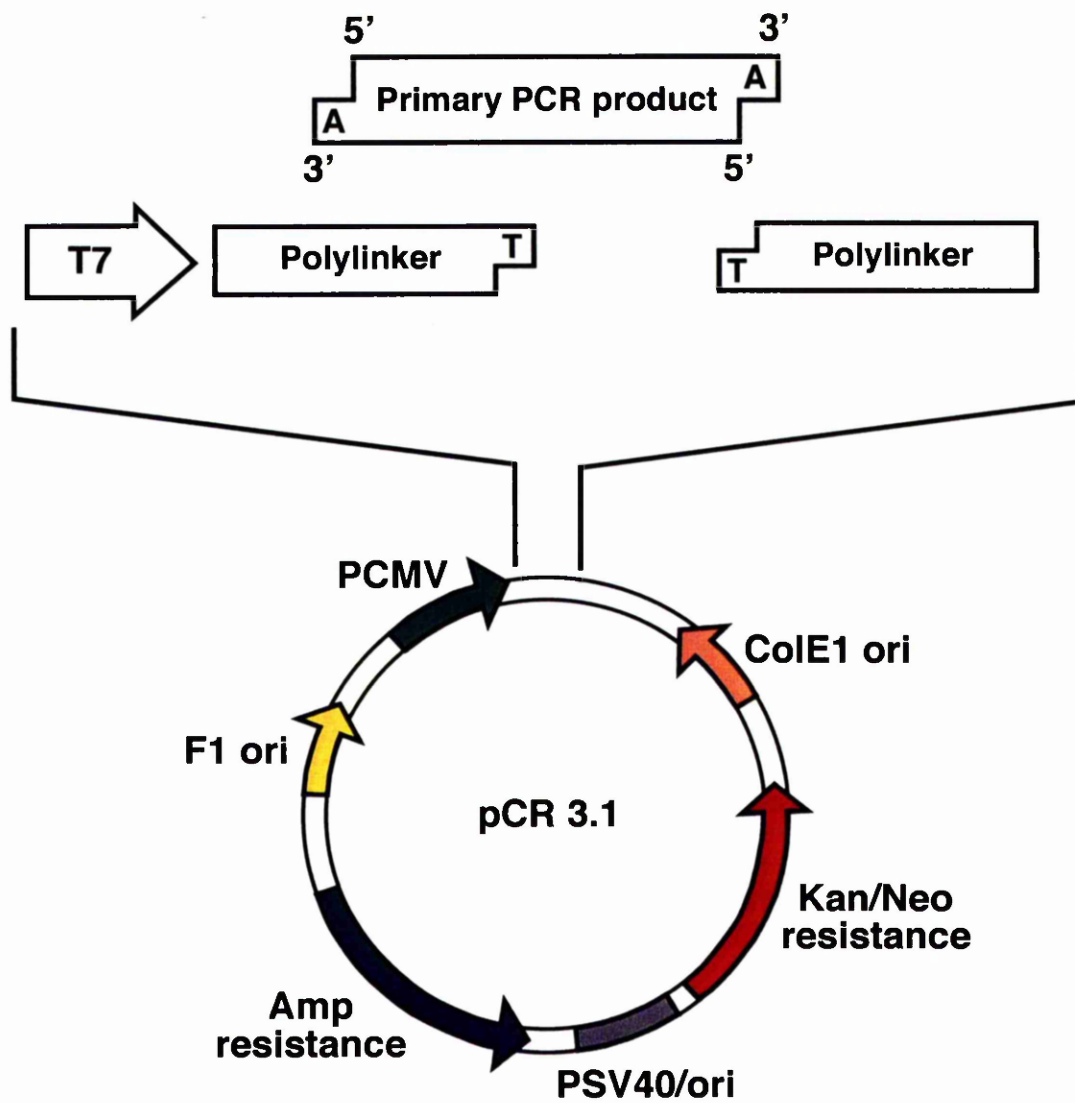
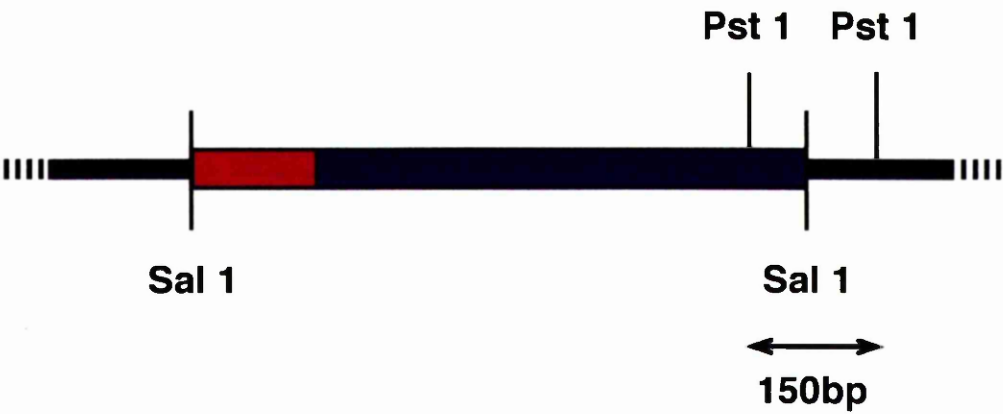


Figure 6.7

Restriction Digestion Analysis of Chimera GLUT4N/2

This diagram shows the position of the cleavage sites of the restriction enzymes used to determine the orientation of the GLUT2/GLUT4 chimera GLUT4N/2 in the vector pCR®3.1. GLUT2 sequence is shown in blue and GLUT4 sequence is shown in red. The extreme carboxy-terminal portion of GLUT2 contains a *Pst* I site that is not present on the sequence of GLUT4. The vector pCR®3.1 contains only one *Pst* I site that is located 3' to the chimeric insert sequence in the vector. Thus, restriction digestion with *Pst* I yields different sized fragments depending on the orientation of the ligated insert. Chimeric sequence inserted in the correct orientation i.e. for transcription driven by the T7 promoter, yields two fragments of approximately 6350bp and 150bp. Insert ligated in the incorrect orientation results in the production of two fragments of 5150bp and 1350bp in length. The fragments produced by electrophoresis were separated by agarose gel electrophoresis (section 2.12.1) and the sizes of the fragments were determined by comparison against a *Bst*E II-digested lambda DNA molecular weight marker loaded on the same gel.

Correct orientation



Incorrect orientation

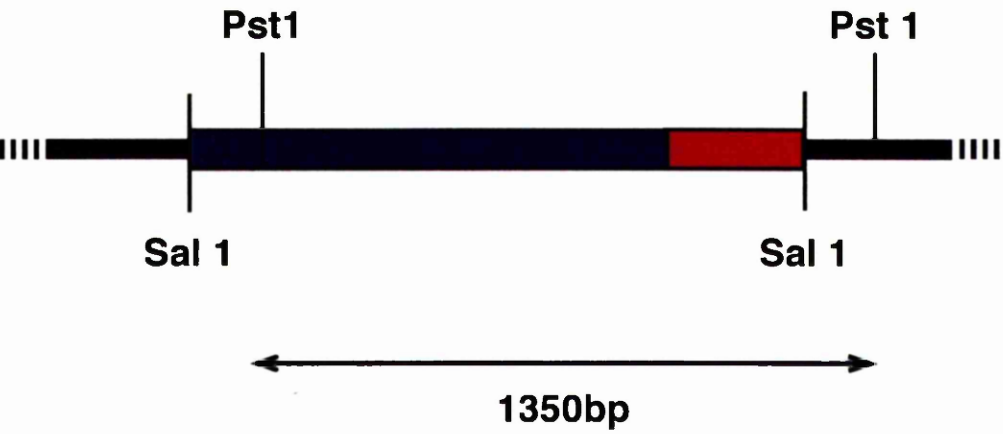


Figure 6.8

Restriction Digestion Analysis of Chimera GLUT2N/4

This diagram shows the position of the cleavage sites of the restriction enzymes used to determine the orientation of the GLUT2/GLUT4 chimera GLUT2N/4 in the vector pCR®3.1. GLUT2 sequence is shown in blue and GLUT4 sequence is shown in red. The vector pCR®3.1 contains only one *Bam* HI site that is located 5' to the chimeric insert sequence in the vector. Thus, restriction digestion with *Bam* HI yields different sized fragments depending on the orientation of the ligated insert. Chimeric sequence inserted in the correct orientation i.e. for transcription driven by the T7 promoter, yields two fragments of approximately 6400bp and 100bp. Insert ligated in the incorrect orientation results in the production of two fragments of 4900bp and 1600bp in length. The fragments produced by electrophoresis were separated by agarose gel electrophoresis (section 2.12.1) and the sizes of the fragments were determined by comparison against a *Bst*E II-digested lambda DNA molecular weight marker loaded on the same gel.

Correct orientation



Incorrect orientation

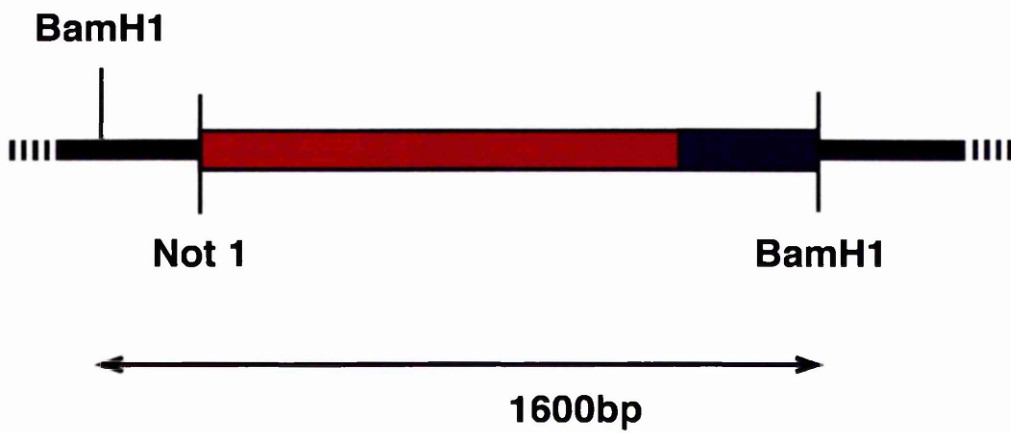
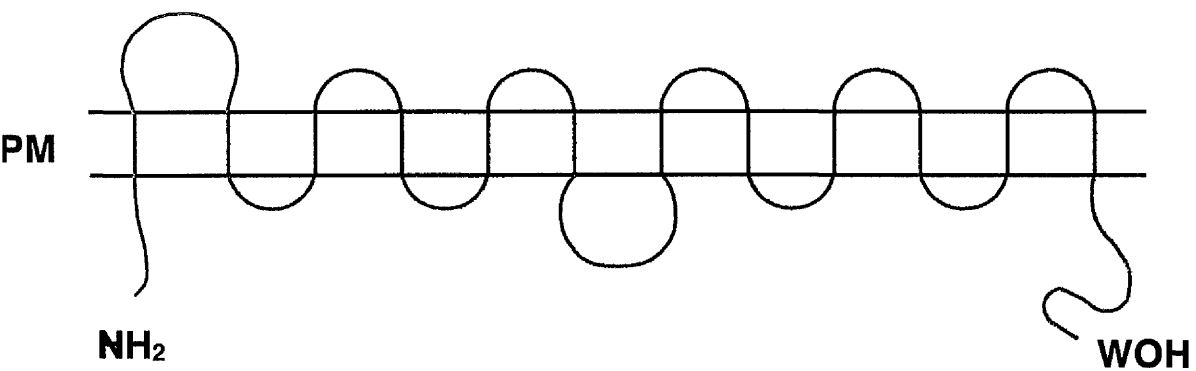


Figure 6.9

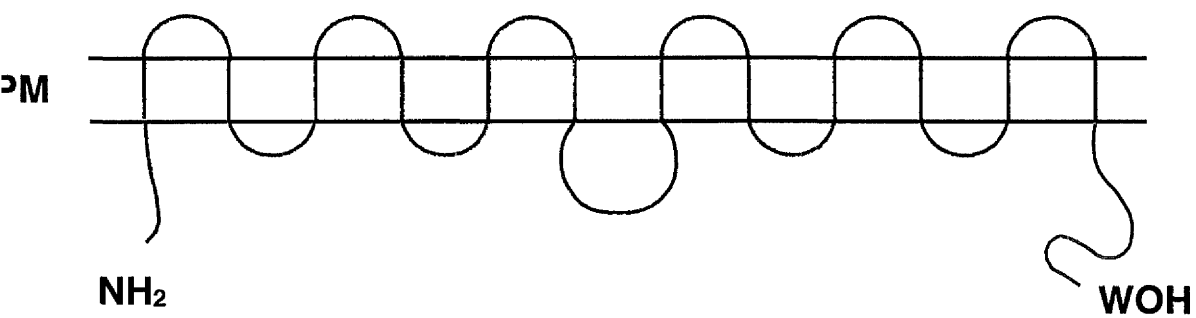
Schematic Representation of Complementary GLUT2/GLUT4 Chimeras

This is a schematic representation of the complementary GLUT2/GLUT4 transporters transfected into 3T3-L1 adipocytes using cDNAs supplied by Dr. Bernard Thorens, University of Lausanne, Switzerland. GLUT2 sequence is represented in red and GLUT4 sequence is represented in blue.

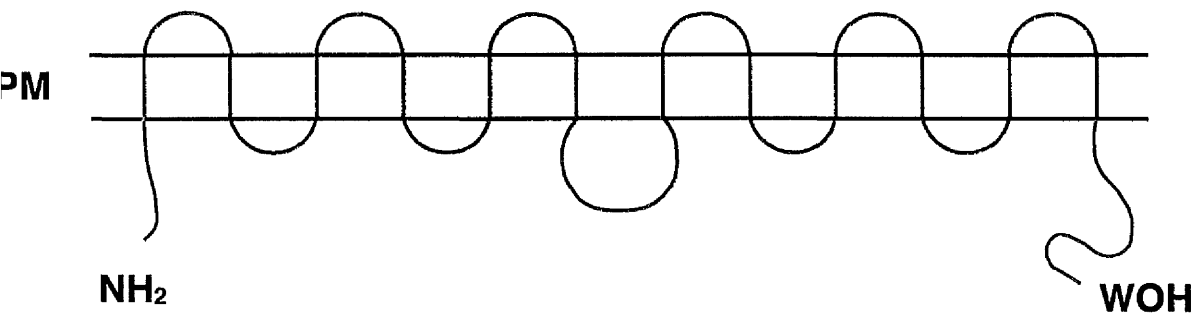
GLUT 2/4



GLUT 4/2C



GLUT 2N/4/2C



— GLUT 2
— GLUT 4

Table 6.1

**Sequences of Oligonucleotide Primers Used to Generate
GLUT2/GLUT4 Chimeras**

Sequences corresponding to GLUT4 are underlined. Sequences which encode a restriction site used in the subcloning of PCR fragments are written in lower case italics. All oligonucleotides are written in the 5' to 3' direction.

Table 6.1
Sequences of Oligonucleotide Primers Used to Generate GLUT2/GLUT4 Chimeric Transporters

3' External Primers

G2-End	5'	<i>gtcgacgtcga</i> CAGACGGTTCCTTATTGTTCTGT	3'
G4-End	5'	<i>gcggccgcgcgg</i> <u>CCCGCAGCTGGCTCTCCCA</u> CCCTG	3'

5' External Primers

G2/G4	5'	<i>ggctccggatcc</i> ATGACAGAGATAAGTGACTGGGACCCCTGGTCTTGCTGTTC	3'
G4/G2	5'	<i>gtcgacgtcga</i> <u>ATGCCGTGCGCTTCCAA</u> CAGATAGGCTCCGTCACCTGGACCCCTG	
		GTTTCACTGTCACTCACTGTGTGCTGGGTTC	3'

6.4 Results

Using the TA cloning strategy and the Calcium Phosphate method of transfection I have managed to successfully stably express both GLUT4N/2 and GLUT2N/4 in 3T3-L1 adipocytes. In addition to this I have also stably expressed the series of complementary GLUT2/GLUT4 chimeras. A range of clones expressing these species have been isolated and stored.

6.4.1 Subcellular Fractionation of GLUT2/GLUT4 Chimeras

The subcellular distribution of the GLUT2/GLUT4 chimeras between the plasma membrane and the low and high density microsomal membranes was investigated by employing the technique of subcellular fractionation (section 2.5.3). This technique generated the following subcellular membrane fractions: plasma membranes (PM) \pm insulin, low density microsomal membranes (LDM) \pm insulin, high density microsomal membranes (HDM) \pm insulin, and soluble proteins (SP) \pm insulin. Figures 6.10A-C are representative immunoblots of the results to date in this study.

Figures 6.10A and 6.10B show the subcellular distribution of the chimeras GLUT4N/2 and GLUT4/2C. These display a pattern of distribution similar to wild-type GLUT4, with a predominantly intracellular distribution in the basal state which is shifted significantly to the cell surface in response to insulin. A concomitant decrease is observed in the level of intracellular GLUT4N/2 and GLUT4/2C after insulin-stimulation. Thus the introduction of GLUT4 cytoplasmic amino-terminal trafficking signals to a predominantly GLUT2-based chimera or a chimera specifically lacking the GLUT4 carboxy-terminal region appears sufficient to shift their distribution

from a primarily cell surface localisation to an intracellular locale which is insulin-responsive.

Figure 6.10C displays the subcellular distribution of the chimeric glucose transporter GLUT2/4. This chimera demonstrates a distribution pattern that is also similar to wild-type in nature. It is localised in a predominantly intracellular location in the absence of insulin and is translocated to the cell surface in a manner similar to wild-type GLUT4 in response to insulin. This result suggests that the presence of the trafficking signals in the carboxy-terminus of GLUT4 are sufficient to overcome the loss of the amino-terminal signal sequences and can maintain the GLUT4-like subcellular distribution of this chimera.

6.4.2 Compartment Ablation Analysis of GLUT2/GLUT4 Chimeras

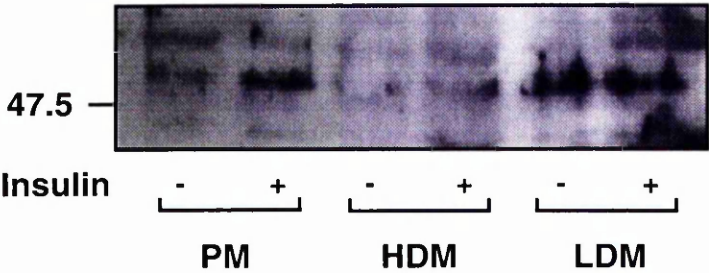
The intracellular targeting of the GLUT2/GLUT4 chimeras between the ablatable and non-ablatable GLUT4 pools was examined using the compartment ablation technique (sections 2.5.1-3). Figure 6.11 is a representative immunoblot of the results using this technique with the aforementioned chimeric transporters. Lack of time has precluded a detailed analysis using this method, therefore the data is inconclusive. Hence, at this time it is not possible to draw conclusions as to the effects of replacing signal sequences on the distribution of these chimeras between the two intracellular GLUT4 pools discussed in Chapter 3.

Figure 6.10

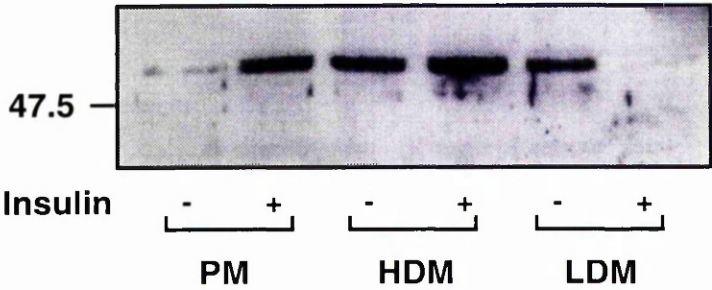
Subcellular Fractionation of GLUT2/GLUT4 Chimeras

3T3-L1 adipocytes stably expressing the recombinant GLUT2/GLUT4 chimeras were subjected to subcellular fractionation as described in section 2.5.3. Cells were incubated in the absence (–) or presence (+) of insulin and the following subcellular fractions: plasma membranes (PM) ± insulin, low density microsomal membranes (LDM) ± insulin, high density microsomal membranes (HDM) ± insulin, were produced. These subcellular fractions (20 µg protein) were immunoblotted with antibodies specific for either the amino- or carboxy-terminus of GLUT2. Representative immunoblots are shown for (A) one clone of chimera GLUT4N/2, (B) one clone of chimera GLUT4/2C and (C) one clone of chimera GLUT2/4.

A. Subcellular Fractionation of GLUT4N/2



B. Subcellular Fractionation of GLUT4/2C



C. Subcellular Fractionation of GLUT2/4

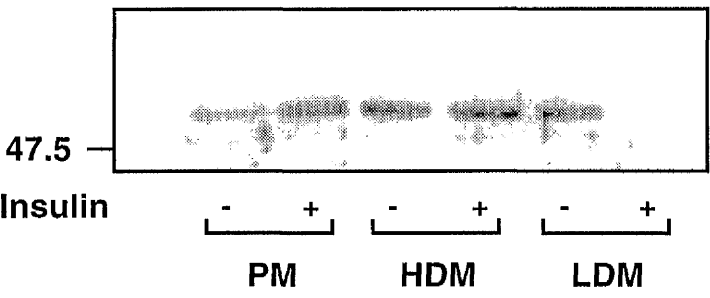
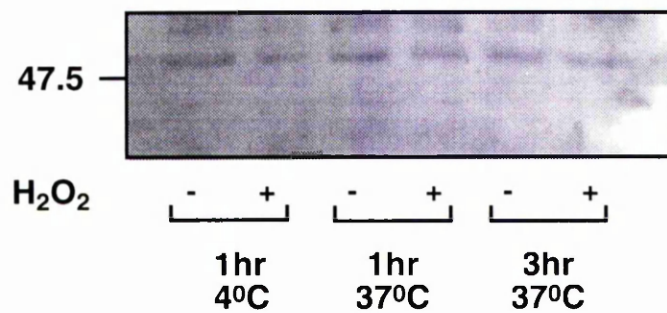


Figure 6.11

Compartment Ablation Analysis of GLUT2/GLUT4 Chimeras

LDM membranes were prepared from 3T3-L1 adipocytes loaded with Tf-HRP for 1hr at 4°C, 1hr at 37°C or 3hr at 37°C, before and after ablation (- and + hydrogen peroxide) as indicated. In these ablation experiments, cells were loaded with Tf-HRP exposed to DAB in the presence and absence of peroxide as indicated. LDM membranes were prepared, 20µg of each fraction were electrophoresed and immunoblotted using anti-GLUT2 antibodies to study the effect of ablation on the intracellular content of the chimeras.



6.5 Discussion

As stated above (section 6.4.1), the chimera GLUT4N/2 displays a primarily wild-type subcellular distribution in 3T3-L1 adipocytes. This indicates that the presence of signal motifs in the cytoplasmic amino-terminal domain of GLUT4 are sufficient to confer an intracellular distribution on this predominantly GLUT2-based chimera. This result is in agreement with published data which has stated that the amino-terminus of GLUT4 is both necessary and sufficient for intracellular sequestration of GLUT1/GLUT4 chimeric glucose transporters [Piper *et al.* (1992), Piper *et al.* (1993b)]. These studies also concluded that the ⁵FQQI⁸ motif mediates intracellular sequestration, at least in part by facilitating the interaction of the transporter with endocytic machinery (clathrin lattices) located at the cell surface. Further studies using GLUT4-transferrin receptor chimeras demonstrated that mutation of the phenylalanine at position 5 did not significantly alter the rate at which the chimeras were recycled back to the cell surface, suggesting that the major function of the amino-terminal domain is to promote the effective internalisation of GLUT4 from the cell surface, via a functional phenylalanine-based internalisation motif, rather than to promote retention of the transporter within intracellular structures [Garripa *et al.* (1994)].

It can be clearly seen from Figure 6.10A that the chimera GLUT4N/2 undergoes translocation to the cell surface in response to insulin. This result is in contrast to the published literature which reports that a chimera containing the amino-terminal 183 amino acids of GLUT4 married to a predominantly GLUT1 sequence, although intracellularly expressed, exhibited no significant translocation from the intracellular site to the

plasma membrane [Verhey *et al.* (1995)]. These workers interpreted this to mean that the amino-terminal domain of GLUT4 contains information involved in internalisation, but not in targeting to an insulin-responsive compartment. In contrast, the data presented in Chapter 3 of this thesis proposes a trafficking scheme for GLUT4 within which the amino-terminal ⁵FQQI⁸ motif is responsible for both internalisation and targeting of GLUT4 to an insulin-responsive compartment (section 3.5.3). It must be clarified however, that the insulin-responsive compartments to which GLUT4 is trafficked by the ⁵FQQI⁸ motif are represented by the early-endosomal (X_{ee}) and *trans*-Golgi (X_{tgn}) compartments, and not by the tubulo-vesicular storage compartment (X_{tv}) (previously termed the insulin-responsive compartment in the published literature). Therefore, the aforementioned scheme would explain the trafficking behaviour of the GLUT4N/2 chimera.

Figures 6.10B and 6.10C demonstrate that the chimera GLUT2/4 also has a intracellular distribution in the basal state in 3T3-L1 adipocytes. This can be explained by the presence of the di-leucine motif at positions 489 and 490, which has been shown to be capable of directing chimeric GLUT1/GLUT4 species to an intracellular location by two studies in 3T3-L1 adipocytes [Marsh *et al.* (1995), Verhey *et al.* (1995)]. However, the di-leucine motif is thought to be neither the major nor the dominant internalisation signal within GLUT4. The demonstration that the FAG mutant is expressed mainly at the plasma membrane even at very low levels of expression argues that the ⁵FQQI⁸ motif at the amino-terminus is the dominant internalisation motif [Marsh *et al.* (1995)]. This is in agreement with previous studies in which the amino-terminus has been

shown to function autonomously in heterologous cells to mediate intracellular sequestration [Piper *et al.* (1992), Garippa *et al.* (1994)].

After insulin treatment the chimera GLUT2/4 moves to the cell surface. This result is as expected as a previous study has shown that signal(s) contained within the carboxy-terminus of GLUT4 are essential for sorting to the tubulo-vesicular compartment, but interestingly, that the L⁴⁸⁹L⁴⁹⁰ motif is not involved in this sorting [Verhey *et al.* (1995)]. The possibility that further trafficking signals are present in the carboxy-terminus of GLUT4 is discussed in further detail in Chapter 5 of this thesis.

It must be noted that the above study is at present incomplete. In order to gain a clearer and more complete picture of the roles of the amino- and carboxy-terminal domains of GLUT4 in the intracellular trafficking of this isoform, further analysis of all of the stated chimeric transporters (sections 6.3.2a-b, 6.3.5a-c) requires to be performed.

With respect to the above data, it would be expected that a difference in the extent of translocation of the GLUT4N/2 and GLUT2/4 chimeras would be observed. GLUT4N/2 should display approximately a 3-fold increase at the cell surface after insulin treatment as it is predominantly located in the X_{ee} and X_{tgn} compartments. Previous studies have demonstrated this magnitude of insulin-stimulated movement for endosomal proteins such as the TfR and GLUT1 [Tanner & Leinhard (1987), Calderhead *et al.* (1990), Robinson *et al.* (1992)]. In contrast, it would be expected that the chimera GLUT2/4 would translocate to a much greater extent (e.g. 10-30-fold) as it is trafficked to the tubulo-vesicular compartment, which is proposed to be the GLUT4 storage compartment that is involved in the massive increase

in GLUT4 at the plasma membrane in response to insulin. Further experiments are needed to address this point.

Furthermore, I would expect that the chimera GLUT2/4 would be ablated to a much more significant degree than GLUT4N/2. This assumption is based on my findings in Chapter 3 which show that mutation of the F⁵ motif results in a massive increase in the extent of ablation, indicating that removal of this motif causes accumulation of transporters in the ablatable endosomal pool. In contrast, GLUT4N/2, complete with the ⁵FQQI⁸ sequence, would be expected to be trafficked to the non-ablatable GLUT4 pool.

6.6 Summary

In this study I have shown that the recombinant chimeric GLUT2/GLUT4 transporters examined adhere to the trafficking scheme proposed in Chapter 3 of this thesis. The amino-terminus of GLUT4 functions to promote internalisation of the chimera GLUT4N/2, and also traffics it to the insulin-responsive pools: the early endosomes and the *trans*-Golgi. The carboxy-terminus of GLUT4 also functions as a less dominant internalisation motif, but is sufficient to promote intracellular sequestration of the chimera GLUT2/4. Signal(s) in the carboxy-terminal motif appear to target GLUT2/4 to a maximally insulin-responsive intracellular location, most likely the tubulo-vesicular compartment.

It must be noted that the preliminary results gained from analysis of the two documented chimeras are very similar in nature and are not particularly illuminating in assisting in the further understanding of GLUT4 trafficking. This is perhaps testament to the limitations of the recombinant chimeric approach, which has perhaps been exhausted as a tool for examining the recycling of these proteins. As such, in this thesis, greater emphasis has been placed on other methods of investigation, such as the introduction of point mutations or the mutation of short motifs within the sequence of GLUT4. It is clear that these methods have been more productive in yielding more novel and interesting results, and in helping to produce a clearer picture of the pattern of GLUT4 trafficking.

Chapter 7

Analysis of the Expression Levels of SNARE Proteins Associated with GLUT4 Trafficking in Animal Models of Diabetes Mellitus

7.1 Aims

The aims of this chapter are:

1. To determine the levels of expression of proteins associated with GLUT4 trafficking (SNARE proteins) in a range of animal models of Diabetes Mellitus.
2. To assess whether a correlation exists between the expression levels of GLUT4 trafficking proteins and the disease state of such animal models.
3. To characterise the subcellular localisation of ARF-5 in adipose and hindlimb skeletal muscle tissue from Sprague-Dawley normal rats under basal and insulin-stimulated conditions.

7.2 Introduction

7.2.1 Possible Defects in GLUT4 Trafficking Responsible for Non-Insulin-Dependent Diabetes Mellitus

A recent study has proposed that a defect in GLUT4 trafficking and targeting causes human insulin resistance and is common to both skeletal muscle and adipose tissue [Garvey *et al.* (1998)]. This defect leads to GLUT4 accumulation in dense membrane compartments from which transporters are unable to be recruited to the cell surface membranes in response to insulin. This mechanism of insulin resistance is operative in adipocytes but appears to be relegated to secondary importance by the profound reduction in GLUT4 expression in non-insulin-dependent diabetes [Garvey *et al.* (1998)]. However, this mechanism is proposed to dominate in skeletal muscle where normal expression of GLUT4 is maintained [Garvey *et al.* (1998)].

The biochemical basis of defects in GLUT4 trafficking remains to be defined. A translocation effect *per se* could be caused by either impaired insulin signal transduction or lie intrinsic to the glucose transporter effector system [Goodyear *et al.* (1995), Garvey *et al.* (1998)]. However, the translocation defect proposed by Garvey *et al.* is independent of insulin, occurring under basal conditions. The clear implication here is that the abnormality in basal GLUT4 targeting or trafficking is a distinct defect intrinsic to the glucose transport system, which is mechanistically linked to impaired translocation. GLUT4 trafficking is constitutive, highly regulated, multi-compartmental [Czech (1995)], and involves multiple proteins that also direct the trafficking of neurosecretory vesicles [Sollner &

Rothman (1996)]. It is therefore feasible that defects at any of several steps could alter trafficking and targeting of GLUT4 to produce the novel pattern of abnormalities observed in human skeletal muscle.

As stated above, homologues of the SNARE proteins involved in small synaptic vesicle (SSV) trafficking are important factors in the unique trafficking of the insulin-regulatable glucose transporter isoform, GLUT4. The role of these proteins has been discussed in greater detail in section 1.9 of this thesis.

These proteins represent a possible site of dysfunction in the disease states of insulin resistance and non-insulin-dependent diabetes mellitus. In this study I applied the technique of subcellular membrane fractionation to hindlimb skeletal muscle and adipose tissue from a number of animal models of non-insulin-dependent and insulin-dependent diabetes mellitus, to examine the expression and subcellular distribution of these proteins in an attempt to determine if any correlation exists between altered levels of protein expression or altered distribution, and the manifestation of a particular disease state. The following results suggest that expression levels of specific SNARE proteins are altered in certain animal models of non-insulin-dependent diabetes mellitus, and are affected by treatment with BRL49653, a thiazolidinedione (TZD) compound (section 7.2.3), also called Rosiglitazone.

7.2.2 Thiazolidinediones in the Treatment of NIDDM

Thiazolidinediones are a class of orally active pharmacological agents that enhance the actions of insulin. These agents increase insulin-dependent glucose disposal and reduce the hepatic glucose output that is commonly elevated in non-insulin-dependent diabetes mellitus. The metabolic changes produced by these drugs result primarily from the increased sensitivity of insulin-sensitive tissues and are observed in numerous animal models of insulin resistance, such as *ob/ob* mice, *db/db* mice and the Zucker *fa/fa* rat [Fujita *et al.* (1983), Fujiwara *et al.* (1988), Stevenson *et al.* (1990), Bowen *et al.* (1991)].

Recent studies have unveiled PPAR- γ as the major receptor for the thiazolidinedione class of insulin-sensitising drugs [Harris & Kletzien (1994), Lehmann *et al.* (1995), Forman *et al.* (1995)]. PPAR- γ is a member of the peroxisome proliferator activated receptor (PPAR) subfamily of nuclear hormone receptors. PPAR- γ is expressed in an adipose-selective fashion in both rodents and humans, being 10-30-fold higher in fat than most other tissues [Tontonez *et al.* (1994)]. The TZDs have been identified as direct ligands of PPAR- γ with positive activity on gene transcription [Lehmann *et al.* (1995), Forman *et al.* (1995)].

These studies also revealed that TZDs were potent and effective at stimulating adipogenesis in cells containing endogenous or ectopically expressed PPAR- γ [Lehmann *et al.* (1995), Forman *et al.* (1995)], confirming that PPAR- γ , expressed at or below levels seen in fat tissue, can convert nearly every fibroblastic cell in a given culture into a fully differentiated adipocyte.

It has been shown that TZD drugs bind to and activate PPAR- γ in the same concentration range that has antidiabetic activity, and that the rank order of their antidiabetic activities closely matches the rank order of their affinities [Willson *et al.* (1996)]. Furthermore, no other receptor for TZD drugs has currently been identified. Taken together, the above data make a compelling case that PPAR- γ is the major functioning receptor for the common TZD actions in diabetes.

Presently it is thought that TZDs function to increase insulin-sensitivity in a number of ways. Firstly, the action of TZDs to promote adipose cell differentiation would be expected to produce more fat cells of a smaller average size. Because smaller adipose cells are usually more sensitive to insulin, such a differentiative response would be expected to produce greater insulin-dependent glucose uptake [Hallakou *et al.* (1997)]. In addition, because insulin is a powerful anti-lipolytic agent, smaller fat cells with increased insulin sensitivity would be expected to have lower relative rates of lipolysis. Because high levels of free fatty acids may be causally involved in the induction of insulin resistance, this could affect insulin-sensitivity at sites such as muscle and liver [Rebrin *et al.* (1995), Rebrin *et al.* (1996)].

The possibility also exists that PPAR- γ activation may control one or more genes that regulate systemic insulin-sensitivity. Two interesting candidate genes in this regard are TNF- α and leptin. An increasing body of data suggests that TNF- α is overexpressed in obesity and insulin resistance and may interfere with proximal events in insulin signalling [Spiegelman & Flier (1996), Peraldi *et al.* (1997)]. TZDs appear to decrease TNF- α mRNA expression in adipose tissue and block the ability of TNF- α to interfere with

insulin signalling [Hofman *et al.* (1994), Peraldi *et al.* (1997)]. Some reports indicate that leptin also might interfere with insulin signalling in certain cell types [Muller *et al.* (1997)], and TZDs have been implicated in the regulation of leptin expression [Kallen & Lazar (1996)].

Which potential target genes for PPAR- γ are most relevant for the antidiabetic action of the TZDs remain to be defined. In differentiated cells and tissues TNF- α and leptin expression are reduced by PPAR- γ activation. Another potentially important target gene for PPAR- γ is GLUT4. The expression of this gene is increased in cultured adipocytes and fat tissue through PPAR- γ activation by TZDs [Young *et al.* (1995), Wu *et al.* (1998)], and this could contribute to reduced hyperglycaemia. One major point that has to be addressed is that, because muscle is the major sink for insulin-dependent glucose disposal, it will be fundamental to determine whether GLUT4 is induced by TZD treatment in muscle.

7.2.3 ARF Proteins

The ADP-ribosylation factor (ARF) GTP-binding proteins are believed to play an important role in membrane trafficking and secretory processes in eukaryotic cells [Boman & Kahn (1995)]. The ARF family consists of 15 structurally related gene products that include 6 ARF proteins and 11 ARF-like (ARL) proteins. The ARF proteins are divided into 3 classes on the basis of size and amino acid identity. ARFs 1 to 3 form class I, ARF-4 and 5 form class II and ARF-6 forms class III. All the ARFs contain a glycine at position 2 that is a site for N-terminal myristoylation [reviewed in Donaldson & Klausner (1994), Moss & Vaughan (1995)].

ARF proteins are known to be involved in various intracellular trafficking events, including endocytosis [D'Souza-Schorey *et al.* (1995)] and endosome fusion [Lenhard & Kahn (1992)]. However, they are most notably associated with the secretory pathway, a process in which ARF-1 plays an important role [Chen & Shields (1996), Ktistakis *et al.* (1996)]. As a member of the Ras superfamily, ARF-1 interconverts between an inactive GDP-bound form and an active GTP-bound form as it cycles between the cytosol and the Golgi membranes. On binding to the Golgi, ARF-1 promotes binding of the adaptor protein 1 (AP-1), a component of the clathrin-coat [Traub *et al.* (1993), Seaman *et al.* (1996)], and coatamer, the promoter of the COP1 coat [Donaldson *et al.* (1992)] to the membrane allowing the budding of secretory vesicles [Chen & Shields (1996), Ktistakis *et al.* (1996)].

As stated above, ARF proteins have been implicated in the regulation of vesicular transport through the secretory pathway [reviewed in Moss & Vaughan (1995)]. Recent studies have shown that ARFs may play a role in both the formation of secretory vesicles [Chen & Shields (1996)], and the initiation or facilitation of vesicle fusion at the plasma membrane in endocrine cells [Galas *et al.* (1997)]. As insulin-stimulated GLUT4 translocation to the cell surface in adipocytes exhibits many similarities to regulated secretion in neuroendocrine and endocrine cells, it is of interest to investigate whether ARF proteins may also be an important component of the GLUT4 trafficking machinery.

In this study I examined the subcellular distribution of another member of the ARF family, ARF-5, in the membranes of SD normal rat adipose and hindlimb skeletal muscle tissue. My results show that, as occurs in 3T3-L1 adipocytes [C. A. Millar and G. W. Gould (unpublished data)], ARF-5 is translocated from an intracellular location to the cell surface in response to insulin, in a similar fashion to GLUT4.

7.3 Materials and Methods

7.3.1 Animal Models

The animal models used in this study were as follows:

1. Sprague-Dawley (SD) Normal Rats
2. Zucker *fa/fa* Rats (ZDF)
3. Streptozotocin-treated (STZ) Sprague-Dawley Rats
4. *ob/ob* Mice

All of the above animal models were supplied by SmithKline Beecham Pharmaceuticals, New Frontiers Science Park, Harlow, Essex, England. For details of the phenotype of these animal models see section 1.11.

7.3.1a Sprague-Dawley Normal Rats

SD normal rats were purchased from Charles River Breeding Laboratories, UK. Animals were fed standard chow, specifically RM1 diet from Special Diet Services. Rats were processed as near as possible to the optimum body weight of 180-200g.

7.3.1b Zucker *fa/fa* Rats (ZDF)

ZDF rats were purchased from Genetic Models Inc., USA, and were fed standard chow, RM1 diet from Special Diet Services.

Rats were divided into four groups by drug treatment regime:

Group A	Lean rats	Vehicle control diet
Group B	ZDF rats	Vehicle control diet
Group C	ZDF rats	BRL 49653 30 μ mol/kg body weight
Group E	ZDF rats	BRL 49653 3 μ mol/kg body weight

7.3.1c Streptozotocin-treated (STZ) Sprague-Dawley Rats

SD normal rats (section 7.3.1a) were injected with streptozotocin when at a body weight of 200g. Streptozotocin was made up in 10mM Citrate buffer; pH 4.5 (section 2.2.2), at 80mg/ml (0.3M). Rats were injected intravenously (tail vein, 1ml/kg body weight, i.e. 0.2ml/rat), using a fresh syringe each time, as streptozotocin is degraded on contact with blood. Animals were processed a week later, following confirmation of hyperglycaemia by blood glucose measurement.

Animals were fed standard chow, specifically RM1 diet from Special Diet Services.

7.3.1d *ob/ob* Mice

ob/ob mice were purchased from Jackson Labs, USA, and were fed standard chow, RM1 diet from Special Diet Services.

Mice were divided into three groups by drug treatment regime:

Group A	Obese mice	Diet control
Group B	Obese mice	Troglitazone 3000 μ mol/kg of diet
Group C	Obese mice	BRL 49653 3 μ mol/kg of diet

7.3.2 BRL 49653 (Avandia)

BRL 49653 (Avandia) is a member of the thiazolidinedione class of insulin-sensitising drugs, currently in the final stages of product development with SmithKline Beecham Pharmaceuticals.

7.4 Results

In all of the experiments discussed below, the amount of protein in samples loaded onto SDS-PAGE gels for Western blotting was equally loaded. The protein recovery from all tissue samples was determined by Bradford's and Quantigold assay (section 2.7). Total protein recovery in all tissue fractions did not vary significantly between animal groups (data not shown).

7.4.1 Analysis of SNARE Proteins in Adipose Tissue from Sprague-Dawley (SD) Normal Control Rats

Adipocytes produced from fresh normal SD rat adipose tissue were subjected to the subcellular fractionation procedure outlined in section 2.6.1 of this thesis. This technique yielded the following subcellular fractions: plasma membranes (PM) \pm insulin, low density microsomal membranes (LDM) \pm insulin, high density microsomal membranes (HDM) \pm insulin, and soluble proteins (SP) \pm insulin.

Western blotting (sections 2.8-9) of these subcellular fractions was carried out for the following proteins: (1) GLUT4, (2) Cellubrevin, (3) Syntaxin4, and (4) VAMP2 (Figure 7.1).

The subcellular distribution of GLUT4 was as expected, with the majority of the protein located in the LDM fraction in the basal state, and displaying significant translocation to the PM in response to insulin stimulation (Figure 7.1). Similarly, cellubrevin and syntaxin4 demonstrated a wild-type distribution, with the majority of cellubrevin expressed intracellularly in

the LDM fraction and translocating to the PM in response to insulin [Martin *et al.* (1996)], and syntaxin4 showing significant localisation at the PM [Volchuk *et al.* (1996)] (Figure 7.1). The immunoblot of VAMP2 was less clear, but indicated that it was expressed predominantly in an intracellular location in the absence of insulin and moves to the cell surface in response to insulin (data not shown). These results demonstrate that the adipose tissue fractionation technique and antibodies employed in this analysis are functioning efficiently.

7.4.2 Analysis of SNARE Proteins in Hindlimb Skeletal Muscle Tissue from Sprague-Dawley Normal Control Rats

Freeze-clamped hindlimb skeletal muscle tissue was subjected to the subcellular fractionation technique detailed in section 2.6.2, producing the following subcellular membrane fractions: plasma membranes (PM) \pm insulin, intracellular membranes (IM) \pm insulin, and soluble proteins (SP) \pm insulin.

These subcellular fractions were immunoblotted for the following proteins: (1) GLUT4, (2) Cellubrevin, (3) Syntaxin4, and (4) VAMP2.

The results of these immunoblots demonstrated that all of the above proteins are expressed in SD rat hindlimb skeletal muscle tissue (data not shown).

7.4.3 Analysis of SNARE Proteins in Hindlimb Skeletal Muscle Tissue from ZDF Rats Treated with BRL 49653

Freeze-clamped hindlimb skeletal muscle tissue from ZDF rats was taken and prepared by the technique of subcellular fractionation. Samples were processed from the four treatment groups listed in section 7.3.1b, allowing a comparative analysis of expression levels of GLUT4 and the SNARE proteins between lean controls and untreated ZDF rats and also analysis of the effects of BRL 49653 treatment at two doses on diabetic rats.

The expression level of GLUT4 appeared to be similar in lean controls -v- untreated ZDF rats, a result consistent with the data available in published literature [Pedersen *et al.* (1990), Garvey *et al.* (1992)] (Figure 7.2). In contrast, treatment with the TZD compound BRL 49653 appeared to upregulate the expression of this protein at both dosages (3 μ mol/kg and 30 μ mol/kg) (Figure 7.2).

Cellubrevin expression levels were increased in untreated diabetic rats in comparison to lean controls (Figure 7.2). Interestingly, the levels of expression of this protein were normalised by BRL 49653 treatment at 30 μ mol/kg but remained elevated at when treated with the lower dosage of the TZD compound (Figure 7.2).

Expression levels of syntaxin4 were also increased in untreated ZDF rats with respect to lean controls (Figure 7.2). Again, similar to cellubrevin, the expression level of syntaxin4 are normalised by treatment with the higher dose of BRL 49653, but not by the lower dosage (Figure 7.2).

The expression of VAMP2 was also subject to the same phenomenon as cellubrevin and syntaxin4, i.e. it was increased in diabetics relative to lean controls, and was normalised by the higher dose of BRL 49653 (Figure 7.2).

Muscle tissue from the four treatment groups was also analysed for the expression levels of GLUT1 and γ -adaplin. Interestingly, the levels of GLUT1 appeared to be increased in untreated diabetic animals when compared to lean controls (Figure 7.3). Furthermore, levels of GLUT1 were normalised by treatment with BRL 49653. Analysis of γ -adaplin revealed that expression remained unaltered between lean controls and untreated diabetics (Figure 7.3).

Similar analysis was performed on adipose tissue from the above animals. Results from this analysis were inconclusive, but suggested that there were little, if any, significant changes in the expression levels of the SNARE proteins. GLUT4 levels were reduced in diabetics compared to lean controls, as was expected, and appeared to be upregulated by treatment with BRL 49653 (data not shown).

Table 7.1 provides *in vivo* details regarding the effect of BRL 49653 on ZDF *fa/fa* rats. The physiological parameters listed are: (1) body weight, (2) blood glucose concentration, and (3) plasma insulin concentration. The insulin-sensitising effects resulting from repeated treatment with BRL 49653 can be clearly observed through the normalisation of blood glucose and plasma insulin levels after 24 weeks.

7.4.4 Expression Levels of SNARE Proteins in Hindlimb Skeletal Muscle Tissue from Streptozotocin-treated (STZ) Rats

Two different analyses were performed to examine the expression levels of GLUT4 and the SNARE proteins in the hindlimb skeletal muscle tissue of STZ rats. These tissues were subjected to an identical subcellular fractionation procedure as ZDF muscle tissue in section 7.4.2. No analysis was attempted on adipose tissue from these animals as the tissue yield from dissection was extremely low.

7.4.4a Comparison of SNARE Protein Expression Levels in STZ -v- Normal SD Rats

A direct comparative analysis was carried out of the expression levels of GLUT4 and the SNARE proteins in STZ rats against expression levels in SD normal controls.

Western blotting indicates that GLUT4 expression is reduced in the LDM fraction of the STZ diabetic rats with respect to the levels of GLUT4 expression observed in the same subcellular fraction of SD normal controls (Figure 7.4). However, there was no significant change in the level of cellubrevin expression between these two groups, and a similar result was observed for VAMP2 (Figure 7.4). An increase in syntaxin4 expression in the PM of the STZ diabetic rats was observed, compared to wild-type expression levels of this protein (Figure 7.4).

7.4.4b Effect of Hyperglycaemia on SNARE Protein Expression in STZ Rats

I undertook to examine possible effects of high levels of circulating blood glucose on the expression of GLUT4 and the SNARE proteins. In order to achieve this, the STZ rats were divided into two subgroups according to the extent of their hyperglycaemia. Animals with blood glucose levels of 20-30mM (hyperglycaemia) were classified as high blood [glucose], whereas animals with blood glucose levels of 10-15mM (mild hyperglycaemia) were classified as low blood [glucose].

Subcellular membrane fractions of these tissues were immunoblotted for the proteins GLUT4, cellubrevin, syntaxin4 and VAMP2 (Figure 7.5). The results indicate that there is no significant modulation of the expression levels of any of these proteins by differing levels of blood [glucose]. Thus, the extent of hyperglycaemia displayed by a streptozotocin-induced diabetic model is not influential on the expression of GLUT4 or the SNARE proteins.

7.4.5 Expression Levels of SNARE Proteins in Hindlimb Skeletal Muscle Tissue from *ob/ob* Mice

Hindlimb skeletal muscle tissue from *ob/ob* mice was subcellularly fractionated and Western blotted for the following proteins: (1) GLUT4, (2) GLUT1, (3) Cellubrevin, and (4) Syntaxin4.

I had no access to lean control tissues, so the following experiments analyse the effects of treatment with the TZD compounds Troglitazone and BRL 49653 (dosages detailed in section 7.4.1d) on the expression levels of the above proteins compared to obese control animals.

The quality of the immunoblots from these experiments was poor, possibly as a consequence of low protein yields (Figure 7.6). Therefore, definitive conclusions cannot be drawn. However, these data indicated that expression of the SNARE proteins remained consistent in all three treatment groups. There was no significant change in the level of expression of GLUT4 between the three treatment groups.

7.4.6 Characterisation of ARF-5 in Adipose and Muscle Tissues

It has recently been shown that the small molecular weight GTP-binding protein ARF-5 translocates from low density microsomal membranes to the cell surface in response to insulin in 3T3-L1 adipocytes [Millar, C. A. and Gould, G. W. (unpublished data)]. This mimics the translocation of GLUT4 to the PM in response to insulin stimulation and thus implies that this protein may play a role in the unique trafficking of GLUT4. Further studies demonstrated that translocation of GLUT4 to the cell surface in 3T3-L1 adipocytes could be inhibited by up to 50% by the introduction of synthetic peptides corresponding to the N-terminus of ARF-5 by α -toxin treatment [Millar, C. A. and Gould, G. W. (unpublished data)]. The above data provides a convincing argument that this protein does indeed play an important role in GLUT4 trafficking. In order to complement these studies I investigated the subcellular localisation of this protein under both basal

and insulin-stimulated conditions in the adipose and hindlimb skeletal muscle tissue of SD normal rats.

Adipose and hindlimb skeletal muscle tissue were prepared by subcellular fractionation (as detailed in sections 2.6.1-2). Insulin stimulation of hindlimb skeletal muscle tissue was achieved by injection of a bolus of insulin into the hepatic portal vein of the animals.

My results show that, as in 3T3-L1 adipocytes, the small molecular weight GTP-binding protein ARF-5 demonstrates a predominantly intracellular location in the low density microsomal membranes in the absence of insulin, and shifts significantly to the cell surface in response to insulin treatment (data not shown). This phenomenon occurs in both adipose and hindlimb skeletal muscle tissue, suggesting that the translocation of ARF-5 previously observed in 3T3-L1 adipocytes is not an artefact associated solely with this cultured cell line, but is a genuine physiological cellular trafficking event.

Figure 7.1

SNARE Protein Expression Levels in Sprague-Dawley Normal Adipose Tissue

This figure shows the comparative expression levels of GLUT4 and the SNARE proteins (1) Cellubrevin and (2) Syntaxin4 in the subcellular membrane fractions of adipose tissue from a normal Sprague-Dawley rat. 20 μ g of membrane protein from each fraction were electrophoresed on 4-12% gels and immunoblotted using the relevant antibodies.

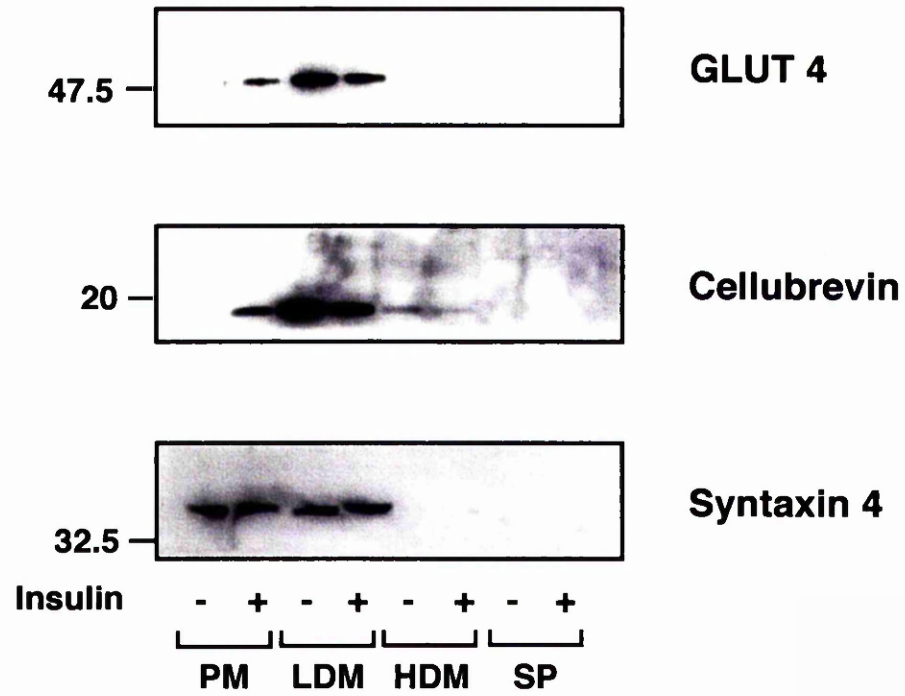


Figure 7.2

SNARE Protein Expression Levels in Zucker *fa/fa* Rat Hindlimb Skeletal Muscle Tissue

This figure is a representative immunoblot of expression levels of GLUT4 and the SNARE proteins (1) Cellubrevin, (2) VAMP2 and (3) Syntaxin4 in the subcellular membrane fractions of hindlimb skeletal muscle tissue from a Zucker *fa/fa* rat. The rats examined in this experiment were divided into four groups by drug treatment regime: (a) Group A; Lean rats on a vehicle control diet, (b) Group B; ZDF rats on a vehicle control diet, (c) Group C; ZDF rats treated with BRL 49653 at a dose of 30 μ mol/kg body weight, and (d) Group E; ZDF rats treated with BRL 49653 at a dose of 3 μ mol/kg body weight. Shown here are comparative total intracellular membrane fractions for GLUT4, Cellubrevin and VAMP2, and plasma membrane fractions for Syntaxin4. 20 μ g of membrane protein from each fraction were electrophoresed on 4-12% gels and immunoblotted using the relevant antibodies.

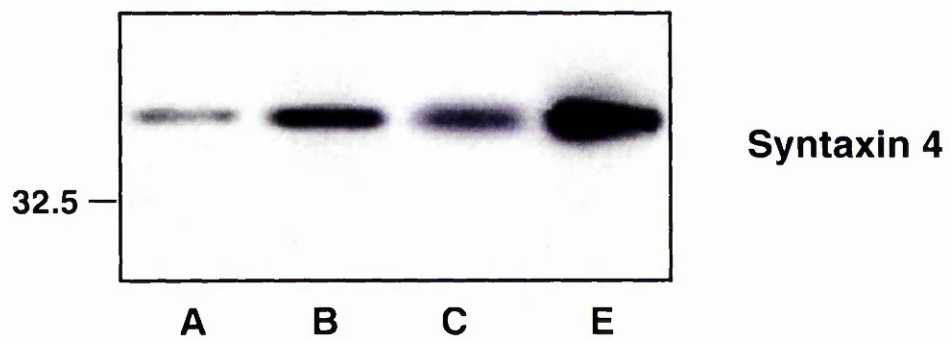
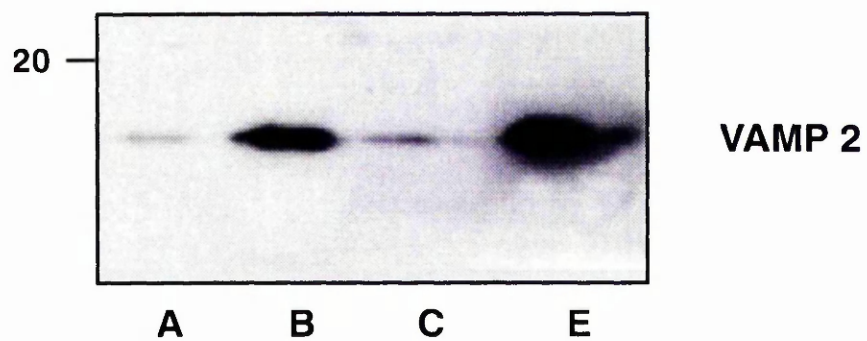
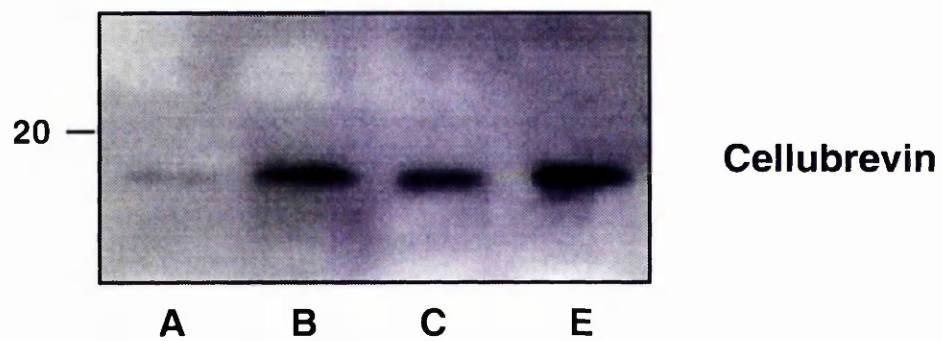
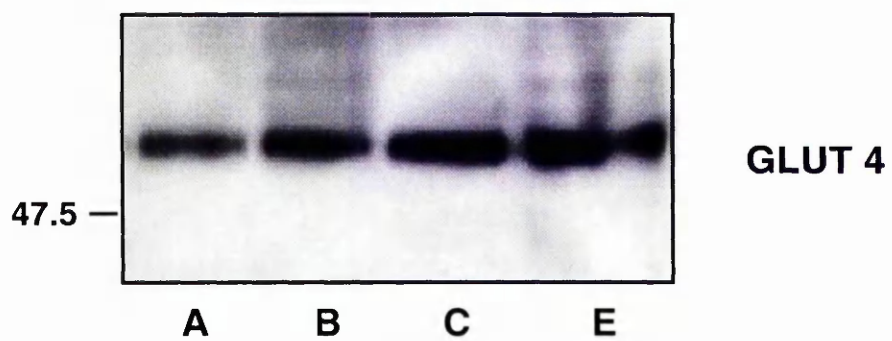


Figure 7.3

Expression Levels of GLUT1 and γ -adaptin in Zucker *fa/fa* Rat Hindlimb Skeletal Muscle Tissue

This is a representative immunoblot of the expression levels of GLUT1 and γ -adaptin in the subcellular membrane fractions of hindlimb skeletal muscle tissue from a Zucker *fa/fa* rat. The rats examined in this experiment were divided into four groups by drug treatment regime: (a) Group A; Lean rats on a vehicle control diet, (b) Group B; ZDF rats on a vehicle control diet, (c) Group C; ZDF rats treated with BRL 49653 at a dose of 30 μ mol/kg body weight, and (d) Group E; ZDF rats treated with BRL 49653 at a dose of 3 μ mol/kg body weight. Shown here are comparative total intracellular membrane fractions for GLUT1 and a comparison of treatment groups A and B for γ -adaptin. 20 μ g of membrane protein from each fraction were electrophoresed on 4-12% gels and immunoblotted using the relevant antibodies.

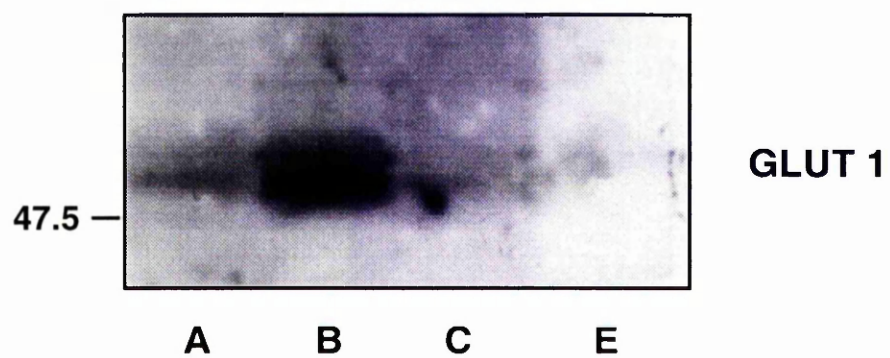
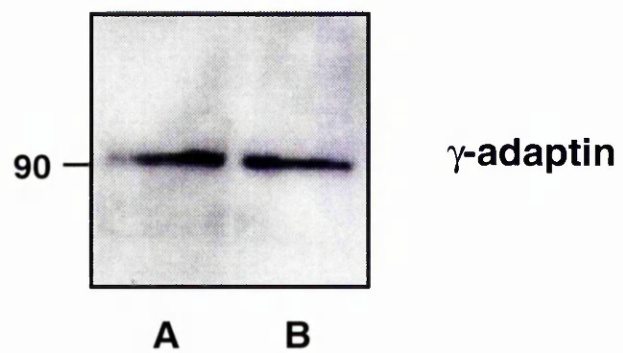


Table 7.1

Effects of BRL 49653 on ZDF *fa/fa* Rats *in vivo*

This table details physiological parameters of the ZDF *fa/fa* rats which received repeated treatment with BRL 49653. The rats examined were classified by drug treatment regime: (a) Group A; Lean rats on a vehicle control diet, (b) Group B; ZDF rats on a vehicle control diet, (c) Group C; ZDF rats treated with BRL 49653 at a dose of 30 $\mu\text{mol/kg}$ body weight.

Table 7.1**Effects of BRL 49653 on ZDF *fa/fa* Rats *in vivo***

Parameter	Group A	Group B	Group C
Body weight (g)			
wt @ 11 wks	269 ± 26	331 ± 11	341 ± 18
wt @ 24 wks	423 ± 35	409 ± 58	732 ± 38*
Blood Glucose (mM)			
@ 11 wks	4.42 ± 0.36	13.56 ± 4.59	19.92 ± 7.25
@ 24 wks	5.33 ± 0.41	27.43 ± 2.37	6.35 ± 0.9
Plasma Insulin (ng/ml)			
@ 11 wks	1.9025 ± 0.55	20.27 ± 6.14	14.22 ± 5.18
@ 24 wks	1.29 ± 0.28	5.66 ± 6.27**	2.37 ± 0.62

* Represents drug-driven adipogenesis, more marked in this sort of model than in man

** Represents considerable islet damage i.e. animals at transition from late-phase NIDDM to IDDM

Figure 7.4

Comparison of Expression Levels of GLUT4 and SNARE Proteins Between Sprague-Dawley Normal Rats and Streptozotocin-Treated Diabetic Rats

This figure shows the comparative expression levels of GLUT4 and the SNARE proteins (1) Cellubrevin, (2) VAMP2 and (3) Syntaxin4 in the subcellular membrane fractions of hindlimb skeletal muscle tissue. Shown here are comparative total intracellular membrane fractions for GLUT4, Cellubrevin and VAMP2, and plasma membrane fraction for Syntaxin4. 20µg of membrane protein from each fraction were electrophoresed on 4-12% gels and immunoblotted using the relevant antibodies.

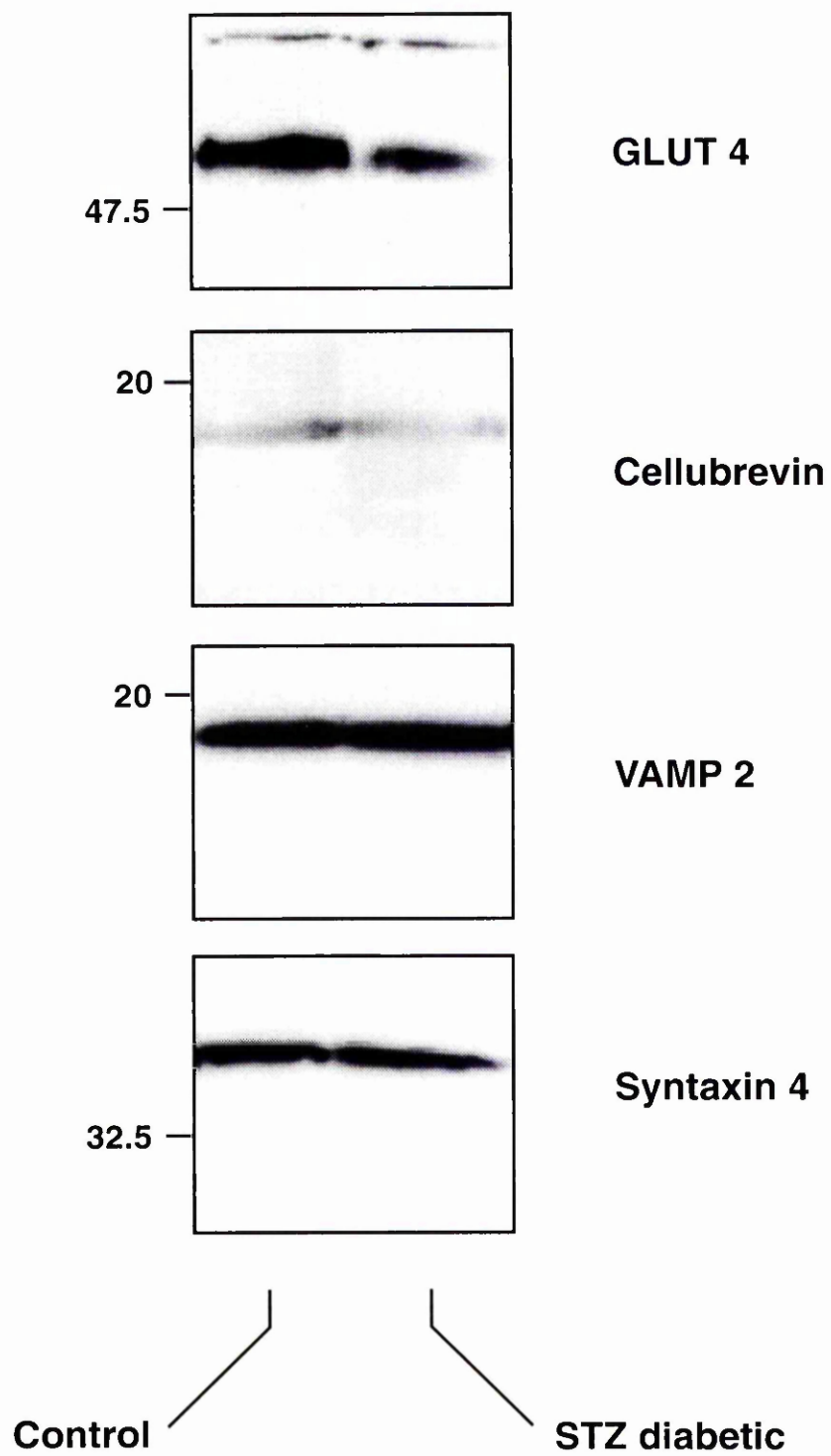


Figure 7.5

Effect of Hyperglycaemia on SNARE Protein Expression in Streptozotocin-Treated Diabetic Rats

In this figure the expression levels of GLUT4 and the SNARE proteins (1) Cellubrevin, (2) VAMP2 and (3) Syntaxin4 are compared between two animal groups displaying different levels of hyperglycaemia. The group classified as low blood [glucose] display blood glucose levels of 10-15mM (mild hyperglycaemia), whereas the group classified as high blood [glucose] display blood glucose levels of 20-30mM (hyperglycaemia). Shown here are comparative membrane fractions for GLUT4, Syntaxin4, Cellubrevin and VAMP2. 20µg of membrane protein from each fraction were electrophoresed on 4-12% gels and immunoblotted using the relevant antibodies.

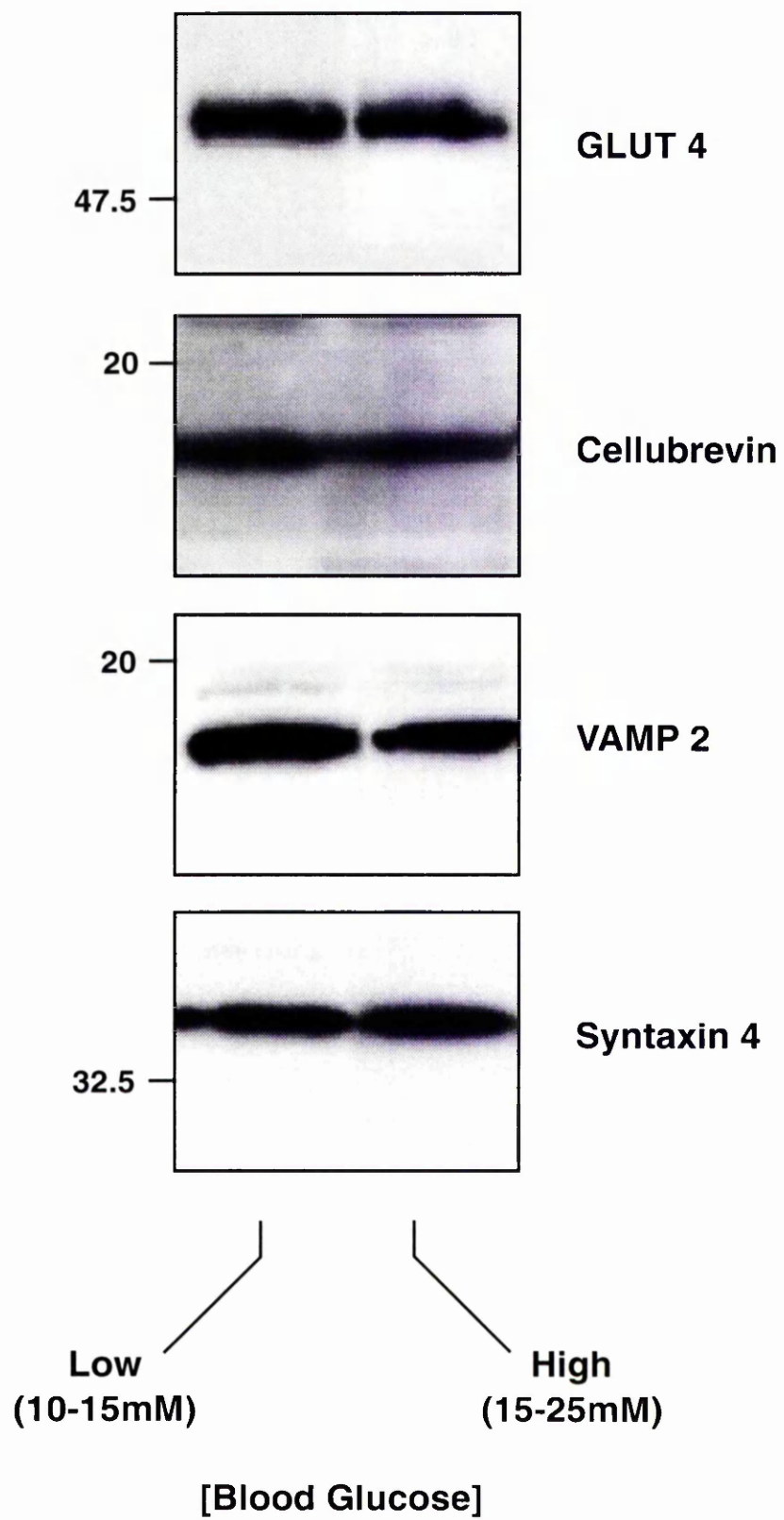
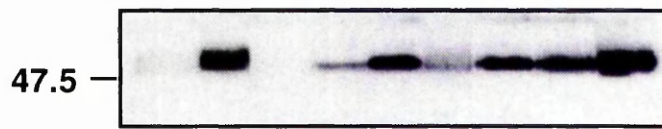


Figure 7.6

SNARE Protein Expression Levels in *ob/ob* Mouse Hindlimb Skeletal Muscle Tissue

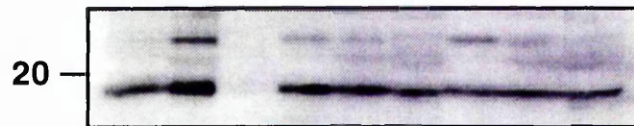
This figure is a representative immunoblot of expression levels of GLUT4 and the SNARE proteins (1) Cellubrevin, (2) VAMP2 and (3) Syntaxin4 in the subcellular membrane fractions of hindlimb skeletal muscle tissue from *ob/ob* mice. The mice examined in this experiment were divided into three groups by drug treatment regime: (a) Group A; Obese mice on a vehicle control diet, (b) Group B; Obese mice treated with Troglitazone at a dose of 3000 μ mol/kg of diet, (c) Group C; Obese mice treated with BRL 49653 at a dose of 3 μ mol/kg of diet. Shown here are comparative 25%, 30% and 35% membrane fractions. 20 μ g of membrane protein from each fraction were electrophoresed on 4-12% gels and immunoblotted using the relevant antibodies.



GLUT 4



VAMP 2



Syntaxin 4

25 30 35 25 30 35 25 30 35

A

B

C

7.5 Discussion

7.5.1 Expression of SNARE Proteins in Animal Models of Diabetes Mellitus

The above results suggest that in the hindlimb skeletal muscle tissue of the Zucker diabetic *fa/fa* animal model of non-insulin-dependent diabetes mellitus there are selective changes in the expression of proteins involved in the trafficking of the insulin-regulatable glucose transporter isoform, GLUT4. Alongside examination of the expression levels of GLUT4 itself, the SNARE proteins that I have primarily concentrated on in this study are as follows. (1) the t-SNARE syntaxin4, which is localised primarily at the cell surface in 3T3-L1 adipocytes and is thought to act as a PM docking protein for GLUT4-containing vesicles [Volchuk *et al.* (1996), Tellam *et al.* (1997)]. (2) the v-SNARE cellubrevin, which is expressed in 3T3-L1 adipocytes, co-localising with GLUT4 in endosomes [Volchuk *et al.* (1995)], where it is thought to mediate the constitutive endosomal trafficking of this protein [Rea & James (1997)]. (3) the v-SNARE VAMP2, which also colocalises with GLUT4 in 3T3-L1 adipocytes, mainly in the GLUT4 storage compartment [Martin *et al.* (1996)], and is proposed to specifically regulate the docking of GLUT4 vesicles in response to insulin stimulation [Rea & James (1997)].

My results indicate that in the subcellular fractions of obese Zucker rat hindlimb skeletal muscle tissue, the expression level of GLUT4 is not significantly different between lean and diabetic controls (Figure 7.2), in agreement with published data [King *et al.* (1992)]. However, it appears that treatment with the TZD compound, BRL 49653, at a dosage of either

3 μ mol/kg body weight or 30 μ mol/kg body weight, results in an upregulation in the level of GLUT4 expression (Figure 7.2). This result is perhaps not unexpected as a similar phenomenon is observed in adipose tissue from obese mice [Young *et al.* (1995)] and cultured adipocytes [Wu *et al.* (1998)], where GLUT4 expression is increased through PPAR- γ activation by TZDs, implying that GLUT4 is an important target gene for PPAR- γ in this tissue. The above results provide some of the first evidence to suggest that BRL 49653 can upregulate GLUT4 levels in the muscle tissue of obese Zucker rats and may help explain the mode of action of this compound in improving insulin-sensitivity in diabetic sufferers. Presumably any increase in GLUT4 levels resulting from treatment with TZDs could contribute to reduced hyperglycaemia, a major component of insulin resistance and non-insulin-dependent diabetes mellitus. It seems that, as in adipose tissue, GLUT4 may be an important target gene for PPAR- γ . It is obviously of major importance to determine the effects of BRL 49653 and other TZD compounds in muscle as this tissue represents the major sink *in vivo* for insulin-dependent glucose disposal.

Further analysis of obese Zucker hindlimb skeletal muscle tissue revealed that, for some of the SNARE proteins involved in GLUT4 translocation (cellubrevin, syntaxin4 and VAMP2), selective changes occurred in the level of their expression. The expression of each of these SNARE proteins was upregulated in diabetic controls compared to lean controls (Figure 7.2). This is perhaps suggestive of a physiological mechanism that is attempting to compensate for the diminished insulin-stimulated glucose uptake observed in all major muscle groups [Zarjevski *et al.* (1992), Kahn & Pedersen (1993)], which is thought to be resultant from impaired translocation of GLUT4 to the plasma membrane [King *et al.* (1992), Garvey

et al. (1998)]. Furthermore, it was noted that treatment with the TZD compound, BRL 49653, appeared to downregulate the elevated levels of expression of the above SNARE proteins to a level more consistent with that observed in the non-diabetic controls (Figure 7.2). This is the first time that such a phenomenon has been reported, and suggests that the genes controlling the expression of these proteins may be potential targets for PPAR- γ .

Immunoblotting of the above tissues was also performed for the ubiquitous glucose transporter isoform, GLUT1, and γ -adaptin, a component of the AP-1 complex. The results indicated that GLUT1 expression was increased in untreated diabetic animals when compared to lean controls (Figure 7.3). This suggests that perhaps levels of GLUT1 are upregulated in diabetic animals in an attempt to compensate for the reduction in insulin-stimulated glucose uptake caused by possible defects in the translocation of the dominant transporter isoform, GLUT4. Furthermore, levels of GLUT1 appeared to be normalised by BRL 49653 treatment, indicating that the TZD may act to control expression of this protein. Analysis of γ -adaptin revealed that expression remained unaltered between lean controls and untreated diabetics (Figure 7.3). I was unable to determine whether BRL 49653 treatment had any effect on the expression of this protein.

The above data provides evidence to support the theory that human insulin resistance involves a defect in GLUT4 trafficking and targeting which leads to an accumulation of this key protein in a dense membrane compartment from which insulin is unable to recruit GLUT4 to the cell surface [Garvey *et al.* (1998)]. It is possible that such a defect may be

manifest at the level of the regulated recycling of GLUT4 which is controlled by insulin and facilitated by the SNARE proteins. As such alterations in their expression levels in the diabetic state could result in aberrant trafficking and/or targeting of GLUT4, resulting in a state of insulin resistance.

As stated previously (section 7.4.3), similar analysis was performed on subcellular fractions of adipose tissue from the same animal model. The results in this case were inconclusive, but suggested that there were no significant changes in the levels of expression of the SNARE proteins between lean and diabetic controls, and that no major regulation of expression levels was apparent after repeated treatment with BRL 49653. These experiments need to be repeated if it is to be conclusively determined whether SNARE protein expression changes in the adipose tissue of diabetic sufferers and if so, whether TZD treatment has a normalising effect as observed in muscle tissue. It was apparent, however, that as expected, GLUT4 expression was downregulated in diabetic controls compared to lean controls, similar to results from the adipose tissue of obese mice [Young *et al.* (1995)] and human diabetes sufferers [Garvey *et al.* (1991)]. After repeated treatment with BRL 49653, GLUT4 expression appeared to be upregulated towards a level consistent with normal lean controls, again in concert with previous experiments in obese mice [Young *et al.* (1995)] which point to GLUT4 being an important target gene for PPAR- γ .

I also investigated the levels of expression of GLUT4 and the SNARE proteins in adipose and hindlimb skeletal muscle tissue of another animal model of non-insulin-dependent diabetes mellitus, the *ob/ob* mouse. The

results from this analysis were ambiguous, and thus no specific conclusions can be drawn from them concerning the expression of the SNARE proteins after treatment with the TZD compounds troglitazone and BRL 49653 other than that they did not appear to be significantly altered by either treatment.

A further investigation was carried out comparing the expression levels of GLUT4 and the SNARE proteins in an animal model of insulin-dependent diabetes mellitus, streptozotocin-treated (STZ) rats. In this case, the levels of expression of the aforementioned proteins were directly compared to expression levels in normal SD rats. It appeared that GLUT4 levels were reduced only in the LDM fraction of STZ rats, suggesting that reduced intracellular levels of this protein could be significant in this condition. There was no discernible differences in the levels of v-SNARE expression (cellubrevin and VAMP2) but the t-SNARE syntaxin4 was expressed at a higher level in the PM of STZ animals. It is not clear why this should be the case, as the primary defect in these animals is their lack of β -cell function. However, studies have shown that GLUT4 levels are reduced in muscle from STZ rats.

The effect of hyperglycaemia on GLUT4 and SNARE protein expression was investigated by comparison of expression levels of these proteins between two groups of STZ rats displaying different (high or low) blood glucose levels (section 7.4.4b). The results indicate that the levels of expression of all of the proteins examined are probably not modulated by the extent of hyperglycaemia exhibited by animals suffering from streptozotocin-induced diabetes.

By considering all of the above results, I propose that the selective changes in expression of the SNARE proteins observed in the muscle tissues of the ZDF model of non-insulin-dependent diabetes mellitus are a consequence of the state of hyperinsulinaemia that is prevalent in these animals. This hypothesis is supported by the fact that sensitiser (TZD) treatment is known to normalise, or at least massively reduce, hyperinsulinaemia, which would explain the normalisation of SNARE protein expression that is observed in this tissue after repeated treatment with BRL 49653. I have also shown, in streptozotocin-treated diabetic rats, that hyperglycaemia appears to have no effect on SNARE protein expression, and this further endorses the proposal that this phenomenon is governed by hyperinsulinaemia, as this state is not manifest in STZ rats and thus no change in expression levels would be expected.

7.5.2 Role of ARF-5 in GLUT4 Trafficking

I undertook to investigate the subcellular distribution of the ARF protein, ARF-5, under basal and insulin-stimulated conditions in adipose and hindlimb skeletal muscle tissue from normal SD rats. The results showed that, in agreement with previous investigations in 3T3-L1 adipocytes [Millar, C. A. and Gould, G. W. (unpublished data)], ARF-5 undergoes translocation from an intracellular location to the cell surface in response to insulin-stimulation (data not shown). This phenomenon is observed in both adipose and hindlimb skeletal muscle tissue indicating that it is an important cellular trafficking event. Parallel examination of GLUT4 in the same tissues showed that GLUT4 levels increased within the plasma membrane fraction in response to insulin, concomitant with a decrease in the intracellular (LDM) fraction, as expected.

Further studies by Millar and Gould have demonstrated that insulin regulates the redistribution of both GLUT4 and ARF-5 to the plasma membrane in 3T3-L1 adipocytes in a PI 3-kinase dependent manner. On the basis of this and the above data it seems reasonable to propose that ARF-5 plays a crucial role in insulin-stimulated GLUT4 translocation.

7.6 Summary

In this study I have demonstrated selective upregulation of the levels of expression of the SNARE proteins, cellubrevin, VAMP2 and syntaxin4 in the diabetic state compared to lean controls in hindlimb skeletal muscle tissue from ZDF rats. I have also shown that in the same tissue the expression levels of these proteins are normalised by repeated treatment with the TZD insulin-sensitising compound, BRL 49653. Furthermore, I have demonstrated that GLUT4 levels are not significantly altered between normal and diabetic ZDF muscle tissue, but are upregulated by repeated treatment with BRL 49653. This is in contrast to the expression levels of the above proteins in streptozotocin-treated rats, where no pattern of selective regulation of expression levels was observed, leading to the proposal that these selective changes are a consequence of the state of hyperinsulinaemia that is prevalent in the ZDF animals but does not occur in the STZ rats.

I have also demonstrated that a member of the ARF family of proteins, ARF-5, displays a pattern of insulin-stimulated translocation from an intracellular location to the cell surface in adipose and hindlimb skeletal muscle tissue in SD normal rats. This data adds to a growing body of

evidence which proposes that this protein plays a key role in the translocation of GLUT4 in response to insulin.

Chapter 8

Discussion

Elucidation of the mechanism by which GLUT4 is trafficked and targeted within insulin-responsive cells remains a key goal in the search to define cellular dysfunctions which may be causally related to the prevalent metabolic diseases of insulin resistance and non-insulin-dependent diabetes mellitus. Of prime interest in this respect is the manner in which the insulin-responsive glucose transporter isoform, GLUT4, is targeted to an 'insulin-responsive' intracellular location, trafficked to the cell surface in response to insulin, and re-internalised post-insulin-stimulation.

Previous studies have demonstrated that the trafficking of GLUT4, and other recycling proteins, such as the transferrin receptor and the cation-independent mannose 6-phosphate receptor, is governed, at least in part, by specific amino acid targeting motifs that are found on the sequence of such proteins. The nature of certain of these targeting motifs has been identified, and those considered in this thesis can be classified into two categories: (1) YXXØ-type motifs, where Y is an aromatic amino acid, X is any amino acid and Ø is an amino acid with a bulky hydrophobic group, and (2) di-leucine (or isoleucine-leucine) motifs.

To date, two specific targeting motifs have been identified on the sequence of GLUT4, one from each of the above categories. Several groups discovered that a sequence in the cytoplasmic amino-terminal domain of GLUT4, ⁵FQQI⁸, functions as a dominant internalisation signal in the trafficking of this protein [Piper *et al.* (1992). Piper *et al.* (1993b), Garippa *et al.* (1994)]. Further research has revealed that the 30 carboxy-terminal amino acids contain a di-leucine motif analogous to that found in the mannose 6-phosphate receptor, which is involved in the re-internalisation of GLUT4 from the cell surface after insulin-stimulation [Verhey *et al.*

(1993), Corvera *et al.* (1994), Verhey & Birnbaum (1994)]. The present school of thought also indicates that this carboxy-terminal cytoplasmic domain of GLUT4 also contains signal(s) which are responsible for the targeting of this protein to specific intracellular compartments. This hypothesis is based on analyses of chimeric transporter proteins expressed in insulin-responsive cells [Haney *et al.* (1995), Verhey *et al.* (1995)].

This thesis attempted to further characterise the roles of the aforementioned motifs in GLUT4 trafficking. Specifically, this study wished to determine whether these motifs were capable of governing more than one aspect of GLUT4 trafficking within the complex multi-compartmental assembly that constitutes the intracellular environment, and also to discover if further targeting motifs were present within the carboxy-terminal domain.

To this end, I examined the subcellular distribution of mutant glucose transporters in which the F⁵ residue was swapped for A⁵, and the L⁴⁸⁹L⁴⁹⁰ motif was altered to A⁴⁸⁹A⁴⁹⁰. Results indicated that both of these motifs do indeed play an important role in the internalisation of GLUT4, but also function to target this protein between distinct intracellular compartments known to be involved in the GLUT4 trafficking pathway. It appears that the ⁵FQQI⁸ sequence regulates the sorting of GLUT4 into the TGN, and that the L⁴⁸⁹L⁴⁹⁰ governs the trafficking of this protein from the TGN back into early endosomes. These results were gained primarily through applying the techniques of buoyant density and compartment ablation analysis to the aforementioned GLUT4 mutants stably expressed in 3T3-L1 adipocytes. These results led to the proposal of an alternative trafficking pathway for GLUT4, which involves the addition of a further intracellular GLUT4 pool,

namely the TGN, to the original 3-pool model advocated by the groups of Holman and Birnbaum [Holman *et al.* (1994), Yeh *et al.* (1995)]. This model provides an attractive scheme within which it is possible to reconcile not only the results of this study, but all previous studies addressing the question of GLUT4 trafficking. It is noteworthy that this is the first model to achieve this objective.

A further study was performed to examine the role of the residues distal to the di-leucine motif in the carboxy-terminal cytoplasmic tail of GLUT4 in targeting this isoform to a post-endocytic compartment in adipocytes, from where it can be translocated to the cell surface in response to insulin. Mutation of the residues ⁴⁹⁸TELEYLGP⁵⁰⁵, but not ⁵⁰⁶DEND⁵⁰⁹, resulted in a redistribution of the protein to the cell surface in an insulin-dependent manner. A more dominant effect on targeting was observed after mutation of ⁴⁹⁸TELE⁵⁰¹, which resulted in an accumulation of GLUT4 in endosomes. It was noted that none of these mutations abrogated the ability of insulin to translocate to the cell surface.

This thesis also tackles the question of whether the trafficking of GLUT4 is regulated by a process of phosphorylation. The role of the major site of phosphorylation in GLUT4, a serine residue at position 488, has been investigated. This site is unique to GLUT4 and is immediately adjacent to the L⁴⁸⁹L⁴⁹⁰ motif in the cytoplasmic carboxy-terminal domain. It was found that mutation of S⁴⁸⁸ to alanine, which prevents the phosphorylation of GLUT4, does not appreciably disrupt the regulated trafficking of GLUT4 in 3T3-L1 adipocytes. The data from this study indicates that the phosphorylation state of S⁴⁸⁸ is not involved in the

insulin- or okadaic acid-elicited recruitment of GLUT4 to the plasma membrane, but may play a role in the sorting of this protein at the TGN.

As a complement to the above studies, I undertook the construction and analysis of a series of recombinant GLUT2/GLUT4 chimeric glucose transporters. These recombinant species were constructed by the reciprocal exchange of domains between GLUT4 and the liver-type glucose transporter isoform, GLUT2, and subsequent analysis of the subcellular distributions of these chimeras in 3T3-L1 adipocytes was performed by application of the techniques of subcellular fractionation and compartment ablation. This study is at present incomplete, and as such, only preliminary data is included in this thesis for discussion only. The results are broadly in agreement with previous studies that have employed recombinant GLUT1/GLUT4 chimeras [Piper *et al.* (1992), Piper *et al.* (1993b), Czech *et al.* (1993), Marshall *et al.* (1993), Verhey *et al.* (1993), Verhey *et al.* (1995), Verhey & Birnbaum (1994)], and also concur strongly with the alternative model of GLUT4 trafficking that has been proposed in this thesis. The one difference from published data is that the results detailed here indicate a role for the cytoplasmic amino-terminus of GLUT4 in trafficking this isoform to an 'insulin-responsive' intracellular location, most likely early endosomes or the TGN.

In order to look at the process of GLUT4 trafficking from a different perspective, I performed a study (in conjunction with SmithKline Beecham Pharmaceuticals) which examined the expression levels of proteins known to be involved in the regulated recycling of GLUT4 in animal models of diabetes mellitus. These were proteins associated with Rothman's SNARE hypothesis of regulated exocytosis in synaptic vesicles

[Rothman (1993)], homologues of which have been identified in insulin-responsive cells e.g. cellubrevin, syntaxin4 and VAMP2 [Volchuk *et al.* (1995), Volchuk *et al.* (1996), Martin *et al.* (1996)]. The results from this study indicated that selective changes take place in expression levels of these proteins in the skeletal muscle of untreated diabetic samples, and also that these selective changes in expression can be normalised by repeated treatment with a thiazolidinedione insulin-sensitising compound. It is proposed that these selective changes are a consequence of the hyperinsulinaemic state of these animals and are not affected by increased blood glucose levels.

Clearly the movement of GLUT4 in insulin-responsive cells is a highly regulated and complex process. It requires the trafficking of this glucose transporter isoform through multiple intracellular compartments and is governed by specific motifs within the sequence of the protein that most likely interact with 'adaptor molecules' which expedite sorting and targeting. The molecules involved encompass general factors utilised by the recycling endosomal pathway to the specific machinery that facilitates the unique sorting, targeting, trafficking and fusion of the GLUT4 storage compartment and GLUT4 vesicles. The, perhaps multiple, roles of these molecules and signal motifs in the process of GLUT4 trafficking remain to be defined completely and this will constitute a primary goal of research in this field. Ultimately, such knowledge should be of central importance in the rational design of drugs intended for the treatment of insulin resistance and non-insulin-dependent diabetes mellitus.

References

- Allard, W. J. and Leinhard, G. E. (1985) *J. Biol. Chem.* **260**, 8668-8675.
- Alvarez, J., Lee, D. C., Baldwin, S. A. and Chapman, D. (1987) *J. Biol. Chem.* **262**, 3502-3509.
- Anderson, T., Martin, S., Berka, J., James, D. E., Slot, J. W. and Slow, J. (1998) *Am. J. Physiol: Renal Physiol.* **274**, F26-F33
- Araki, S., Yang, J., Hashiramoto, M., Tamori, Y., Kasuga, M. and Holman, G. D. (1996) *Biochem. J.* **315**, 153-159.
- Asano, T., Takata, K., Katagiri, H., Tsukuda, K., Lin, J. -L., Ishihara, H., Inukai, K., Hirano, H., Yazaki, Y. and Oka, Y. (1992) *J. Biol. Chem.* **267**, 19636-19641.
- Baldwin, S. A., Baldwin, J. M., Gorga, F. R. and Leinhard G. E. (1979) *Biochim. Biophys. Acta.* **552**, 183-188.
- Baldwin, S. A., Gorga, J. C. and Leinhard, G. E. (1981) *J. Biol. Chem.* **256**, 3685-3689.
- Baldwin, S. A., Baldwin, J. M. and Leinhard, G. E. (1982) *Biochemistry* **21**, 3837-3842.
- Banerjee, A., Barry, V. A., DasGupta, B. R. and Martin, T. F. J. (1996) *J. Biol. Chem.* **271**, 20223-20226.
- Bell, G. I., Kayano, T., Buse, J. B., Burant, C. F., Takeda, J., Lin, D., Fukumoto, H. and Seino, S. (1990) *Diabetes Care* **13**, 198-206.
- Bell, G. I., Burant, C. F., Takeda, J. and Gould, G. W. (1993) *J. Biol. Chem.* **268**, 19161-19164.
- Birnbaum, M. J. (1989) *Cell* **57**, 305-315.

- Boman, A. L. and Kahn, R. A. (1995) *Trends Biochem. Sci.* **20**, 147-150.
- Bowen, L., Steven, P. P., Stevenson, R. and Shulman, C. I. (1991) *Metabolism* **40**, 1025-1030.
- Brant, A. M., Jess, T. J., Milligan, G., Brown, C. M. and Gould, G. W. (1993) *Biochem. Biophys. Res. Commun.* **192**, 1297-1302.
- Brant, A. M., Martin, S. and Gould, G. W. (1994) *Biochem. J.* **304**, 307-315.
- Bremnes, T., Lauvrak, V., Lindqvist, B. and Bakke, O. (1998) *J. Biol. Chem.* **273**, 8638-8645.
- Breuer, P., Korner, C., Boker, C., Herzog, A., Pohlmann, R. and Braulke, T. (1997) *Molec. Biol. Cell* **8**, 567-576.
- Brozinick, J. T., Etgen, G. J., Yaspelkis, B. B. and Ivy, J. L. (1994) *Am. J. Physiol.* **267**, R236-R243.
- Burant, C. F., Takeda, J., Brot-Laroche, E., Bell, G. I. and Davidson, N. O. (1992) *J. Biol. Chem.* **267**, 14523-14526.
- Cain, C. C., Trimble, W. S. and Leinhard, G. E. (1992) *J. Biol. Chem.* **267**, 11681-11684.
- Calderhead, D. M. and Leinhard, G. E. (1988) *J. Biol. Chem.* **263**, 12171-12174.
- Calderhead, D. M., Kitigawa, K., Tanner, L. I., Holman, G. D. and Leinhard, G. E. (1990) *J. Biol. Chem.* **265**, 13800-13808.
- Carruthers, A. (1990) *Physiol. Rev.* **70**, 1135-1176.
- Carruthers, A. (1991) *Biochemistry* **30**, 3898-3906.
- Charron, M. J., Brosius, F. C., Alper, S. L. and Lodish, H. F. (1989) *Proc. Natl. Acad. Sci. USA* **86**, 2535-2539.

- Chen, Y. -G. and Shields, D. (1996) *J. Biol. Chem.* **271**, 5297-5300.
- Chin, J. J., Jung, E. K. Y. and Jung, C. Y. (1986) *J. Biol. Chem.* **261**, 7101-7104.
- Coleman, D. L. (1982) *Diabetes* **31**, (Suppl 1) 1-6.
- Collawn, J. F., Stangel, M., Kuhn, L. A., Esekogwu, V., Jing S. Q., Trowbridge, I. S. and Tainer, J. A. (1990) *Cell* **63**, 1061-1072.
- Colville, C. A., Seatter, M. J., Jess, T. J., Gould, G. W. and Thomas, H., M. (1993) *Biochem. J.* **290**, 701-706.
- Corvera, S., Jaspers, S. and Pasceri, M. (1991) *J. Biol. Chem.* **266**, 9271-9278.
- Corvera, S., Chawla, A., Chakrabarti, R., Joly, M., Buxton, J., and Czech, M. P. (1994) *J. Cell. Biol.* **126**, 979-989.
- Cushman, S. W., and Wardzala, L. J. (1980) *J. Biol. Chem.* **255**, 4758-4762.
- Czech, M. P., Chawla, A., Woon, C., Buxton, J., Armoni, M., Wang, W., Joly, M., and Corvera, S. (1993) *J. Cell. Biol.* **123**, 127-135.
- Czech, M. P. (1995) *Annu. Rev. Nutr.* **15**, 441-471.
- Davidson, N. O., Hausman, A. M. L., Ifkovits, C. A., Buse, J. B., Gould, G. W., Burant, C. F. and Bell, G. I. (1992) *Am. J. Physiol.* **262**, C795-800.
- Davies, A., Meeran, K., Cairns, M. T. and Baldwin, S. A. (1987) *J. Biol. Chem.* **262**, 9347-9352.
- Davis, C. G., Lehrman, M. A., Russell, D. W., Anderson, R. G., Brown, M. S. and Goldstein, J. L. (1986) *Cell* **45**, 15-24.
- Dell'Angelica, E. C., Ohno, H., Ooi, C. E., Rabinovich, E., Roche, K. W. and Bonifacino, J. S. (1997) *EMBO J.* **16**, 917-928.

- Denzer, K., Weber, B., Hille-Rehfeld, A., von Figura, K. and Pohlmann, R. (1997) *Biochem. J.* **326**, 497-505.
- Dietrich, J., Kastrup, J., Nielsen, B. L., Odum, N. and Geisler, C. (1997) *J. Cell Biol.* **138**, 271-281.
- Dittrich, E., Haft, C. R., Muys, L., Heinrich, P. C. and Graeve, L. (1996) *J. Biol. Chem.* **271**, 5487-5494.
- Donaldson, J. G., Finazzi, D. and Klausner, R. D. (1992) *Nature* **360**, 350-352.
- Donaldson, J. G. and Klausner, R. D. (1994) *Curr. Opin. Cell Biol.* **6**, 527-532.
- D'Souza-Schorey, C., Li, G., Colombo, M. I. and Stahl, P. D. (1995) *Science* **267**, 1175-1178.
- Elliot, K. R. F. and Craik, J. D. (1982) *Biochem. Soc. Trans.* **10**, 12-13.
- Fasshauer, D., Otto, H., Eliason, W. K., Jahn, R. and Brunger, A. T. (1997) *J. Biol. Chem.* **272**, 28036-28041.
- Flier, J. S., Meuckler, M., McCall, A. and Lodish, H. F. (1987) *J. Clin. Invest.* **79**, 657-661.
- Forman, B. M., Tontonoz, P., Chen, J., Brun, R. P., Spiegelman, B. M. and Evans, R. M. (1995) *Cell* **83**, 803-812.
- Froehner, S. C., Davies, A., Baldwin, S. A. and Leinhard, G. E. (1988) *J. Neurocytol.* **17**, 173-178.
- Fujita, T., Sugiyama, Y., Takeotomi, S., Shoda, T., Kawamatsu, Y., Iwatsuka, H. and Suzuoki, Z. (1983) *Diabetes* **32**, 804-810.
- Fujita, Y., Sasaki, T., Fukui, K., Kotani, H., Kimura, T., Hata, Y., Sudhof, T. C., Scheller, R. H. and Takai, Y. (1996) *J. Biol. Chem.* **271**, 7265-7268.

Fujiwara, T., Yoshioka, S., Yoshioka, T., Ushiyama, I. and Horikoshi, H. (1988) *Diabetes* **37**, 1849-1888.

Fukumoto, H., Seino, S., Imura, H., Seino, Y., Eddy, R. L., Fukushima, Y., Byers, M. G., Shows, T. B. and Bell, G. I. (1988) *Proc. Natl. Acad. Sci. USA* **85**, 5434-5438.

Fukumoto, H., Kayano, T., Buse, J. B., Edwards, Y., Pilch, P. F., Bell, G. I. and Seino, S. (1989) *J. Biol. Chem.* **264**, 7776-7779.

Galas, M. C., Helms, J. B., Vitale, N., Thierse, D., Aunis, D. and Bader, M. F. (1997) *J. Biol. Chem.* **272**, 2788-2793.

Garripa, R. J., Judge, T. W., James, D. E. and McGraw, T. E. (1994) *J. Cell. Biol.* **124**, 705-715.

Garippa, R. J., Johnson, A., Park, J., Petrusch, R. L. and McGraw, T. E. (1996) *J. Biol. Chem.* **271**, 20660-20668.

Garvey, W. T., Heucksteadt, T. P., Matthei, S. and Olefsky, J. M. (1988) *J. Clin. Invest.* **81**, 1528-1536.

Garvey, W. T., Maianu, L., Heucksteadt, T. P., Birnbaum, M. J., Molina, J. M. and Ciaraldi, T. P. (1991) *J. Clin. Invest.* **87**, 1072-1081.

Garvey, W. T., Maianu, L., Hancock, J. A., Golichowski, A. M. and Baron, A. D. (1992) *Diabetes* **41**, 465-475.

Garvey, W. T., Maianu, L., Zhu, J. -H., Brechtel-Hook, G., Wallace, P. and Baron, A. D. (1998) *J. Clin. Invest.* **101**, 2377-2386.

Glickman, J. N., Conibear, E. and Pearse, B. M. (1989) *EMBO J.* **8**, 1041-1047.

Goodyear, L. J., Giorgiano, F., Sherman, L. A., Carey, J., Smith, R. J. and Dohm, G. L. (1995) *J. Clin. Invest.* **95**, 2195-2204.

Gould, G. W., Derechin, V., James, D. E., Tordjman, K., Ahern, S., Gibbs, E. M., Leinhard, G. E. and Meuckler, M. (1989) *J. Biol. Chem.* **264**, 2180-2184.

Gould, G. W., Thomas, H. M., Jess, T. J. and Bell, G. I. (1991) *Biochemistry* **30**, 5139-5145.

Gould, G. W. and Holman, G. D. (1993) *Biochem. J.* **295**, 329-341.

Gould, G. W. [Editor] (1997) *Facilitative Glucose Transporters*. Molecular Biology Intelligence Unit.

Hallakou, S., Doare, L., Fougelle, F., Kergoat, M., Guerre-Millo, M., Berthault, M. F., Dugail, I., Morin, J., Auwerx, J. and Ferre, P. (1997) *Diabetes* **46**, 1393-1399.

Haney, P. M., Slot, J. W., Piper, R. C., James, D. E. and Meuckler, M. (1991) *J. Cell. Biol.* **114**, 689-699.

Haney, P. M., Levy, M. A., Strube, M. S. and Meuckler, M. (1995) *J. Cell. Biol.* **129**, 641-658.

Hanson, P. I., Roth, R., Morisaki, H., Jahn, R. and Heuser, J. E. (1997) *Cell* **90**, 523-535.

Harris, P. K. and Kletzien, R. F. (1994) *Mol. Pharmacol.* **45**, 439-445.

Hediger, M. A., Coady, M. J., Ikeda, T. S. and Wright, E. M. *Nature* **330**, 379-381.

Heilker, R., Manning-Kreig, U., Zuber, J. -F. and Speiss, M. (1996) *EMBO J.* **15**, 2893-2899.

Herman, G. A., Bonzelius, F., Cietuat, A. -M. and Kelly, R. B. (1994) *Proc. Natl. Acad. Sci. USA* **91**, 12750-12754.

Hofman, C., Lorenz, K., Braithwaite, S. S., Colca, J. R., Palazuk, B. J., Hotamisligil, G. S. and Spiegelman, B. M. (1994) *Endocrinology* **134**, 264-270.

Holman, G. D., Kozka, I. J., Clark, A. E., Flower, C. J., Saltis, J., Habberfield, A. D., Simpson, I. A. and Cushman, S. W. (1990) *J. Biol. Chem.* **265**, 18172-18179.

Holman, G. D., Leggio, L. L. and Cushman, S. W. (1994) *J. Biol. Chem.* **268**, 17516-17524.

Hudson, A. W., Ruiz, M. and Birnbaum, M. J. (1992) *J. Cell. Biol.* **116**, 785-797.

Hughes, S. D., Johnson, J. H., Quaade, C. and Newgard, C. B. (1992) *Proc. Natl. Acad. Sci. USA* **89**, 677-692.

Hunziker, W. and Fumey, C. (1994) *EMBO J.* **13**, 2963-2969.

James, D. E., Strube, M., and Meuckler, M. (1989a) *Nature* **338**, 83-87.

James, D. E., Hiken, J. and Lawrence, J. C. (1989b) *Proc. Natl. Acad. Sci. USA* **86**, 8368-8372.

James, D. E., Piper, R. C. and Slot, J. W. (1993) *J. Cell Science* **104**, 607-612.

James, D. E., Piper, R. C. and Slot, J. W. (1994) *Trends Cell Biol.* **4**, 120-126.

Jing, S. Q., Spencer, T., Miller, K., Hopkins, C. R. and Trowbridge, I. S. (1990) *J. Cell. Biol.* **119**, 249-257.

Johnson, K. F., Chan, W. and Kornfeld, S. (1990) *Proc. Natl. Acad. Sci. USA* **87**, 10010-10014.

Johnson, K. F. and Kornfeld, S. (1992a) *J. Biol. Chem.* **267**, 17110-17115.

Johnson, K. F. and Kornfeld, S. (1992b) *J. Cell. Biol.* **119**, 249-257.

Jullien, D., Tanti, J. F., Heydrick, S. J., Gautier, N., Gremeaux, T., Van Obberghen, E. and Le Marchand-Brustel, Y. (1993) *J. Biol. Chem.* **268**, 15246-15251.

Kaestner, K. H., Christy, R. J., McLenithan, R. J., Briterman, L. T., Cornelius, P., Pekala, P. H. and Lane, M. D. (1989) *Proc. Natl. Acad. Sci. USA* **86**, 3150-3154.

Kahn, B. B. & Pedersen, O. (1993) *Endocrinology* **132**, 13-22.

Kahn, C. R. (1994) *Diabetes* **43**, 1066-1084.

Kahn, C. R. (1995) *Current Opinion in Endocrinology and Diabetes* **2**, 283-284.

Kallen, C. B. and Lazar, M. A. (1996) *Proc. Natl. Acad. Sci. USA* **93**, 5793-5796.

Kandror, K. V., Coderre, L., Pushkin, A. V. and Pilch, P. F. (1995) *Biochem. J.* **307**, 383-390.

Kandror, K. V. and Pilch, P. F. (1996) *J. Biol. Chem.* **271**, 21703-21708.

Kasahara, M. and Hinkle, P. C. (1977) *J. Biol. Chem.* **252**, 7384-7390.

Kayano, T., Fukumoto, H., Eddy, R. L., Fan, Y. -S., Byers, M. G., Shows, T. B. and Bell, G. I. (1988) *J. Biol. Chem.* **263**, 15245-15248.

Kayano, T., Burant, C. F., Fukumoto, H., Gould, G. W., Fan, Y. -S., Eddy, R. L., Byers, M. G., Shows, T. B., Seino, S. and Bell, G. I. (1990) *J. Biol. Chem.* **265**, 13276-13282.

King, P. A., Horton, E. D., Hirshman, M. F. and Horton, E. S. (1992) *J. Clin. Invest.* **90**, 1568-1575.

Kishida, Y., Olsen, B. R., Berg, R. A. and Prockop, D. J. (1975) *J. Cell. Biol.* **64**, 331-339.

Klip, A., Ramlal, T., Young, D. A. and Holloszy, J. O. (1987) *FEBS Letters* **224**, 224-230.

Klumperman, J., Hille-Rehfeld, A., Veenendaal, T., Oorschot, V., Stoorvogel, W., von Figura, K. and Geuze, H. J. (1993) *J. Cell. Biol.* **121**, 997-1000.

Kobayashi, M., Nikami, H., Morimatsu, M. and Saito, M. (1997) *Neurosci. Letts.* **213**, 103-106.

Kreig, P. A. and Melton, D. A. (1984) *Nucleic Acid Research* **12**, 7057-7070.

Ktistakis, N. T., Brown, H. A., Waters, M. G., Sternweis, P. C. and Roth, M. G. (1996) *J. Cell. Biol.* **134**, 295-306.

Lawrence, J. C., Hiken, J. F. and James, D. E. (1990a) *J. Biol. Chem.* **265**, 2324-2332.

Lawrence, J. C., Hiken, J. F. and James, D. E. (1990b) *J. Biol. Chem.* **265**, 19768-19776.

Le Borgne, R., Schmidt, A., Mauxion, F., Griffiths, G. and Hoflack, B. (1993) *J. Biol. Chem.* **268**, 22552-22556.

Lehmann, J. M., Morre, L. B., Smith-Oliver, T. A., Wilkinson, W. O., Wilson, T. M. and Kleiwer, S. A. (1995) *J. Biol. Chem.* **270**, 12953-12956.

Lenhard, J. M. and Kahn, R. A. (1992) *J. Biol. Chem.* **267**, 13047-13052.

Letourneur, F. and Klausner, R. D. (1992) *Cell* **69**, 1143-1157.

Lewin, D. A. and Mellman, I. (1998) *Biochim. Biophys. Acta* **1401**, 129-145.

Livingstone, C., James, D. E., Rice, J. E., Hanpeter, D. and Gould, G. W. (1996) *Biochem. J.* **315**, 487-495.

Lobel, P., Fujimoto, K., Ye, R. D., Griffiths, G. and Kornfeld, S. (1989) *Cell* **57**, 787-796.

Lombardo, Y. B. and Menahan, L. A. (1979) *Horm. Metab. Res.* **11**, 9-14.

Malide, D., St-Francois, J. F., Keller, S. R. and Cushman, S. W. (1997) *FEBS Letters*. **409**, 461-468.

Marks, M. S., Woodruff, L., Ohno, H. and Bonifacino, J. S. (1996) *J. Cell. Biol.* **135**, 341-354.

Marks, M. S., Ohno, H., Kirchhausen, T. and Bonifacino, J. S. (1997) *Trends Cell Biol.* **7**, 124-128.

Marsh, B. J., Alm, R. A., McIntosh, S. R. and James, D. E. (1995) *J. Cell. Biol.* **130**, 1081-1091.

Marsh, B. J., Martin, S., Melvin, D. R., Martin, L. B., Alm, R. A., Gould, G. W. and James, D. E. (1998) *Am. J. Physiol.* **275**, E412-422.

Marshall, B. A., Murata, H., Hresko, R. C., and Meuckler, M. J., (1993) *J. Biol. Chem.* **268**, 26193-26199.

Martin, S., Reaves, B., Banting, G. and Gould, G. W. (1994) *Biochem. J.* **300**, 743-749.

Martin, S., Tellman, J., Livingstone, C., Slot, J. W., Gould, G. W. and James, D. E. (1996) *J. Cell. Biol.* **134**, 625-635.

Martin, S., Rice, J. E., Gould, G. W., Keller, S., Slot, J. W. and James, D. E. (1997) *J. Cell. Sci.* **110**, 2281-2291.

Matter, K., Yamamoto, E. M. and Mellman, I. (1994) *J. Cell. Biol.* **126**, 991-1004.

Mauxion, F., Le Borgne, R., Munier-Lehmann, H. and Hoflack, B. (1996) *J. Biol. Chem.* **271**, 2171-2178.

McCall, A. L., van Bueren, A. M., Huang, L., Stenbit, A., Celnik, E. and Charron, M. J. (1996) *Brain Res.* **744**, 318-326.

Mellman, I. (1996) *Annu. Rev. Cell. Dev. Biol.* **12**, 575-625.

Meuckler, M., Caruso, C., Baldwin, S. A., Panico, M., Blench, I., Morris, H. R., Allard, W. J., Leinhard, G. E. and Lodish, H. F. (1985) *Science* **229**, 941-945.

Moss, J. and Vaughan, M. (1995) *J. Biol. Chem.* **270**, 12327-12330.

Motta, A., Bremnes, B., Morelli, M. A., Frank, R. W., Saviano, G. and Bakke, O. (1995) *J. Biol. Chem.* **270**, 27165-27171.

Muller, G., Ertl, J., Geri, M. and Prebisch, G. (1997) *J. Biol. Chem.* **272**, 10585-10593.

Nagamatsu, S., Kornhauser, J. M., Burant, C. F., Seino, S., Mayo, K. E. and Bell, G. I. (1992) *J. Biol. Chem.* **267**, 467-472.

Naim, H. Y. and Roth, M. G. (1994) *J. Biol. Chem.* **269**, 3928-3933.

Nichols, B. J., Ungermann, C., Pelham, H. R., Wickner, W. T. and Haas, A. (1997) *Nature* **387**, 199-202.

Nishimura, H., Saltis, J., Habberfield, A. D., Garty, N. B., Greenberg, A. S., Cushman, S. W., Londos, C. and Simpson, I. A. (1991) *Proc. Natl. Acad. Sci. USA* **88**, 11500-11504.

Ohno, H., Fournier, M. -C., Poy, G. and Bonifacino, J. S. (1996) *J. Biol. Chem.* **271**, 29009-29015.

Orci, L., Thorens, B., Ravazzola, M. and Lodish, H. F. (1989) *Science* **245**, 295-297.

Page, L. J. and Robinson, M. S. (1995) *J. Cell. Biol.* **131**, 619-360.

- Pearse, B. M. F. and Robinson, M. S. (1990) *Ann. Rev. Cell. Biol.* **6**, 151-171.
- Pedersen, O., Bak, J. F., Andersen, P. H., Lund, S., Moller, D. E., Flier, J. F. and Khan, B. B. (1990) *Diabetes* **39**, 865-870.
- Pedersen, O., Khan, C. R., Flier, J. S. and Kahn, B. B. (1991) *Endocrinology* **129**, 771-777.
- Peraldi, P., Xu, M. and Spiegelman, B. M. (1997) *J. Clin. Invest.* **100**, 1863-1869.
- Pevsner, J., Hsu, S. -C., Braun, J. E. A., Calakos, N., Ting, A. E., Bennett, M. K. and Scheller, R. H. (1994) *Neuron* **13**, 353-361.
- Piper, R. C., Hess, L. J. and James, D. E. (1991) *Am. J. Physiol.* **260**, C570-C580.
- Piper, R. C., Tai, C., Slot, J. W., Hahn, C. S., Rice, C. M., Huang, H. and James, D. E. (1992) *J. Cell. Biol.* **117**, 729-743.
- Piper, R. C., James, D. E., Slot, J. W., Puri, C. and Lawrence, J. C. (1993a) *J. Biol. Chem.* **268**, 16557-16563.
- Piper, R. C., Tai, C., Kulesza, P., Pang, S., Warnock, D., Baenziger, J., Slot, J. W., Geuze, H. J., Puri, C., and James, D. E. (1993b) *J. Cell. Biol.* **121**, 1221-1232.
- Pond, L., Kuhn, L., Teyton, L., Schutze, M. -P., Tainer, J. A., Jackson, M. R. and Peterson, P. A. (1995) *J. Biol. Chem.* **270**, 19989-19997.
- Rampal, A. L., Jhun, B. H., Kim, S., Liu, H., Manka, M., Lachaal, M., Spangler, R. A. and Jung, C. Y. (1995) *J. Biol. Chem.* **270**, 3938-3943.
- Rapoport, I., Chen, Y. C., Cupers, P., Shoelson, S. E. and Kirchhausen, T. (1998) *EMBO J.* **17**, 2148-2155.
- Rea, S. and James, D. E. (1997) *Diabetes* **46**, 1667-1677.

- Reaven, G. M. (1988) *Diabetes* **37**, 1595-1607.
- Reaven, G. M., Chang, H., Hoffman, B. and Azhar, S. (1989) *Diabetes* **38**, 1155-1160.
- Rebrin, K., Steil, G. M., Getty, L. and Bergman, R. N. (1995) *Diabetes* **44**, 1038-1045.
- Rebrin, K., Steil, G. M., Mittelman, S. D. and Bergman, R. N. (1996) *J. Clin. Invest.* **98**, 741-749.
- Robinson, L. J., Pang, S., Harris, D. A., Heuser, J. and James, D. E. (1992) *J. Cell. Biol.* **117**, 1181-1196.
- Robinson, M. S. (1994) *Curr. Opin. Cell. Biol.* **6**, 538-544.
- Rodionov, D. G. and Bakke, O. (1998) *J. Biol. Chem.* **273**, 6005-6008.
- Rondinone, C. M. and Smith, U. (1996) *J. Biol. Chem.* **271**, 18148-18153.
- Ross, S. A., Scott, H. M., Morris, N. J., Leung, W. Y., Mao, F., Lienhard, G. E. and Keller, S. R. (1996) *J. Biol. Chem.* **271**, 3328-3332
- Rothman, J. E. (1993) *Nature* **372**, 55-63.
- Rothman, J. E. and Warren, G. (1994) *Current Biology* **4**, 220-233.
- Sandoval, I. V. and Bakke, O. (1994) *Trends Cell Biol.* **4**, 292-297.
- Schafer, W., Stroh, A., Berghofer, S., Seiler, J., Vey, M., Kruse, M. L., Kern, H. F., Klenk, H. D. and Garten, W. (1995) *EMBO J.* **14**, 2424-2435.
- Schurmann, A., Mieskes, G. and Joost, H. G. (1992) *Biochem. J.* **285**, 223-228.
- Seaman, M. N. J., Sowerby, P. J. and Robinson, M. S. (1996) *J. Biol. Chem.* **271**, 25446-25451.

- Seidman, I., Horland, A. A. and Teebor, G. W. (1967) *Biochim. Biophys. Acta* **146**, 600-603.
- Shafrir, E. (1992) *Diabetes/Metabolism Reviews* **8**, 179-208.
- Shepherd, P. R., Gibbs, E. M., Weslau, C., Gould, G. W. and Kahn, B. B. (1992) *Diabetes* **41**, 1360-1365.
- Shepherd, P. R., Gould, G. W., Colville, C. A., McCoid, S. C., Gibbs, E. M. and Kahn, B. B. (1992) *Biochem. Biophys. Res. Comm.* **188**, 149-154.
- Shin, J., Doyle, C., Yang, Z., Kappes, D. and Strominger, J. L. (1990) *EMBO J.* **9**, 425-434.
- Shin, J., Dunbrack, R. L., Lee, S. and Strominger, J. L. (1991) *J. Biol. Chem.* **266**, 10658-10665.
- Simonsen, A., Stang, E., Bremnes, B., Roe, M., Prydz, K. and Bakke, O. (1997) *J. Cell. Sci.* **110**, 597-609.
- Simpson, F., Peden, A. A., Christopoulou, L. and Robinson, M. S. (1997) *J. Cell. Biol.* **137**, 835-845.
- Slot, J. W., Geuze, H. J., Gigengack, S., James, D. E. and Meuckler, M. (1991a) *Proc. Natl. Acad. Sci. USA* **88**, 7815-7819.
- Slot, J. W., Geuze, H. J., Gigengack, S., Leinhard, G. E. and James, D. E. (1991b) *J. Cell. Biol.* **113**, 123-135.
- Slot, J. W., Garruti, G., Martin, S., Oorschot, V., Posthuma, G., Kraegen, E. W., Laybutt, R., Thibault, G. and James, D.E. (1997) *J. Cell. Biol.* **137**, 1-12.
- Sollner, T. H., Whiteheart, S. W., Brunner, M., Erdjument-Bromage, H., Geromanos, S., Tempst, P. and Rothman, J. E. (1993) *Nature* **362**, 318-324.
- Sollner, T. H. and Rothman, J. E. (1996) *Cell Struct. Funct.* **21**, 407-412.

Sosa, M. A., Schmidt, B., von Figura, K. and Hille-Rehfeld, A. (1993) *J. Biol. Chem.* **268**, 12537-12543.

Spiegelman, B. M. and Flier, J. S. (1996) *Cell* **87**, 377-389.

Stevenson, R. W., Hutson, N. J., Krupp, M. N., Volkmann, R. A., Holland, G. F., Eggler, J. F., Clark, D. A., McPherson, R. K. and Hall, K. L. (1990) *Diabetes* **39**, 1218-1227.

Sudhof, T. C. (1995) *Nature* **375**, 645-653.

Suzue, K., Lodish, H. F. and Thorens, B. (1989) *Nucleic Acids Research* **17**, 10099-10107.

Suzuki, K. and Kono, T. (1980) *Proc. Natl. Acad. Sci. USA* **77**, 2542-2545.

Tanner, L. I. and Leinhard, G. E. (1988) *J. Biol. Chem.* **262**, 8975-8980.

Tanner, L. I. and Leinhard, G. E. (1989) *J. Cell. Biol.* **108**, 1537-1545.

Tanti, J. F., Gremeaux, T., Cormont, M., Van Obberghen, E. and Le Marchand-Brustel, Y. (1993) *Am. J. Physiol.* **264**, E868-E873.

Tanti, J. F., Gremeaux, T., Van Obberghen, E. and Le Marchand-Brustel, Y. (1994) *J. Biol. Chem.* **269**, 6051-6057.

Tellam, J. T., MacAuley, S. L., McIntosh, S., Hewish, D. R., Ward, C. W. and James, D. E. (1997) *J. Biol. Chem.* **272**, 6179-6186.

Thomas, H. M., Takeda, J. and Gould, G. W. (1993) *Biochem. J.* **290**, 707-715.

Thorens, B., Sahar, H. K., Kaback, H. R. and Lodish, H. F. (1988) *Cell* **55**, 281-290.

Thorens, B., Cheng, Z. Q., Brown, D. and Lodish, H. F. (1990) *Am. J. Physiol.* **259**, C279-285.

- Thorens, B. and Roth, J. (1996) *J. Cell. Sci.* **109**, 1311-1323.
- Tontonez, P., Hu, E., Graves, R. A., Budavari, A. B. and Spiegelman, B. M. (1994) *Genes Dev.* **8**, 1224-1234.
- Traub, L. M., Ostrom, J. A. and Kornfeld, S. (1993) *J. Cell. Biol.* **123**, 561-573.
- Trowbridge, I. S., Collawn, J. F. and Hopkins, C. R. (1993) *Annu. Rev. Cell. Biol.* **9**, 129-161.
- Ungermann, C., Nichols, B. J., Pelham, H. R. and Wickner, W. T. (1998) *J. Cell. Biol.* **140**, 61-69.
- Verhey, K. J., Hausdorff, S. F. and Birnbaum, M. J. (1993) *J. Cell. Biol.* **123**, 137-147.
- Verhey, K. J. and Birnbaum, M. J. (1994) *J. Biol. Chem.* **269**, 2353-2356.
- Verhey, K. J., Yeh, J. and Birnbaum, M. J. (1995) *J. Cell. Biol.* **130**, 1071-1079.
- Volchuk, A., Sargeant, R., Sumitani, S., Liu, Z., He, L. and Klip, A. (1995) *J. Biol. Chem.* **270**, 8233-8240.
- Volchuk, A., Wang, Q., Ewart, S., Liu, Z., He, L., Bennett, M. K. and Klip, A. (1996) *Mol. Biol. Cell* **7**, 1075-1082.
- Voorhees, P., Deignan, E., van Donselaar, E., Humphrey, J., Marks, M. S., Peters, P. J. and Bonifacino, J. S. (1995) *EMBO J.* **14**, 4961-4975.
- Waddell, I. D., Zomerschoe, A. G., Voice, M. W. and Burchell, A. (1992) *Biochem. J.* **286**, 173-177.
- Wang, G., Witkin, J. W., Hao, G., Bankaitis, V. A., Scherer, P. E. and Baldini, G. (1997) *J. Cell. Sci.* **110**, 505-513.
- Warren, R. A., Green, F. A. and Enns, C. A. (1997) *J. Biol. Chem.* **272**, 2116-2121.

Weber, T., Zemelman, B. V., McNew, J. A., Westermann, B., Gmachl, M., Parlati, F., Sollner, T. H. and Rothman, J. E. (1998) *Cell* **92**, 759-772.

West, M. A., Lucocq, J. M. and Watts, C. (1994) *Nature* **369**, 147-151.

Willson, T. M., Cobb, J. E., Cowan, D. J., Wiethe, R. W., Correa, I. D., Prakash, S. R., Beck, K. D., Moore, L. B., Kleiwer, S. A. and Lehmann, J. M. (1996) *J. Med. Chem.* **39**, 665-668.

Wu, Z., Xie, Y., Butcher, N. L. R. and Farmer, S. R. (1998) *J. Clin. Invest.* **101**, 22-32.

Yang, J., Clark, A. E., Harrison, R., Kozka, I. J. and Holman, G. D. (1992a) *Biochem. J.* **281**, 809-817.

Yang, J., Clark, A. E., Kozka, I. J., Cushman, S. W. and Holman, G. D. (1992b) *J. Biol. Chem.* **267**, 10393-10399.

Yang, J. and Holman, G. D. (1993) *J. Biol. Chem.* **268**, 4600-4603.

Yeh, J. I., Verhey, K. J. and Birnbaum, M. J. (1995) *Biochemistry* **34**, 15523-15531.

Young, P. W., Cawthorne, M. A., Coyle, P. J., Holder, J. C., Holman, G. D., Kozka, I. J., Kirkham, D. M., Lister, C. A. and Smith, S. A. (1995) *Diabetes* **44**, 1087-1092.

Zarjevski, N., Doyle, P. and Jeanrenaud, B. (1992) *Endocrinology* **130**, 1564-1570.

Zhang, Y. and Allison, J. P. (1997) *Proc. Natl. Acad. Sci. USA* **94**, 9273-9278.

Zorzano, A., Wilkinson, W., Kotliar, N., Thoidis, G., Wadzinski, B. E., Ruoho, A. E. and Pilch, P. F. (1989) *J. Biol. Chem.* **264**, 12358-12363.

